THE UNIVERSITY
of EDINBURGH

Control of regulatory T cell activity by endogenous and pathogen-derived EGFR ligands

Jame Christopher McCrae

Submitted for the Degree of Doctor of Philosophy

The University of Edinburgh

Doctor of Philosophy - The University of Edinburgh - 2019

For Alana

Table of Contents

Table of Figures

Table of Tables

Declaration

I declare that I have composed this thesis, and that the work is my own unless clearly stated otherwise. I also declare that this work has not been submitted for any other degree or professional qualification.

Student's Signature

Jame McCrae

Supervisor's signature

Dr Dietmar Zaiss

9 April 2020

Acknowledgements

My thanks to my supervisor Dietmar Zaiss, for his support and guidance before, during and after my PhD. My assistant supervisor, Matthew Taylor was also very supportive, and assisted in particular with my work on *Litomosoides sigmodontis*. My thanks also to my clinical supervisor, Professor David Webb, who was instrumental in my obtaining funding from the Medical Research Council. Without his help I wouldn't have been able to set my sights on this degree.

I am grateful to others in the Zaiss group who assisted me, either with technical advice and guidance (Carlos Minutti in particular) or more coffee-oriented support (Felicity MacDonald, Matthew Sinton). My thanks to Andrew Muir also, for showing me the ropes in the lab when I first came to the department. We all helped each other, and that's what made working in the group enjoyable.

I am grateful also to Martin Waterfall, whose expertise in flow cytometry was essential to my obtaining good-quality data for this thesis (as it has been in many others). Alison Fulton, Nicola Logan and Rucha Modak helped with experimental harvesting and data acquisition. My thanks also the animal unit staff in Ann Walker and March Building for their assistance with *in-vivo* experiments.

Lastly, my thanks to Laura for her support at home.

Abstract

Regulatory T cells (Treg) are $CD4^+$ $FOXP3^+$ T lymphocytes whose function is to prevent autoimmunity and immune cell-mediated damage on infected tissues. They carry out their suppressive effects either by direct cell-cell contact or through the use of soluble mediators such as IL-10 and TGFβ. Activated Treg express the epidermal growth factor receptor (EGFR), a tyrosine kinase receptor found in most tissue types and leukocytes. EGFR signalling induces behavioural changes in Treg: in particular, the ligand Amphiregulin (AREG) is required for optimal Treg function in various *in-vitro* and *in-vivo* experimental models. The aim of my thesis has been to explore the effects of EGFR signalling on Treg function in the context of infection, induced either from endogenously expressed or pathogen-derived ligands.

In **Chapter 2** I examined the effects of Vaccinia (VACV) virus-derived Vaccinia Growth Factor (VGF), a pathogen-derived soluble protein with EGF-like activity, on Treg function. I showed that Treg function is increased when exposed to UV-inactivated Vaccinia virus, but that this activation can be blocked by deleting EGFR expression on Treg. Using an *in-vivo* pneumonitis model, I showed that mice deficient in EGFR expression on their Tregs were more resistant to VACV infection compared to wildtype, and that following infection there was less bioactive TGFβ in the bronchoalveolar lavage supernatant of these animals. Taken together, these data imply that Vaccinia virus derived VGF enhances the suppressive capacity of Tregs and use this enhanced activation as a means of immune escape.

In **Chapter 3** I used the filariasis model *Litomosoides sigmodontis* (a chronic helminth infection of rodents) to examine the effects of EGFR signalling in Tregs induced by the endogenous ligand Amphiregulin, and to study the effects of EGFR blockade on the helminth-specific immune response using the commercially available tyrosine kinase inhibitor Gefitinib. We found that EGFR deletion on Treg lead to no increase in TH2 cytokine production or parasite rejection. Also, complete deletion of Amphiregulin in *Areg*$^{-/-}$ mice had no significant effect; nor did the administration of Gefitinib over several weeks in WT mice. From these findings, we conclude that AREG-EGFR signalling on Tregs (or EGFR signalling in general) is not a significant factor influencing the immune response to *L.sigmodontis* infection.

In **Chapter 4** I examined the effects of the complete deletion of Amphiregulin in *Areg*$^{-/-}$ mice, and the deletion of Amphiregulin in specific cell types, on the activity of activated Tregs in an airway allergy model. To induce and activate Tregs we used the murine helminth *Heligmosomoides polygyrus,* which infects the gastrointestinal tract but also induces Treg expansion systemically. Previous work in our group had determined that Amphiregulin deletion in mice led to a decreased Treg-mediated immunosuppression following *H. polygyrus* infection and airway OVA challenge, as evidenced by greater eosinophilia in the lungs of *Areg*$^{-/-}$ than wildtype mice. However, I failed to replicate the initial findings of our group's work, seeing no difference in Treg activity or TH2 response between infected and noninfected animals, and also no significant differences in different mouse strains with a cell type-specific deletion of Amphiregulin.

Taken together, my thesis provides evidence for the enhanced suppressive capacity of Tregs by a viral pathogen derived EGFR ligand, in order to create a local immunosuppressive environment. To our knowledge, this is the very first time such an immune escape mechanism has been demonstrated. It also demonstrates that in the face of helminth-mediated activation of Treg, EGFR signalling is not a significant factor contributing to local immune suppression. This further clarifies the role of EGFR signalling on Tregs in the setting of both acute and chronic infection.

Lay Summary

Regulatory T cells (Treg) are a type of white blood cell whose function is to prevent autoimmune disease and stop other white blood cells damaging infected tissues. They do this either by directly contacting cells and giving a suppressive signal, or by releasing chemicals into the environment such as IL-10 and TGFβ. Activated Treg express a receptor on their cell surface called the Epidermal Growth Factor Receptor (EGFR), which is also present on many other cells. When EGFR is activated by specific proteins, for example by Amphiregulin (AREG), the cell is activated and starts suppressing other white blood cells. The aim of my thesis was to clarify the effects of EGFR activation on Treg function, either when EGFR is activated by AREG or by a virus-derived protein that behaves similarly to AREG.

In **Chapter 2** I use a virus called Vaccinia (VACV), which produces a protein called VGF that can activate EGFR. Using virus that can't replicate, but can make VGF protein, I showed that Treg can suppress other cells when they are exposed to the nonreplicating virus. Treg that don't have EGFR on their cell surfaces don't do this. Then, using mice infected with VACV in their lungs, I show that normal mice are much more susceptible to infection than animals with EGFR deleted on the cell surface of their Tregs. The gene-deficient mice also had less of the suppressive chemical TGFβ in their lungs, implying that their Treg were less activated than those in the normal mice. Taken together, these data imply that Vaccinia virus uses VGF to activate Tregs, which in turn will suppress the rest of the immune response to infection, ultimately harming the host and benefiting the virus.

In **Chapter 3** I used a helminth worm infection of rodents called *Litomosoides sigmodontis*, to look at the effects of AREG produced by the host's own body on Tregs, and with a drug called Gefitinib tried to block this signal. Comparing normal mice to mice with EGFR deleted on their Tregs, I found no differences in the immune response to *L.sigmodontis* infection. Using mice with the gene for AREG deleted completely also didn't change this. Finally, I tried administering Gefitinib to block AREG-EGFR signals, and again this did not have an effect compared to mice who didn't receive Gefitinib. In conclusion, AREG-EGFR signalling on Tregs, or using a drug to block EGFR signals in general, doesn't affect the immune response to or outcome of *L.sigmodontis* infection.

In **Chapter 4** I looked at AREG-EGFR signalling in a mouse airway allergy model. To induce Treg production in some mice, I infected half of my animals with a gut worm called *Heligmosomoides polygyrus*: the infected mice would have more Treg in the lungs, as *H.polygyrus* infection makes the host body to produce Tregs. We had expected to see a reduced Treg response in the lungs of mice where the AREG gene has been deleted, as previous work in our lab had shown this, and it is known that AREG is an important EGFR signal for Tregs in general. We were then going to use mice with the AREG gene deleted on specific white blood cell types in order to determine where the AREG is coming from that is activating the Treg in the lungs. However, we weren't able to repeat the initial findings, and didn't see any difference between wildtype animals and animals where AREG is deleted completely. No other

strains of mice we used had significant differences when compared to wildtype animals either.

In summary, I have shown that in an acute infection that viruses can exploit EGFR signalling by using their own proteins to activate regulatory T cells. This in turn makes them suppress the rest of the immune system, to the benefit of the virus and detriment of the host. AREG-EGFR signalling is not a significant factor in the activation of regulatory T cells in *L.sigmodontis* infection.

Abbreviations

3H-TdR	Tritiated thymidine
A431	Human epidermal cell line
ADAM10	A disintegrin and metalloproteinase protein 10
AKT	Transcription factor (not an abbreviation)
ANOVA	Analysis of variance
APC	Antigen-presenting cell
APS	Ammonium Persulphate
AREG	Amphiregulin
ATP	Adenosine triphosphate
B16	Mouse melanoma cell line
BAL	Bronchoalveolar lavage
BALF	Bronchoalveolar lavage fluid
Bcl-2	B-cell lymphoma 2-encoded protein
Bcl-3	B-cell lymphoma 3-encoded protein
BSA	Bovine serum albumin
BSC-1	Biologics Standards Cercopithecus-1 (monkey kidney cell line)
C11R	Vaccinia Growth Factor gene
CD	Cluster of Differentiation
CEV	Cell-associated enveloped virion
cGAS	Cyclic GMP-AMP Synthase
CMV	Cytomegalovirus
CPXV	Cowpoxvirus
CTLA4	Cytotoxic T-lymphocyte-associated protein 4
CTV	CellTrace Violet
CXCL12	C-X-C motif chemokine 12
CXCR4	C-X-C chemokine receptor type 4
D4R	Smallpox Growth Factor gene
DMSO	Dimethylsulfoxide
DNA	Deoxyribonucleic acid
DNA-PK	DNA-dependent protein kinase
dsDNA	Double-stranded DNA
DTT	Dithiothreitol
EBV	Epstein-Barr virus
ECL	Enhanced chemiluminescence
EDTA	Ethylenediaminetetraacetic acid
EEV	Extracellular enveloped virion
EGF	Epidermal growth factor
EGFR	Epidermal growth factor receptor
egr-1	Early growth response protein 1
ErbB	Avian erythroblastosis oncogene B Tyrosine kinase receptor family
ERK	Extracellularly regulated kinase
FACS	Fluorescence activated cell sorting
FCεRI	Fc IgE receptor
FCS	Fetal calf serum
FOXP3	Forkhead box protein 3
FSc	Forward scatter
GATA3	GATA-binding protein 3
gB	Glycoprotein B
GI	Gastrointestinal

GITR	Glucocorticoid-induced TNFR-related protein
Gq/11	Gq protein
GRB2	Growth factor receptor-bound protein 2
HaCaT	Human keratinocyte cell line
HBEGF	Heparin-binding epidermal growth factor
HBV	Hepatitis B virus
HCl	Hydrogen chloride
HCV	Hepatitis C virus
Hep2	A hepatocyte cell line
HER	Human epidermal receptor
HIV	Human immunodeficiency virus
HNSCC	Head and neck squamous cell carcinoma
HSV	Herpes simplex virus
IAV	Influenza A virus
ICOS	Inducible T cell co-stimulator
IEV	Intracellular enveloped virion
IFNα	Interferon alpha
IFNγ	Interferon gamma
IGF-1	Insulin-like growth factor type 1
IgG	Immunoglobulin G
IL	Interleukin
IL-33R	Interleukin 33 receptor
ILC2	Innate Lymphoid Cell type 2
IRF3	Interferon Regulatory Factor 3
IMDM	Iscove's modified Dulbecco's medium
IMV	Intracellular mature virion
kDa	Kilodalton
KRAS	Kirsten RAt Sarcoma oncogene
L1R	Gene for poxvirus protein L1
LCMV	Lymphocytic choriomeningitis mammarenavirus
LMP1	Latent membrane protein
MACS	Magnetic Cell Separation (Miltenyi Biotec)
MEK	MAPK/ERK Kinase
MHC	Major histocompatibility complex
MMP	Matrix metalloproteinase
mTOR	Mechanistic target of rapamycin
MUC5AC	Mucin 5AC gene
MVA	Modified Vaccinia Ankara
NaCl	Sodium chloride
NF-κB	Nuclear factor kappa-B
NK	Natural Killer
NP-40	Nonylphenoxypolyethoxylethanol
OVA	Ovalbumin
PAGE	Polyacrylamide gel electrophoresis
PAI-1	Plasminogen activator inhibitor 1
PBS	Phosphate-buffered saline
PC61	Anti-CD25 antibody
PDGFR	Platelet-derived growth factor receptor
pEGFR	Phosphorylated EGFR
PFU	Plaque-forming units
PI3K	Phosphatidylinositol-3-kinase

PKC	Protein kinase C
PKCδ	Protein kinase C delta
PLCγ1	Phospholipase C gamma 1
PLEC	Pleural exudate cells
PMP21	Polymorphic membrane protein 21
PVDF	Polyvinylidene fluoride
RAF	RAF proto-oncogene serine/threonine-protein kinase
RAG	Recombination activating gene
RAS	RAt Sarcoma GTPase
Rck	Resistance to complement killing protein
RNA	ribonucleic acid
RORγt	RAR-related orphan receptor gamma T
RSV	Respiratory syncytial virus
SDS	Sodium dodecyl sulphate
SOPF	Specific opportunistic pathogen free
SPF	Specific pathogen free
SPGF	Smallpox growth factor
SSc	Side scatter
STAT5	Signal transducer and activator of transcription 5
STING	STimulator of IFN Gene
TACE	TNF alpha converting enzyme
Tbet	T-Box Expressed in T Cells
TBK1	Tank-Binding Kinase 1
TBST	Tris-Buffered Saline with Tween-20
TCR	T cell receptor
TEMED	Tetramethylethylenediamine
TGFα	Transforming Growth factor alpha
TGFβ	Transforming growth factor beta
TH	Helper T cell
TKI	Tyrosine kinase inhibitor
TLR	Toll-like receptor
TMLC	Transgenic Mink Lung Epithelial Cells
TNFα	Tumour necrosis factor alpha
TNFR25	Tumour necrosis factor receptor superfamily member 25
Tr1	Type 1 regulatory cell
Treg	Regulatory T cell
TRM	Tissue-Resident Memory T cell
UV	Ultraviolet
VACV	Vaccinia virus
VARV	Variola virus
VGF	Vaccinia growth factor
WT	Wildtype

Chapter 1: Introduction

1 Overview of the immune system

1.1 The immune system's evolution over time is defined by increasing complexity, leading to the development of adaptive immunity

With the development of multicellular life (metazoans) came a requirement for successful organisms to defend against invasion by parasites (Beutler 2004; Akira, Uematsu, and Takeuchi 2006; Cosson and Soldati 2008). Cells with a similar phenotype to amoeba (migrate along chemoattraction gradients, consume nonself microbes) were essential for this, and are the likely origins of phagocytic cells that constitute the innate immune system (Cosson and Soldati 2008; Wynn, Chawla, and Pollard 2013). The innate immune system's main function is to recognise pathogens and eliminate them without damaging host tissues in the process (i.e. there must be self-tolerance) (Beutler 2004). It is composed of a variety of barrier methods (e.g. skin, mucosa, coagulation cascade, mucus production) and phagocytic cells such as the macrophages mentioned above (Beutler 2004; Akira, Uematsu, and Takeuchi 2006). These cells function by constitutively recognising pathogen-associated molecular antigens, and then triggering an immune response to those pathogens.

The adaptive immune system responds to pathogens by clonal amplification of specific lymphocytes with affinity for the pathogen's antigenic structure(s), differentiation of those lymphocytes and production of antibodies against that specific pathogen (Cooper and Alder 2006; Flajnik and Kasahara 2010). Increasing parasite burden seems to be the main driver for the development of adaptive immunity, which has evolved separately on at least 2 occasions: once in jawed vertebrates (Gnathostomes), and a second time in jawless fish (Agnathostomes) (Cooper and Alder 2006; Flajnik and Kasahara 2010). There are 2 types of lymphocyte, B cells and T cells, which are subdivided into Cytotoxic (express CD8 on their cell surface) and 'Helper' (Express CD4). CD4+ T cells are discussed below.

1.2 CD4 T cells are an essential component of adaptive immunity

CD4+ T cells are termed Helper T cells, and function to establish and maintain the immune response to infection, tissue homeostasis, and the generation of immunological memory (Kumar, Connors, and Farber 2018). They do this via recognition of a diverse range of antigens from pathogens, tumour cells and the environment via the T cell receptor (TCR) (Zhu, Yamane, and Paul 2010). The TCR binds to antigen presented in a peptide-MHC complex, either from an infected cell or an antigen-presenting cell (Murphy and Reiner 2002). T cell phenotype is then decided both by the

nature of antigen binding to the TCR and the surrounding cytokine milieu (Zhu, Yamane, and Paul 2010; Murphy and Reiner 2002; Mosmann et al. 1986; O'Garra and Murphy 1994).

Naïve T cells differentiate to either TH1, TH2 or TH17 cells by means of transcription factors that alter gene expression: Tbet promotes a TH1 phenotype, without which the activated cell will 'default' to TH2 or TH17. The main transcription factors for TH2 and TH17 cells are GATA3 and RORγt, respectively. Once the relevant transcription factor is acquired, expression and activity of the others is suppressed (Yu et al. 2015; Kanhere et al. 2012; Murphy and Reiner 2002). Tbet promotes expression of IFNγ by using chromosomal looping to bring the IFNγ gene closer to a promoter region; GATA3 does the same to the genes for IL-4, IL-5 and IL-13 (Kanhere et al. 2012). Note that the above picture is simplified, and many other extrinsic signals affect the T cell's eventual fate (Murphy and Reiner 2002).

TH1 cells are responsible for cell-mediated defence against intracellular pathogens; they produce large amounts of IFNγ and lymphotoxin in order to facilitate this (Glimcher and Murphy 2000; Murphy and Reiner 2002; Chakir et al. 2003).

TH2 cells are produced in response to extracellular parasites with complex antigenic structures, such as helminth worms, as well as chronic infections such as tuberculosis (Gomez-Escobar, Gregory, and Maizels 2000; Elson et al. 1998). They are involved in the generation of a type 2 immune response, where cytokines such as IL-4, IL-5, IL-10, IL-13 and Amphiregulin are present (Zaiss et al. 2006; Chen et al. 2012; Gomez-Escobar, Gregory, and Maizels 2000; Haben et al. 2013; Glimcher and Murphy 2000; O'Garra and Murphy 1994; Romagnani 2000). As well as repelling the pathogen, type 2 immune responses aim to minimise tissue damage caused by a runaway immune response (Allen and Sutherland 2014; Gause, Wynn, and Allen 2013). Derangement of the TH2 response contributes to the development of atopic reactions and allergy (Elson et al. 1998).

TH17 cells are involved in mucosal immunity, and are produced in response to a variety of bacterial and fungal pathogens, where they play a protective role (Pan et al. 2011; Abi Abdallah et al. 2011; Guglani and Khader 2010). Naïve CD4 T cells express the transcription factor RORγt in response to TGFβ, IL-6 and IL-21 signals, though TH17 cells can also be produced upon exposure to IL-1β, IL-6 and IL-21 without TGFβ (Ghoreschi et al. 2010; Pan et al. 2011; Lee et al. 2009). TH17 cells express high levels of IL-17, as well as IL-17F and IL-22. As well as functioning in pathogen clearance, TH17 cells are implicated in autoimmunity and inflammatory conditions such as

multiple sclerosis, collagen-induced arthritis and colitis (Korn et al. 2009; Guglani and Khader 2010).

A fourth kind of T cell, the regulatory T cell, is discussed below.

2 Regulatory T cells are essential for optimal immune function

Regulatory T cells (Treg) are defined as CD4 T cells which express the intracellular transcription factor Forkhead Box Protein 3 (FOXP3) (Li et al. 2008; Veiga-Parga, Sehrawat, and Rouse 2013). FOXP3 in turn binds and regulates up to 700 other genes as well as various microRNAs to generate the Treg 'phenotype'. The main function of Treg is to prevent immunopathology, either from autoimmune disease or direct damage of infected tissue by the host immune response (Veiga-Parga, Sehrawat, and Rouse 2013; Li et al. 2008); and depletion of Treg leads to both more autoimmune lesions and increased effector T cell-mediated tissue damage.

Tregs maximally activate when they have migrated to the site of inflammation (Zhang et al. 2009). There they expand in response to TCR activation, typically from dendritic cells, but also ILC2 cells as well as costimulatory signals, such as IL-2 and ICOS (Li et al. 2008; Redpath et al. 2013; Veiga-Parga, Sehrawat, and Rouse 2013; Halim et al. 2018). Treg are more sensitive to IL-2 than effector T cells, and IL-2 is essential for the generation of tolerance.

2.1 Classification of regulatory T cells

Tregs have been divided into 2 subsets, natural (nTreg) and induced (iTreg). nTreg are derived from thymic tissue, where T cell precursors with self-affinity are retained, express FOXP3 and proliferate when they exit the thymus in response to specific signals. They mostly reside in the skin and mucosa, and are activated by a range of signals, including Toll-like receptors, antigen-presentation, and cytokines from virus-infected antigen-presenting cells (IL-2, TGFβ, TNFα); their main role is in suppressing autoimmunity (Veiga-Parga, Sehrawat, and Rouse 2013). Their mechanism of action is antigen-specific, and works via membrane-bound TGFβ, or by cytoplasmic transfer of granzyme-B and galectin-1 in order to kill specific cells (usually effector T cells).

It is proposed that iTreg 'class-switch' from other T cell subsets in the infective milieu (e.g. naïve or effector T cells) in response to certain signals (e.g. antigen presentation, IL-2 & TGFβ), and start to express both FOXP3 and CD25 (Li et al. 2008; Veiga-Parga, Sehrawat, and Rouse 2013; Yu et al. 2015). Their main role is in altering the antigen-specific immune response, and this is achieved through soluble mediators such as IL-10 and TGFβ. Treg function is variable, and can be suppressed by activated NK cells, IL-6 and TLR signalling (Veiga-Parga, Sehrawat, and Rouse 2013; Zaiss et al. 2013; Brillard et al. 2007; Okoye et al. 2014)

It should be noted that neither Treg subtype uses these mechanisms of action exclusively; nor are these the only regulatory cells: Tr1 cells are $FOXP3^{-}$ $CD4^{+}$ T cells that produce mostly IL-10, and are induced by chronic antigenic stimulation in the presence of IL-10 (Zeng et al. 2015; Veiga-Parga, Sehrawat, and Rouse 2013; Brockmann et al. 2018).

2.2 Treg immunotherapy

Researchers have investigated the utility of Tregs as a therapy against conditions where there is an excessive immune response: These involve either transfusion of activated and expanded Tregs or attempts to induce Treg production in the host (Kretschmer et al. 2006). This can be done using TGFβ, galectins 1 & 9, and an IL-2-IL-2 monoclonal antibody, as well as antibodies to TNF-R25 (Reddy et al. 2012; Veiga-Parga, Sehrawat, and Rouse 2013).

The utility of Tregs as a therapy to prevent established disease was confirmed in a T cell colitis model, where transfer of $CD4^{+}$ $CD25^{+}$ cells rescued $RAG1^{-/-}$ mice from further injury, and in fact reversed the colitis (Mottet, Uhlig, and Powrie 2003). Since then Treg therapy has been trialled in graft-versus-host disease, as well as autoimmune conditions such as type 1

diabetes; whilst *in-vivo* work in mice has helped to clarify the signals and mechanisms which influence Treg function, First-In-Human trials are less impressive (Read et al. 2006; Marek-Trzonkowska et al. 2014; Whibley, Tucci, and Powrie 2019; Hartemann et al. 2013; Heinrichs et al. 2016; Hull, Peakman, and Tree 2017; Marco Romano et al. 2019). Notably, phase I/II trials in type 1 diabetic patients have produced more impressive results, and phase II studies are ongoing (Hartemann et al. 2013).

In infectious disease models, such as HSV keratosis, transfusion of Tregs also appears to be effective at preventing immunopathology (Veiga-Parga, Sehrawat, and Rouse 2013). Expansion of Treg populations using anti-TNF-R25 also reduces inflammation in this model system; however, use after D6 postinfection also expanded proinflammatory effector T cells, which also express TNF-R25 (Reddy et al. 2012). Hence, it appears that the timing of therapy, and method of expansion is important to the final outcome.

3 The Epidermal Growth Factor Receptor is a Tyrosine Kinase Receptor with Numerous Functions Across Multiple Cell Types

The Epidermal Growth Factor Receptor (EGFR) was the first tyrosine kinase receptor to be identified in 1975: initially the effects of epidermal growth factor (EGF) were noted when Cohen and colleagues injected a submandibular gland extract (containing EGF) into neonatal mice, and induced hyperproliferation and keratinisation of epithelial cells (Levi-Montalcini and Cohen 1960); the receptor for EGF was found shortly after, and was noted to incorporate radiolabelled phosphorus after stimulation with EGF (Carpenter, King, and Cohen 1978). Molecular methods soon clarified EGFR's structure as a tyrosine kinase receptor, the first of its kind to be identified (Chen et al. 2016; Gschwind, Fischer, and Ullrich 2004).

EGFR (also termed Human epidermal receptor type 1 [HER1]) is the first in the ErbB superfamily of tyrosine kinase receptors (Zhang et al. 2007). ErbB receptors are composed of monomers that are activated upon dimerisation and binding to specific ligands (see below) (Avraham and Yarden 2011). There are 4 monomers, termed ErbB1-4. EGFR (HER1) is a homodimer composed of two ErbB1 monomers, HER2 (also called Neu in mice) has two ErbB2 monomers, HER3 has two ErbB3 monomers, and HER4 two ErbB4

monomers. In addition to these receptor homodimers, heterodimers can occur, and in fact HER2 is the preferred 'partner' fort ErbB3/4 (Zhang et al. 2007; Tzahar et al. 1996). In order to dimerise, an ErbB1 monomer bound to a ligand undergoes a conformational change revealing a dimerization 'arm', which can then initiate contact with another ErbB monomer. In ErbB2 this dimerization 'arm' is permanently exposed, explaining its constitutive activity (Linggi and Carpenter 2006).

3.1 Intracellular signalling from EGFR

Once a ligand binds to a receptor (except HER2/neu, which is constitutively active), various tyrosine residues are phosphorylated, which then act as docking sites for intracellular messenger molecules: these occur via 2 main signal transduction pathways.

In the first pathway, GRB2 is phosphorylated and subsequently recruits RAS; subsequent signalling cascades down RAF – MEK – ERK, which when phosphorylated triggers downstream signals that regulate entry into the cell cycle. In the second pathway, PI3K – AKT – mTOR signalling triggers a propensity for reduced apoptosis and cell survival. After internalisation the receptor-ligand complex can continue to signal, though AKT signalling is rapidly terminated (Avraham and Yarden 2011; Gschwind, Fischer, and

Ullrich 2004). Overall, at EGFR engages with at least 6 separate biochemical pathways (Avraham and Yarden 2011).

Note that the 2 signal transduction pathways described do not account for all the downstream effects of EGFR activation; ligands have different affinities for different receptors, activation can result in different tyrosine residues being phosphorylated, and the effect can vary by cell type; but in general, stimulation of EGFR usually triggers proliferation or differentiation of the target cell (Avraham and Yarden 2011; Schlessinger 2000).

3.2 Tissues expressing EGFR

3.2.1 Epithelial cells

EGFR is mandatory for optimal epithelial cell development. EGFR signalling is required for development and migration of epithelial tissue during embryogenesis, explaining the near-lethality of a full deletion in mice (Bublil and Yarden 2007); EGFR knockout mice either die in-utero or survive for a few weeks postpartum, and show defects in epithelial development in the skin, kidney, lung and GI tract (Threadgill et al. 1995; Miettinen et al. 1995; Sibilia and Wagner 1995). By contrast, deletion of genes for individual EGFR ligands results in mild or no abnormal phenotype, indicating considerable ligand redundancy.

In addition to this, EGFR signalling has some importance in maintenance of optimal tissue function in infection: EGFR ligands EGF and Amphiregulin both promote migration of gut epithelial cells after injury, and EGF has protective effects in bowel perforation sepsis models in mice (Clark et al. 2008). This may be by encouraging the preservation of bowel epithelial integrity, and minimising subsequent bacterial translocation from the GI tract to the systemic circulation (Liu et al. 1997). EGFR responses in the lung include epithelial and goblet cell proliferation and mucin production (Burgel and Nadel 2004); hence, EGFR signalling partially contributes to the barrier function of the innate immune system in the lung and GI tract.

3.2.2 Leukocytes, including regulatory T cells, express EGFR

In recent years EGFR has been detected on the cell surfaces of various leukocytes, including monocytes, plasma cells and myeloma cells (Mahtouk et al. 2005; Chan, Nogalski, and Yurochko 2009). Activated CD4 T cells also express EGFR, which is the most upregulated transmembrane receptor after STAT5 signalling (Liao et al. 2008; Zaiss et al. 2013).In addition to the above, EGFR signalling influences T cell function: Garrido and colleagues showed that T cells were essential for the antimetastatic effect of a monoclonal antibody to EGFR in a murine lung carcinoma model. (Garrido et al. 2007).

Previous work in our lab has shown that regulatory T cells express EGFR: the receptor was detected on 15% of resting Treg in healthy volunteers, and 100% of activated Treg *in-vitro*. These findings were confirmed in a murine B16 melanoma model (Zaiss et al. 2013). Others have found increased EGFR expression in a skin wound model, and kinome profiling in human Tregs has shown that EGFR is strongly upregulated after Treg activation (Nosbaum et al. 2016; Tuettenberg et al. 2016). Thus, activated Treg express EGFR and respond to EGFR signalling.

3.3 EGFR signalling and cancer

Over 60% of tumour cells contain abnormal ErbB receptors. (Yang et al. 2005), and EGFR in particular is notable for its presence (and overactivity) on several epithelial cancers such as pancreatic, breast, brain, colorectal, non-small cell lung cancer and head and neck squamous cell carcinoma (HNSCC) (Boran et al. 2012). Overexpression of EGFR in these tumours (e.g. HNSCC) is associated with increased mortality (Dassonville et al. 1993; Chung et al. 2006; Kumar et al. 2008).

Additionally, some tumours such as myeloma, overproduce the EGFR ligand Amphiregulin, which signals via the PI3K-AKT pathway, and contributes to myeloma cell proliferation by inducing IL-6 production from bone marrow

stromal cells (Mahtouk et al. 2005). Interestingly, blocking EGFR signalling induced apoptosis in myeloma cells.

The high prevalence of EGFR overexpression (or ligand production) in various tumours led to the development of EGFR antagonist agents, namely monoclonal antibodies (e.g. cetuximab) and small molecule tyrosine kinase inhibitors of EGFR (e.g. Gefitinib, erlotinib etc.), which have been used to treat a number of cancers (Boran et al. 2012). By inhibiting EGFR signalling the tumour cells are denied a growth signal and are more susceptible to destruction either by the immune system or chemotherapeutic agents (Mahtouk et al. 2005; Garrido et al. 2007). Resistance to these agents has been documented, either by modification of EGFR in lung cancer, or the generation of KRAS mutants (Boran et al. 2012). However, it has also been noted that some EGFR-negative tumours appear to respond to EGFR blockade: this interesting observation led researchers to examine the peritumoural space, where activated regulatory T cells inhibit antitumour responses (Zitvogel et al. 2008). Potentially this has the advantage of limiting tissue damage, but would also impair cytotoxic T cell activity against cancer cells, allowing tumour growth (Garrido et al. 2007). As discussed, activated Treg express EGFR, and blocking this signal appears to shift the peritumoural environment to a more proinflammatory state; for example, Garrido and colleagues found that in the presence of a monoclonal antibody antagonist of EGFR that dendritic, NK and T cells infiltrated a murine lung

tumour in a T-cell dependent manner (Garrido et al. 2007). Others have found the same, and hypothesised that tumour responses to EGFR blockade may rely partially on Treg deactivation (Zaiss et al. 2013; Ferris, Jaffee, and Ferrone 2010; MacDonald and Zaiss 2017).

3.4 Ligands for EGFR have different effects in different cell types

After the discovery of epidermal growth factor (EGF), several other ErbB ligands have been identified. These are Heparin-Binding Epidermal Growth Factor (HBEGF), Amphiregulin, Transforming Growth Factor alpha (TGFα), Epiregulin, Betacellulin, Epigen and Neuregulins 1-4 (Avraham and Yarden 2011; Monick 2004). Not all ErbB receptors respond to all of these: EGFR binds to all except the Neuregulins; HER2/Neu doesn't bind to any known ligand; HER3 only binds Neuregulins 1 & 2, and ErbB4 binds all ligands except EGF, TGFα and Epigen (Linggi and Carpenter 2006). ErbB ligands are synthesised as type 1 transmembrane precursor proteins, which once inserted into the cell membrane undergo extracellular domain cleavage to release the soluble ligand that is capable of binding ErbB receptors (Singh, Carpenter, and Coffey 2016; Singh and Coffey 2014; Schneider and Yarden 2014).

These ligands can be subdivided according to their affinity: high-affinity EGFR ligands, such as EGF, TGFα and HBEGF, induce a strong but transient signal, as high-affinity ligand-EGFR binding induces rapid internalization and degradation of the EGFR by negative-feedback (Zaiss et al. 2013; 2015). Subsequent signalling is 'oscillatory' (Shankaran et al. 2009), and typically would result in cell proliferation.

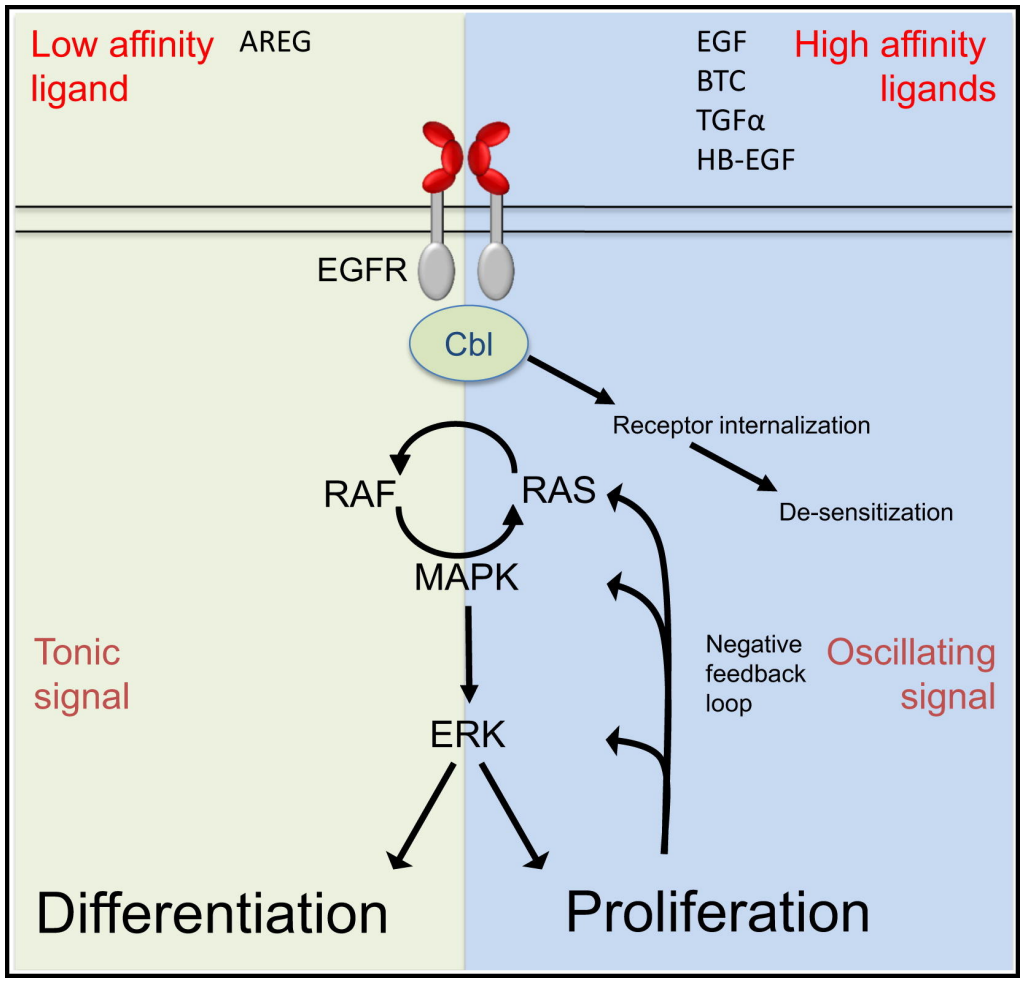

Figure 3-1 Illustration of the differing outcomes when EGFR is bound to a high-affinity ligand (e.g. HBEGF) as opposed to a low-affinity ligand (AREG). Reproduced with permission from (Zaiss et al. 2015)

3.4.1 Amphiregulin is a weak-affinity EGFR ligand which functions as a type 2 cytokine

In contrast to the above, Amphiregulin (AREG) activates in a more sustained, tonic manner, due to a point mutation in the EGFR binding site leading to weaker ligand-EGFR binding, and subsequent weaker activation of the receptor (Zaiss et al. 2015; 2013; Zaiss et al. 2006; Chen et al. 2012; Solic and Davies 1997). Subsequent signalling is more tonic and sustained, which does not promote internalisation and destruction of the ligand-EGFR complex, but instead promotes cell activation/differentiation (Stern, Place, and Lill 2008; Zaiss et al. 2015). Though AREG displays a preference for ErbB1/ErbB1 homodimers (i.e. the EGFR), or for ErbB1/ErbB2 heterodimers, it has, surprisingly, also been shown to work via ErbB3/4 in an oncology model (Mahtouk et al. 2005).

AREG is classified as a type 2 cytokine, whose main functions are to promote tissue integrity and promote tolerance to pathogens, so as to enable tissue repair and prevent loss of function (Zaiss et al. 2015; Zaiss et al. 2006). AREG is constitutively expressed by a variety of epithelial and mesenchymal tissues (Berasain and Avila 2014), but notably also in several types of leukocyte, including dendritic cells, ILC2s, Plasma cells, neutrophils, eosinophils, basophils and mast cells in response to a variety of inflammatory stimuli (Zaiss et al. 2006; Bles et al. 2010; Monticelli et al. 2011; Adib-Conquy et al. 2008; Matsumoto et al. 2009; Wang et al. 2005; Mahtouk et al. 2005;

Zaiss et al. 2013). In addition to the above, AREG has also been isolated from murine cytotoxic T cells in response to TGFβ, Prostaglandin E_2 or IGF-1 signals (Qi et al. 2012; Zhou et al. 2012). TH2 cells also produce AREG upon TCR stimulation (Qi et al. 2012; Zaiss et al. 2006). Finally, an IL-33R-positive subset of tissue-residential Tregs can also produce AREG (Burzyn et al. 2013).

AREG has been studied in association with several inflammatory states, including asthma, cancer, and acute and chronic infection (Monick 2004; Zaiss et al. 2006). AREG can also affect tissue repair in unexpected ways: tissue macrophages release AREG after detecting tissue damage, which stimulates EGFR on pericytes (myofibroblast precursor cells). These cells in turn activate integrin-αV complexes on target cells, which cleave latent TGFβ to its active form; TGFβ then gives the pericytes a differentiation signal, maturing them into myofibroblasts, which aids in the restoration of tissue barrier function (Minutti et al. 2019).

Interestingly, AREG appears to have different effects in acute and chronic infections: for example, RSV promotes MMP-mediated cleavage of pro-AREG to free AREG, which in turns activates EGFR in a paracrine manner; this promotes local cell survival in the short-term, and so improves virus proliferation (Monick 2004). However, in the helminth infection *Trichuris muris*

Areg$^{-/-}$ mice had significantly reduced clearance rates at D14 postinfection, indicating that AREG was crucial to TH2-mediated clearance of the parasite (Zaiss et al. 2006). AREG-EGFR stimulation is also required for IL-33 mediated release of IL-13 from TH2 cells, which contributes to the expulsion of the gastric helminths *Heligmosomoides polygyrus* and *Nippostrongylus brasiliensis* (Minutti et al. 2017). Hence, AREG can be both beneficial and damaging to the parasite depending on the nature of infection.

AREG in particular appears to be a prominent EGFR signal for regulatory T cells; total deletion of AREG in *Listeria* infection resulted in enhanced production of antigen-specific CD4 T cells (Zaiss et al. 2013), and further work with an *in-vivo* colitis model showed that activated Mast cells upregulate AREG production, and this was required for optimal Treg function. As well as promoting Treg activation, AREG could also be promoting the integrin-αV mediated conversion of inert to active TGFβ, which is known to be an important mechanism Tregs use to mediate their immunosuppressive function (Worthington et al. 2015).

4 Pathogens manipulate both EGFR signalling and regulatory T cells to facilitate their own survival and proliferation.

As pathogens have evolved alongside their host organisms, they have developed strategies both to aid their own proliferation and escape or minimise the host immune response. As both EGFR and T cells are strongly evolutionarily conserved, they are excellent candidates for manipulation by pathogens wishing to facilitate their own survival. A brief discussion of the evidence base in this field follows.

4.1 Manipulation of regulatory T cells

As Treg suppress the immune response to infection, they are an obvious target for manipulation by parasites. Consequently, there is evidence that many different pathogens include Treg activation/manipulation as a survival strategy.

4.1.1 Viruses

Viruses generally manipulate Tregs to decrease the effector T cell response to infection. However, it should be noted that with some acute infections such

as influenza and LCMV depletion of Tregs makes little difference, either because the environment is too proinflammatory or there are mechanisms for suppressing Treg induction/function in the context of acute infection (Veiga-Parga, Sehrawat, and Rouse 2013; Pasare and Medzhitov 2003).

Blood-borne viruses tend to be chronic, and so are obvious candidates for viruses that would wish to manipulate Tregs. Hepatitis C virus (HCV) expands Tregs using specific HCV peptides; this leads to a decrease in cytotoxic T cell activity, as evidenced by IFNγ production (Dietze et al. 2011; Li et al. 2008). Interestingly, a subset of chronic HCV-infected patients have decreased levels of Treg in their blood, and are more prone to developing mixed cryoglobulinaemia, an autoimmune B cell disorder, indicating that Treg are also benefitting the host despite being induced (in part) by the virus (Boyer et al. 2004).

Hepatitis B virus (HBV) carriers and chronic active HBV patients also display high levels of circulating Treg, though whether this is induced by the virus or a host immunotolerant response is unclear (Yang et al. 2007). Treg suppressive activity correlated with impaired viral clearance and higher HBVDNA levels in plasma. This was especially the case for HBV carriers who have detectable levels of ‘e’ antigen in their plasma, who are known to have higher numbers of Treg in peripheral blood samples. Yang and colleagues showed that higher Treg levels correlated with higher levels of

TGFβ, and hypothesised that this was driving Treg conversion from naïve CD4 T cells.

HIV is a lifelong infection, and is known to induce Treg-mediated immunosuppression separately to its effects on the CD4 T cell population (Dietze et al. 2011); HIV antigens induce Treg proliferation, and subsequently T cell responses (cytotoxic and noncytotoxic, including IFNγ production) are suppressed (Li et al. 2008). HIV can also induce/expand Treg indirectly through infection of dendritic cells (DC), promoting an immature DC phenotype; immature DCs are more likely to promote naïve CD4 T cells to differentiate into Treg (Li et al. 2008).

In the murine Friend Virus infection model Tregs are induced to proliferate by the virus in an organ-specific manner (Zelinskyy et al. 2009), and depletion of Tregs leads to an increased effector T cell response and long-term suppression of viral load, likely due to increased cytotoxicity and IFNγ production (Li et al. 2008; Dietze et al. 2011).

Finally, HSV appears to decrease T cell migration and activation, acting via activated Tregs; this prolongs the duration of infection, but also appeared to reduce TH1-mediated corneal damage in a HSV keratitis model (Sehrawat et

al. 2008; Li et al. 2008). Hence, Treg responses in viral infections can benefit the host by reducing tissue damage, at the expense of prolonging the infection.

In addition to the above, some viruses attempt to mimic the immunosuppressive effects of Tregs by encoding for homologues of IL-10, termed vIL-10; these proteins have been identified by members of the Herpesviridae, Alloherpesviridae and Poxviridae families (though not Vaccinia virus) (Ouyang et al. 2014). These display variable sequence homology to the host IL-10, but have suppressive effects that are beneficial to the virus; human CMV, for example, encodes a vIL-10 with little sequence homology to human IL-10, but binds with equal efficacy, and induces IL-10 production in dendritic cells, macrophages and monocytes, and polarises macrophages towards an M2 phenotype (Rojas et al. 2017). A latent form of vIL-10 also contributes to CMV viral latency. EBV vIL-10, by contrast, appears to be important in acute infection only; it is 92% homologous to human IL-10, but binds IL-10R with much less affinity; this results in signalling which reduces production of proinflammatory cytokines, but not the stimulation of thymocytes and mast cells, as well as polarisation of macrophages to an M2 phenotype (Rojas et al. 2017; Jog et al. 2018).

In contrast to the above, Cowpoxvirus appears to induce the expression of host IL-10 (*in-vitro* work suggests possibly from dendritic cells or macrophages), which has an immunosuppressive effect; compared to intranasal infection with vaccinia virus, Cowpoxvirus-infected mice had more than double the amount of soluble IL-10 in bronchoalveolar lavage samples, and fewer numbers of dendritic, CD4 and CD8 T cells in lung samples, and IL-$10^{-/-}$ mice were more susceptible to reinfection with Cowpoxvirus (Spesock et al. 2011). Hence, viruses can induce Treg-style suppression either by use of viral IL-10 homologues or by induction of host IL-10.

4.1.2 Helminths

Many helminth infections appear to be associated with an expansion of Treg populations. This can be because of a response to chronic infection from the host, or as part of a deliberate strategy from the parasite to generate an immunosuppressive environment. There is evidence of an expansion of Treg populations in infections with *Heligmosomoides polygyrus*, *Trichinella spiralis*, and *Schistosoma mansoni,* amongst others (McSorley et al. 2008).

Additionally, a number of helminths produce TGFβ analogues, which in turn expand Treg populations and generate an immunosuppressive environment: the trematode *Schistosoma mansoni* egg antigen induces Treg formation from naïve CD4 T cells in a TGFβ -dependent manner, which contributes to

generating a locally immunosuppressive environment in the host (Zaccone et al. 2009).

The human filariasis *Brugia malayi* promotes Treg proliferation by the secretion of a retinoic acid analogue, which synergises with TGFβ to induce Treg expansion (McSorley et al. 2008), and also secretes a TGFβ analogue termed TGH-2, which ligates the mammalian TGFβ receptor and suppresses T cell responses (Gomez-Escobar, Gregory, and Maizels 2000). Treg are induced and recruited to the site of *B.malayi* infection; notably, asymptomatic carriers have higher amounts of circulating IL-10 than controls, implying a role for Treg in parasite tolerance. *Litomosoides sigmodontis* also appears to produce a secretory product that promotes Treg expansion by stimulating TGFβ signalling, but this secreted product was not amenable to neutralisation by anti-TGFβ antibody (Hartmann, Schramm, and Breloer 2015).

Finally, the murine helminth *Heligmosomoides polygyrus* produces a TGFβ mimic several times larger than the TGFβ molecule itself, called TGM (Grainger et al. 2010; Maizels, Smits, and McSorley 2018).

A summary of the different pathways of Treg manipulation by the above pathogens is given below:

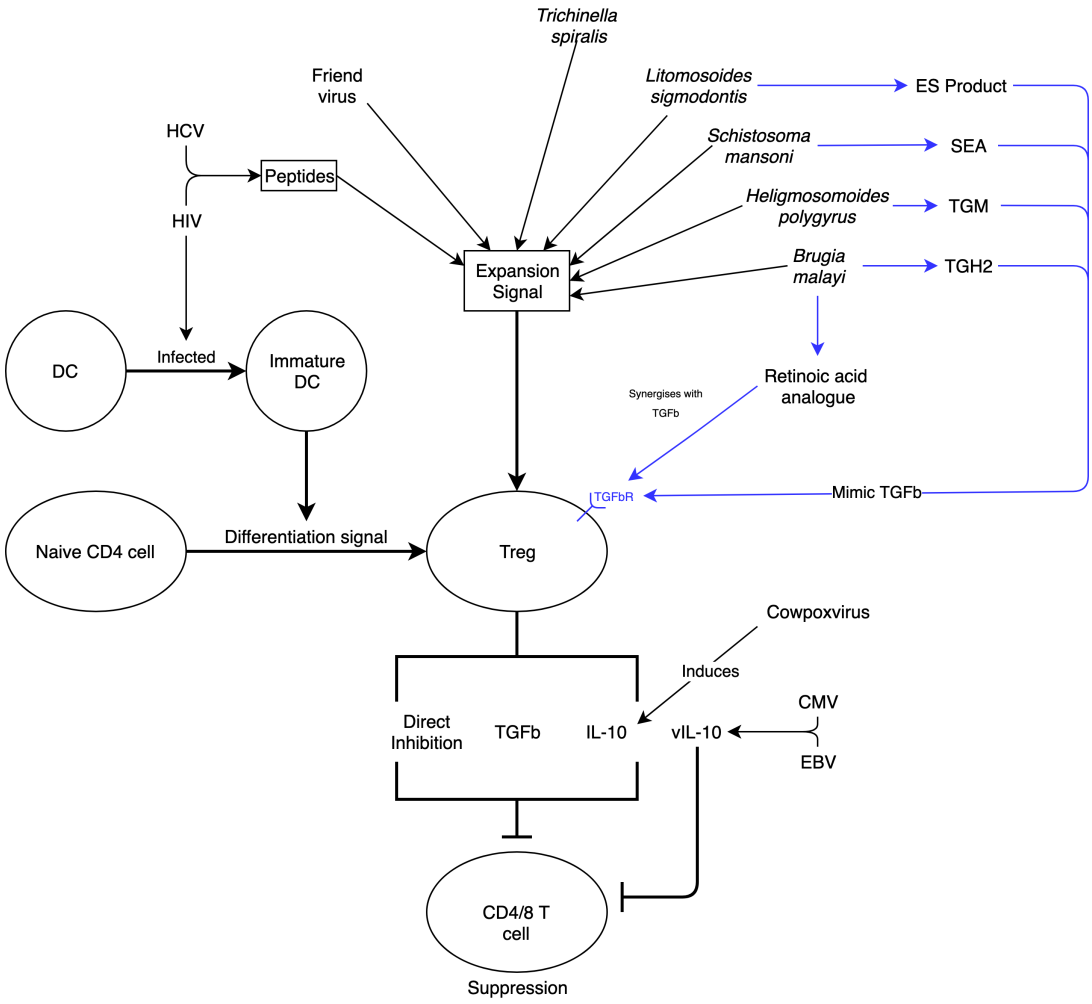

Figure 4-1: Treg manipulation by viruses and helminths. As well as nondefined expansion signals, particular methods of Treg expansion are described, including viral IL-10 (vIL-10) production, IL-10 induction, immature dendritic cell formation postinfection with HIV, and manipulation of the TGFβ pathway through various secreted products by helminth worms. HCV, Hepatitis C virus; HIV, Human immunodeficiency virus; DC, dendritic cell; TGFβ, TGF beta; CMV, cytomegalovirus; EBV, Epstein-Barr virus; TGFβR, TGF beta receptor; TGH2, TGFβ homologue 2; TGM, TGFβ mimic; SEA, Schistosomal Egg Antigen; ES product, Excreted-Secreted product.

4.2 Manipulation of EGFR signalling

4.2.1 Viruses

Viruses have been shown to use EGFR signalling to promote their own survival (Zheng, Kitazato, and Wang 2014). Many of these have been shown to use EGFR as an attachment point to facilitate entry into the cell, but others have phenotypic effects beyond this, and still others act through promoting the release of EGFR ligands (including pathogen-derived EGF homologues).

Influenza A virus (IAV) haemagglutinin, for example, binds sialic acid residues on the cell surface, which leads to lipid clustering and raft formation. Co-localisation of EGFR monomers in these rafts (along with other receptors) leads to their dimerization and activation, resulting in virion internalisation (Eierhoff et al. 2010). Notably, infection of epithelial cells promoted excretion of AREG and TNFα, and IAV binding onto the cell surface resulted in upregulated ERK, PKC and PI3K signalling. Increased production of the mucin MUC5AC was dependent on activation of these pathways (Barbier et al. 2012; Eierhoff et al. 2010).

Epstein-Barr Virus (EBV) protein LMP1, traditionally described as a constitutively active TNFα analogue that enables transformation of B cells to apoptosis-resistant host cells, also has effects on EGFR signalling; LMP1

activates PKCδ, which in turn generates a signalling cascade involving STAT3, Bcl-3 and NF-κB to upregulate expression of EGFR on the target cell. At the same time, PKCδ directly upregulates ERK signalling, and mildly upregulates epiregulin production. Thus, stimulation of EGFR-ERK signalling by LMP1 promotes cell survival, and directly contributes to the oncogenicity of EBV (Kung, Meckes, and Raab-Traub 2011; Miller, Earp, and Raab-Traub 1995; Pratt, Zhang, and Sugden 2012).

Respiratory Syncytial Virus (RSV) upregulates EGFR ligands rather than the receptor: the virus contains proteins that promote MMP-mediated cleavage of membrane-bound AREG to the soluble form; AREG then activates EGFR-ERK signalling to promote infected cell survival (Monick 2004).

Cytomegalovirus (CMV) envelope glycoprotein B (gB) binds EGFR (and possibly also PDGFR), triggering internalisation of the receptor (and so also the virus) (Monick 2004; Wang et al. 2003; Soroceanu, Akhavan, and Cobbs 2008). However, gB activates EGFR differently in different cell types: in fibroblasts and trophoblasts the activation signal is more oscillatory, whereas in epithelial cells or monocytes the stimulation is more tonic (Chan, Nogalski, and Yurochko 2009). This results in different behaviours from the host cell: monocytes, for example, differentiate into a mobile, proinflammatory, macrophage-like phenotype which aids viral spread to other tissues (Chan,

Nogalski, and Yurochko 2009). This is not seen when epithelial cells are infected. Therefore, CMV does not just use EGFR as a means of cell entry, but also as a way of promoting cross-infection of tissues; chronic CMV infection also leads to upregulation of EGFR expression on the host cell (Melnick, Deluca, et al. 2013). Furthermore, CMV can induce AREG secretion, and subsequent EGFR-ERK signalling, by activating NFκB; downstream ERK signalling was in fact essential for pathogenicity in a submandibular gland model of disease (Melnick et al. 2011). Treatment of CMV-infected cells with EGFR inhibitors results in partial rescue, which can be improved to full rescue when combined with aciclovir (Melnick et al. 2011; Melnick, Sedghizadeh, et al. 2013), and pre-treatment with EGFR inhibitors in-vitro reduces viral entry into cells by 50% (Chan, Nogalski, and Yurochko 2009).

Rhinovirus appears to manipulate EGFR-ERK signalling to facilitate spread; Rhinovirus dsRNA stimulation of TLR3 upregulates the EGFR ligands AREG and TGFα, which in turn stimulate EGFR-ERK signalling and mucin expression via an autocrine/paracrine loop (Zhu et al. 2009).

Herpes-simplex virus (HSV) also uses EGFR-PI3K-ERK signalling to indirectly trigger viral entry; binding of HSV-1 envelope activates EGFR-PI3K-

ERK, leading to cofilin phosphorylation and F-actin polymerization, lipid raft clustering and subsequent virus internalisation (Zheng et al. 2014).

There is some evidence that chronic viral infections also utilise EGFR signalling: Hepatitis C virus replication is improved in the presence of bile salts; it appears that bile salts promote EGFR-ERK signalling, which leads to HCV-infected cells entering S-phase, aiding their survival; furthermore, blocking this signalling pathway either at the level of EGFR or ERK inhibited HCV replication, and re-established the antiviral effects of IFNα (Patton, George, and Chang 2011).

Poxviruses are known to produce soluble EGFR ligands, but this will be discussed in chapter 2.

4.2.2 Bacteria

Bacteria have also evolved strategies to manipulate EGFR signalling, typically by increasing the availability of EGFR ligands to the target cell.

Helicobacter pylori is a gram-negative bacteria that infects the gastric mucosa. It increases EGFR-ERK signalling by promoting MMP-mediated

cleavage of membrane-bound AREG and HBEGF to their free forms, which then act in a paracrine/autocrine manner (Romano et al. 1998; Keates et al. 2001). *H.pylori* also upregulates EGFR expression in infected cells, presumably in order to maximise the cell's response to EGF ligands (Keates et al. 2007; Hardbower et al. 2016). EGFR stimulation has an antiapoptotic effect on the host cell, which favours parasite survival but is also implicated in the generation of gastric epithelial neoplasms (Yan et al. 2009).

Haemophilus influenzae produces an EGF analogue that directly activates EGFR-ERK signalling, which amongst other effects downregulates TLR2 expression, thereby limiting the innate immune response to the host cell (Mikami et al. 2005).

Chlamydia species are obligate intracellular bacteria that have been known to exploit EGFR: The *Chlamydia pneumoniae* invasin protein PMP21 attaches to EGFR, and modification of EGFR reduces both the amount of adhesion and bacterial cell internalisation. Blockade of either EGFR or ERK with monoclonal antibodies had no effect on attachment but abrogated internalisation, implying that *C.pneumoniae* uses EGFR as a cell entry mechanism (Mölleken, Becker, and Hegemann 2013). *Chlamydia trachomatis*, the causative agent of trachoma, attaches to EGFR when in their sporoid infectious form (termed Elementary Bodies), and triggers

phosphorylation of tyrosine residue pTyr1173, with downstream signalling via PLC-γ1, Akt and STAT5 (Patel et al. 2014).

Neisseria species recruit a range of ErbB monomers, and it is noteworthy that ErbB2 monomers accumulate underneath the attachment point of *N.meningitidis*, and that HER2 inhibition prevents cell entry (Hoffmann et al. 2001). Either *N.meningitidis* is 'riding in' on an internalisation signal brought about by HER2 dimerisation and autophosphorylation, or it is itself attaching to HER2 in a ligand-like fashion. On top of this, *N.meningitidis* promotes HBEGF release from infected cells, which then activate EGFR and ErbB4 receptors (Slanina et al. 2014). *N.gonorrhoea* recruits EGFR and ErbB monomers underneath its attachment point, and once entered upregulate production of HBEGF, AREG and TGFα, which presumably act in a paracrine/autocrine manner (Swanson et al. 2011).

Pasteurella multocida secretes a dermatonecrotic toxin responsible for much of its virulence. This toxin appears to activate intracellular Gq/11 protein, which in turn can intracellularly activate EGFR-ERK signalling, which has a mitogenic effect on the host cell (Seo et al. 2000).

Pseudomonas aeruginosa is an important human pathogen of the respiratory and urinary tract; some strains create biofilms, which help the pathogen 'hide' inside host mucus in the lungs and provide an optimal environment for the bacteria (Kohri et al. 2002). MMP and TACE activity is increased in *Pseudomonas*-infected cells, leading to increased 'shedding' of HBEGF and TGFα, leading to EGFR-ERK/PI3K signalling, and ultimately delayed apoptosis in the target cell (Zhang et al. 2004; Burgel and Nadel 2004). *Pseudomonas*-mediated EGFR-ERK signalling also increases MUC5AC production from lung epithelial cells, resulting in mucin hypersecretion (Kohri et al. 2002; Burgel and Nadel 2004).

Finally, *Salmonella enterica* use EGFR as a secondary invasion mechanism: Rck binds EGFR tightly and triggers internalisation (Wiedemann et al. 2016). Historically, *S.typhimurium* has also been shown to enter epithelial cells in an EGFR-dependent manner (Galán, Pace, and Hayman 1992).

4.2.3 Protozoans (Toxoplasma)

There is some (limited) evidence for EGFR manipulation by protozoa also: Toxoplasma infects epithelial and microglial cells and appears to use micronemal proteins (containing EGF domains) to stimulate EGFR-Akt signalling. This signalling reduces the chances of lysosome fusion with the parasite's vacuole, thus aiding its survival (Muniz-Feliciano et al. 2013).

5 Summary

Based on the above data, we observed that EGFR and regulatory T cells are common targets for exploitation by pathogens. It is also established that EGFR is expressed on Treg both at rest and when activated. Whether pathogens exploit Treg through direct manipulation of EGFR signalling, or if endogenous Amphiregulin affects Treg function in the context of infection, is not clear. My thesis will aim to answer these questions using virus and helminth models to examine EGFR-Treg interactions in both acute and chronic infections.

6 Hypothesis

We hypothesise that regulatory T cells can be activated by EGFR signalling, either from endogenous or pathogen-derived ligands, and that this will affect Treg function *in-vivo*.

Chapter 2: Vaccinia Virus Growth Factor activates regulatory T cells through the Epidermal Growth Factor Receptor as a method of immune escape

7 Abstract

Poxviruses such as Vaccinia Virus (VACV) encode soluble growth factors such as Vaccinia Growth Factor (VGF), which work by activating the Epidermal Growth Factor Receptor (EGFR) on epithelial cells to encourage cell proliferation, ultimately promoting spread of the virus. Whether there is an interaction between VACV-derived VGF and regulatory T cells (Treg) via the EGFR has remained unknown. Here we show that VGF enhances the suppressive capacity of EGFR-expressing Treg.

Using an *in-vitro* Treg suppression assay, we show that UV-inactivated virus (which cannot replicate, though should still express early genes such as VGF) can induce Treg activity, measured as proliferation of cocultured effector T cells. Coculturing effector T cells and VACV without Treg had no effect on proliferation, and Treg suppressive capacity was not increased upon exposure to a strain of VACV which does not express VGF.

Furthermore, mice with Treg deficient for EGFR (*Egfr*$^{fl/fl}$ *x FoxP3*^{cre}) were more resistant to VACV infection, with less weight loss, more cellular lung infiltrate, and lower lung viral titres at D7 postinfection compared to wildtype C57BL/6. These findings correlated with a lower level of bioactive TGFβ in bronchoalveolar lavage supernatant.

These data reveal a novel mechanism by which VACV creates a local immunosuppressive environment as a method of immune escape, i.e. through the VGF-EGFR mediated activation of Treg.

8 Introduction

8.1 Poxviruses

Poxviruses are large enveloped DNA viruses, which are characterised by linear dsDNA of length 150-300kbp, a cytoplasmic site of DNA replication, large size and complex internal structure (Fields et al. 2013).

Poxviruses are divided into those with vertebrate (Chordopoxvirinae) and invertebrate hosts (Entomopoxvirinae). Of the former, Orthopoxviruses are the commonest studied genus, as it includes several human pathogens of importance, including Variola virus (VARV), Vaccinia virus (VACV), Cowpox (CPXV) and monkeypox. VARV and molluscum contagiosum virus are obligate human pathogens, but the remainder are zoonoses that infect humans to varying degrees (Fields et al. 2013). Of the above Variola virus, the causative agent of Smallpox, has had the most substantial effect on the human population due to its lethality on the general population, children in particular (Jacobs et al. 2009; Smith 2011). It was a major burden of disease up until its eradication through the use of mass-vaccination programmes (using Vaccinia virus and, to a lesser extent, cowpoxvirus), and remains a potential agent of bioterrorism, as most of the world's population are now not vaccinated, and therefore susceptible (Jacobs et al. 2009; Smith 2011; Yang

et al. 2005; Langhammer et al. 2011; Clark 2006; Vermeer et al. 2007). Of all orthopoxviruses the most heavily studied is Vaccinia virus.

8.2 Vaccinia

8.2.1 History

Historically, immunisation against smallpox was conducted by variolation, which involved transdermal inoculation with infected smallpox tissue taken from pox lesions of patients. Though less lethal than the disease itself (1-2% vs 20-30%), it still resulted in significant mortality (Smith 2011). Jenner's development of the procedure of vaccinating individuals with samples of cowpox virus was much less lethal, produced only mild symptoms in vaccine recipients, and was similarly efficacious. The practice slowly supplanted variolation in the 19th century, and smallpox vaccination slowly became a standard preventative healthcare measure, eventually resulting in the worldwide eradication of endemic smallpox by 1980 (Jacobs et al. 2009; Smith 2011).

With the advent of genetic testing, it became clear that smallpox vaccine was derived not only of cowpox, but also a separate viral species, which was termed Vaccinia virus (VACV). Subsequent gene sequencing has demonstrated that these viruses are significantly different from one another (Fields et al. 2013; Li et al. 2006). The original host of VACV is not currently

known, though it is theorised that Jenner's original vaccine was derived from horsepox lesions rather than cowpox; there is some genetic evidence to support this (Smith 2011; Huygelen 1996; Schrick et al. 2017).

The means by which two viruses were used for vaccination against smallpox is unclear, but following this discovery purified Vaccinia virus was chosen as the agent of choice, due to its low pathogenicity (Jacobs et al. 2009). Due to its ubiquity, use as a vaccine and relative safety (compared to Smallpox), Vaccina virus has been used for research in preference to other orthopoxviruses, and so has become the 'default' for study.

8.2.2 Structure

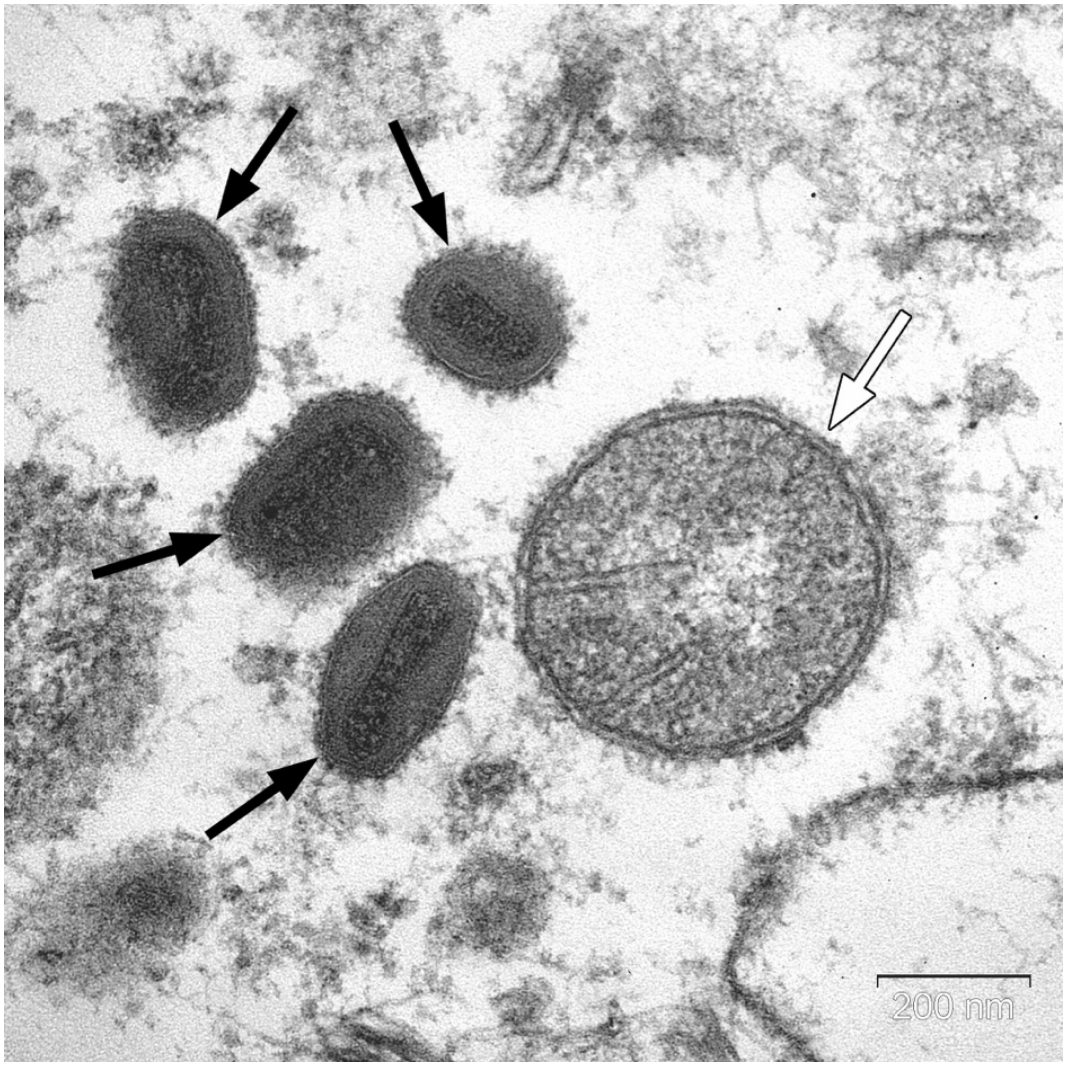

Figure 8-1 Scanning Electron Micrograph showing mature VACV virions (dark arrows) in the cytoplasm of a human carcinoma cell. Light arrow shows a mitochondrion. Note internal double-concave structure of capsid. VACV virions rival intracellular organelles in size, and are the largest viruses discovered. Licensed from ZE Vladimirovich, distributed under CC-ASA 4.0 license, available here: https://commons.wikimedia.org/wiki/File:Vaccinia_virus_particles.jpg

VACV virions are noted for their complex internal structure, and individual particles approach 300nm in size (Fields et al. 2013). DNA is arranged linearly alongside several proteins in a nucleosome, contained within a protein core (the double-concave internal structure seen in Figure 8-1).

Internal structure is revealed in Figure 8-2. Outside the virus core are 2 proteinaceous lateral bodies, which contain a variety of viral factors which modify host cell function and optimise the intracellular environment for virus replication (Bidgood and Mercer 2015). Surrounding this is a lipid bilayer which contains both host and virus-derived proteins (Moss 2016; Chung et al. 2006; Yoder et al. 2006; Resch et al. 2007). The origin of this is not quite settled on, but likely derives from the endoplasmic reticulum (Moss 2015). On the surface of this are a variety of viral proteins (Moss 2016), as well as host proteins acquired along with the membrane (Resch et al. 2007).

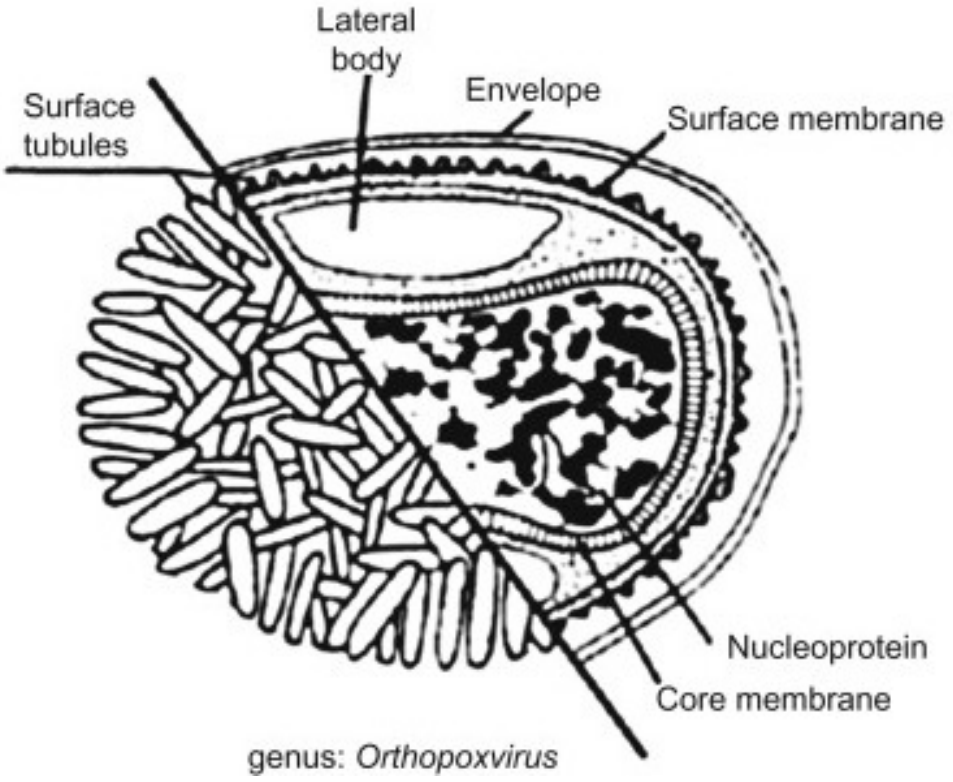

Figure 8-2 Internal structure of Vaccinia virus. Image from (Fields et al. 2013)

There are several types of virion: Intracellular mature virions (IMV) are as described above: They make up 98-99% of virus particles, remain in the cell, are released on cell lysis and are responsible for host-host transmission (Moss 2012; Smith, Vanderplasschen, and Law 2002; Harrison et al. 2016). The remaining 1-2% are cell-associated enveloped virions (CEV) or extracellular enveloped virions (EEV). These acquire 2 more membranes, likely by manipulation of retrograde cellular transport pathways (Harrison et al. 2016; Pechenick Jowers et al. 2015), to become intracellular enveloped virions (IEV). This appears to be determined by just a few viral proteins (A27, B5 & F13), as deleting these genes stops the formation of IEVs (Bidgood and Mercer 2015). The outer membranes appear to also integrate a number of host proteins that have an effect on the virus' virulence; purified EEVs express human proteins CD45, CD55, CD59, CD71, CD81 and MHC-I, and are resistant to complement-mediated lysis (as compared to EEVs generated & purified from a rat cell line which does not contain human CD55/CD59) (Vanderplasschen et al. 1998). Travelling to the cell surface, virions exit the cell by fusion of the outer (3rd) membrane with the plasma membrane (Smith, Vanderplasschen, and Law 2002). If the virion remains attached to the cell surface these are termed CEVs, and are implicated for local cell-cell transmission via the formation of actin 'tails' (Smith, Vanderplasschen, and Law 2002; Harrison et al. 2016). CEVs that leave the cell surface are termed Extracellular Enveloped Viruses (EEVs) and spread in a paracrine fashion to other cells. EEVs are hypothesised to be the main method for in-host dissemination, as a) antibodies targeting EEV are more effective than those

targeting IMV; b) EEV are relatively resistant to the effects of antibodies and complement, and c) VACV strains that do not produce EEVs cannot replicate *in-vivo* (Roberts and Smith 2008).

Once a CEV/EEV encounters an uninfected cell an interaction with glycosaminoglycans disrupts the outer (2^{nd}) membrane to 'reveal' the inner (Moss 2012). The virion enters the cell either by direct fusion with the cell membrane or an acidified endosome following macropinocytosis (NB: there is some evidence that Western Reserve strain of VACV favours endosomal entry (Townsley et al. 2006)). There are 4 attachment proteins, which bind chondroitin, heparan and laminin on the cell surface, and an Entry Fusion Complex composed of 11 fusion proteins, that facilitate the viral core's entry into the cytoplasm (Moss 2016).

8.2.3 Replication

Once inside the host cell, the viral core travels to a juxtanuclear position within the cytoplasm. From here it will 'breach', releasing viral DNA into the cytoplasm; this area will become the "virus factory". At this point early genes are transcribed using pre-existing viral factors and produce proteins essential for DNA/RNA replication and synthesis of intermediate genes. Intermediate and late genes occur post-replication and are transcribed from progeny DNA

(Fields et al. 2013; Moss 2013). Intermediate genes facilitate late gene expression, DNA packaging and the construction of core-associated proteins; late genes encode transcription factors (that will be packaged into new virions) and mature virion membrane proteins, including attachment proteins and the Entry Fusion Complex.

Following viral assembly, naked virions are enveloped in one membrane (the source of which is controversial, but likely derived from modified endoplasmic reticulum) to become intracellular mature virions (Moss 2015; Smith, Vanderplasschen, and Law 2002).

8.3 Vaccinia Growth Factor

Of the roughly 200 genes encoded by VACV, almost half are not involved in viral replication, and are immunomodulatory (Clark 2006). Many of these target the immune system, aiming to thwart the host response to infection. These include various inhibitors of complement (Vaccinia Complement Protein), Interferon (various), NF- κB (various), and numerous cytokines such as IL-1, 18, TNF, chemokines and the apoptotic Bcl-2 proteins (Fields et al. 2013; Smith et al. 2013; Becker 2003). For an excellent review of these, see (Smith et al. 2013).

Vaccinia Growth Factor is a small, soluble, heavily glycosylated protein composed of 77 amino acids that has considerable sequence homology to Epidermal Growth Factor (EGF) and Transforming Growth Factor alpha (TGFα) (Stroobant et al. 1985; Kim et al. 1995), as well as 95% sequence homology to the closely related Smallpox Growth Factor (SPGF) (Kim et al. 2004). It is the product of the C11R gene, which is contained in the inverted terminal repeat sequences at either end of the VACV genome (though some strains contain only one copy) (Buller et al. 1988; Kim et al. 2004; Lai and Pogo 1989; Martin, Harris, and Shisler 2012). An early gene product, it is secreted 2-8 hours postinfection (Beerli et al. 2019), after viral uncoating but *before* viral replication occurs (Buller et al. 1988).

Early reports stated that VGF was found in the medium of VACV-infected cells in-vitro, leading to the assumption that VGF was excreted from infected cells (Stroobant et al. 1985; Kim et al. 1995). Further characterisation of this has revealed that after secretion to the cell surface, a 25kDa precursor form is cleaved by ADAM10 to a 22kDa soluble form that then acts in a paracrine/autocrine manner (Beerli et al. 2019; Chang et al. 1988). This is remarkably similar to the extracellular cleavage processing undergone by native ErbB ligands, particularly EGF and betacellulin, which are also cleaved by ADAM10 (Singh and Coffey 2014; Singh, Carpenter, and Coffey 2016).

In contrast to other poxviral growth factors, but not SPGF, VGF binds preferentially to EGFR, and at a much lower affinity than EGF (Tzahar et al. 1998; Kim et al. 2004). Following this, downstream signalling occurs via the MAP kinase pathways MEK/ERK, as well as PLC-γ1 and NF-κB. These signals result in host cell proliferation, survival and motility, even before viral replication has occurred in the host cell (Postigo et al. 2009; Beerli et al. 2019; Buller et al. 1988; Kim et al. 1995; Andrade et al. 2004; Prenzel 2001). Additionally, VGF has been shown to synergise with other signals, such as the viral antiapoptotic protein F1L, and promote expression of the mitotic gene *egr-1* in host cells (Postigo et al. 2009; Andrade et al. 2004). Proliferation can even be induced in uninfected cells, demonstrating that VGF acts in a paracrine as well as autocrine manner (Buller et al. 1988). Deletion of VGF results in reduced downstream activation (particularly ERK), resulting in suboptimal viral proliferation, virulence, and replication in-vitro (particularly resting cells) and *in-vivo* (Buller et al. 1988; Andrade et al. 2004; Lai and Pogo 1989).

At one time EGFR was proposed as a receptor used for entry into host cells, but this has been rejected as further research clarified the structure and function of the proteins comprising the attachment proteins and entry fusion complex (Lai and Pogo 1989; Moss 2016; Townsley et al. 2006; Marsh and

Eppstein 1987). Poxviruses can also enter EGFR-deplete cell lines in-vitro, though it should be noted that growth factor-mediated activation of EGFR seems to be required for optimal poxvirus cell entry (Buller et al. 1988; Stroobant et al. 1985).

Upon exposure to VGF several behavioural changes are evident in epithelial cells: cell proliferation and motility are increased, resulting in rapid growth and dehiscence from the epithelial basement membrane, leading to the characteristic ‘pox’ lesions (Beerli et al. 2019; Buller et al. 1988; Tzahar et al. 1998). in-vitro viral plaques are smaller in VGF-deplete mutants, likely due to reduced motility of infected cells (Beerli et al. 2019; Yang et al. 2005).

8.3.1 Vaccinia virus blocks intracellular cytoplasmic DNA sensing to improve survival

Previous work has shown that poxviruses manipulate ErbB receptors to facilitate their own survival: cytosolic DNA is a pathogen-associated signal, recognised by several intracellular pattern-recognition receptors, including DNA-dependent Protein Kinase (DNA-PK) and cyclic GMP-AMP Synthase (cGAS). Following recognition of this DNA, these proteins trigger the phosphorylation of STING (STimulator of IFN Gene), an endoplasmic reticulum-bound receptor that in turn activates Tank-Binding Kinase 1

(TBK1). TBK1 phosphorylates Interferon Regulatory Factor 3 (IRF3), which controls the expression of Type 1 interferons; these are deleterious to the virus (Dai et al. 2014; Ferguson et al. 2012; Liu et al. 2015).

Several viruses produce proteins which interfere with STING function, including CMV, Human Papillomavirus and Dengue (Liu et al. 2015). Poxviruses do this also: VACV protein C16 inhibits IRF3 activation by disrupting dsDNA recognition by DNA-PK (Peters et al. 2013). It has also been observed that expression of type 1 interferons is reduced in VACV-infected cells, together with reduced levels of STING phosphorylation and dimerization (which are prerequisites for downstream signalling). This signal is also seen even in the related poxviruses Cowpoxvirus and Ectromelia virus, as well as a C16-deficient strain of VACV, (Liu et al. 2015; Georgana et al. 2018). Cells infected with Modified Vaccinia Ankara (MVA, a highly attenuated strain of VACV which cannot replicate in human cells), on the other hand, exhibit activated IRF3, STING dimerization and phosphorylation. The mechanism by which non-MVA VACV produces this effect is unclear.

Recent work has demonstrated that HER2/neu, a member of the ErbB receptor family, can inhibit STING function: Wu et al. found that HER2 bound to STING, leading to its dissociation from TBK1 and inhibition of downstream expression of type 1 interferons (Wu et al. 2019). The mechanism by which

HER is internalised and co-locates with STING is unknown, but is triggered after detection of DNA by cGAS. This effect was not seen with other ErbB receptor family members, including EGFR, and in fact EGF-EGFR signalling somewhat potentiated DNA sensing. However, this mild EGFR-induced activation of cGAS–STING signalling is similar in the absence or presence of HER2, suggesting that ErbB1-ErbB2 heterodimers do not participate in STING regulation. Nonetheless, it is clear that ErbB receptor family members are involved in the regulation of the immune response to infection, and that blockade of ErbB signalling has the potential to aid or diminish pathogen survival.

8.3.2 Blockade of EGFR signalling in Vaccinia infection

Due to ongoing concerns regarding the use of Variola virus as a bioterrorism agent, research into antiviral treatments for poxviruses has been ongoing. Mass-vaccination of the human population is no longer viable for reasons of cost, and not an option for certain risk groups (e.g. immunocompromised, though vaccination with the attenuated strain Modified Vaccinia Ankara [MVA] could be used in these groups (Stittelaar et al. 2001)) as the vaccine consists of live virus (Kim et al. 2004; Langhammer et al. 2011). The only current treatment option is Cidofovir, which a) the virus can become resistant to, b) is only available intravenously, and c) causes renal impairment to a substantial minority of patients, requiring it to be coadministered with

probenecid and IV fluid to reduce nephrotoxicity (UpToDate 2019). As a Smallpox outbreak is a low probability but high impact event, this has driven further research into possible ways of counteracting poxvirus infections.

Deletion of VGF reduces virulence, and this has been used to 'temporise' VACV to enable its use as a vector for antitumour immunotherapy (McCart et al. 2001; Foy et al. 2016), and wound healing (Norton, Peplinski, and Tsung 1996). VGF-deplete VACV can be several orders of magnitude less infectious than wildtype counterparts (Lai and Pogo 1989). Therefore, some researchers have attempted to examine the effects of EGFR inhibition on viral proliferation and survival, *in-vitro* and *in-vivo*.

Poxviral EGFR ligands, such as SPGF, have been studied *in-vitro* using small molecule tyrosine kinase inhibitors (TKI) of EGFR: Yang and colleagues used the TKI CI-1033 (Canertinib, now discontinued) to examine the effects of EGFR blockade on SPGF-mediated cell activity *in-vitro*. They found reduced EGFR internalisation, downstream phosphorylation and cellular DNA synthesis (Yang et al. 2005). Secondary viral spreading in-vitro (on BSC-40 cells) was also inhibited. Following on from this, Langhammer et al. observed paracrine 'priming' of Hep2 cells *in-vitro* for subsequent infection when exposed to Vaccinia virus, and activation of EGFR-ERK signalling in infected cells. Application of the EGFR TKI Gefitinib abrogated this effect,

reducing EGFR phosphorylation at Tyrosine residue 1068, which led to reduced ERK signalling, smaller plaque size and number, and loss of the 'priming' effect in uninfected cells surrounding the plaque.

In-vivo, results have been more mixed. In 2004 Kim et al. examined the effects of SPGF-neutralising antibodies on VACV in an *in-vivo* pneumonitis model. They found the SPGF neutralising antibody 13E8 failed to reduce mortality or lung viral titre at D7 when used in isolation. However, when combined with the IMV-neutralising antibody anti-L1R there was enhanced clearance of the virus in association with augmented CD8 T cell responses (seen in spleen and lung) (Kim et al. 2004).

Following on from the above, Yang and colleagues examined the effects of the EGFR-blocking antibody CI-1033 (Canertinib) in an *in-vivo* VACV pneumonitis model; here, CI-1033 improved survival if given from the day of infection (out to D14), and increased T cell antiviral cytokine production. However, if given from D2 onwards, there was no effect on mortality unless again the drug was combined with anti-L1R antibody. Administration of CI-1033 from D2 onwards did, however, result in lower lung viral titres and stronger CD8 T cell responses (Yang et al. 2005).

Thus, it would appear that tyrosine kinase inhibitors of EGFR are effective *in-vivo* when compared to antibodies against poxviral growth factors, though overall the results are more muted when compared to *in-vitro* data.

8.3.3 Vaccinia and regulatory T cells.

Expansion and activation of regulatory T cells is a noted feature of multiple chronic viral infections: Hepatitis B and C are both associated with Treg expansion and resultant immunosuppression (though with HBV there is conflicting evidence) (Dietze et al. 2011; S. Li et al. 2008; Veiga-Parga, Sehrawat, and Rouse 2013), and HIV is also associated with Treg-mediated immunosuppression (Dietze et al. 2011). As these are chronic infections, it is perhaps not surprising that these pathogens have mechanisms to suppress the immune response long-term.

The evidence for acute viral pathogens manipulating Treg to their own benefit is less clear. Treg depletion using anti-CD25 antibody improves CD8 T cell response to VACV infection (Amoah et al. 2013), and it has been previously noted that Treg tend to expand by D5-6 postinfection, particularly if the virus burden is high. Additionally, in a MVA-OVA viral vector study of CD8 T cell response, Treg led to decreased expression of T cell costimulatory molecules CD80 & CD86 on dendritic cells, leading to a decrease in endogenous IL-2

production by antigen-specific T cells and a reduction in CD8 T cell expansion, which could be overridden by application of IL-2/antibody complexes (Kastenmuller et al. 2011). As CD8 T cells are the main method of control for Vaccinia infection, manipulating Treg to control CD8 T cells would be beneficial to the virus.

Bearing this in mind, it is possible that there is an indirect interaction between poxviruses and regulatory T cells, perhaps using their soluble EGFR-stimulating factors.

9 Hypothesis

We hypothesised that poxvirus-derived EGFR ligands could activate regulatory T cells via the EGFR, creating a locally immunosuppressive environment to aid virus survival.

10 Methods

10.1 Western Blot

10.1.1 Protocol

HaCaT cells (RRID: CVCL_0038) (Boukamp et al. 1988) were cultured in Iscove's Modified Dulbecco's Medium (IMDM) supplemented with 10% Fetal Calf Serum (FCS; South America, Gibco), 1% L-glutamine, 1% penicillin/streptomycin and 5 x 10^{-5}M 2-mercaptoethanol (hereafter termed "complete IMDM") and incubated at 37 ^{o}C in a humidified atmosphere at 5% CO2.

For experiments, HaCaT cells were seeded into 24-well plates at a concentration of 4 x 10^{5} cells/well and incubated (as above) in serum-free media overnight (i.e. otherwise "complete" IMDM **without** FCS). The following day wells were exposed to serum-free IMDM only (negative control), or serum-free IMDM containing either HBEGF 10ng/ml (positive control) or the virus of interest for 20 minutes. Following this, cells were placed on ice and lysed with 72μl NP40 lysis buffer (50 mM Tris-HCl [pH 7.6], 150 mM NaCl, 5 mM EDTA, 1% NP-40, 0.05% Sodium Azide) supplemented with protease inhibitors (Phenylmethylsulfonyl fluoride 200mM) and phosphatase inhibitors (Sodium fluoride 100mM and Sodium Orthovanadate 100mM) for 10 minutes. Lysates were then mixed with 18μl 5x Laemmli

loading buffer (60 mM Tris-Cl pH 6.8, 2% sodium dodecyl sulphate [SDS], 10% glycerol, 5% 2-mercaptoethanol, 0.01% bromophenol blue) for a total volume of 90μl, of which 35-40μl samples were resolved onto a 10% SDS-PAGE gel.

SDS-PAGE gel was made up according to the following recipe (Available from Cytographica (Cytographica.com 2007). Recipe is per gel):

	10% Separating Gel:	6% Stacking Gel:
Distilled H_2O	3.2ml	2.6ml
30% Acrylamide	2.67ml	1ml
1.5 M Tris HCl pH 8.8	2ml	
0.5 M Tris HCl pH 6.8		1.25ml
10% SDS	80µl	50µl
10% Ammonium Persulphate (APS)	80µl	50µl
Tetramethylethylenediamine (TEMED)	8µl	5µl
Total Volume (ml)	8	5

TEMED and APS were not added the mixture initially. 1ml of the 10% mixture was taken, and 8μl of both APS and TEMED added; this was then injected into the gel mold and left to polymerise at the bottom, so as to form a 'plug' and prevent leaks. 10 minutes following this, the remaining 7ml of 10% gel mixture had proportional amounts of TEMED and APS added, and then was poured in on top of the 'plug'. Following this, a 2-3mm film of isopropanol was gently pipetted on top of the gel, so that the boundary between the

separating and stacking gel was smooth and even. This mixture was left for 15-30 minutes to set.

Following this, the isopropanol was tipped out of the gel mould, and the remainder blotted with Whatman paper (#CHR1128, SLS). After this, the 6% stacking gel was finished with APS and TEMED, and the mixture added on top of the separating gel. The combs were instantly inserted, and any excess gel mixture blotted off. The gels were left to set for another 15-30 minutes. Gels were normally made up just prior to experimentation; if made up in advance, they were stored in Tris-Buffered Saline with 0.1% Tween-20 (TBST; see 10.1.2 for recipe) at 4^{o}C for no more than 72h.

For examination of phosphorylated (pTyr1068) and total EGFR, samples were resolved onto the above gel for 12-24h at 70v continuously. Following this, the gels were removed from the tank apparatus and washed in Wet Tank Transfer Buffer (see 10.1.2 for recipe), as were 4 Whatman sheets cut to the size of the gel, and a nitrocellulose 0.45μm membrane (#1620155, Bio-Rad). These were loaded into a wet transfer tank lattice in the following order: Absorbent sponge – 2 Whatman sheets – Gel – Nitrocellulose membrane – 2 Whatman sheets – Sponge. This lattice was then set to transfer overnight at 25v. Effective transfer was confirmed in the morning using Ponceau staining (Proteomics-grade, #K793-500, Amresco). Following

this, membranes were blocked using 5% Blocking Buffer (see 10.1.2) for 2-4 hours, then washed with TBST (for 15 minutes x3) and incubated with primary antibodies against phospho-EGFR Tyr1068 (#2234, Cell Signalling Technologies) or total EGFR (#2232, Cell Signalling Technologies) at concentrations of 1:10,000 in 10ml 5% Blocking buffer + Sodium Azide 0.02% overnight at 4^{o}C. After further washing in TBST (15 minutes x3) membranes were incubated with Goat anti-rabbit Horseradish Peroxidase-conjugated secondary IgG antibody (1:2000, #P0217, DakoCytomation) in 10ml 5% Blocking buffer for 1h at room temperature. Membranes were then exposed to ECL reagents (see 3.1.2) and visualised using a MI-5 automatic X-ray film processor (Medical Index GMBH) at various timepoints.

10.1.2 Recipes

TBST: Tris-buffered Saline with Tween 0.1% (Tris 20mM, NaCl 150mM), made up as follows:

- Water 900ml
- Tris 10x Buffer 100ml
- Tween20 1ml

Tris 10x Buffer

- 24 g Tris base (formula weight: 121.1g)
- 88 g NaCl (formula weight: 58.4g)
- Dissolve in 900mL distilled water
- Adjust pH to 7.6 with HCl.
- Add distilled water to a final volume of 1 L

Wet Tank Transfer Buffer

- Water 700ml
- Methanol 100% 200ml
- Wet Tank 10x Transfer Buffer 100ml:
  - Water 800ml
  - Glycine 144g
  - Tris HCl 30.3g
  - Total volume adjusted with water to 1L.

Blocking Buffer 5%:

- TBST: 100ml
- Bovine Serum Albumin (#A3294-100G, Sigma): 5g

ECL Reagent Recipes:

- ECL buffer (Tris pH 8.2, 100mM) 10ml (5ml in two tubes)
- Luminol 50μl (added to tube 1)
- Coumaric acid 22μl (added to tube 1)
- Hydrogen peroxide 30% 6μl (added to tube 2)

Both tubes were kept in the dark and mixed just prior to exposing the membrane.

10.1.3 Optimisation

10.1.3.1 Cell lines: A431 vs HaCaT

Vaccinia virus has been shown to favour epithelial cells, and poxvirus derived growth factors are implicated in the formation of the classic 'pox' lesion seen in smallpox (Tzahar et al. 1998). A431 cells (RRID: CVCL_0037), a human epidermoid carcinoma cell line, were initially chosen for experimentation as they are a cell line which readily expressed the EGFR, and used for many studies of EGFR-related intracellular signalling (Graness et al. 2000). However, when used for Western Blot there was a high background phosphorylation that made interpretation of pEGFR signalling impossible. Incubation for 24h in serum-free media prior to exposure to experimental

conditions did not decrease the size of background signal. Reculturing A431 cells from fresh aliquots also did not remedy the issue.

It was then decided to change over to HaCaT cells, an immortalized nontumorigenic human epidermal cell line (Boukamp et al. 1988). The HaCaT cell line mimics many of the properties of normal epidermal keratinocytes, expresses the EGFR, and can differentiate under appropriate experimental conditions (Boukamp et al. 1988; Koivisto et al. 2006). Previous *in-vitro* experiments with Vaccinia virus have also been conducted using HaCaT cells (Martin, Harris, and Shisler 2012). Western blots were subsequently conducted with HaCaT cells alone.

10.1.3.2 Wet vs Semi-dry transfer methods

Initial Western blots were performed with an Owl HEP series Hep-1 Semidry Electroblotter (Thermo fisher). However, we determined that electroblotting of a large protein such as EGFR (molecular weight 175kDa for both phosphorylated and total products) was inefficient, and often failed to transfer the larger proteins from the gel to the blotting paper. After moving to Wet tank transfer, it was determined that a slow overnight transfer at low voltage gave best results.

10.1.3.3 Membrane: Nitrocellulose vs PVDF

Both nitrocellulose and PVDF membranes were tried; PVDF membranes were first soaked in methanol 100% for 2-5 minutes before soaking in Wet Tank Transfer Buffer and proceeding as normal. No improvement in protein transfer was seen when assessed by Ponceau staining, and success with PVDF membranes was variable between experiments. Therefore, nitrocellulose membranes were used for all experiments shown.

10.2 Regulatory T Cell Suppression Assay

10.2.1 Protocol

Regulatory T cell suppression assays were carried out as previously described (Collison and Vignali 2011). Mouse splenocytes were obtained by homogenisation in a cell strainer (70μm nylon, #352350, Corning), using either end of the plunger of a 5ml syringe, and collected in a 50ml Falcon tube. Following this, cells were suspended in 10ml complete IMDM and left for 2-5 minutes, before transferring the suspension (but not any clumps that had aggregated at the base of the tube) to a new 15ml Falcon tube and centrifuged (300g, 10min, 4^{o}C). The supernatant was discarded, and the cells resuspended by use of a plate shaker for 3-5 seconds. Cells were then resuspended in MACS buffer (see 10.2.2), using 450μl per spleen (estimate of 16-20 million CD4 T cells per spleen (Miltenyi Biotec 2018)), and to this

50μl CD4 (L3T3) MACS beads (#130-049-201, Miltenyi Biotec) were added. After incubation for 15 minutes at room temperature, the suspension was washed in 15ml MACS buffer, centrifuged (300g, 5min, 4°C; NB all further centrifugation steps use these settings unless otherwise stated), the supernatant discarded, and the cells resuspended in 1.5ml MACS buffer. Following this, the cell suspension was then pipetted into a LS MACS column (#130-042-401, Miltenyi Biotec) held in a magnetic cell separator. The suspension was added 0.5ml at a time, separated by 60 seconds. Following this the column was washed with 3ml MACS buffer 3x, leaving 2-5 minutes between washes.

$CD4^-$ cells were collected if needed for subsequent experimentation in a 50ml Falcon, centrifuged and resuspended in 5ml Red Cell Lysis buffer (#R7757, Sigma-Aldrich). After 5 minutes at room temperature the solution was quenched with 35ml complete IMDM, and then centrifuged again. Following resuspension in 5ml complete IMDM, the $CD4^-$ cells were taken to a GSR C1 irradiator and exposed to 40 Grays radiation. After this Cells were sieved with a 70μm cell strainer to remove dead cells, centrifuged, resuspended in complete IMDM and kept for use as antigen-presenting “feeder” cells.

$CD4^+$ cells were collected after the LS MACS column was removed from the magnetic cell separator, placed over a 15ml Falcon tube and washed with

3ml MACS buffer x4, the last 3ml pushed through the column with the plunger provided. $CD4^+$ cells were centrifuged and resuspended in 400μl complete IMDM containing antibodies for CD4 (AF700, #100536, BioLegend), CD25 (APC, #553101, BD Pharmingen) and CD45rb (PE, #557192, BD Pharmingen) at concentration 1:100; samples were stored for 20 minutes at 4°C. Following this, cells were washed (centrifuged and resuspended) in 1ml FACS buffer (see 10.2.2) two times, and then sorted by flow cytometry into Treg (defined as $CD4^+$ $CD25^{HI}$ $CD45RB^{LO}$) and naïve effector T cells (defined as $CD4^+$ $CD25^{LO}$ $CD45RB^{HI}$), to a purity of ≥98% on a BD FACS Aria flow cytometer.

After sorting, Effector T cells were then washed in phosphate-buffered saline (PBS) twice, then centrifuged again and resuspended in 1ml PBS containing 0.5μM CellTrace Violet (CTV, #C34557, Invitrogen), and left at room temperature for 5-10 minutes. After this 5x original staining volume of complete IMDM was added, and the sample incubated for 5 minutes; this was repeated once more. The stained effector T cells were then centrifuged and resuspended in complete IMDM and incubated for a further 10 minutes at room temperature, before recounting with a haematocytometer. Cell loss varied between 30-95% depending on experimental conditions.

Treg and CTV-labelled effector Ts were recombined in a ratio 1:4 – 1:8 together with 2 x 10^5 $CD4^-$ APC feeder cells per well in a 96-well plate, along with 2 μg/ml stimulatory anti-CD3 antibody (#553058, BD Pharmingen) in a final volume of 200μl complete IMDM per well. Wells were exposed in multiples of 3 or 4 to various experimental conditions and then incubated for 72h. On the day of analysis samples were centrifuged and resuspended in PBS, before being centrifuged again. Live/dead stain (Zombie Aqua Fixable Viability Kit, #423101, Biolegend, diluted 1:500 in PBS) was added (20μl/well), and the cells left at room temperature for 10 minutes. Following this, cells were surface stained using CD4 (AF700, #100536, BioLegend) and Fc block (1mg/ml) in FACS buffer, each at a concentration of 1:200 (50μl per well) and left for 30 minutes at 4°C. Samples were then washed with 100μl FACS buffer, centrifuged and resuspended in 100μl FACS buffer for acquisition by flow cytometry.

Proliferation of effector T cells was determined by measurement of CellTrace Violet dilution using a FACSCanto (BD Biosciences), after gating for singlets, live cells and staining for CD4. Proliferation was assessed using division index (average number of divisions of the whole cell population including undivided cells) and percentage divided (of the cell population of interest). FACS data was acquired using Flowjo v9.9.6, (Flowjo LLC). A typical gating strategy is shown below (Figure 10-1).

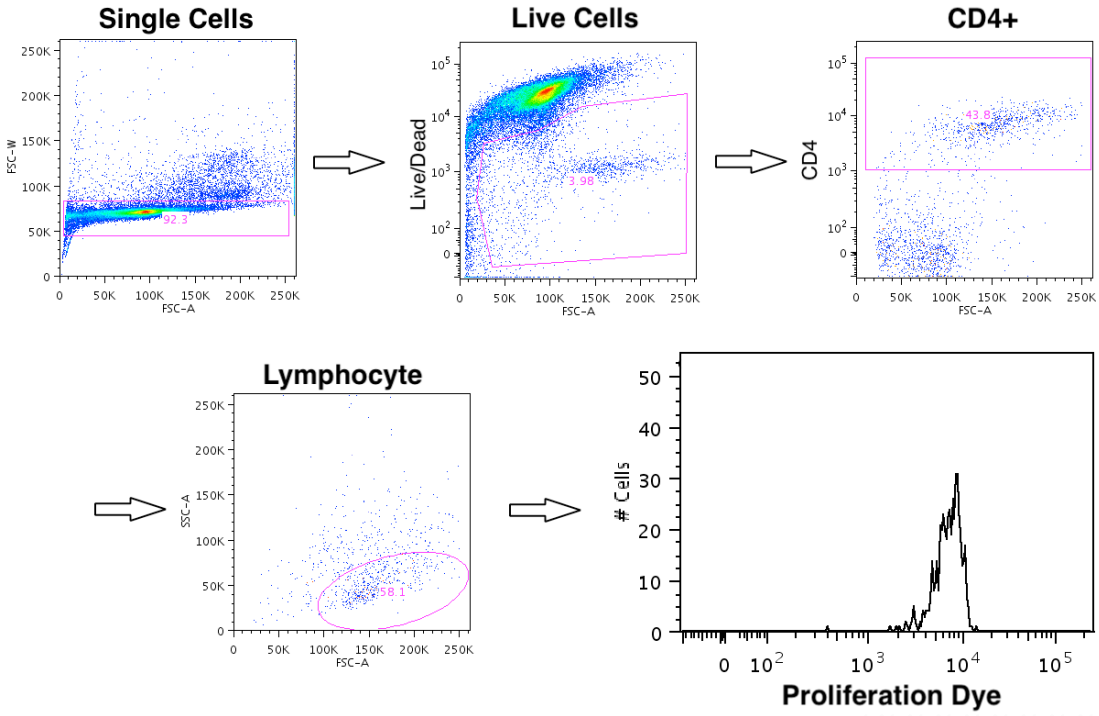

Figure 10-1 Gating strategy used to assess CVT dilution in effector T cells after incubation with Treg. Cells shown have not divided.

10.2.2 Recipes

MACS Buffer:

- PBS (pH 7.2) 500ml
- BSA 0.5% (2.5g per 500ml PBS)
- EDTA 2mM

FACS Buffer:

- PBS (pH 7.2) 500ml
- FCS 2% (10ml per 500ml PBS)

10.2.3 Optimisation

10.2.3.1 Cell Proliferation Readout: Tritiated Thymidine vs CellTrace Violet

Initially these experiments were performed with tritiated thymidine (3H-TdR) according to the protocol in Appendix A. However, despite variations in experimental conditions and time of acquisition, proliferation rates (as measured by radioactivity of samples) remained low. 3H-TdR has been replaced by other proliferation agents and dilution dyes, as they are poorly suited to analysis of specific cell populations, and only inform you about the

total amount of radioactivity in the sample, from which proliferative activity is inferred. Additionally, cell proliferation can only be analysed at one endpoint with 3H-TdR, as opposed to multiple timepoints with cell proliferation dyes (Lim, Berger, and Su 2016; Tario et al. 2018). CellTrace Violet is a reliable intracellular amine dye, which labels cells brightly and evenly, distributes equally to daughter cells, and as minimal transfer to nonlabelled cells in culture (Filby et al. 2015).

Additionally, there were logistical issues that triggered a change to CTV as the proliferative agent of choice:

1. Moving to CTV eliminated the need to work with radioactivity completely, which eliminated the chance of contamination of the laboratory environment.
2. After working with 3H-TdR appropriate monitoring of the laboratory environment involved swabbing specific areas for analysis in a beta-radiation-counter (Beckmann Coulter LS6500). These machines were located in another building on the King's Buildings (KB) site, in near-constant use and regularly broke down.
3. The Scintillation reader used for data acquisition was located on another campus (Queen's Medical Research Institute, Edinburgh), which necessitated transfer of radioactive samples by bicycle.

4. The Scintillation reader (1450 Microbeta Trilux, Wallac) was several decades old, required a 3.5” floppy disk to load its operating system when turned on, and inconsistently linked up to an attached Windows 95 computer on which the analysis software resided. As far as I could tell, no quality control was performed on the machine in the time I was using it. Data readout was in the form of a table (showing scintillation counts per minute per well), which could be exported as a CSV file, but only onto a 3.5” floppy disk. A Floppy drive-to-USB-A extension was available, but difficult to locate within the institute and did not sync to my computer (a 2015 MacBook, via a USB-C to USB-A dongle). To get around these limitations, a photo was taken of the table and the results manually transcribed into Excel. Despite visual verification of correct transcription twice (once by row, once by column) the possibility of human error using this method cannot be excluded.
5. Following the above, the Scintillation reader was cleaned, and swabs taken for beta-radiation counting. For the first year of experiments a beta-counter was only available on the KB site, requiring a bicycle ride with the samples to KB (and a repeat of this if the beta-counters showed contamination, as the machine would have to be recleaned and swabbed).

For the above reasons, CTV incorporation was selected as the proliferation readout of choice.

10.2.3.2 Optimisation of CellTrace Violet assay

Initial conditions for CTV proliferation assay were related to those for 3H-TdR assay. To verify that these were the correct conditions to use, a titration assay for various experimental conditions were carried out as follows:

1. Time of Analysis: Wells were incubated for 72, 96 or 120 hours, and analysis of Division Index, Proliferation Index and Percent Divided was Performed. Cells incubated for 72h consistently showed significantly increased cell proliferation than later timepoints (Figure 14-2).
2. Amount of feeder APC cells: The 72h samples were analysed for proliferation depending on the amount of feeder cells per well (1 or 2 x 10^5). 2 x 10^5 feeder cells per well produced consistently more cell proliferation than 1 x 10^5 at all concentrations of anti-CD3 antibody (Figure 14-3).
3. Concentration of stimulatory anti-CD3 antibody per well: the 72h samples with 2 x 10^5 feeder cells per well were analysed for optimal concentration of stimulatory anti-CD3 antibody (Figure 14-4). Concentrations ranged from 0.1μg per well (0.5μg/ml final concentration) to 0.8 μg/well (4μg/ml final concentration). ANOVA showed statistical significance for all analysis methods, and subsequent t-testing with correction for multiple comparisons was carried out, comparing 0.4μg/well (final concentration 2μg/ml) with others. 0.4μg/well caused variably superior proliferation

relative to the 0.1 and 0.2μg/well samples, and an increase above this did not reliably improve proliferation metrics.

Therefore, the optimal experimental conditions for CTV proliferation assays were selected as follows: Incubation time 72h, feeder cells 2 x 10^5/well, CD3 antibody final concentration 2μg/ml. This is similar to the experimental conditions that were used for the 3H-TdR assays.

10.3 *In-vivo* Vaccinia Pneumonitis Model

10.3.1 Animal strains used

C57BL/6J mice (*Egfr*$^{fl/fl}$, *Egfr*$^{fl/fl}$ *x FoxP3*^{cre} and *Egfr*$^{fl/fl}$ *x CD4*^{cre}, Hereafter referred to as WT, EGFR$^{\Delta FOXP3}$ and EGFR$^{\Delta CD4}$ respectively), and RAG1$^{-/-}$ mice (JAX stock #002216) were bred and maintained at the University of Edinburgh in specific pathogen free conditions. All mice were housed in individually ventilated cages at the Ashworth 3 Level 5 animal unit, King's Buildings, University of Edinburgh, until required for experiments, when they were transferred either to the Ann Walker Unit or March Building, King's Buildings Campus, University of Edinburgh. Both sexes were used for experiments, but all mice in one experiment were of the same sex. Mice were 6-8-weeks old at the start of the experiment. Cages were randomly assigned to a treatment group; mice were not randomised within the cages

themselves, but cages could contain mice of mixed genotype or all one genotype. Experiments were performed in accordance with the United Kingdom Animals (Scientific Procedures) Act of 1986, and all researchers were accredited by the UK Home Office. Dispensation to carry out animal research at The University of Edinburgh was approved by the University of Edinburgh Animal Welfare and Ethical Review Body and granted by the UK government Home Office; all research was carried under the project licence 70/8470. All in-vivo experiments were conducted with groups of 5-7 animals unless otherwise stated, and all results shown are representative of at least 2 experiments.

10.3.2 Infection Protocol

C57BL/6J mice aged 6-12 weeks were transferred to the experimental site a minimum of 24h prior to start of experiment (and usually 48h), to acclimatise to a new environment.

On the day of inoculation an aliquot of VACV stock (1 x 10^6 Plaque-Forming Units [PFU] in 100μl Tris-HCl 1mM pH 8.8), either $VACV^{WR}$ or $VACV^{\Delta VGF}$, was removed from a -20°C freezer and thawed in a water sonicator for 30 seconds, then diluted 1:2 with Tris-HCl 1mM pH 8.8 to form a final concentration of 5 x 10^5 PFU/100μl. 20μl was then used to inoculate mice,

giving an inoculation dosage of 1 x 10^5 PFU per mouse. If higher amounts of VACV needed to be given (i.e. in dose-titration experiments as detailed below) then undiluted virus stock was used. The maximum volume inoculated was 50μl.

Mice were place in a fume hood, then anaesthetised with isofluorane gas in a chamber until their respiratory rate had started to slow. They were then intranasally inoculated with 1 x 10^5 PFU VACV (in 20μl Tris-HCl pH 8.8) using a 200μl pipette tip, over 3-5 seconds. Mice were then returned to their cage and observed until awake and mobile.

Mice were observed and weighed daily, and culling occurred early if any mouse in the group exhibited weight loss of greater than 20% of baseline (weight at Day 0, at time of inoculation). In all but one experiment the same set of scales was used for all measurements; where the same set of scales was not available for one experiment, standardised weights were used to determine a conversion factor between the 2 sets of scales to allow for comparison of weights taken with the different scales.

Animals were sacrificed at 7 days (or earlier if indicated), as has been used in previous experiments (Buller et al. 1988; Kim et al. 2004; Yang et al.

2005). For studies where Bronchoalveolar Lavage Fluid (BALF) samples were not taken, mice were culled using CO2, then death confirmed with terminal exsanguination. For studies where BALF was required, culling using CO2 produced a marked decrease in viable cells, so the primary method was changed to overdose of anaesthesia using Pentobarbital 150μl/mouse (Euthatal 200mg/ml, Merial), and death confirmed by dislocation of the neck.

Following this mice were dissected, and the spleen removed and placed in 2ml complete IMDM (see 10.1.1) on ice. BALF was obtained by cannulating the trachea with a needle (19g, 1.1 x 40mm), and washing with BAL wash (see 10.3.7), 0.5ml, slowly 4 times, with the aim of recovering at least 1500μl in an Eppendorf tube, which was then placed on ice. Following this, the lungs were removed and placed in a 7ml Bijou tube and frozen. For some experiments the thoracic lymph nodes (paramediastinal and parathymic) were also removed and placed in 2ml complete IMDM on ice.

10.3.2.1 Administration of PC61 antibody

For experiments where we wished to deplete regulatory T cells, the anti-CD25 antibody PC61 was used as previously described (Setiady, Coccia, and Park 2010). Briefly, mice were injected with 200μg PC61 antibody (kind donation from Dr Van Kooten, Utrecht University, Netherlands) at 3 and 1

days prior to inoculation with VACV; as viral infections typically only ran for 7 days, this should have been enough to deplete Treg for the duration of the experiment.

10.3.2.2 Administration of Gefitinib

Gefitinib was administered by daily gavage, at a dose of 200mg/kg dissolved first in DMSO (5mg Gefitinib per 50μl DMSO), then Corn oil (450μl per 50μl DMSO). This fixed volume was administered to mice in both groups (placebo group: 50μl DMSO & 450μl corn oil only) daily from D0 to D7.

10.3.3 Plaque Assay

BSC-1 cells (RRID: CVCL_0607) were incubated (37^{o}C, 5% CO2) in 150ml flasks in 20ml IMDM supplemented with 10% FCS, 1% L-glutamine, 1% penicillin/streptomycin but WITHOUT 2-mercaptoethanol. Flasks were split into new flasks 2-3 times weekly, when reaching 80% confluence. New flasks were seeded with 1 x 10^6 cells at a time.

The day before a plaque assay was to be performed, BSC-1 cells were harvested from a flask and resuspended in IMDM as above, then seeded

onto 6-well tissue culture plates at a concentration of 5 x 10^5 cells/well in IMDM supplemented with 2.5% FCS, 1% L-glutamine and 1% penicillin/streptomycin (hereafter termed “virus IMDM”) and incubated overnight. Plaque assay was performed the following day.

Lung samples were suspended in liquid nitrogen for a few seconds, then crushed with a mortar and pestle and resuspended in 3ml Tris-HCl 1mM, pH 8.8 and transferred to a 15ml Falcon tube. After incubation on ice for 15 minutes, samples were transferred to a Dounce Homogeniser. Samples were homogenised by raising and lowering the piston slowly 25 times, then transferred into fresh 15ml Falcon tubes. These were centrifuged (750g, 5min, 4^{o}C) and the supernatant discarded. The cell pellet was resuspended in 1ml Tris-HCl 1mM, pH 8.8, and either frozen until required or used immediately (no difference was observed in the yield of the same sample used immediately or within 1 week of preparation).

On the day of initiating the assay, lung samples were thawed in a water bath sonicator for 1 minute, then a 10^{-1} solution prepared using 100μl lung sample and 900μl virus IMDM. Subsequent tenfold dilutions were made up from 0.5ml of the previous dilution mixed with 4.5ml virus IMDM (e.g. the 10^{-2} solution was made up of 0.5ml 10^{-1} solution and 4.5ml virus IMDM). Once tenfold serial dilutions from were made up to 10^{-8}, these were seeded in

triplicate on the 6-well plates containing confluent BSC-1 cells, then incubated for 1-2h. After this, wells were aspirated and washed with 2ml PBS, then overlaid with 2ml virus IMDM, and incubated for 36h.

At the time of analysis, media was removed from the wells and the cells stained with 2ml Crystal Violet solution (see 10.3.7). Wells were incubated for 15-30 minutes at room temperature, then washed in water. Plaques were then counted by eye, and an average for each dilution step produced (NB: As no agar or carboxymethylcellulose was used to limit viral spread via the medium, small 'daughter' plaques were ignored, and only large plaques were counted; additionally, wells with <20 or >200 plaques/well were not counted unless they were the only wells available for analysis). After a plaque count for the dilution step was established, a PFU value for the whole mouse lung was calculated.

10.3.4 Flow Cytometric sample preparation and analysis

Single cell suspensions for each cell sample were prepared as follows:

- Spleen: samples were forced through a 70μm cell strainer, followed by treatment with 5ml Red Cell Lysis buffer (#R7757, Sigma-Aldrich) for 5 minutes, quenching in 25ml complete IMDM, centrifuged (5m, 300g,

4°C) and resuspended in 5ml complete IMDM. 0.5ml of this suspension (i.e. 10% of the spleen sample) was used for analysis.

- BALF: samples were centrifuged (5m, 300g, 4°C) and resuspended in 1ml complete IMDM; the supernatant was used for TGFβ quantification as per section 10.3.5. The whole sample was used for analysis.
- Thoracic Lymph Node: Samples were homogenised as per spleen, then resuspended in 1ml complete IMDM. The whole sample was used for analysis.

Samples were incubated for 6h in 200μl complete IMDM with the VACV immunodominant epitope $B8R_{20-27}$ (concentration 2 μg/ml) and monensin 10μM (Invitrogen), or monensin alone, in FACS tubes. Following this, samples were washed in 3ml FACS buffer, centrifuged (5m, 300g, 4°C) and resuspended in 150μl PBS, then transferred to a 96-well plate.

Following centrifugation, wells were viability stained (10-20μl/well, see 10.3.7 for details) and left at room temperature for 10 minutes. Following this, samples were stained with antibodies for surface markers (as detailed in 10.3.7) and incubated at 4°C for 30 minutes. For intracellular staining, samples were fixed with 2% paraformaldehyde (in PBS) 100μl/well at room

temperature for 20 minutes, then permeabilised with 0.5% Saponin at room temperature for 20 minutes. Samples were then stained with intracellular antibodies for 30 minutes at 4°C. Following fixation with 2% paraformaldehyde (100μl/well, room temperature, 20 minutes), Samples were analysed by flow cytometry using a BD FACSCanto flow cytometer and FlowJo software v10.3 (FlowJo LLC).

Cells were identified after gating for singlets and live cells, and CD45 positivity for surface staining (for intracellular cytokine staining lymphocytes were gated by typical appearance on forward and side scatter). Cell types were gated as follows:

- CD4 T cells: Lymphocyte (FSc x SSc) – CD3+ – CD4+
- CD8 T cells: Lymphocyte (FSc x SSc) – CD3+ – CD4-
- B cells: Lymphocyte (FSc x SSc) – CD19+
- Alveolar Macrophages: CD11c + / SigF + / F4/80 +
- Neutrophils: Ly6G +
- Eosinophils: CD11c - / SigF +
- Monocytes: Ly6G - / Ly6C +

Intracellular cytokine staining samples were gated as follows: Singlets – Live – Lymphocyte gate on FSc x SSc – CD4 or CD8, followed by intracellular cytokine staining.

10.3.5 Measurement of Bioactive TGFβ

This analysis was conducted by a colleague, Dr Rucha Modak. Bioactive TGFβ from BALF supernatant was quantified using Transgenic Mink Lung Epithelial Cells (TMLCs). TMLCs express luciferase downstream of the PAI-1 promoter activated by TGFβ; thus, luciferase expression correlates with bioactive TGFβ (Abe et al. 1994). The assay was carried out as described in Wipff et al. (Wipff et al. 2007). In brief, TMLCs were plated at a density of 2.5 x 10^4 cells/well in a 96 well tissue culture plate and allowed to adhere for 3 hours. Subsequently, well supernatant was replaced with either 100µl of TGF-β standards (20 – 2000 pg/ml), prepared in cell culture medium containing 2% FCS or BALF supernatant. Plates were then incubated for 20 hours. Following this the TMLCs were washed twice with PBS and lysed using Firefly Lysis Buffer (#99923, Biotium). The lysate was read for luciferase activity using luciferase assay buffer (See 10.3.7) to which 750 µM ATP (Abcam) and 800 µM D-luciferin sodium salt (Cayman Chemicals) were freshly added prior to data acquisition on a Varioskan Flash spectral scanning reader (Thermo Scientific). Data was represented as pg/ml of TGFβ in the respective sample.

10.3.6 Statistics

Student's t-test was performed with GraphPad Prism 7 (GraphPad Software Inc.), with corrections for multiple comparisons where appropriate (See figure legends for details). Significant results were reported as follows: * = $p<0.05$, ** = $p<0.01$, *** = $p<0.001$.

10.3.7 Recipes

Tris-HCl 1mM pH 8.8

- Water: 500ml
- Tris base: 605mg
- Hydrochloric acid (Add base to Tris & 400ml water and mix; adjust pH to 8.8; add remaining water).

BAL wash:

- PBS 40ml
- BSA 1% 10ml (BSA 5% stock)
- EDTA 0.01mM 1μl (EDTA 0.5M stock)

Crystal Violet Solution:

- Water 160ml
- Methanol 30ml
- Crystal Violet (Sigma HT901-8F0Z) 10ml

FACS Buffer (PBS with 2% FCS):

- PBS 500ml
- Fetal Calf Serum 10ml

Viability Stains:

- Intracellular cytokine stains:
    - Zombie Aqua Fixable Viability Kit, #423101, Biolegend
    - Dilute 1:500 in PBS, use 20μl per well.
- Surface stain for cellular characterisation in BALF samples:
    - Live/Dead Fixable Blue Dead Cell Stain Kit, L34961, Invitrogen
    - Dilute 1:300 in PBS, use 10μl per well.

Antibodies used:

Antigen	Fluorophore	Product code	Manufacturer
CD3	BV421	100228	Biolegend
CD4	AF700	100536	Biolegend
CD4	FITC	11-0041-82	eBioscience
CD8	PCP/Cy5.5	100734	Biolegend
CD8	PE	553032	BD Pharmingen
CD11b	BV711	101241	Biolegend
CD11c	BV605	117334	Biolegend
CD19	APC	17-0193-82	eBioscience
CD45.2	PCP	108926	Biolegend
F4/80	Pe-Cy7	25-4801-82	eBioscience
IFNγ	FITC	505806	Biolegend
Ly6c	AF700	128024	Biolegend
Ly6g	APC-Cy7	127624	Biolegend
SiglecF	PE	552126	BD Pharmingen

Surface Staining Recipe (per sample):

- FACS buffer: 50µl
- Fc Block (1mg/ml) 0.25µl
- Surface Antibody 1:200 0.25µl

Intracellular Cytokine Staining Recipe (per sample):

- 0.5% Saponin (in FACS buffer): 50µl
- Intracellular antibody 1:200 0.25µl

Luciferase Assay Buffer:

Reagent	**Final concentration**
Tricine	20mM (pH7.8)
$Mg(CO_3)_4$. $Mg(OH)_2$.$5H_2O$	1.07 mM
$MgSO_4$	2.67 mM
EDTA	100 µM
DTT	33.3 mM

10.4 Vaccinia Virus Culture & UV inactivation

10.4.1 Viral culture & Purification

The following is a modification from a previously published protocol (Cotter et al. 2015). In order to prepare cultures of Vaccinia virus (both $VACV^{WR}$ and $VACV^{\Delta VGF}$) a culture of RK-13 cells (RRID: CVCL_3155) was prepared. Six $150cm^2$ flasks of 80-90% fully confluent RK13 cells was infected with the relevant virus with an MoI of 0.1. Flasks were checked daily for signs of cytopathic effect. After ~48h, cells were freed into the media using a cell scraper, and the flask contents collected into a 50ml tube. Samples were centrifuged (1500g, 10mins, 4^{o}C) and the supernatant discarded. Samples were resuspended in 50ml PBS, and centrifuged again (150g, 5mins, 4^{o}C). The supernatant was again discarded; at this point the pellet could be frozen overnight if required.

The pellets were resuspended in 10ml Tris-HCl (1mM, pH 8.8) and kept on ice for 15 minutes. Samples were then transferred to a Dounce homogeniser and homogenised as per 10.3.3, transferred to a 15ml tube and centrifuged (750g, 5min, 4^{o}C). The supernatant was removed from these tubes, leaving the pellet.

A 36% sucrose cushion was prepared using 100ml Tris-HCl 1mM pH 8.8, to which 36g Sucrose crystals were added and the solutions magnetically stirred for 5-10mins at room temperature. 9ml of this solution was added to a polypropylene centrifuge tube (#331374, Beckman Coulter), and the supernatant gently poured on top; the remainder of the tube was filled with Tris-HCl 1mM pH 8.8. These tubes were then ultracentrifuged (SW28 Rotor, 13,500rpm, 80mins, 4^{o}C). Following this, the supernatant was aspirated and discarded, and the pellet resuspended in 1ml Tris-HCl 1mM pH8.8. This 1ml preparation was aliquoted, and a plaque assay conducted to determine PFU concentration (see 10.3.3 for details). Using the results of these plaque assay, samples were standardised to a concentration of 1 x 10^6 PFU/100μl.

10.4.2 UV Inactivation

In order to UV inactivate vaccinia virus, a sample of 1 x 10^6 PFU virus in 1ml Tris-HCl 1mM pH 8.8 was added to one well of a 6-well plate. This was kept

on ice, placed in a CL-1000 UV crosslinker (UVP) and exposed for 15 minutes. Following this, a plaque assay was performed on a part of the sample to confirm UV inactivation. If necessary this process was repeated until UV inactivation was confirmed.

11 Results

11.1 Early EGFR phosphorylation occurs when cells are exposed to Vaccinia virus *in-vitro*

It has been noted that EEVs (which are the main means of cell-cell spread *in-vivo*) appear to enter EGFR-rich cells better in the absence of EGFR blockade, implying that cell entry is partially dependent on EGFR signalling (possibly as macropinocytosis is upregulated by EGFR activation) (Mercer et al. 2010). Interestingly, Western Reserve VACV appears to favour entry into cells via macropinocytosis (Townsley et al. 2006). Data connecting VGF with the function of Extracellular Enveloped Virions (EEV) has been published previously: Yang and colleagues found that infection with VACV deficient in VGF led to smaller plaque size and comet formation on BSC40 cells (Yang et al. 2005).

To determine if there was a detectable difference in EGFR phosphorylation, we exposed HaCaT cells to two strains of UV-inactivated virus: Western Reserve ($VACV^{WR}$), and a strain with the VGF gene deleted ($VACV^{\Delta VGF}$). We exposed HaCaT cells to 1 x 10^4 PFU of each strain for 20 minutes; This is not enough time for virus replication or early gene expression (or barely for cell entry), but enough time for any VGF present in the virus sample to

stimulate EGFR. We also exposed cells to HBEGF as a positive control, or vehicle only (FCS-deplete IMDM; negative control).

Here we saw early phosphorylation induced by HBEGF, a well-known high-affinity ligand for EGFR, but also with $VACV^{WR}$ (but not $VACV^{\Delta VGF}$; see Figure 11-1). The degree of phosphorylation was roughly the same between HBEGF and $VACV^{WR}$. This indicates that our purified UV-inactivated virus stock contains enough VGF that significant EGFR phosphorylation can occur. Whether this VGF is embedded in the viral envelope or present as a soluble protein in the purified virus stock is unclear.

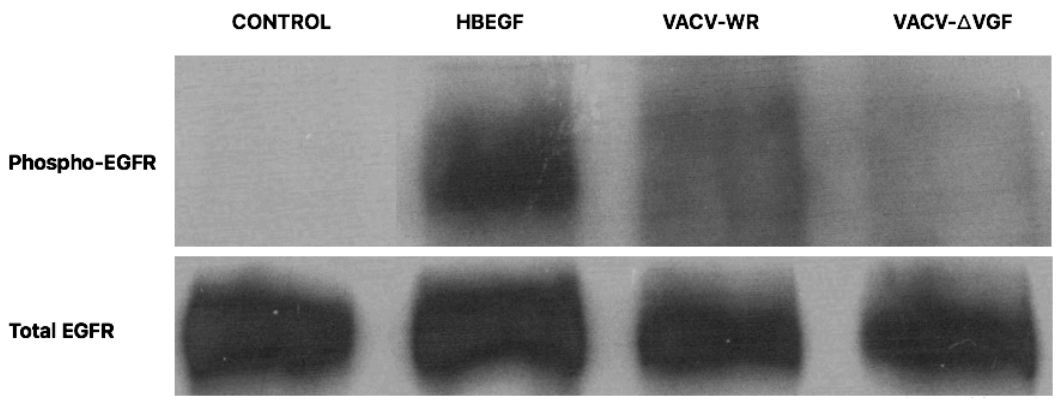

Figure 11-1: HaCaT cell phosphorylation upon exposure to Vaccinia virus. Top row samples were stained for pTyr1068, as described previously (Langhammer et al. 2011).

11.2 Regulatory T cell Suppression Assay

Regulatory T cell suppressive capacity can be determined by use of an *in-vitro* assay (Collison and Vignali 2011), in which Treg are cocultured with naïve effector CD4 T cells (Teff), and the degree of proliferation of Teff quantified at a later timepoint.

To compare the suppressive capacity of regulatory T cells exposed to UV-inactivated virus (won't replicate, but should express early genes such as the VGF gene C11R) (Tsung et al. 1996), we took $CD4^+$ mouse splenocytes from WT or $EGFR^{\Delta CD4}$ mice and sorted them into Treg ($CD25^{HI}$ $CD45RB^{LO}$) and Teff ($CD45RB^{HI}$, $CD25^{LO}$). $CD4^-$ cells were kept, irradiated (40 Grays) to prevent them replicating, and used as APC 'feeder' cells: these provide CD28 co-stimulation to the T cells, which along with a stimulatory anti-CD3 antibody promotes T cell activation and proliferation. We incubated $EGFR^{\Delta CD4}$ feeder cells and Teff for 72h, in the presence of a stimulatory CD3 antibody, with either WT or $EGFR^{\Delta CD4}$ Tregs, with or without UV-inactivated VACV, 1,000–10,000 PFU/well. These virions, as stated above, do not replicate, but have the ability to infect any live cell in the well to which they were added. As the total Multiplicity of Infection was low (0.016-0.16) and would not result in full infection of the cell, we did not think this would affect the outcome of our experiment. Additionally, it has previously been shown that non-inactivated VACV prefer to infect non-T cell leukocytes (Sánchez-Puig et al. 2004); given

this, we it is likely that the UV-inactivated VACV preferentially infected the $CD4^-$ APCs rather than the T cells directly.

11.2.1 Determination of ideal VACV inoculation dosage.

Early-phase experimentation using tritiated thymidine as our readout had demonstrated that doses of 1000 PFU/well or above provided optimal suppression of Teff proliferation (Figure 14-1). In fact, for wells containing WT Treg, incubation with 100 or 1000 PFU/well $VACV^{WR}$ was enough to generate enhanced (statistically significant) suppression when compared to wells incubated with $VACV^{\Delta VGF}$, which was not seen when Treg from $EGFR^{\Delta CD4}$ mice were used.

However, as tritiated thymidine incorporation is a flawed readout, as well as the logistical issues outlined above (in 10.2.3.1), we decided to move to CellTrace Violet (CTV) as our readout for future experiments, and to try and quantify the nature of the proliferation signal we were seeing in more detail.

As no suppression signal was seen with $VACV^{\Delta VGF}$, it was not used further.

11.2.2 Naïve Effector T cells are not affected by EGFR ligand signalling

One explanation for the suppressive effect seen so far is that VGF being released by virus-infected cells is acting directly on the Teff cells via EGFR. Our group has previously shown that naïve effector T cells are *not* directly affected by EGFR ligands such as Amphiregulin (Zaiss et al. 2013), and was also shown to be the case specifically with soluble VGF protein alone (Abdullah et al. 1989). Additionally, previous work has shown that VACV preferentially infects non-T cell leukocytes; an MoI of 10 resulted in a 2% infection rate (Sánchez-Puig et al. 2004). Wishing to corroborate this, we incubated Teff WITHOUT Treg, but with $VACV^{WR}$ (please note figure 14-1, where no suppression signal was seen with $VACV^{\Delta VGF}$). Here we saw no difference between Teff incubated with $VACV^{WR}$ or vehicle alone (Figure 11-2). We concluded that any suppression signal seen was not operating directly through Teff. In any case, as EGFR signals tend to cause proliferation or differentiation (Zaiss et al. 2015), it is unlikely that a direct VGF-EGFR interaction on Teff would suppress Teff proliferation. To summarise, even if some Teff are infected with UV-inactivated VACV, proliferation of these cells is not significantly affected.

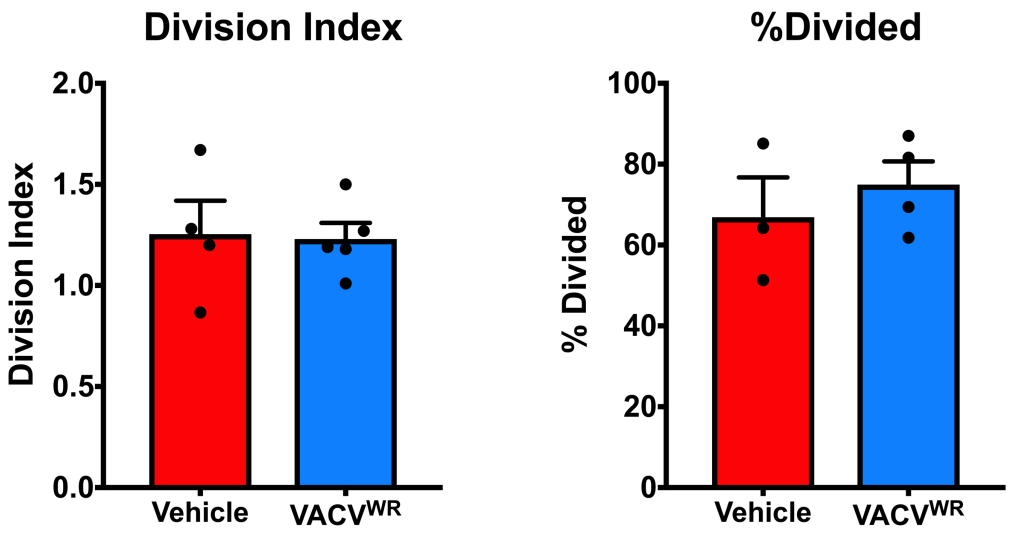

Figure 11-2 Proliferation of Teff exposed to 1000 PFUs UV-inactivated Vaccinia virus (VACV^{WR}) in the absence of Treg; 72h incubation, proliferation measured by CTV dilution.

11.2.3 Regulatory T cells and Vaccinia Virus

We then examined the effect of regulatory T cells in the presence or absence of $VACV^{WR}$. We found that in the presence of WT Tregs, EGFR–deficient naïve T cells proliferated less in the presence of $VACV^{WR}$. By contrast, when the Treg were deficient in EGFR ($EGFR^{\Delta CD4}$) this effect was not observed (Figure 11-3).

From this we concluded that effector T cell proliferation was being suppressed in the presence of VACV; that this interaction was occurring indirectly via the co-cultured Treg; and that the EGFR was essential for this interaction to occur, as deletion of EGFR on Treg abolished this effect. We suggest that this is a VGF-EGFR signal, as in our preliminary work with tritiated thymidine and $VACV^{\Delta VGF}$, no such signal was seen.

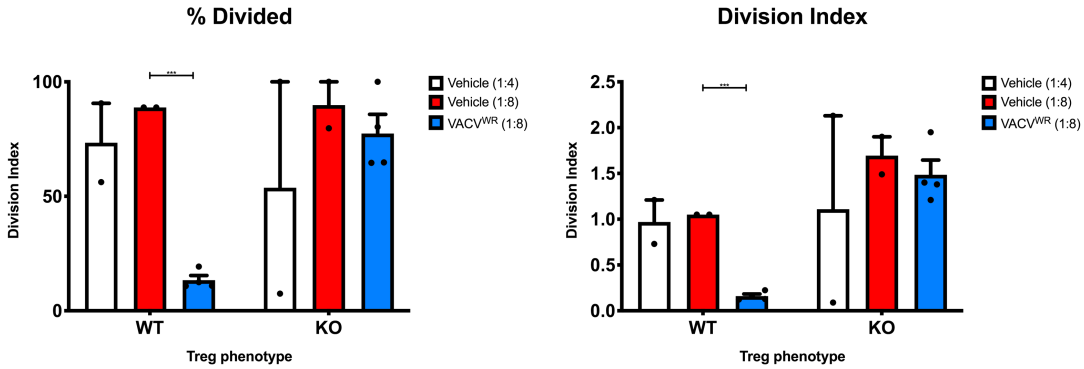

Figure 11-3 Proliferation of Teff in presence of WT or EGFR-deficient Treg after incubation with 1000 PFUs UV-inactivated VACV^{WR} or vehicle only. 1:8 Treg:Teff ratio. Representative of 2 experiments. Vehicle-exposed 1:4 Treg:Teff samples included for comparison.

11.3 Vaccinia Pneumonitis Model

11.3.1 Vaccinia virus dose optimisation

To test the physiological relevance of our *in-vitro* data, we decided to move to an *in-vivo* model of infection, namely pneumonitis brought about by intranasal inoculation of VACV. This has been used by multiple researchers, using inoculation doses ranging between 5 x 10^3 – 5 x 10^7 PFU per mouse (Yang et al. 2005; Tscharke et al. 2005; Stack et al. 2005; Becker 2003). Using wildtype (WT) C57BL/6 mice, we started with a VACV inoculation dose of 1 x 10^4 PFU/mouse and compared weight loss to an uninfected control group. We observed no statistically significant weight loss (compared to baseline weight at inoculation) in any of the 3 groups (Figure 11-4).

We therefore decided to carry out a dose-titration, to determine the optimal inoculation dosage for our particular mice (It has been shown that C57BL/6 mice of different origins respond to VACV infection differently (Tscharke et al. 2005)).

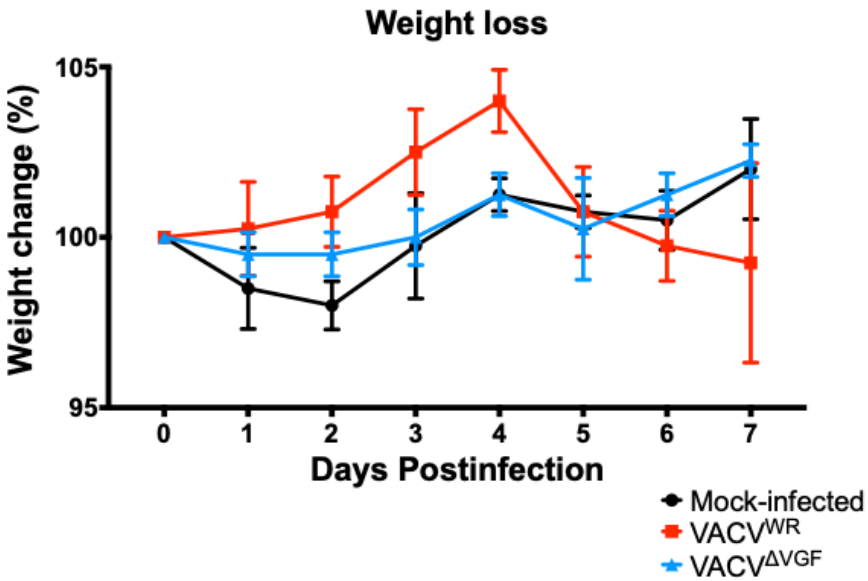

Figure 11-4 Weight change from baseline in WT mice inoculated with 1 x 10^4 PFU $VACV^{WR}$, $VACV^{\Delta VGF}$, or mock infection, over 7 days.

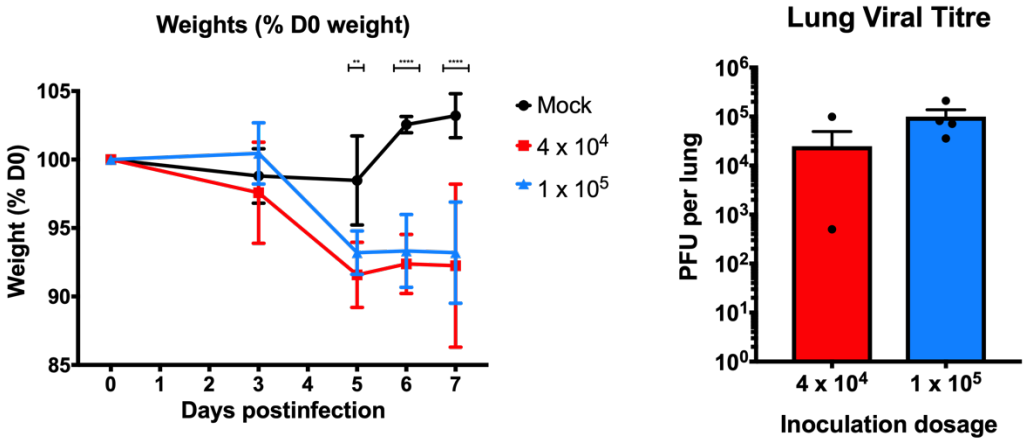

Figure 11-5 Effects of increased $VACV^{WR}$ inoculation dosages on WT C57BL/6 mice; weight change and lung viral titre. Animals were culled at 7 days. Statistical analyses are t-tests with correction for multiple comparisons where appropriate.

Figure 11-5 shows the effects of 4 x 10^4 and 1 x 10^5 inoculations on weight loss and lung viral titre. Weight loss compared to mock-infected mice was similar between the 2 infected groups, but the higher inoculation dose produced an increase in lung viral titre that was trending to significance (p=0.15). It was therefore selected as the inoculation dose to be used in subsequent experiments, unless otherwise stated.

11.3.2 Comparison of virulence

After establishing an inoculation dose of $VACV^{WR}$ that would produce symptoms in wildtype C57BL/6 mice, we proceeded to compare the virulence of our 2 virus strains. We infected $RAG1^{-/-}$ C57BL/6, as they do not develop mature B and T cells, and would not be able to mount a substantial immune response to VACV infection (Mombaerts et al. 1992). We inoculated mice with 1 x 10^5 PFU of either $VACV^{WR}$ or $VACV^{\Delta VGF}$ and monitored the animals over 7 days. Results are shown in figure 11-6.

$VACV^{WR}$ was significantly more virulent, producing pronounced weight loss when compared to $VACV^{\Delta VGF}$-infected mice that was statistically significant at 4 days. Additionally, lung viral titres between the two groups were

significantly different, with $VACV^{\Delta VGF}$ infection producing a lung viral titre mean of ~1400 PFU (as opposed to ~240,000 PFU with $VACV^{WR}$).

Based on these data, we decided to repeat infection with $VACV^{\Delta VGF}$, using different inoculation doses, in order to find a dose which provided a similar level of pathology to 1 x 10^5 PFU of $VACV^{WR}$.

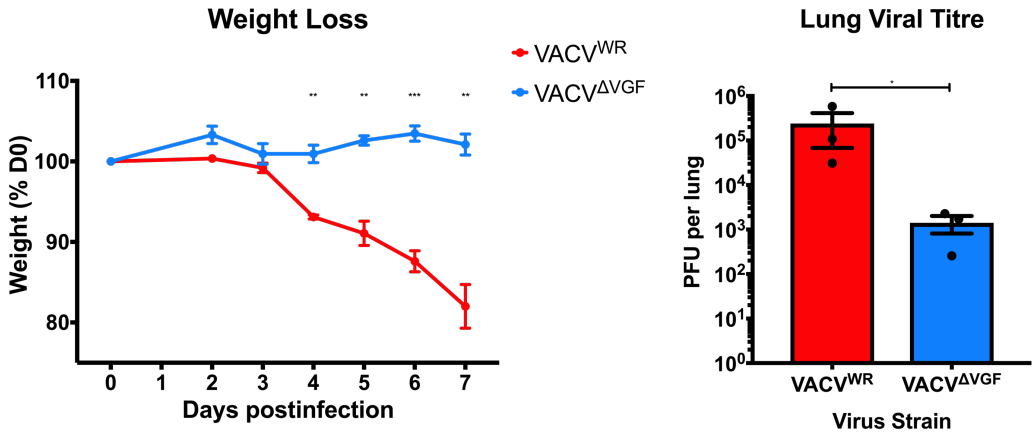

Figure 11-6 Weight loss and lung viral titre of RAG1$^{-/-}$ mice infected with VACV^{WR} or VACV$^{\Delta VGF}$. Animals were harvested for lung sample acquisition at 7 days. Analyses are t-tests with correction for multiple comparison where appropriate. Note lung viral titre is on logarithmic scale.

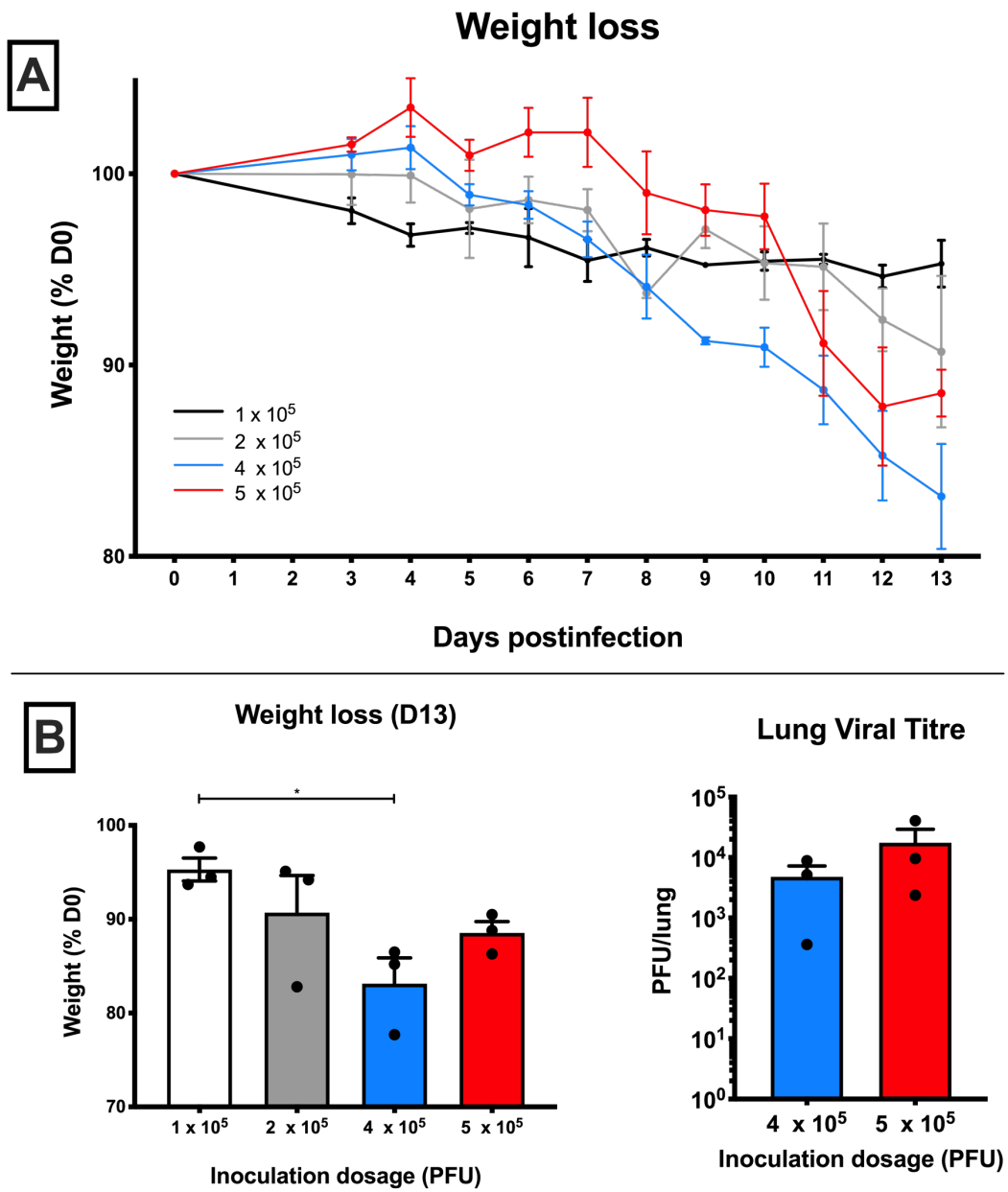

Figure 11-7 Effects of different VACV$^{\Delta VGF}$ inoculation doses on weight loss and lung viral titre in RAG1$^{-/-}$ mice. A) Weight loss of all groups out to end of experiment. B) End of experiment weights and lung viral titre (4 and 5 x 10^5 inoculation doses only). Analyses are t-tests with correction for multiple comparison where appropriate.

Figure 11-7 shows that weight loss was more gradual with $VACV^{\Delta VGF}$ as compared to $VACV^{WR}$, with mice only approaching 20% weight loss 2 weeks after infection with 4 – 5 x 10^5 PFU. Lung viral titres were obtained from these 2 groups; Even an inoculation dose of 5 x 10^5 PFU only produced a mean lung viral titre of 17,500 PFU – significantly less than those seen with inoculations of 1 x 10^5 $VACV^{WR}$. The difference in weight loss at D13 between the 4 x 10^5 and 5 x 10^5 groups doesn't correlate with the lung viral titre results but can be explained by a) natural variation in susceptibility to the virus, b) different starting weights in each group, and c) variation in actual administered dose during inoculation.

From this we concluded that comparisons could not be made between animals of similar genotype infected with different strains of VACV, as these strains have markedly different virulence *in-vivo*, as had been previously described by other researchers (Buller et al. 1988; Lai and Pogo 1989).

11.3.3 Vaccinia Growth Factor promotes *in-vivo* immunosuppression via EGFR-mediated activation of regulatory T cells

Having established that our viral strains could not be directly compared, we conducted experiments using 2 strains of C57BL/6 mice: $Egfr^{fl/fl}$ (should be

phenotypically normal, hence hereafter termed WT), and *Egfr$^{fl/fl}$ x FoxP3^{cre}* (hereafter termed EGFR$^{\Delta FOXP3}$), a strain in which EGFR is missing from FOXP3-expressing cells (i.e. Regulatory T cells).

We started by infecting each strain with 1 x 10^5 PFU of VACV^{WR} intranasally. By D3 there was a significant difference in weight loss between the groups, and this divergence continued until harvest at D7 (Figure 11-8 A). At the same time, we repeated this experiment with an inoculation dose of 1 x 10^5 PFU VACV$^{\Delta VGF}$ and saw no weight loss (Figure 11-8 B). We did not expect to see weight loss due to our previous findings with RAG$^{-/-}$ mice (see 11.3.2).

We then went on to analyse lung viral titre and found that EGFR$^{\Delta FOXP3}$ mice were significantly more resistant to VACV^{WR} infection, with VACV titres two orders of magnitude below that of WT mice. When this was repeated with VACV$^{\Delta VGF}$, the effect was not seen, and both mouse strains were equally resistant to the virus, producing lung viral titres similar to that of EGFR$^{\Delta FOXP3}$ mice infected with VACV^{WR}.

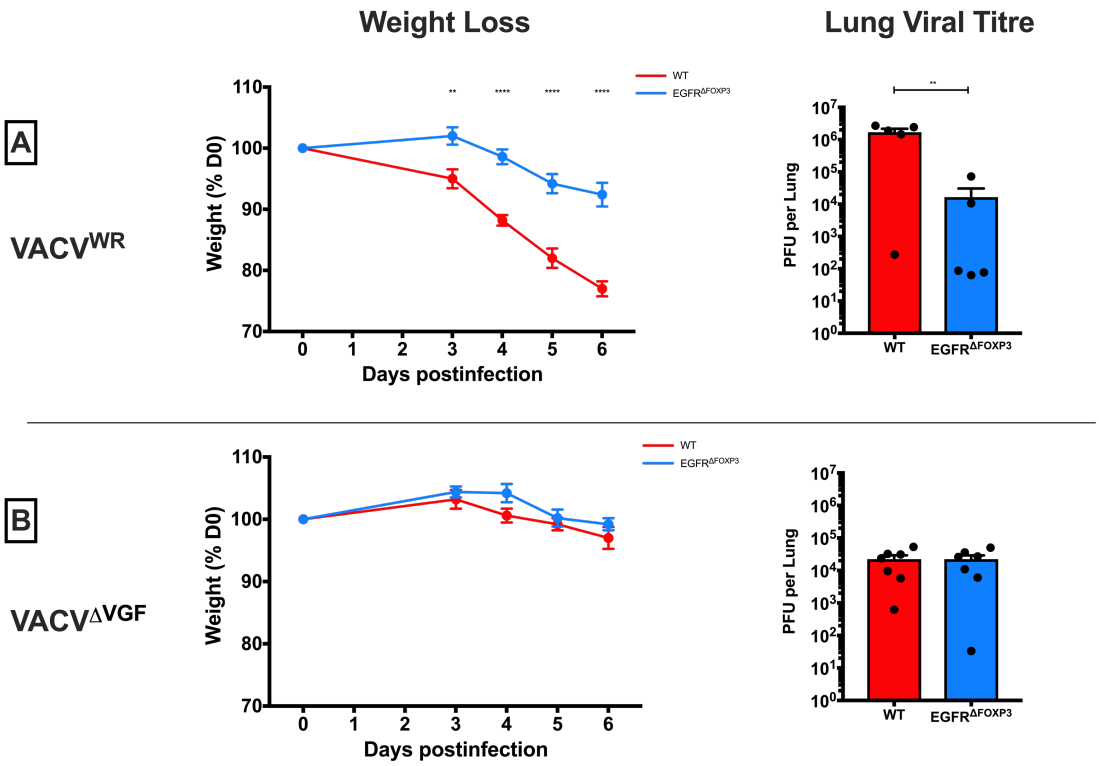

Figure 11-8 Weight loss and lung viral titre in mice infected with 100k PFUs of A) VACV^{WR} and B) VACV$^{\Delta VGF}$ virus; culled and lungs harvested at 6 days postinfection. Results representative of at least 2 experiments; statistical analyses t-test with correction for multiple comparison where appropriate.

From this we concluded that deletion of EGFR on Tregs confers resistance to VACV infection (Figure 11-8 A), and that this improved resistance is not seen in an infection using a VGF-deplete form of Vaccinia (Figure 11-8 B). This implies a VGF-EGFR interaction on regulatory T cells in this Vaccinia pneumonitis model.

11.3.4 EGFR$^{\Delta FOXP3}$ mice infected with VACV^{WR} have more cellular BALF, predominantly alveolar macrophages.

We then proceeded to analyse the cellular components of bronchoalveolar lavage fluid (BALF) from mice infected with VACV^{WR} virus. BALF of EGFR$^{\Delta FOXP3}$ mice contained more leukocytes than WT ($p=0.04$), and this seemed to be driven by an overall increase in cellularity, with no one cell population significantly increased in EGFR$^{\Delta FOXP3}$ mice compared to WT (Figure 11-9 A–D).

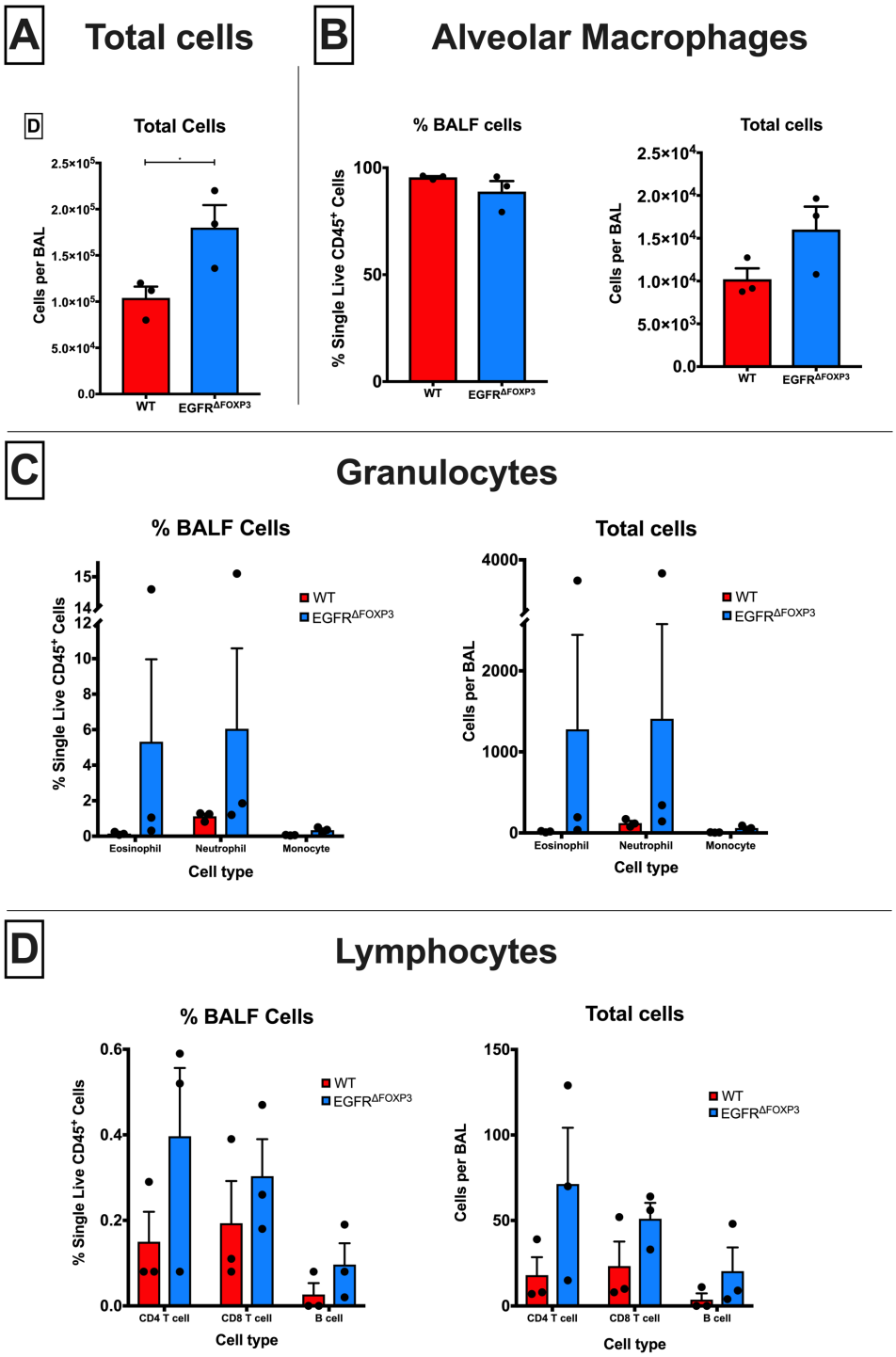

Figure 11-9 Cellular component of BAL fluid in mice infected with 100k PFUs VACV^{WR} and culled at 7 days postinfection. A) Total cellularity, B) Alveolar macrophages, C) other granulocytes, D) lymphocytes. For details of cell gating strategy see 10.3.4. Statistical analyses are t-tests.

11.3.5 CD8 T cell responses

CD8 T cells are a major means of clearing viral infections in general, and poxviruses in particular (Goulding et al. 2012; van Helden et al. 2012; Salek-Ardakani et al. 2008; Goulding et al. 2014). We therefore took single cell preparations and stimulated them either with anti-CD3 or the synthetic VACV peptide $B8R_{20-27}$ (Tscharke et al. 2005), in the presence of monensin, to stimulate production of intracellular cytokines. Staining was then carried out for CD4/CD8 and cytokine staining for CD8 IFNγ.

Figure 11-10 shows the effects of $VACV^{WR}$ infection on CD8 T cell responses in BALF, thoracic lymph node (tLN, as defined in methods) and spleen in WT and $EGFR^{\Delta FOXP3}$ mice. Across multiple experiments we saw either no change or a decrease in CD8 T cells present in BALF, and a trend to decreased responsiveness to restimulation with VACV peptide $B8R_{20-27}$. Spleen-derived CD8 T cells from $EGFR^{\Delta FOXP3}$ mice consistently were less responsive to restimulation across multiple experiments. The reason for this is unclear but may relate to improved early viral clearance in $EGFR^{\Delta FOXP3}$ animals. These data do not support the hypothesis that an increase in activated CD8 T cell function is the cause of increased viral clearance in $EGFR^{\Delta FOXP3}$ mice.

Figure 11-11 shows similar data in mice infected with VACV$^{\Delta VGF}$. We again saw reductions in CD8 T cells in BALF, but not tLN or spleen, and a nonsignificant reduction in CD8 T cell responsiveness to restimulation. This signal was now completely absent in spleen samples.

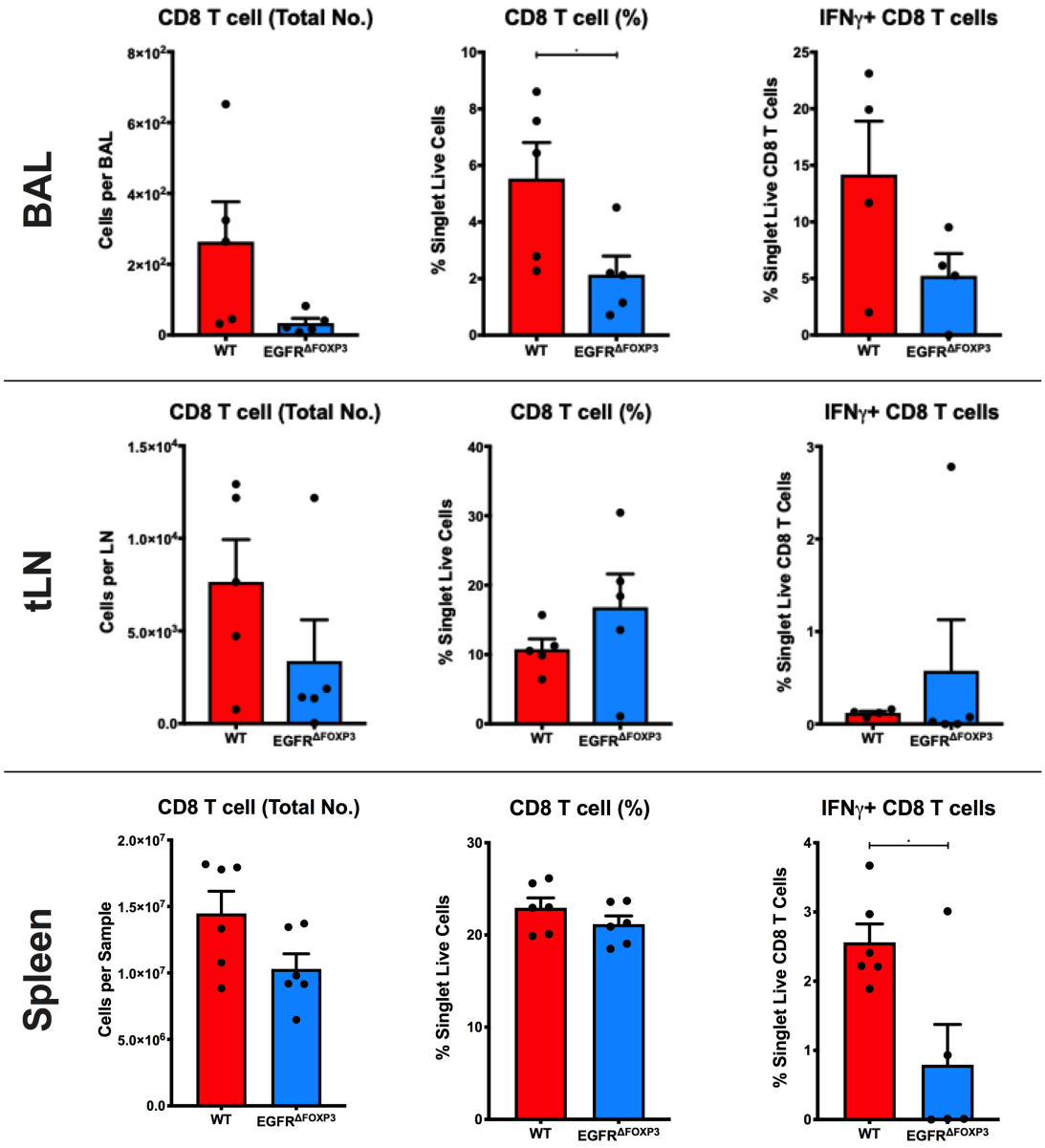

Figure 11-10 CD8 T cell responses in BAL fluid, thoracic LN and spleen of WT and EGFR$^{\Delta FOXP3}$ mice infected with 100k PFUs VACV^{WR}, and culled at 7 days. See 10.3.4 for gating parameters. Statistical analyses are t-tests, figure representative of ≥2 experiments.

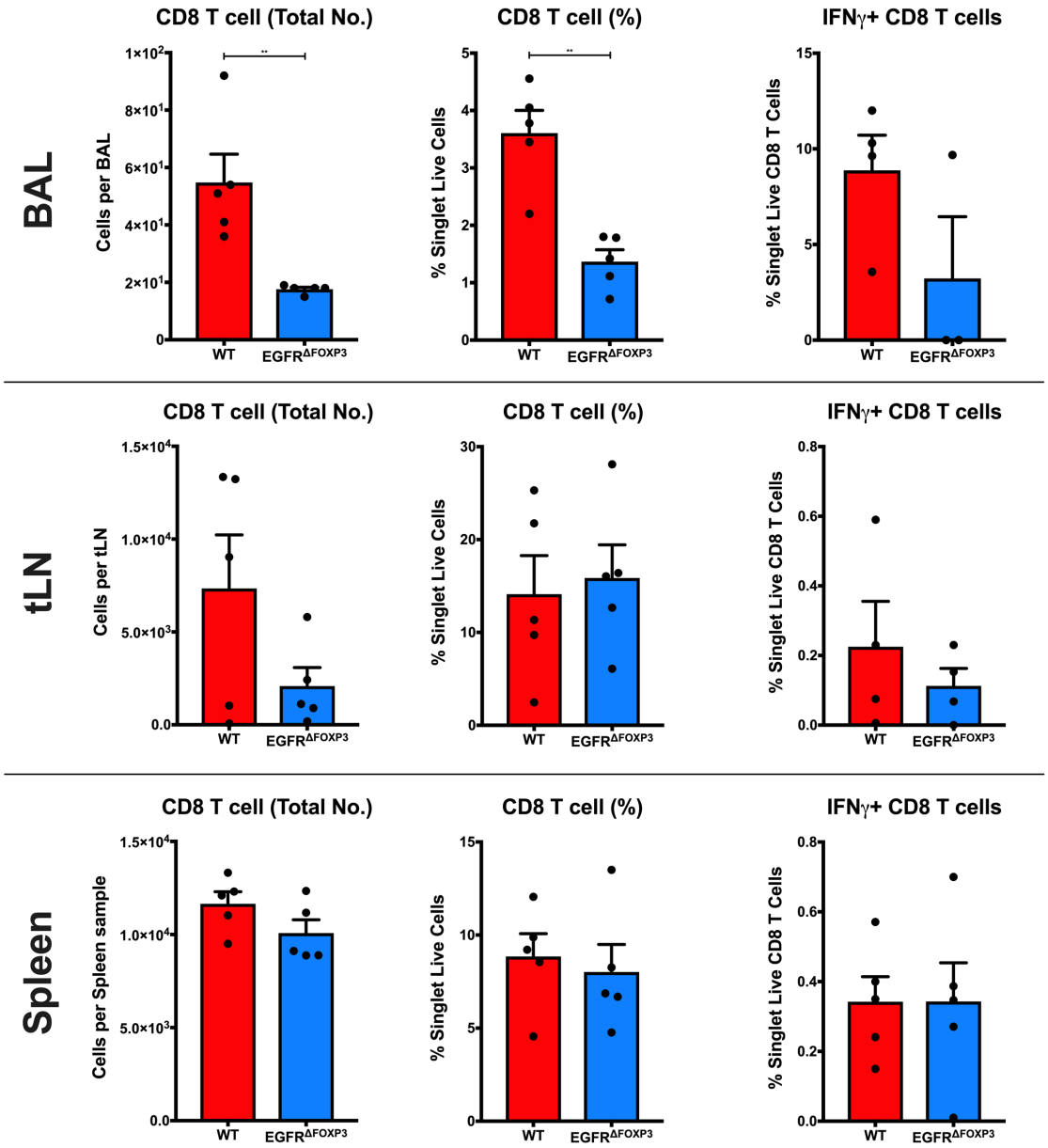

Figure 11-11 CD8 T cell responses in BAL fluid, thoracic LN and spleen of WT and EGFR$^{\Delta FOXP3}$ mice infected with 100k PFUs VACV$^{\Delta VGF}$, and culled at 7 days. See 10.3.4 for gating parameters. Statistical analyses are t-tests, figure representative of ≥2 experiments.

In summary, $EGFR^{\Delta FOXP3}$ mice infected with either strain of VACV demonstrate a reduction in BALF CD8 T cells, with a nonsignificant decrease in CD8 T cell activation. Spleen-derived CD8 T cells from $EGFR^{\Delta FOXP3}$ mice infected with $VACV^{WR}$ show reduced CD8 T cell expression of IFNγ. These data do not support the hypothesis that CD8 T cells are the main method of VACV clearance in these experiments.

11.3.6 TGFβ is reduced in the BAL Fluid of $EGFR^{\Delta FOXP3}$ mice infected with $VACV^{WR}$

As stated above, TGFβ is an essential component of Treg function, and has been linked to the function of EGFR ligands such as Amphiregulin (Budhu et al. 2017; Minutti et al. 2019). Therefore, we decided to analyse the BALF supernatant for bioactive TGFβ. Here we found that the BALF of $EGFR^{\Delta FOXP3}$ mice had significantly less TGFβ than WT mice (Figure 11-12).

This suggests that Tregs of $EGFR^{\Delta FOXP3}$ mice are producing less TGFβ than their WT counterparts, and therefore are less inhibitory. This would explain the general increase in cellularity seen in BALF of $EGFR^{\Delta FOXP3}$ mice.

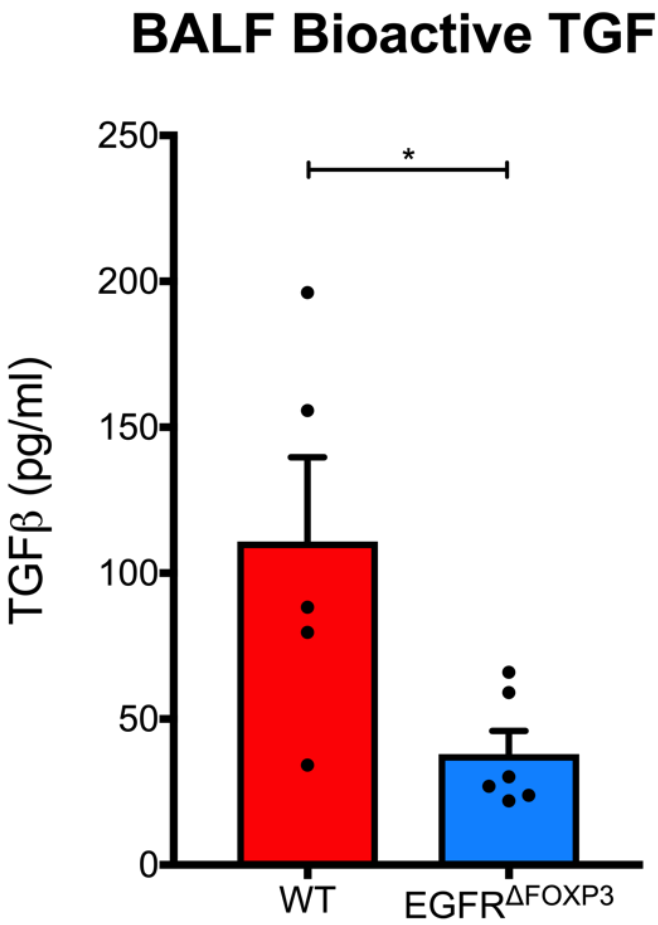

Figure 11-12 Bioactive TGFβ in mice infected with 100k PFUs VACV^{WR} and culled at 7 days. BAL fluid was then harvested, and the cell-free supernatant analysed for bioactive TGFβ by means of a luciferase assay. Statistical analysis: t-test

11.3.7 Effects of Treg depletion

Treg depletion has previously been shown to be effective in reactivating antiviral T cells and reducing viral load (Reuter et al. 2012). Assuming that VACV is manipulating Treg via EGFR using VGF, we hypothesised that depletion of regulatory T cells may be enough to protect mice from VACV infection. We inoculated WT mice with 200k PFU of $VACV^{WR}$ and injected one group with the CD25-depleting anti-PC61 antibody (Setiady, Coccia, and Park 2010) on Day -3 and Day -1 preinfection. We observed similar levels of weight loss and lung viral titre in both groups out to D6 (Figure 11-13 A), despite a near-halving of spleen $FOXP3^{+}$ CD4 T cells (Figure 11-13 C). PC61-treated mice had similar numbers of CD4 & CD8 T cells in, though the proportion of CD4 T cells was slightly greater (Figure 11-13 C). CD8 T cells in both BAL fluid and spleen (Figure 11-13 B & C) had had significantly reduced expression of IFNγ upon restimulation with the VACV peptide $B8R_{20-27}$ (NB: in BAL there was a nonsignificant trend in this direction).

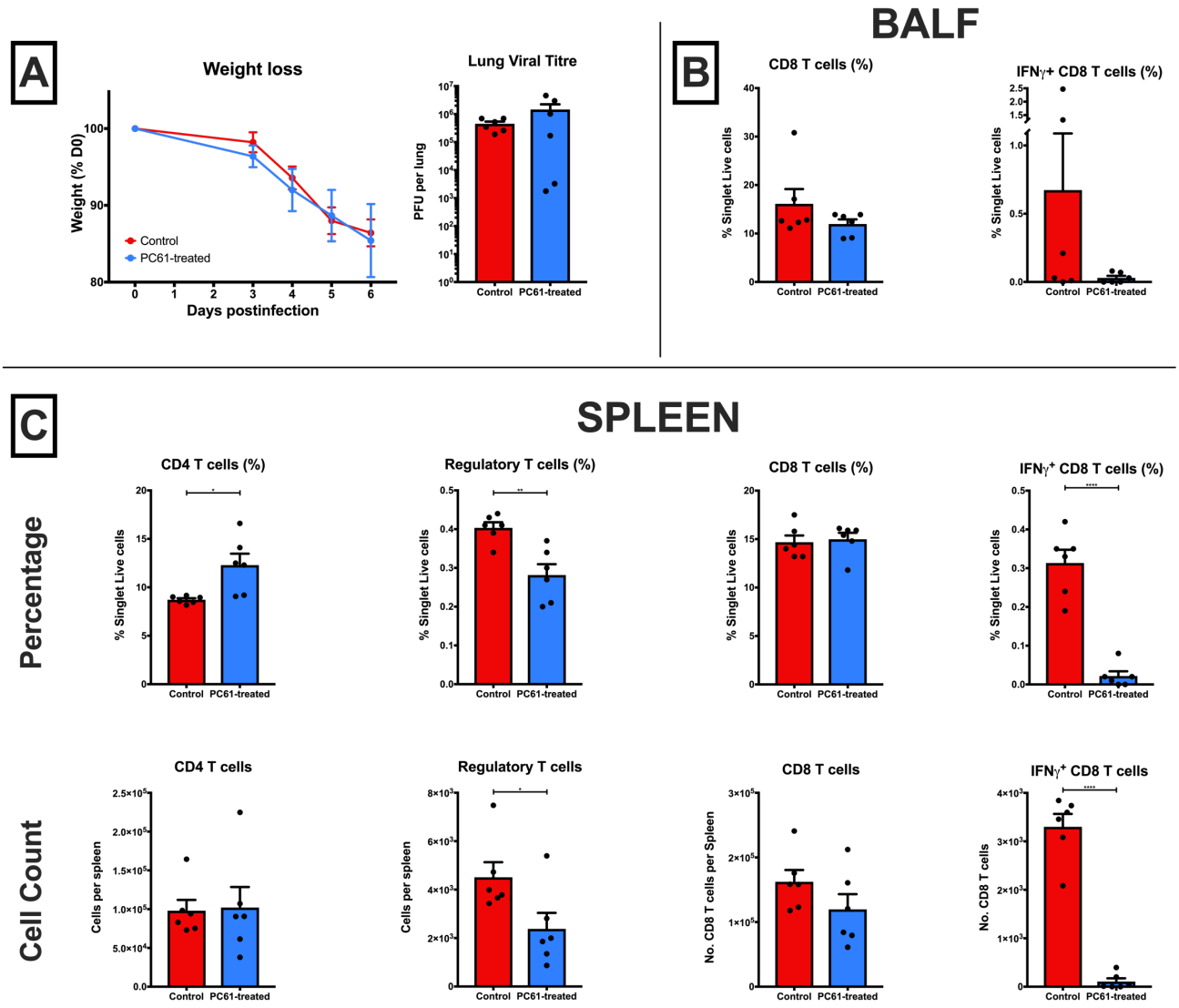

Figure 11-13 Effects of Treg depletion (by administration of PC61 anti-CD25 antibody on D-3 & D-1) on A) weight loss, lung viral titre and CD8 T cell responses in B) BAL fluid and C) spleens of mice infected with 100k PFUs VACV^{WR}. Statistical analyses are t-tests.

11.3.8 Effects of EGFR blockade (Gefitinib)

Finally, we attempted to test the effects of EGFR blockade in our VACV pneumonitis model. We inoculated WT mice with 100k PFU $VACV^{WR}$, and gave Gefitinib 200mg/kg by daily gavage, or vehicle only. Unfortunately, due to poor tolerance of drug administration in both the placebo and Gefitinib group, faster than expected weight loss and unexpected deaths in both experimental groups, this experiment was abandoned, and not repeated.

12 Discussion

Here we have shown that mice whose regulatory T cells are deficient for EGFR are more resistant to vaccinia infection, and clear the virus faster; that the BAL fluid of $EGFR^{\Delta FOXP3}$ mice is more cellular compared to wildtype; and that when $VACV^{\Delta VGF}$ is used both WT and $EGFR^{\Delta FOXP3}$ mice are equally resistant. From this we hypothesise that Vaccinia virus has the ability to manipulate Treg using the EGFR, and that this signal likely occurs via VGF-EGFR signalling. It does this in order to produce a locally immunosuppressive environment in which the virus can replicate unchallenged. In support of this, $EGFR^{\Delta FOXP3}$ mice had more cellular BAL fluid than WT, indicating a greater immune response to infection.

$VACV^{\Delta VGF}$ infection did not replicate any of these differences, indicating that both mouse strains are equally resistant to infection with this VACV mutant. $EGFR^{\Delta FOXP3}$ mice had less TGFβ in their BAL fluid, which could be as a result of less Treg activation in these mice compared to WT (assuming Treg are the main source of TGFβ, or are influencing the source cells). One interesting future avenue of inquiry would be to examine the effect of this reduced TGFβ on the formation of tissue-resident memory CD8 T cells (TRMs); TRMs are a phenotypically distinct group of memory cells that remain within their 'home' organ, tend to be positive for CD103 and/or CD69, and generate a rapid

immune response to reinfection (Muruganandah et al. 2018; Wu et al. 2018; Schenkel and Masopust 2014). Interestingly, it seems that TGFβ is the main cytokine for maintaining the TRM phenotype in the long term (Nath et al. 2019), and in some tissues is the signal that promotes the conversion of effector T cells to TRM (Ma et al. 2017). TRMs have been shown to be important in Vaccinia infection, where higher numbers correlated with rapid viral clearance upon reinfection (Gilchuk et al. 2016); they also are induced within days of infection, and are detectable by D7 postinfection (Jiang et al. 2012; Iborra et al. 2016; Kadoki et al. 2017; Puksuriwong et al. 2019). It is therefore possible that in subsequent exposure to Vaccinia infection, our $EGFR^{\Delta FOXP3}$ mice would be less protected against the virus due to defective formation of TRMs.

In-vitro, we showed that cultured virus stock (purified through a sucrose gradient) contained sufficient amounts of VGF to elicit phosphorylation of EGFR in HaCaT cells. We did not attempt to qualify this further; one possibility is that, as the viral membranes are acquired from endoplasmic reticulum or the ER-Golgi intermediate compartment (Harrison et al. 2016; Moss 2015; Pechenick Jowers et al. 2015; Smith, Vanderplasschen, and Law 2002), and VGF is assumed to be transported in precursor form to the cell surface before cleavage to a soluble form (Beerli et al. 2019; Chang et al. 1988), that VGF is being passively integrated into the virus membrane. It has long been assumed that VGF is not present on the virus particle itself.

However, recent data from the group of Dr Buck (personal communication) has suggested that VGF may be present in extracellular vesicles harvested from the supernatants of infected cell cultures; if so, then it is possible that VGF precursors could become embedded in membranes other than the host cell plasma membrane, and so may find itself in membranes of viruses. The alternative explanation is the virus stock contained soluble VGF as impurities. One way to detect this would be to look for soluble VGF in our virus stock by SDS-PAGE; however, we did not pursue this any further due to time constraints and a desire to proceed to *in-vivo* experiments.

As VGF is an early protein, it is still transcribed/translated by cells infected with UV-inactivated virions (Tsung et al. 1996). In our *in-vitro* assay of Treg function, effector T cell proliferation was suppressed by Treg when incubated with UV-inactivated $VACV^{WR}$, but only when EGFR was present on the Treg cell surface. This was not due to a direct effect on the effector T cells, as incubation of these cells with $VACV^{WR}$ in the absence of Treg did not affect proliferation when compared to controls. As far as we can see, this is the first time the effect of VGF on regulatory T cells has been examined *in-vitro*. Given the increasing evidence of the importance of EGFR signalling on T cell function (Dai et al. 2015; Nosbaum et al. 2016; Tuettenberg et al. 2016; Wang et al. 2016; Zaiss et al. 2013), it is important to determine if this receptor can be manipulated by pathogens such as poxviruses, especially

given the potential for using EGFR-inhibiting drugs to treat such infections in outbreaks.

For *in-vivo* experiments a VACV pneumonitis model was chosen due to its history of use in studying poxvirus infections, the well-described host response, and lung samples could be used for viral titres. $EGFR^{\Delta FOXP3}$ mice were more resistant to $VACV^{WR}$ infection than WT, with less weight loss, lower lung viral titres, greater cellular infiltrate in BAL fluid, and lower levels of bioactive TGFβ in BAL fluid supernatant. These effects were not seen when $VACV^{\Delta VGF}$ was used as the inoculation agent. These data imply that VGF derived from $VACV^{WR}$ is interacting with regulatory T cells via the EGFR, resulting in their activation and release of bioactive TGFβ into the environment (cellular source undetermined); this then suppresses the local immune response to infection.

It is interesting to note that depletion of WT mice Treg using anti-CD25 to near 50% baseline was not enough to replicate the effects seen when $EGFR^{\Delta FOXP3}$ mice were used. Clearly the protective effect we saw with $EGFR^{\Delta FOXP3}$ Tregs cannot be replicated by a ~50% depletion of WT Treg, as these mice lost similar amounts of weight compared to untreated. In contrast to this, previous work has noted an association between more severe Treg

depletion and enhanced antiviral CD8 T cell responses previously (Haeryfar et al. 2005). Other methods of Treg depletion exist, namely the use of DEREG mice (Lahl and Sparwasser 2011), which are considered to produce greater Treg depletion than that seen in my experiment, for a period of 6-8 days (which would have been sufficient to cover a 7-day experiment) (Kastenmuller et al. 2011). Use of DEREG mice may have produced more consistent and more specific Treg depletion, which in turn may have affected the outcome of these experiments.

The reduced CD8 T cell responses to restimulation with Vaccinia immunodominant epitope $B8R_{20-27}$ in $EGFR^{\Delta FOXP3}$ mice is difficult to explain; this trend was consistently seen across multiple experiments. Given that CD8 T cells are a major means of clearing viral infections (Goulding et al. 2012; van Helden et al. 2012; Salek-Ardakani et al. 2008), and previous authors have found that Treg depletion led to enhanced antiviral responses (see above) our findings were confusing. However, Freyschmidt and colleagues studied the effector CD8 T cell response in cutaneously-infected WT and $FOXP3^{-/-}$ mice (Freyschmidt et al. 2010), and found that $FOXP3^{-/-}$ mice failed to generate VACV-specific CD8 T cells, and those cells did not produce significant amounts of IFNγ. They hypothesised that Treg deficiency led to a disordered T cell response to infection, and polarisation towards a Th2 response. Our data on the face of it seems to reflect this, in that CD8 T cells of $VACV^{WR}$-infected $EGFR^{\Delta FOXP3}$ mice had significantly lower levels of IFNγ

expression; however, their FOXP3^{KO} mice had worse outcomes compared to WT, whereas we found the reverse to be true in our EGFR$^{\Delta FOXP3}$ mice. One possible explanation is that, by interrupting VGF-EGFR signalling and Treg activation, the rest of the immune system is 'unleashed' from TGFβ-mediated suppression, and so enhances viral clearance despite a relative lack of antiviral CD8 T cells, explaining the general increase in BAL cellularity in EGFR$^{\Delta FOXP3}$ mice. Another is that antiviral CD8 T cells are being sequestered in lung tissue, which we did not analyse for. Finally, the enhanced viral clearance seen in EGFR$^{\Delta FOXP3}$ mice may result in lower numbers of CD8 T cells at the time of analysis (almost always D7); Goulding and colleagues found that IFNγ levels in VACV-infected lung peaked at D3-6 in WT animals (but was detectable out to D14) (Goulding et al. 2014); If the antiviral response in EGFR$^{\Delta FOXP3}$ mice was more pronounced, perhaps their population of Vaccinia-specific CD8 T cells had been depleted at the time of experimental harvest; this could have been determined by harvesting some experiments at earlier and later timepoints. Further studies could also look at alternative markers for CD8 T cell activation in Type 1 infections, such as IL-2 or TNFα, as has been done elsewhere (Rodo et al. 2019; Kastenmuller et al. 2011); it is known that T cells produce various cytokines at multiple timepoints, and that polyfunctionality (production of multiple cytokines) is associated with improved response to infections and vaccination (Han et al. 2012). However, in VACV infection models naïve CD8 T cells produce TNFα early, and subsequently acquire the ability to express IFNγ as they

proliferate/differentiate (Brehm, Daniels, and Welsh 2005; Xiao et al. 2007). Other researchers have found that all CD8 T cells produce IFNγ, whereas a subset of cells can make both IFNγ and TNFα, and a third subset producing IFNγ, TNFα and IL-2 (Harrington et al. 2002). For these reasons, we chose the IFNγ as out readout for CD8 T cell activity at the D7 timepoint.

To the best of our knowledge this is the first time that a specific interaction between regulatory T cells and Vaccinia virus via VGF has been proposed. As discussed above, many poxviruses carry EGFR ligands, but notably the smallpox virus gene D4R encodes Smallpox Growth Factor (SPGF), a near-complete homologue of VGF (Kim et al. 2004). For the reasons discussed above, it would be advantageous to have an antiviral agent that could be used to treat patients in the event of a poxvirus outbreak. Perhaps EGFR-blocking agents could be used to limit the severity of infection. This has been discussed previously (Beerli et al. 2019; Kim et al. 2004; Langhammer et al. 2011; Yang et al. 2005), and Langhammer and colleagues have used the commercially licensed TKI Gefitinib in-vitro to block VGF-EGFR interaction, so stopping the paracrine ‘priming’ of uninfected epithelial cells (Langhammer et al. 2011). They also hypothesised that, based on previous work done by Mercer et al., that that Gefitinib could inhibit EGFR-dependent entry into cells, so reducing viral spread (Mercer et al. 2010). Our work would support an additional hypothesis: that EGFR blockade could inhibit host Treg

activation by poxvirus growth factors, and so expedite viral clearance by improving the host response to infection. As tyrosine kinase inhibitors of EGFR are reasonably well-tolerated in humans (Köhler and Schuler 2013), their use as an antiviral in the unlikely event of VARV exposure should be explored further. It was only limitations of time and difficulties with experimental animals' intolerance to drug administration that prevented us from examining Gefitinib's effects on VACV infection *in-vivo*.

13 Appendix: Tritiated Thymidine Protocol for assessment of T cell proliferation

$CD4^+$ mouse splenocytes were selected using a magnetic separation column and sorted into Treg and Teff as stated in 10.2.1, but the labelling of Teff cells with CTV was not performed. Instead, cells were incubated in ratios of 1:4 – 1:8 under various experimental conditions in 200μl complete IMDM with anti-CD3 antibody at a final concentration of 2μg/ml and incubated for 72h. At 66h, 0.1microCurie (3.7 kilobequerel [kBq]) of tritiated thymidine (3H-TdR) was added to each well.

At 72-84h (varied with experimental conditions) plates were frozen to stop cell proliferation. At the time of analysis, frozen plates were transported to the Queen's Medical Research Institute, University of Edinburgh, and thawed by use of a Thermolyne Plate Heater. Following this, wells were placed in a plate harvester and cell samples were washed onto 96-well scintillation paper (Printed Filtermat A, #1450-421, Wallac). Following this, a scintillation sheet (Metilex A, #1450-441, Perkin Elmer) was melted onto the scintillation paper before loading into a Scintillation counter (1450 Microbeta Trilux, Wallac). Samples were then acquired, and radioactivity of each well individually reported as counts per minute (NB: 30,000 cpm = 1kBq). Incorporation of 3H-TdR into cell populations was rarely above 1%.

14 Supplemental Data:

14.1 Initial titration of Vaccinia dosage for in-vitro Treg proliferation assay using Tritiated Thymidine readout.

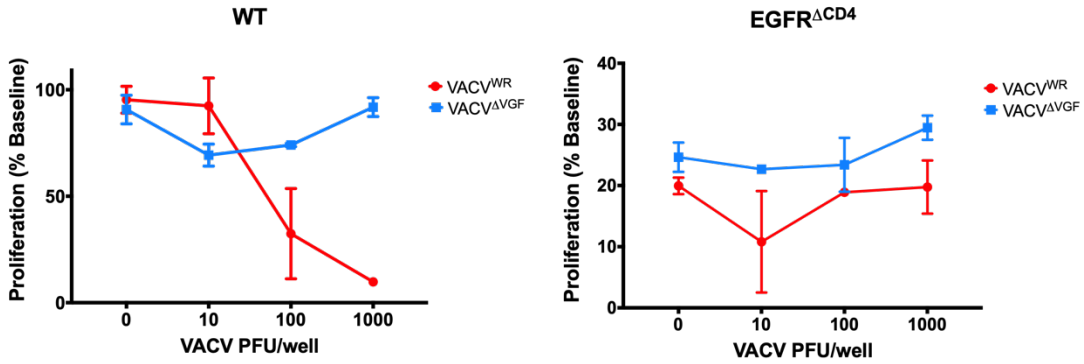

Figure 14-1 Effects of increasing doses of VACV on WT (left) or EGFR$^{\Delta CD4}$ (right) Treg function

14.2 CTV Optimisation

14.2.1 Optimisation of incubation conditions

Optimal proliferation of effector T cells (Teff) was determined as follows, using division index (Mean number of divisions per cell) and % Divided (Number of cells that underwent at least one division).

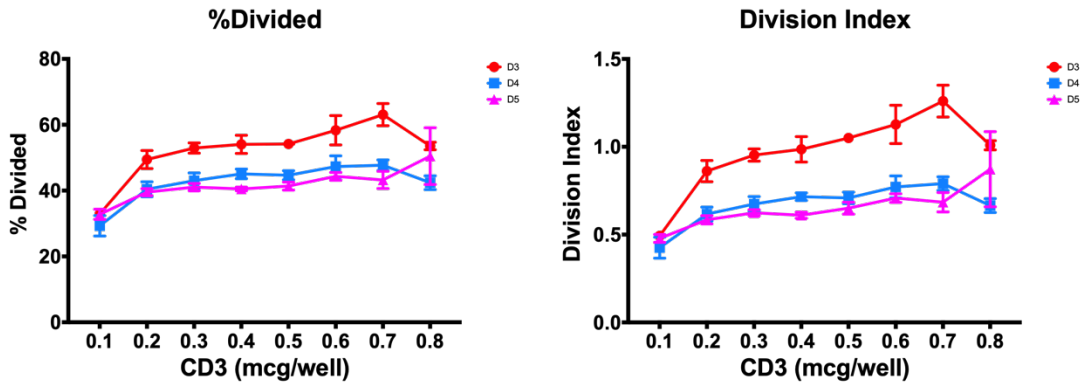

Figure 14-2 Proliferation of Effector T cells incubated for 72, 96 or 120 hours in various experimental conditions

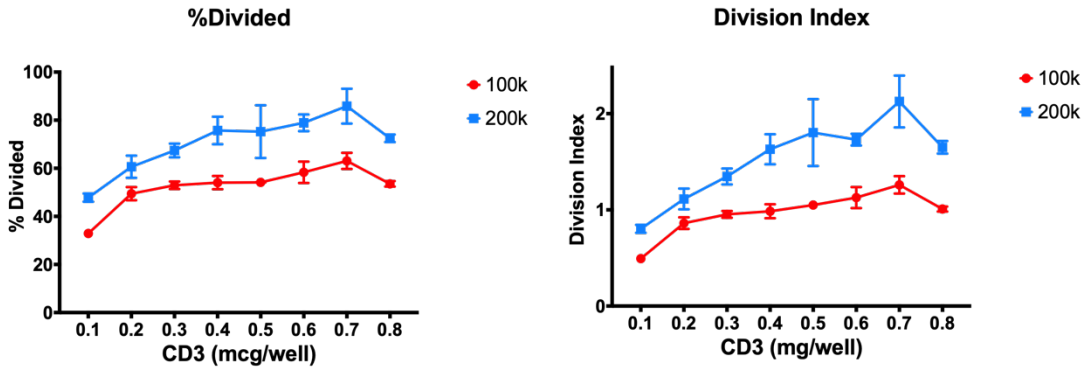

Figure 14-3 Proliferation at 72 hours of Effector T cells incubated with 1 or 2 x 10^5 $CD4^-$ APC feeder cells at various concentrations of CD3 antibody

Figure 14-2 shows that 72h of incubation results in higher division indices and %divided rates at almost all timepoints, likely due to increased cell death in the wells.

Having determined 72h as the optimal analysis timepoint, we compared 1 or 2 x 10^5 $CD4^-$ APC feeder cells per well (Figure 14-3). 2 x 10^5 feeder cells resulted in improved proliferation at all concentrations of CD3 antibody, and so was used for subsequent analysis.

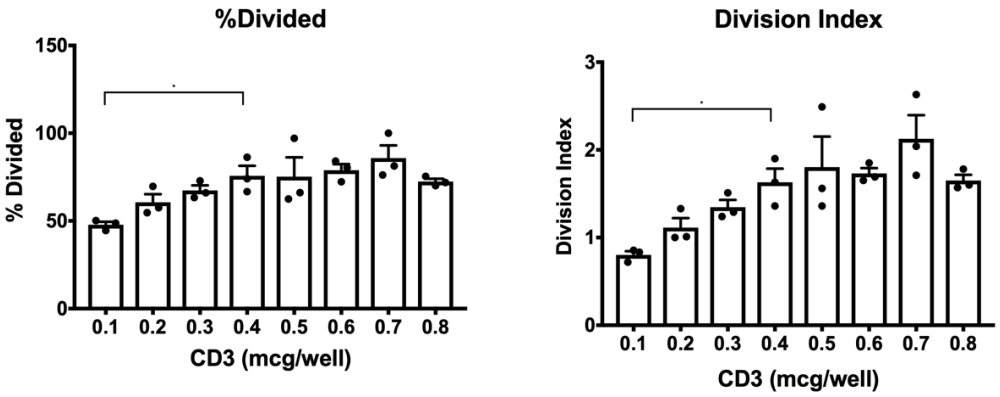

Figure 14-4 Proliferation of Teff at various concentrations of anti-CD3 antibody. (Analyses are Bonferroni-corrected t-tests relative to 0.4μg/well).

Having established optimal incubation time and number of feeder cells, we then analysed optimal concentration of stimulatory CD3 antibody per well. A final concentration of 2μg/ml was already in use in our group: this correlates to 0.4μg in a well filled with 200μl medium, so this was used as a reference for comparison to all other wells.

As demonstrated in 14-4, proliferation was only significantly reduced (relative to the 0.4μg wells) when the concentration of CD3 reached 0.1μg (equivalent to 0.5μg/ml final concentration). There was a trend in increasing proliferation between 0.1 and 0.4μg/well but increasing the dosage above 0.4μg/well did not lead to a significant increase in proliferation.

We therefore determined that optimal conditions for Teff proliferation were:

- 72h incubation
- 200,000 Feeder cells per well
- Anti-CD3 antibody: 2μg/ml final concentration

14.2.2 CellTrace Violet Staining Optimisation

Initial experiments with CTV were hampered by considerable cell death upon exposure to CTV (up to 90%). A CTV dose optimisation experiment was performed, looking at various parameters:

- Incubation volume (1, 2 or 4 ml)
- CTV concentration (0.5 or 0.25 μM).
- Incubation temperature (20 or 37 ^{o}C)
- Incubation time (5 or 10 minutes)

Results are shown in figure 14-5:

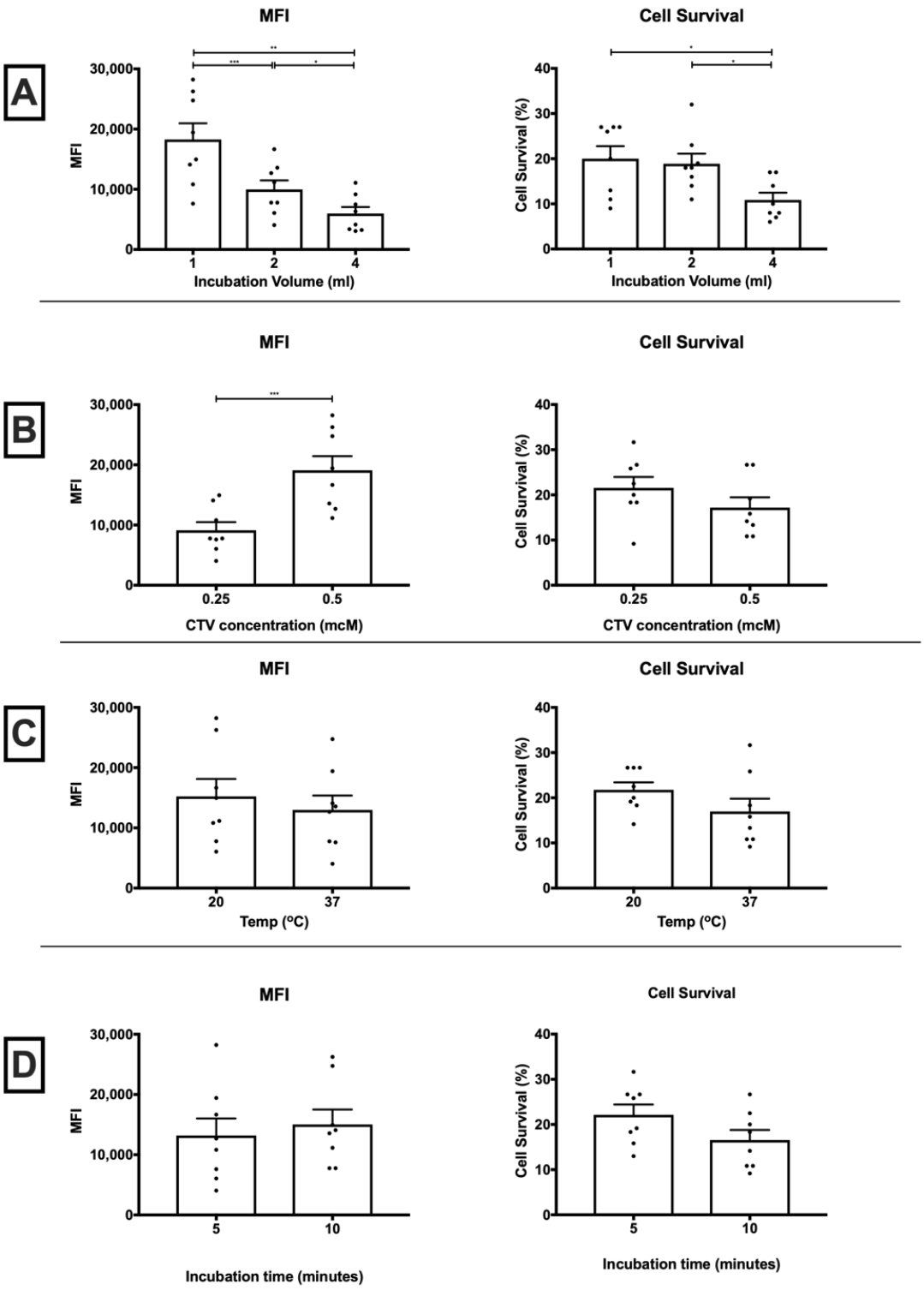

Figure 14-5 CellTrace Violet dose optimisation of Teff cells; A) Incubation volume, B) CTV concentration, C) Temperature, D) incubation time. Statistical analyses are either ANOVA with subsequent paired testing, or paired t-tests where appropriate.

These data were interpreted as follows:

14-5 A): Higher total incubation volumes produced both poorer staining and reduced cell survival. Please note that 4ml sample data was excluded from subsequent analysis.

14-5 B): A final concentration of 0.5mcM produced superior staining with a (nonsignificant) reduced cell survival.

14-5 C): Incubation at 37^{o}C did not improve cell staining, and slightly worsened cell survival (all nonsignificant).

14-5 D) Incubation time of 10 minutes produced a slightly better staining, but slightly worse cell survival (all nonsignificant).

From this the optimal CTV staining protocol was determined to be:

- Incubation volume: 1ml
- CTV final concentration 0.5 μM.
- Incubation temperature 20 ^{o}C
- Incubation time 5 minutes

Chapter 3: EGFR signalling does not significantly affect regulatory T cell function in the murine filariasis model *Litomosoides sigmodontis*

15 Abstract

Helminth worms are multicellular parasites that generate a strong TH2 immune response, including the induction of regulatory T cells (Treg), which may benefit the host (by limiting immune-mediated damage to tissues), but also the parasite. The mouse filarial infection *Litomosoides sigmodontis* induces Tregs early in infection, and these Treg appear to induce a hyporesponsive TH2 response to infection. The aim of this chapter was to determine the extent to which endogenous Amphiregulin signalling on EGFR affected Treg proliferation and function.

Initially we used transgenic C57BL/6 mice (*Egfr*$^{fl/fl}$ *x FoxP3*^{cre}) to assess the effects of EGFR deletion on Treg activity in *L.sigmodontis* infection. We found an increase in TH2 cells in all tissues, but this did not correlate with an increase in TH2 cytokine expression in CD4 cells at early (D14) or later (D40) timepoints. Repeating this with *Areg*$^{-/-}$ mice produced similar results. Using BALB/c mice, which develop full *L.sigmodontis* infection, we examined the effects of EGFR blockade with the commercially available EGFR inhibitor Gefitinib, at a dose of 100mg/kg 3 times weekly. Compared to control mice, we observed no differences in numbers of plasma microfilaria at various timepoints, pleural exudate (PLEC) microfilaria or adult worms at harvest, or lymphocyte populations or cytokine expression in CD4 or TH2 cells. Based on these data, we conclude that AREG-EGFR signalling does not significantly affect the behaviour of Tregs in the context of *L.sigmodontis* infection.

16 Introduction

16.1 Helminths

Helminths are worm-like multicellular parasites that infect vertebrates worldwide, though the burden of human disease is in tropical regions (Lindquist and Cross 2017). They can be either parasitic or free-living, and are typically transmitted by arthropod or mollusc vectors, but also from soil and contaminated food. Helminthoses can occur in any organ system, and are a significant cause of morbidity worldwide, especially in developing countries. In children in particular they are associated with limitations in physical and mental development. Overall, it is estimated that 25% of the world's population are actively infected at any one time (Bethony et al. 2006). The majority of Helminthoses are listed as Neglected Tropical Diseases (WHO 2019). Treatment with anthelminthic drugs (and to a lesser extent doxycycline, which targets the symbiotic *Wolbachia* endobacteria in filarial worms) is commonplace, but must be repeated often as reinfection is common and host resistance limited (Hoerauf et al. 2011; Volkmann et al. 2003).

Helminths are divided into 3 major classifications: Nematodes (roundworms), Trematodes (Flukes) and Cestodes (Tapeworms). Each have distinct anatomy, but all are characterised by an outer layer termed tegument (cuticle in nematodes), that serves to protect the worm from environmental conditions and the host response to

the parasite. Internal structures vary markedly between these 3 groups and will not be discussed further.

16.2 Filarial Nematodes

Filarial (threadlike) worms are nematodes that infect blood and lymph tissue, derived from the *Filarioidea* superfamily. There are eight species of worm that infect humans, but the four commonest pathogens are *Wuchereria bancrofti* and *Brugia malayi/timori* (causative agents of Lymphatic filariasis), *Onchocerca volvulus* (River Blindness) and *Loa Loa* (Loasis). All filarial worms are typified by residence in a human (definitive) host, and release of microfilaria into the bloodstream for uptake by an arthropod vector (Intermediate host), typically a mosquito (Taylor, Hoerauf, and Bockarie 2010). Figure 16-1 shows the typical life cycle of *W.bancrofti*.

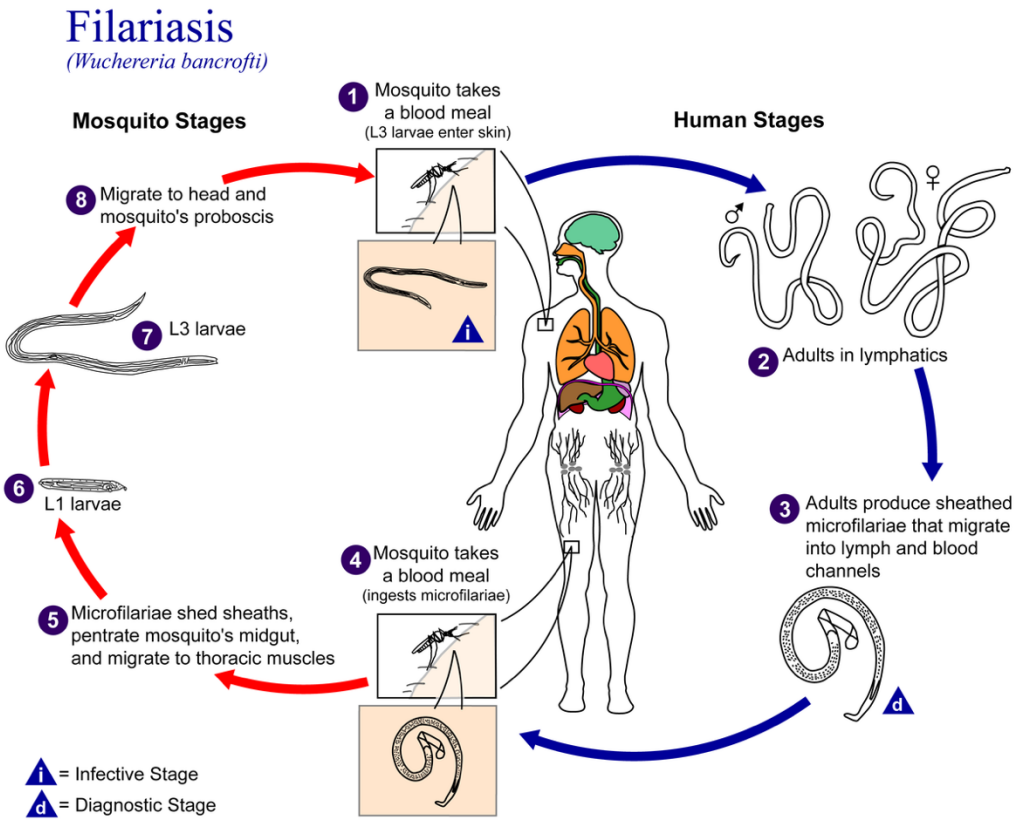

Figure 16-1 Life cycle of W.bancrofti parasite. L3 larvae enter the bloodstream during a blood meal, and then migrate to the site where they will mature into adults (In this case lymphatic vessels). After developing into adults and mating, females will produce microfilaria that will enter the bloodstream at a time optimised for ingestion by their mosquito vector (typically 10pm-4am). After entering the mosquito (Typically Culex and Aedes species) the microfilaria will mature into L1 larvae, then L2, then L3, after which they will migrate into the proboscis ready to infect the next human host. Image distributed under public domain from CDC Public Health Image Library, image credit: CDC/Alexander J. da Silva, PhD/Melanie Moser. (PHIL #3425), 2003.

Filarial infection in the tropics is commonplace, particularly sub-Saharan Africa (see Table 16-1), and though mortality is not high, morbidity with filariases is extensive: Onchocerciasis is a major cause of blindness in sub-Saharan Africa, and Loasis causes painful swellings and joint aches related to worm migration through tissues.

Disease	Causative Agent	Prevalence (million)	Distribution
Loasis	Loa Loa	3-13	West and Central Africa
Lymphatic filariasis	W.bancrofti (90%), B.malayi/timori (10%)	38.4	Sub-Saharan Africa, SE Asia, South America
River Blindness	Onchocerca volvulus	15.5	Sub-Saharan Africa, Brazil, Venezuela

Table 16-1 Overview of important filarial infections. Note most burden of disease is in sub-Saharan Africa (CDC 2018; Vos et al. 2016).

Lymphatic filariasis is typically asymptomatic, allowing for occult transmission in endemic communities, but some individuals generate an abnormally aggressive immune response to the parasite, causing scarring and obstruction of the lymphatic vessel in which the adults reside; the resulting interruption of lymph flow causes irreversible stage 3 lymphoedema, termed Elephantiasis (Hoerauf et al. 2011). This causes significant disfigurement to the host.

Eradication programmes set up by WHO have focused on mass drug administration programmes, tailored to the parasites that reside in that particular area. However, despite a variety of tailored control programmes spanning decades, including vector control, eradication of these diseases has proven difficult (Hoerauf et al. 2011).

16.3 Litomosoides sigmodontis

Litomosoides sigmodontis is a filarial nematode infection used as a model for human filariasis. It is a natural parasite of the cotton rat (*Sigmodon hispidus*), but was found to develop patent infection (defined as microfilaria detectable in blood) in the inbred laboratory mouse strain BALB/c in the 1990's (Petit et al. 1992; Dittrich et al. 2008; Haben et al. 2013). Due to this ability to study patent infection, *L.sigmodontis* infection of BALB/c mice has become the standard model for investigating filarial infections in laboratory settings.

16.3.1 Life cycle

The life cycle of *L.sigmodontis* is maintained in Jirds (*Meriones unguiculatus*) or gerbils as detailed in Fulton et al. (Fulton, Babayan, and Taylor 2018). Briefly, Uninfected *Ornithonyssus bacoti* mites (the intermediate host) are kept in a cage and 'fed' by exposure to an uninfected mouse. When time for infection, the mites are moved to a cage with an infected Jird (definitive host, ~90 days postinfection) and allowed to feed. Microfilariae (L1 larvae) are contracted from the Jird blood and take 12-14 days to develop into L3 larvae in the mites. At this point, the mites are placed in a tissue culture plate with media containing horse serum and crushed, allowing the L3 larvae to escape into the media. They are then aspirated into a pipette and

transferred to a syringe for injection. Mice are infected subcutaneously, but Jirds/Gerbils are infected intraperitoneally.

The above is the conventional way of obtaining L3 larvae, but other methods of infection including recovery of L3 larvae from a recently infected Jird pleural cavity (Hübner et al. 2009) for subsequent subcutaneous inoculation, and direct feeding of mites on BALB/c mice (though inoculation dosage in this method is undetermined). Once injected, L3 larvae migrate via lymphatics to the pleural cavity (D3 postinfection), where they mature to L4 larvae (D8-12), then maturing into adults at D25-30 (Fulton, Babayan, and Taylor 2018; Haben et al. 2013). The difference between BALB/c and other mouse strains is that the adult worms reach sexual maturity, and start to release microfilaria at D50-55, which will be detectable in venous blood. If left unchecked, infection will usually be cleared in wildtype BALB/c mice by 100 days.

16.3.1.1 The immune response to *Litomosoides sigmodontis* infection in C57BL/6 & BALB/c mice

The immune response to *L.sigmodontis* infection mimics that of human filariases (Morris et al. 2013; Taylor et al. 2009), namely there is an upregulation of the Type 2 cytokines IL-4, IL-5 and IL-13, leading to a TH2 dominant response. Individuals with a high parasite burden (but reduced pathology) show reduced T cell proliferative

responses, increased IL-10 and lower levels of IL-5 and IFNγ, suggesting both that these are important for parasite expulsion, and that they are deliberately modified by the parasite to promote survival (see below) (Specht et al. 2012). BALB/c are susceptible hosts as stated above, and have a dominant TH2 response to infection, whereas the resistant C57BL/6 strain demonstrates a mixed TH1/2 response (Le Goff et al. 2002).

Upon translocation to the pleural space, the chemokine CXCL12 is released by mesothelial cells, which attracts $CXCR4^+$ cells (the receptor for CXCL12) such as neutrophils, eosinophils, monocytes and T cells, into the pleural space. From there they expand and work to quickly reduce filarial load (particularly in resistant C57BL/6 strains); this is reduced in BALB/c mice, who produce less CXCL12 overall compared to C57BL/6 (Bouchery et al. 2012).

Pleural macrophages expand quickly in response to infection, and assume a M2 phenotype, facilitating parasite killing. In C57BL/6 mice tissue-resident macrophages expand and are gradually replenished from bone marrow, whereas in BALB/c mice monocytes are recruited to the pleura, and assume an immunosuppressive role, which aids parasite survival (Campbell et al. 2019).

Some of the immune responses to infection do not result in parasite expulsion; they may benefit the host by limiting tissue damage, but also result in parasite survival in both larval and adult forms. This is common to human filariases too, where downregulation of IL-4, IL-5 and IFNγ, together with upregulation of

immunosuppressive cytokines TGFβ and IL-10, has been noted (Taylor et al. 2009). Clearance of *L.sigmodontis* infection in C57BL/6 mice is dependent on the type 2 cytokines IL-4, IL-5 & IL-10 (Specht et al. 2012; Bouchery et al. 2012; Haben et al. 2013). Interference with these cytokines alters the outcome of infection.

In C57BL/6 mice, for example, deletion of the IL-4 gene renders the mice susceptible to patent infection, and in BALB/c mice causes a substantial increase (up to 160x) in microfilaraemia, though the number of adults in the pleural cavity is not increased (Haben et al. 2013; Volkmann et al. 2001, 2003; Bouchery et al. 2012). IL-4 has also been found to be important for control of microfilaria in the murine filariasis *Brugia pahangi*, implying a broadly similar immune response to filariases, namely that IL-4's main effect is by limiting the fecundity of adult females. It seems, therefore, that IL-4 in particular is important for control of microfilaria.

IL-5, too, is important for clearance of the disease, and when knocked out on BALB/c mice results in many more adult worms (up to 200x), though levels of microfilaraemia are similar to IL-$4^{-/-}$ as above(Volkmann et al. 2003; Haben et al. 2013). It appears that IL-5 synergises with IFNγ to increase resistance to the parasite and subsequent expulsion (Haben et al. 2013). However, C57BL/6 IL-$5^{-/-}$ mice infected with *L.sigmodontis* are as resistant to infection as wildtypes, implying that Eosinophils are not required to facilitate parasite expulsion (Le Goff et al. 2002). IL-5 production is opposed by IL-10, typically derived from M2 or alternatively activated Macrophages (Specht et al. 2012).

IL-10 plays an important part in *L.sigmodontis* infection. Infected IL-10$^{-/-}$ mice have smaller populations of T cells (along with B cells a major source of IL-10), and when mice were infected that had a T cell specific IL-10 deletion, they produced more IL-5, IL-13 and IFNγ, and had a higher initial parasite burden (D17 postinfection), though not at later timepoints (D30 & D60). These changes were not seen when mice with a B cell specific IL-10 deletion were infected, implying that T-cell-derived IL-10 affects the TH1/TH2 response to *L.sigmodontis* infection, resulting in a transient improvement in parasite survival (Haben et al. 2013). Other researchers have found that overexpression of IL-10 in macrophages leads to alternative activation, reduced TH2 cytokines and higher parasite counts, confirming the importance of IL-10 mediated suppression of the host response for parasite survival (Specht et al. 2012). Thus, it seems that IL-10 secretion from specific sources leads to tolerance of the parasite and suppression of the TH2 response.

16.3.2 Litomosoides sigmodontis and regulatory T cells

Filarial worms (as well as many other helminths) are known to suppress both TH1 and TH2 responses (Taylor et al. 2005). It has become increasingly clear that regulatory T cells (CD4$^+$ FOXP3$^+$ T cells; Treg) and Tr1 cells (Type 1 Regulatory Cells; CD4$^+$ FOXP3$^-$ T cells that produce IL-10 when activated in an antigen-specific manner (Zeng et al. 2015)) suppress the inflammatory response to infection in filarial disease (Taylor et al. 2009). In *L.sigmodontis*, Treg expansion occurs early, within 7 days of infection with L3 larvae, and depletion of Treg (e.g. with anti-CD25 antibody

prior to infection) results in improved parasite rejection (Taylor et al. 2009; Taylor et al. 2007). At the site of infection Treg appear to promote a hyporesponsive TH2 phenotype, which is mitigated by Treg depletion. Effector T cells themselves appear anergic, and postinfection depletion of Treg alone is not enough to reverse this phenotype: use of stimulatory anti-CTLA4 or anti-GITR monoclonal antibodies 'revitalises' effector T cells, and re-establishes a resistant phenotype in C57BL/6 mice (Taylor et al. 2009).

Clearly, Tregs play a significant role in the suppression of the immune system and immunological tolerance of *L.sigmodontis* infection, being rapidly expanded early and remaining so for the duration of infection. Whether endogenous EGFR signalling is important for the function of Treg in *L.sigmodontis* infection is less clear. It has been previously established that in inflammatory conditions Treg express EGFR, and that Amphiregulin enhances Treg function via EGFR (Chen et al. 2012; Zaiss et al. 2013). We hypothesised, therefore, that endogenous AREG can activate Treg via the EGFR at the site of infection, as has been shown in other inflammatory models. We therefore decided to test this *in-vivo* as detailed below.

17 Hypothesis

We hypothesised that Amphiregulin-EGFR stimulation would lead to the activation of regulatory T cells in a chronic murine filariasis infection, with a resultant decrease in TH2 responses. We also hypothesised that this could be ameliorated through the use of nonspecific EGFR inhibitors such as Gefitinib.

18 Methods

18.1 Animal strains used

BALB/c mice (all wildtype) and C57BL/6J mice (*Egfr*$^{fl/fl}$, *Egfr*$^{fl/fl}$ x *FoxP3*^{cre}, *Areg*$^{-/-}$ and *Areg*$^{fl/fl}$, Hereafter referred to as WT, EGFR$^{\Delta FOXP3}$, AREG$^{-/-}$ and AREG$^{fl/fl}$ respectively) were bred and maintained at the University of Edinburgh in specific-pathogen free conditions. All mice were housed in individually ventilated cages at the Ashworth 3 Level 5 animal unit, King's Buildings, University of Edinburgh, until required for experiments, when they were transferred either to the Ann Walker Unit, King's Buildings Campus, University of Edinburgh. Both sexes were used for experiments, but all mice in one experiment were of the same sex. Mice were 6-8-weeks old at the start of the experiment unless otherwise specified. Cages were randomly assigned to a treatment group; mice were not randomised within the cages themselves. Experiments were performed in accordance with the United Kingdom Animals (Scientific Procedures) Act of 1986, and all researchers were accredited by the UK Home Office. Dispensation to carry out animal research at The University of Edinburgh was approved by the University of Edinburgh Animal Welfare and Ethical Review Body and granted by the UK government Home Office; all research was carried under the project licence 70/8470. All *in-vivo* experiments were conducted with groups of 5-7 animals unless otherwise stated. All results are representative of at least 2 experiments.

18.2 Infection Protocol

For infections, the *L.sigmodontis* life cycle was maintained by Ms A Fulton as detailed in section 16.3.1, in room B57, Ashworth Building 3, King's Buildings Campus, University of Edinburgh. Prior to infection, mice were transferred to the Ann Walker Building and left to acclimatise for 24-48 hours.

On the day of infection, infected mites were collected by Ms Fulton, crushed in a tissue culture plate containing media and horse serum, and left for 20 minutes to allow the L3 larvae to escape into the medium. Individual mites were then aspirated into a pipette, in doses of 30 L3s per pipette, and transferred into a rounded glass and left for 10 minutes. After this time, larvae would have localised to the bottom of the well and could be aspirated into a 1ml syringe via a blue needle (23G, 0.6 x 25mm) in no more than 50μl media. Following this, prepared syringes were transferred to the Ann Walker Building, and mice were inoculated by subcutaneous injection into the dorsal skin. After injection, the needle was kept in the mouse for 3 seconds to allow injected fluid to distribute into the subcutaneous space, then withdrawn slowly. This resulted in minimal 'leak' of serum back out along the needle tract. Mice were monitored for a short period of time afterwards for adverse effects. Anaesthetic was not required or used.

18.3 Administration of Gefitinib

Experiments with BALB/c mice involved the administration of Gefitinib to one or more groups. Gefitinib was purchased from LC laboratories (#G-4408, LC labs) and kept frozen at -20^{o}C until prior to experimentation. When making up aliquots, Gefitinib was dissolved in DMSO (up to 100mg/ml), then stored at -20^{o}C until use.

18.3.1 Dose calculation

For our initial experiment, Gefitinib was added to the cage water to give a calculated dose of 5mg/kg to each mouse, assuming standard rates of water consumption.

For subsequent experiments, a higher dose of 100mg/kg of Gefitinib was used, as this was closer to the equivalent Gefitinib dose used in humans: the standard daily dose of Gefitinib in humans is 250-500mg/d. Assuming a weight of 60kg, this would be per-kilogram dose of 4.17-8.34 mg/kg. Using a standard conversion of 12.3x for human to mouse dosages, 8.3 x 12.3 = 102.09 mg/kg (Center for Drug Evaluation and Research 2005). We considered this dose to be safe, as other researchers had only experienced adverse effects in A/J mice when doses of over 300mg/kg were used (Yan et al. 2006) Additionally, clinical effects have been seen when lower per kg doses have been used (Zheng et al. 2016; Song et al. 2016). We therefore

considered that a dose of 100mg/kg was likely safe and effective, and used this for subsequent experimentation.

18.3.2 Administration

Due to the duration of experiments involving *L.sigmodontis* infection, it was considered unethical to administer Gefitinib by daily gavage. For initial experiments, it was decided to add the drug to the water supply. Using an estimated daily water consumption of 6ml for a 30g BALB/c mouse (Bachmanov et al. 2002), we determined that for a dose of 5mg/kg, 6ml drinking water would have to contain 0.15mg Gefitinib, giving a desired concentration of 0.025mg/ml (note that as smaller mice should drink less, this dosage should remain constant regardless of mouse size). As water bottles contained 250ml, we added 6.25mg Gefitinib to reach this concentration.

When trying to administer 100mg/kg doses (i.e. 125mg per bottle), we found that Gefitinib had the tendency to precipitate out and collect at the bottom of the water bottle. This method of administration was discontinued, and instead Gefitinib was added to food. For this, mouse energy requirements were calculated as follows: daily energy requirements = 160 kCal/$kg^{0.75}$/d (Nutrition 1995). For a 20g mouse, this equates to 8.51kCal/d. Using Dietgel 76A dietary supplement 56g pots (#72-07-5022X, ClearH_2O), which have a calorific content of 0.94kCal/g, we calculated a 20g

mouse should consume 9.05g/d of food, in which there should be 2mg Gefitinib (a dose of 100mg/kg). Therefore, 12.4mg Gefitinib was added to each Dietgel 76A pot (0.221mg/g, or 2mg drug per 9g food). These pots were administered Monday, Wednesday and Friday. On days when pots were not administered mice were allowed standard dry food *ad libitum*.

18.4 Monitoring

L.sigmodontis infection is typically asymptomatic even in the susceptible BALB/c mouse strain. When using C57BL/6 mice, no monitoring during the experiment was performed, and no plasma samples collected for analysis.

18.4.1 Weight monitoring

For BALB/c experiments using Gefitinib, monitoring was performed. For the initial experiment, all groups were weighed daily for the first week, then twice a week for the second week, then weekly for the remainder of the experiment. For subsequent experiments monitoring of weight was less intensive. Mice were also assessed for signs of skin changes (namely rash and alopecia), which are signs of Gefitinib toxicity. None were observed in any experiment.

Water bottles were weighed twice weekly and the amount of water consumed per mouse in each group calculated and compared, to determine if mice were refusing to drink Gefitinib-contaminated water. This could not be done when Gefitinib was added to food, as food tended to be scattered around the cage.

18.4.2 Sampling of venous blood

After 50-55 days, venous blood was drawn from infected BALB/c mice to look for plasma microfilaria; this was repeated every 5 days until the end of the experiment. Venous blood was obtained either by tail snip or tail vein cannulation. For tail snip, the mouse was placed on top of the metal grille of a cage, and a small (submillimetre) section of skin on the distal tail removed by use of a pair of scissors. Following this, the tail veins were 'milked' (gentle pressure applied from the proximal to the distal tail, fingers running laterally over the tail veins) and blood collected onto a plastic surface until 25-30μl had been acquired (varied by experiment). This was then placed in 500μl FACS Lysing Solution (#349202, BD Biosciences). For future collections, the scar on the end of the tail was removed, which produced enough bleeding for further collections of blood. Animals displayed no distress during the procedure and did not need to be immobilised.

Tail vein cannulation was performed as previously described (NC3Rs 2019): the mouse was immobilised in a restraint chamber and the tail vein located on the lateral

side. After puncture with a 25G needle, venous blood was collected onto a waterproof surface until 25-30μl had been acquired and then stored in FACS lysing solution as above.

Following sample acquisition, they were visually inspected for microfilaria by Ms A Fulton using a microscope.

18.5 Experimental harvest

18.5.1 Sample Acquisition

On the day of experimental harvest, animals were culled by exposure to CO2 in rising concentration and confirmed with cervical dislocation. Following this, mice were dissected, and venous blood taken from the inferior vena cava to look for plasma microfilaria on day of harvest (BALB/c experiments only). The spleen was then removed and placed in 2ml complete IMDM (see 10.3.7).

In order to recover a) adult worms and b) Pleural Exudate Cells (PLEC) from the pleural cavity, a small incision was made in the diaphragm at the anterolateral edge. Using a Pasteur pipette and 10ml complete IMDM several irrigations of the pleural cavity were made through this incision. The irrigation fluid was collected in a 15ml tube and kept at 4^{o}C prior to analysis. In BALB/c experiments, a 25μl samples of PLEC fluid was kept for analysing microfilarial numbers in the pleura. Following this,

thoracic lymph nodes (tLN; as described in chapter 2) were dissected out and placed in 1ml complete IMDM.

18.5.2 Adult worm acquisition from PLEC wash

To acquire adult worms from PLEC fluid, PLEC samples were sieved through a 70μm cell strainer (NB: 95% adult worms can be captured using this method (Morris et al. 2013)). Adult worms remained in the 70μm cell strainers, which were placed in 6-well plates containing PBS and stored at 4°C. Worm numbers and length was determined by Ms A Fulton under microscopy.

18.6 Flow Cytometric sample preparation and analysis

Single cell suspensions of tissue samples were prepared as follows:

- Spleen: Samples were forced through a 70 μm cell strainer, and the strainer washed with 10ml complete IMDM. Samples were then centrifuged (300g, 5min, 4°C) and resuspended in Red Cell Lysis buffer (#R7757, Sigma-Aldrich) for 5 minutes. Samples were then quenched with 25ml complete IMDM, centrifuged as above and resuspended in 5ml complete IMDM.
- Thoracic Lymph Node: Samples were homogenised by crushing between 2 pieces of sterilised gauze swabs (in a petri dish containing 1ml complete

IMDM), which were then 'washed' with 1ml complete IMDM on each side to remove as many cells as possible from the swabs. The resulting 5ml complete IMDM containing tLN cells was then centrifuged (300g, 5min, 4°C) and resuspended in 1ml complete IMDM.

- PLEC wash: The entire sample was centrifuged (300g, 5min, 4°C) and resuspended in 5ml Red Cell Lysis buffer (#R7757, Sigma-Aldrich) for 5 minutes. Samples were then quenched with 25ml complete IMDM, centrifuged (300g, 5min, 4°C) and resuspended in 1ml complete IMDM.

Using a Cellometer Auto T4 (Nexelcom), sample concentrations (of live cells, using trypan blue staining) were established, and standardised to a concentration of 2 x 10^7/ml. Thus, a 100μl sample would contain 2 x 10^6 cells, which could be used for surface staining and intracellular cytokine staining (NB: if fewer than 4 x 10^6 cells were available for analysis, the whole sample was used: this was almost always the case with PLEC samples).

100μl samples (containing 2 x 10^6 cells or fewer) were placed into two 96-well plates and used for analysis as stated below.

18.6.1 Surface Staining

For surface staining, samples were kept in 96-well plates and all volumes given are per-well. Samples were washed in 150μl PBS, then centrifuged (300g, 2min, 4°C) and the supernatant removed (shaking the plate forcefully once upside down over a sink; the cells remained pelleted at the bottom of the well), viability stain added (as per section 18.8) and samples left for 10 minutes at room temperature. Following this, samples were incubated with Fc block (1mg/ml, diluted 1:200 in FACS buffer, 10μl/well) to reduce nonspecific staining, and left for a further 10 minutes at room temperature. Then, cells were surface stained for CD4 and CD8 (diluted 1:200 in FACS buffer, 20μl/well) and left for 20min at 4°C. Samples were then washed with 100μl FACS buffer, centrifuged (300g, 2min, 4°C) and resuspended in 100μl Fixation/Permeabilization solution (#00-5521-00, eBioscience). The whole plate was then left overnight at 4°C.

The next day samples were centrifuged (300g, 2min, 4°C) and resuspended in 100μl permeabilization buffer (#00-8333-56, eBioscience, hereafter termed Perm buffer); this step was repeated once. Following this, samples were incubated in Fc block (as above, but with Perm buffer replacing FACS buffer) for 10 minutes at room temperature. Afterwards, samples were exposed to an intracellular staining panel of various factors (see results and 18.8 for details, 20μl/well), and left for 30 minutes at 4°C. Following this samples were washed with 100μl Perm buffer, centrifuged (300g, 2min, 4°C) and resuspended in 100μl Formalin 1% until analysis by flow cytometry.

18.6.2 Intracellular Cytokine Staining

Samples were incubated (37°C, 5% CO2) for 6h in 200μl complete IMDM with a stimulatory anti-CD3 antibody (#553058, BD Pharmingen) at a concentration of 2μg/ml, and monensin 10μM (Invitrogen).

Following the viability and Fc Block steps described above, cells were surface stained with CD4 antibody, 20μl/well, and left for 20min at 4°C. Samples were then washed 1x with FACS buffer 100μl, centrifuged (300g, 2min, 4°C) and fixed with Paraformaldehyde 2% (in PBS; 100μl/well, 20 minutes, room temperature). Depending on experimental timings, samples were sometimes centrifuged (300g, 2min, 4°C), resuspended in 150μl FACS buffer, and kept at 4°C overnight at this point.

For intracellular cytokine staining, samples were resuspended in 0.5% Saponin (in FACS buffer) 100μl for 20 minutes at room temperature. 50μl cytokine staining panel was then added to each well, and samples were stored at 4°C for 30 minutes. Following this samples were centrifuged (300g, 2min, 4°C) and resuspended in 100μl FACS buffer; this was repeated once. Samples were then centrifuged (300g, 2min, 4°C) and resuspended in 100μl Formalin 1%.

18.6.3 Flow Cytometry Analysis

Samples were analysed by flow cytometry using a BD FACSCanto flow cytometer and FlowJo software v10.3 (FlowJo LLC).

Cells were identified after gating for singlets and live cells, and typical lymphocytes appearance on forward and side scatter. CD4 and CD8 cells were then identified by fluorochrome positivity for same (NB: the tLN samples, cells which registered as double-positive were gated out and assumed to be thymic tissue contaminants). Intracellular cytokine and transcription factor staining was then quantified. Cells were classified as follows:

Cell types were gated as follows:

- TH2 CD4+ / GATA3+
- Treg CD4+ / FOXP3+
- TH1 CD4+ / Tbet+

Intracellular cytokine staining samples were gated as follows: Singlets – Live – Lymphocyte gate on FSc x SSc – CD4 +/- TH2, followed by intracellular cytokine staining.

18.7 Statistical Analysis

Student's t-test was performed with GraphPad Prism 7 (GraphPad Software Inc.), with corrections for multiple comparisons where appropriate (See figure legends for details). Significant results were reported as follows: * = $p<0.05$, ** = $p<0.01$, *** = $p<0.001$.

18.8 Recipes

FACS Buffer (PBS with 2% FCS):

- PBS 500ml
- Fetal Calf Serum 10ml

Viability Stains:

- Zombie Aqua Fixable Viability Kit, #423101, Biolegend
- Dilute Stock Zombie dye 1:500 in PBS, use 20μl per well.

Fixation/Permeabilisation Solution:

- Bioscience Foxp3 / Transcription Factor Fixation/Permeabilization concentrate and diluent (00-5521)
    - Concentrate: 1 part
    - Diluent: 3 parts
- Use 100μl/well, i.e. for 20 wells use 500μl concentrate and 1500μl diluent, total volume 2ml.

Permeabilisation buffer:

- eBioscience™ Permeabilization Buffer (10X), 1 part
- Distilled water, 9 parts
- NB: After using eBioscience Fixation/Permeabilisation Solution, all further incubations and wash steps should be performed in Perm buffer.

Surface Staining antibodies:

Antigen	**Fluorophore**	**Dilution**	**Product code**	**Manufacturer**
CD4	PB	1:200	100531	Biolegend
CD8	PCP/Cy5.5	1:200	100734	Biolegend
GATA3	FITC	1:8	130-100-651	Miltenyi Biotec
FOXP3	APC	1:100	17-5773-82	eBioscience
Helios	Pe	1:20	137216	Biolegend
Isotype REA (GATA3 Isotype Control)	FITC	1:8	130-104-611	Miltenyi Biotec
Hamster IgG (Helios Isotype Control)	Pe	1:100	400908	Biolegend

Intracellular Cytokine Staining Antibodies (volumes per well):

- 0.5% Saponin (in FACS buffer) 50μl
- Antibody (1:100) 0.5μl

NB: Surface staining with CD4 carried out in FACS buffer as described above, 20μl/well).

Antigen	**Fluorophore**	**Product code**	**Manufacturer**
CD4	AF700	100536	Biolegend
IFNγ	FITC	505806	Biolegend
IL-2	PeCy7	25-7021-82	eBioscience
IL-4	Pe	504104	Biolegend
IL-5	APC	504306	Biolegend
IL-13	PcPeFl710	46-7133-82	eBioscience
Rat IgG1	FITC	400405	Biolegend
Rat IgG2b	PeCy7	25-4031-82	eBioscience
Rat IgG1	Pe	400407	Biolegend
Rat IgG1	APC	400412	Biolegend
Rat IgG1	PcPeFl710	46-4301-80	eBioscience

19 Results

19.1 C57BL/6 Experiments

As stated above, C57BL/6 mice are considered to be a resistant host for *L.sigmodontis*, as wildtypes animals do not develop patent infection. However, as our transgenic lines are on a C57BL/6 background, we were forced to use C57BL/6 mice for our initial experiments.

19.1.1 Identifying an early timepoint for analysis of T cell responses.

In order to identify the optimal time to look for early T cell responses to infection, we infected 6 wildtype C57BL/6 mice and culled 2 animals on D7, D14 and D21 postinfection. Analysis was of flow cytometry alone. Results are given in supplemental data (21.1, figures 21-1 & 21-2). Over the time period D7 - D21 postinfection we observed a reduction in CD4 T cells early on in all tissues, and an increasing proportion of TH2 cells in thoracic lymph node (tLN) and PLEC wash (but not spleen samples); this was more prominent from D14. We also observed early decreases in IL-2 expression in PLEC and spleen, and IL-5 in LN and PLEC. There was also an early reduction in IL-13 expression in PLEC wash CD4 T cells. Based on these data, it was decided to use D14 as an analysis timepoint for early T cell responses, as that seemed to provide a compromise timepoint where we could

observe both increasing TH2 cell numbers and decreasing expression of TH2 cytokines.

19.1.2 Effects of EGFR deletion on regulatory T cells in *L.sigmodontis* infection: early T cell responses

Using *Egfr*$^{fl/fl}$ *x FoxP3*^{cre} (hereafter termed EGFR$^{\Delta FOXP3}$) and *Egfr*$^{fl/fl}$ (as CRE negative should be phenotypically wildtype, hence hereafter termed WT) were infected with 30 L3 larvae and culled for analysis at 14 days. At this stage we examined cell numbers and T cell responses only; as C57BL/6 mice are a resistant host, we did not think we would see a difference in L4 or worm numbers in the PLEC (see also 19.1.4). There were minor reductions in CD4 & CD8 T cells detected in EGFR$^{\Delta FOXP3}$ spleen samples and infected EGFR$^{\Delta FOXP3}$ mice when compared to infected WT (Figure 19-1 A&B). There were significantly more TH2 cells in infected samples compared to uninfected, but no difference between WT and EGFR$^{\Delta FOXP3}$ (Figure 19-1 C). Treg (Figure 19-1 D) were a lower proportion of singlet live cells in infected spleen samples compared to uninfected in both groups, but only in WT when looking at cell numbers. This was also true for Helios^{+} Treg (Figure 19 E). To summarise, *L.sigmodontis* infection promotes the development of TH2 cells, but the absence of EGFR on Tregs does not affect this significantly compared to WT.

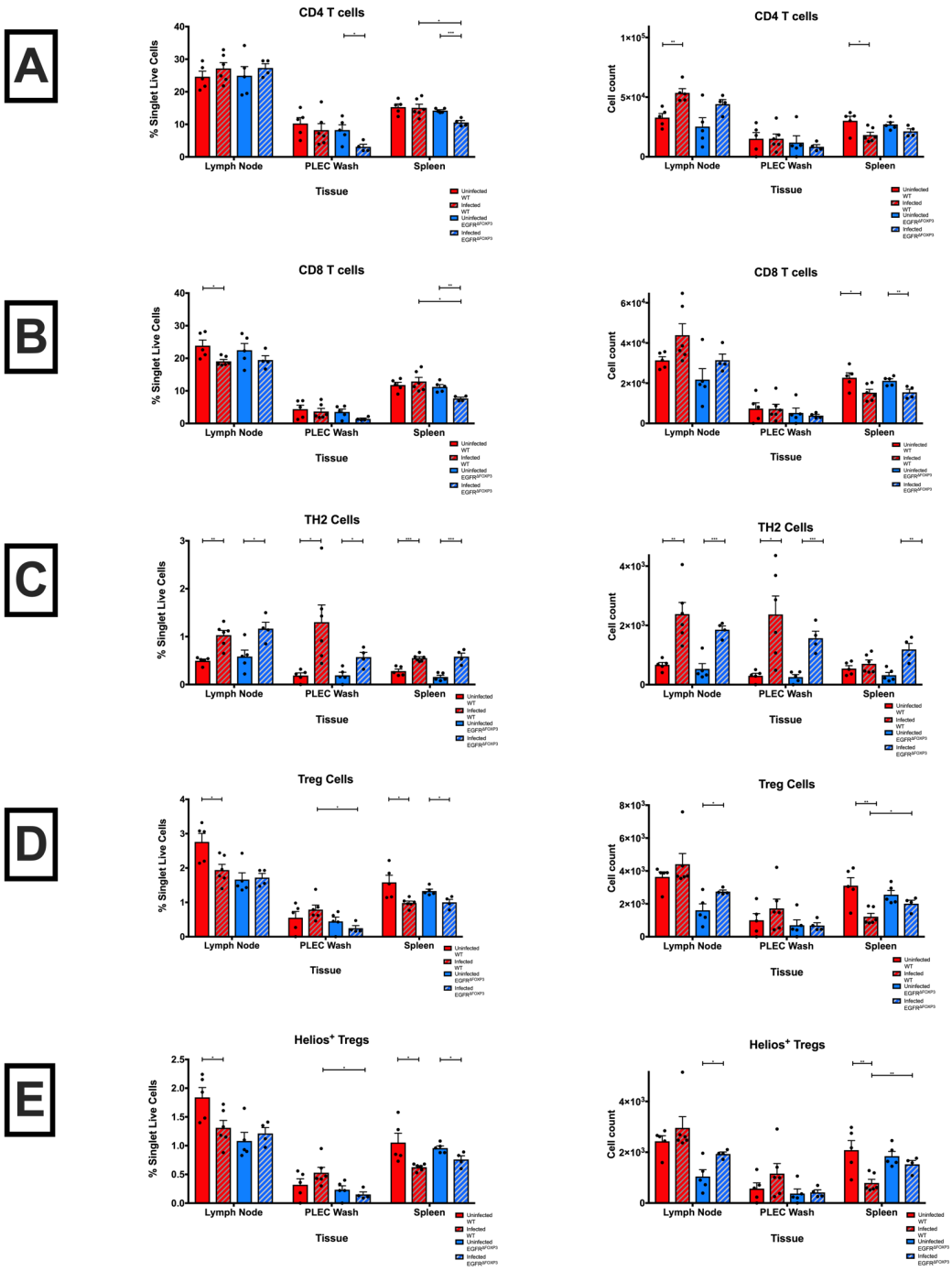

Figure 19-1 Proportions and cell counts of different T cell populations in tissue samples of WT and EGFR$^{\Delta FOXP3}$ mice infected with L.sigmodontis or uninfected; Harvest at 14 days postinfection. A) CD4 T cells, B) CD8 T cells, C) TH2 cells (CD4+ GATA3+ FOXP3-), D) Treg (CD4+ GATA3- FOXP3+), E) Helios^{+} Treg. Statistical analyses are T-tests. Note: Spleen count is for 1/10 of the sample; for LN and PLEC the whole sample was analysed.

Differences in intracellular cytokine staining correlated with this TH2 response, with upregulation of IL-4, IL-5 and IL-13 in infected samples, notably PLEC and to a lesser extent spleen (Figure 19-2). However, no significant differences between infected WT and $EGFR^{\Delta FOXP3}$ mice were noted. Expression of IL-2 and IFNγ was not significantly different between infected groups (except for IFNγ in spleen, where the difference was minor).

In conclusion, *L.sigmodontis* infection of $EGFR^{\Delta FOXP3}$ mice on the C57BL/6 background does not result in an enhanced TH2 response or increased TH2 cytokine expression when compared to WT.

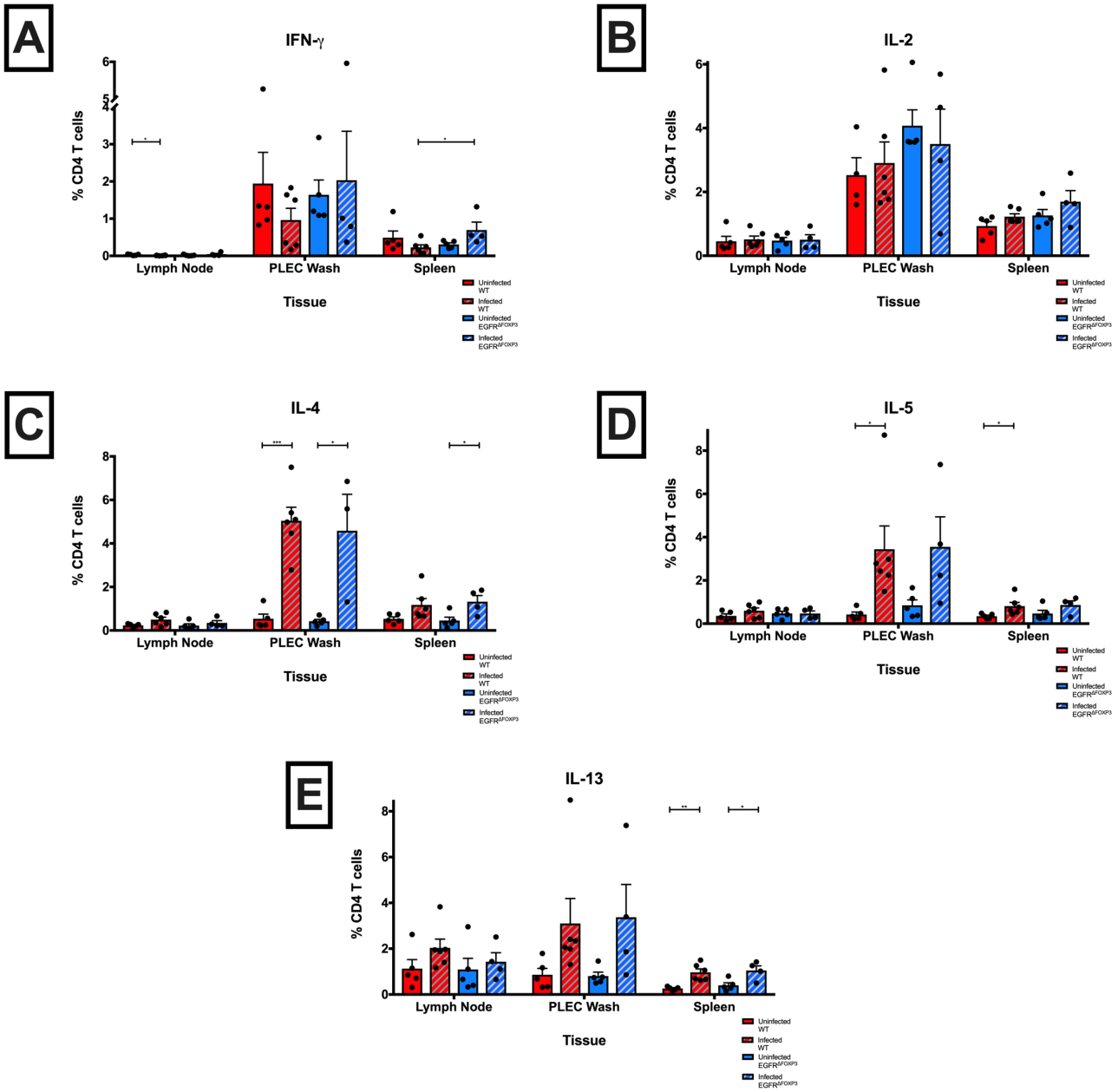

Figure 19-2 Intracellular cytokine staining of CD4⁺ T cells in tLN, PLEC and Spleen of WT and EGFR$^{\Delta FOXP3}$ mice infected with L.sigmodontis or uninfected. A) IFNγ, B) IL-2, C) IL-4, D) IL-5, E) IL-13. Statistical analyses are T-tests.

19.1.3 Effects of EGFR deletion on regulatory T cells in *L.sigmodontis* infection: later T cell responses

We then moved on to analysing the effects of infection at a later timepoint. As expulsion of *L.sigmodontis* adult worms tends to occur roughly at D40 in C57BL/6 mice, we decided to use this as our second timepoint. We infected WT and $EGFR^{\Delta FOXP3}$ mice with 30x L3 larvae as before and culled for analysis at 40 days (NB: We did not include uninfected groups as we were aiming to detect differences between the infected groups as our main readout).

Figure 19-3 shows results for surface staining. PLEC samples from $EGFR^{\Delta FOXP3}$ mice had minor reductions in CD4 and CD8 T cells compared to WT. All tissue samples demonstrated an increase in TH2 cells in $EGFR^{\Delta FOXP3}$ mice compared to WT, but no differences in proportions of Treg or Helios-positive Treg were noted.

To summarise, we saw an increase in TH2 cells in $EGFR^{\Delta FOXP3}$ mice than WT, indicating the response to *L.sigmodontis* infection is pushed in this direction in our $EGFR^{\Delta FOXP3}$ mice; this effect was more pronounced at D40 than at D14.

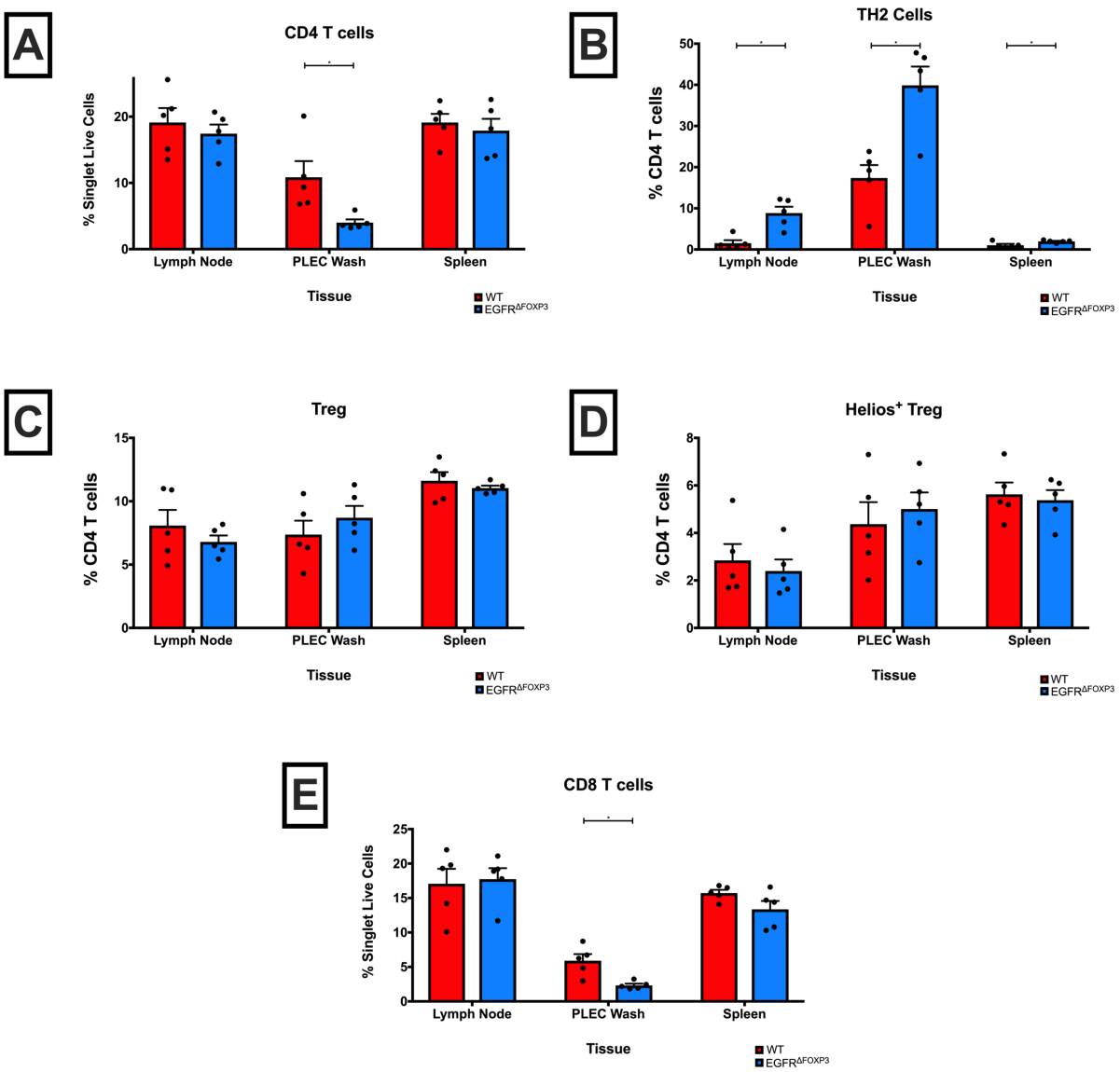

Figure 19-3 Proportions of different T cell populations in tissue samples of WT and EGFR$^{\Delta FOXP3}$ mice infected with L.sigmodontis; Harvest at 40 days postinfection. A) CD4 T cells, B) TH2 cells, C) Treg, D) Treg positive for Helios, E) CD8 T cells. A and E are expressed as percentage of singlet live cells in the sample; B-D are expressed as a percentage of CD4 T cells. Representative of 2 replicates. Statistical analyses are T-tests.

Figure 19-4 shows results for intracellular cytokine staining, where similar to our D14 data, we saw no significant differences between infected WT and $EGFR^{\Delta FOXP3}$ mice (though note the nonsignificant increases of IL-4 and IL-5 expression in $EGFR^{\Delta FOXP3}$ compared to WT samples).

Thus, we conclude that $EGFR^{\Delta FOXP3}$ mice infected with *L.sigmodontis* polarise towards a TH2 response, but that this does not lead to a significant upregulation of Type 2 cytokines in CD4 T cells as a whole.

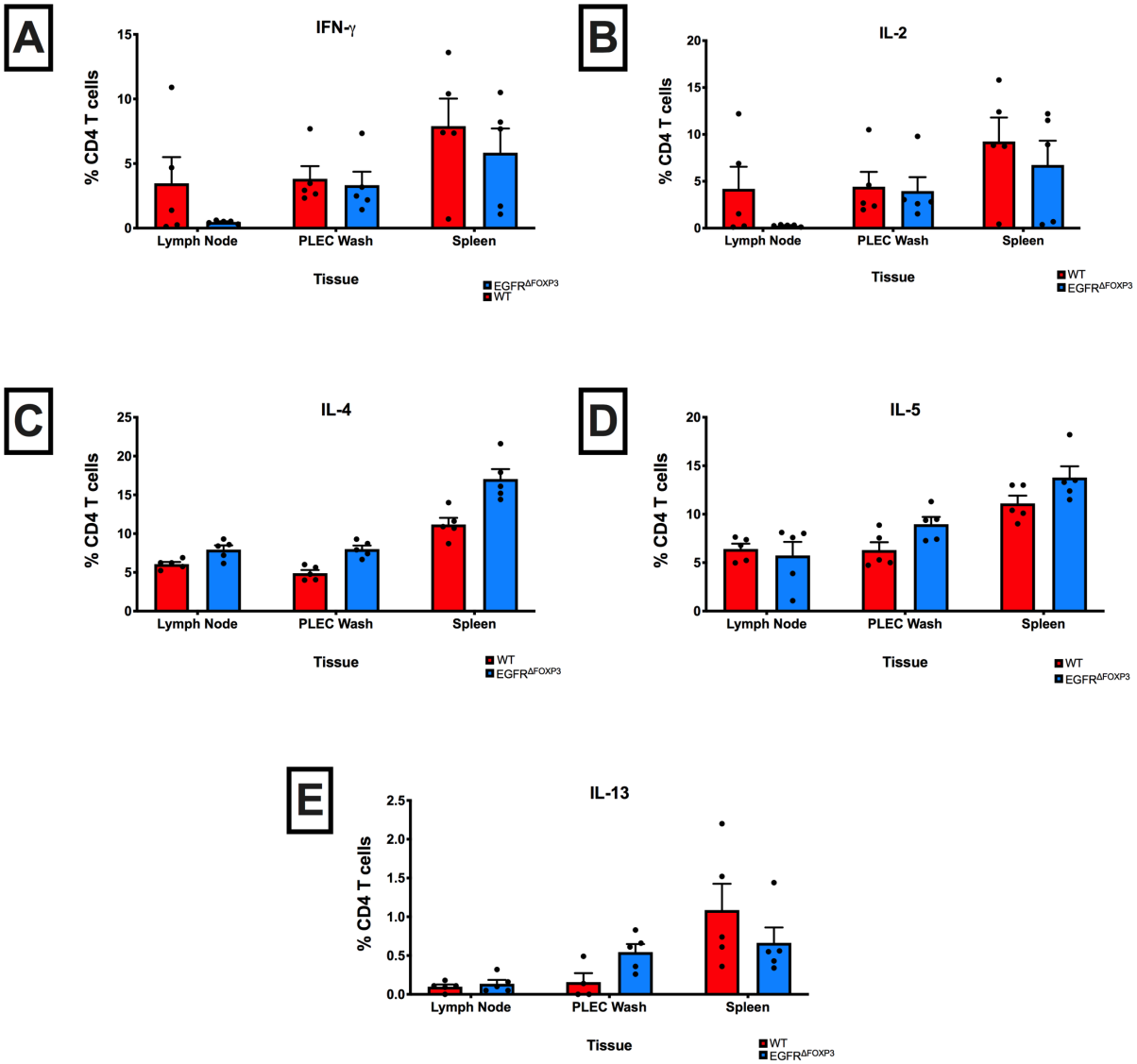

Figure 19-4 Intracellular cytokine staining of CD4⁺ T cells in tissue samples of WT and EGFR$^{\Delta FOXP3}$ mice infected with L.sigmodontis; Harvest at 40 days postinfection. A) IFNγ, B) IL-2, C) IL-4, D) IL-5, E) IL-13. Representative of 2 replicates. Statistical analyses are T-tests.

19.1.4 Effects of Amphiregulin signalling on T cell immune response to *L.sigmodontis*.

Based on the data we obtained with $EGFR^{\Delta FOXP3}$ mice, we hypothesised that the polarisation towards a TH2 response was being driven by AREG-EGFR interactions. AREG-mediated activation of EGFR has been proven to have a significant impact on regulatory T cell function, (Nosbaum et al. 2016; Minutti et al. 2017; Zaiss et al. 2013). As a test of this hypothesis, we infected $AREG^{-/-}$ and $AREG^{fl/fl}$ mice (should be phenotypically wildtype, hence hereafter termed "WT") as per previous experiments, and analysed cell proportions and responses both to each other and uninfected control groups of the same genotype. As this experiment was exploratory, and we were unsure if the $AREG^{-/-}$ phenotype was going to increase or decrease susceptibility to *L.sigmodontis* infection, we also collected adult worms from the PLEC wash for analysis. Harvest date was kept at 40 days.

Figure 19-5 shows the numbers and length of adult worms recovered from PLEC wash of $AREG^{-/-}$ and WT groups (NB: Worm length is indicative of growth and overall health (Taylor et al. 2009)). We saw no significant differences between our 2 groups but note overall numbers of adult worms recovered from the pleural cavity were low.

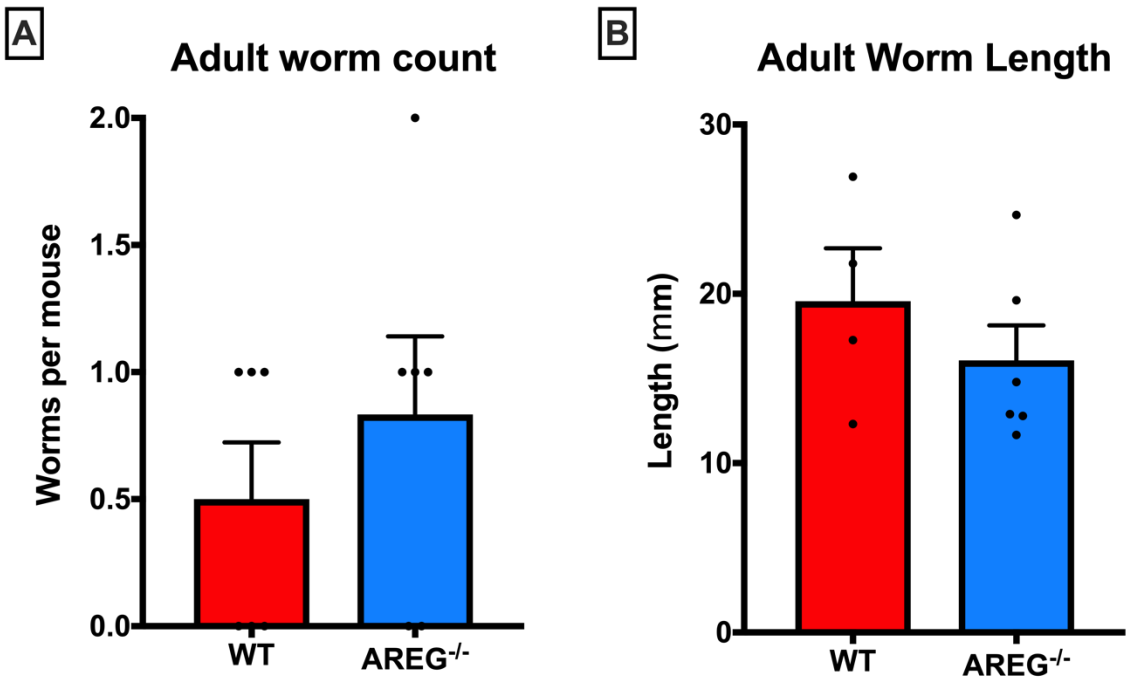

Figure 19-5 A) Number and B) length of adult worms found in the pleural cavity of WT and AREG$^{-/-}$ mice infected with L.sigmodontis. Statistical analyses are T-tests.

We then moved on to FACS analysis. Surface staining revealed a reduction in CD4 and CD8 T cells present in tLN and PLEC (Figure 19-6 A & D), but not spleen samples. There was a greater proportion of TH2 cells in infected samples, but no significant differences between infected WT and AREG$^{-/-}$ groups (Figure 19-6 B). Treg populations did not seem to be significantly different, even between uninfected and infected groups (Figure 19-6 C).

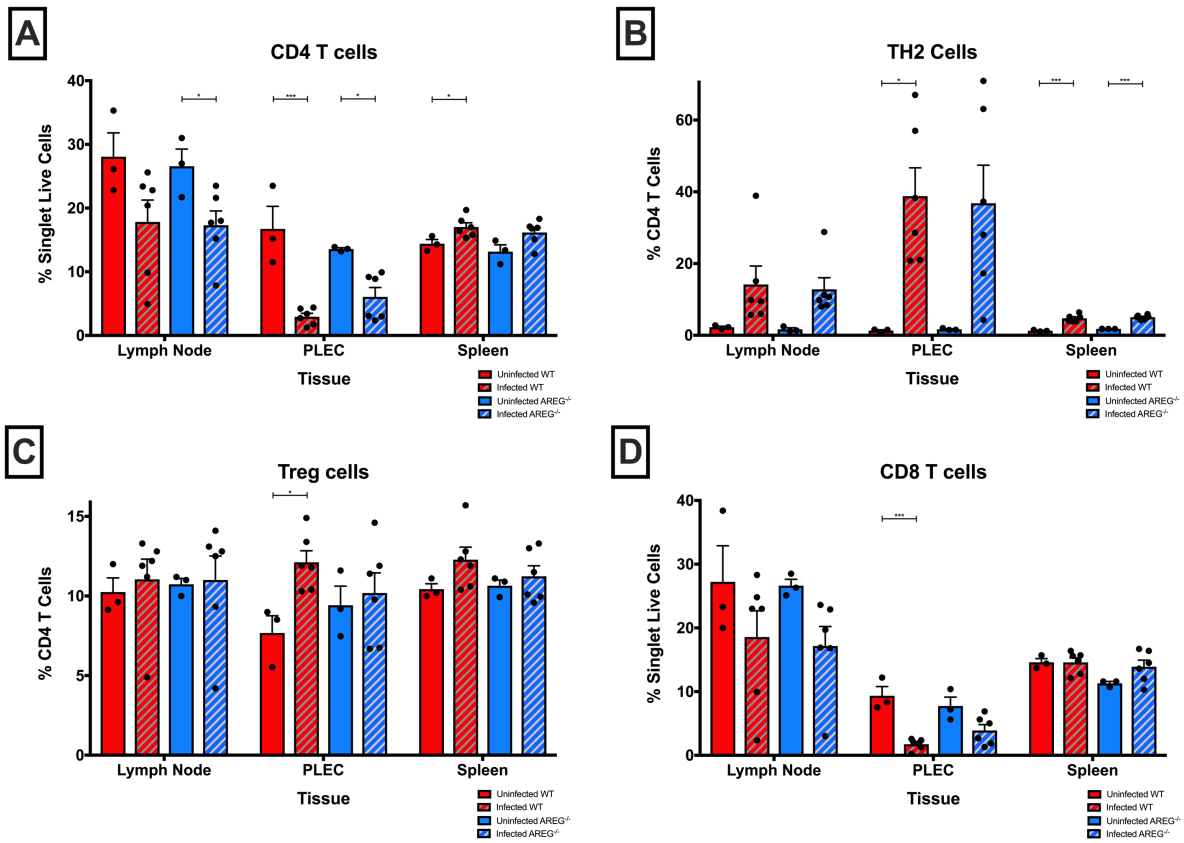

Figure 19-6 Proportions of different T cell populations in tissue samples of WT and AREG$^{-/-}$ mice infected with L.sigmodontis; Harvest at 40 days postinfection. A) CD4 T cells, B) TH2 cells, C) Treg, D) CD8 T cells. A and D are expressed as percentage of singlet live cells in the sample; B & C are expressed as a percentage of CD4 T cells. Statistical analyses are T-tests

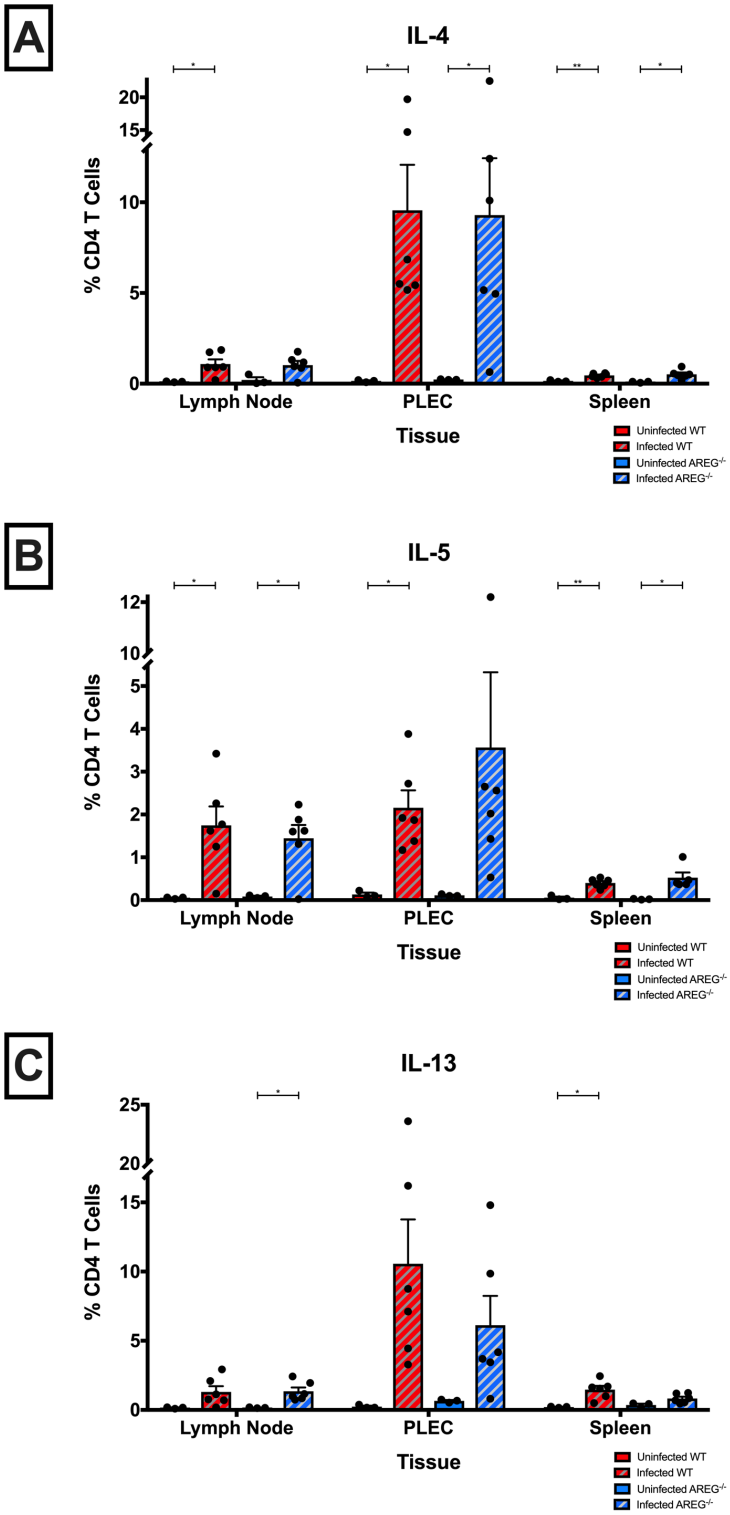

Figure 19-7 Intracellular cytokine staining of CD4^{+} T cells in tissue samples of WT and AREG$^{-/-}$ mice infected with L.sigmodontis; Harvest at 40 days postinfection. A) IL-4, B) IL-5, C) IL-13. Statistical analyses are T-tests.

Analysis for TH2 cytokines showed that infected samples of either WT or AREG$^{-/-}$ mice showed increased percentages of CD4+ T cells expressing IL-4, IL-5 and IL-13 (Figures 19-7 A – C respectively); however, no differences were observed between the infected groups.

These data would indicate that Amphiregulin signalling between T cells is not required for the generation of an immune response to infection with *L.sigmodontis*.

19.2 BALB/c Experiments

When analysing the effects of EGFR blockade with the commercially available EGFR inhibiting TKI Gefitinib, BALB/c mice were used so that they would develop full patent infection, allowing us to assess microfilarial levels and adult worm length/number as well as flow cytometry data.

19.2.1 Establishing tolerance of BALB/c mice to Gefitinib administration

For administering Gefitinib over a long period of time it was decided that gavage would be inappropriate. Instead Gefitinib was be added to the animals' drinking water, which they could consume ad libitum. An initial experiment was performed to

assess if the mice would still consume Gefitinib-laced water at the same rate, with the dose set at 5mg/kg assuming standard consumption rates (see section 18.3.2). Infected and uninfected BALB/c mice given Gefitinib-laced water (Gefitinib group) gained weight at a similar rate to groups with plain water (control group) (Figure 19-8 A), and per-mouse consumption rates averaged over the duration of the experiment did not differ between all four groups (Figure 19-8 B).

Plasma samples were taken from D60-67 and showed no significant differences in microfilaria counts between the 2 infected groups (Figure 19-8 C). Animals were culled at D70; there was no significant difference between the 2 groups in terms of total adult worm count (Figure 19-8 D) or worm length (data not shown). Though the main aim of this initial experiment was to establish if the mice would tolerate Gefitinib administration, we nevertheless performed flow-cytometry on thoracic lymph node, PLEC and spleen cells, analysing proportions of CD4 & CD8 T cells, TH2 cells, Treg, and intracellular cytokine staining for IFNγ, IL-2, IL-4 & IL-5 (in CD4 T cells); no significant differences were observed between the any of the groups (data not shown).

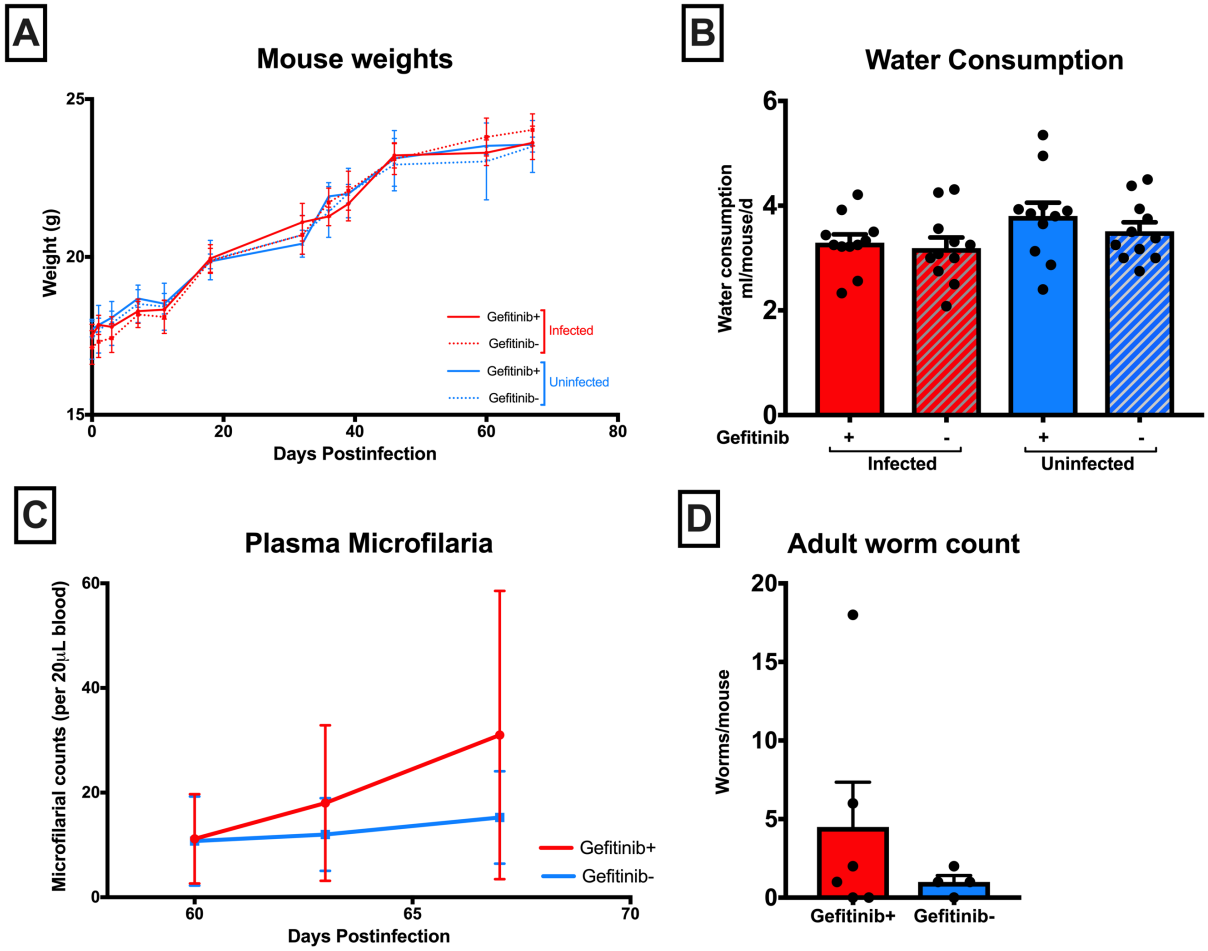

Figure 19-8 BALB/c mice infected with L.sigmodontis and then exposed to Gefitinib 5mg/kg in drinking water 3x weekly, compared to control mice and uninfected groups. A) Weight change over the duration of experiment, B) average water consumption by group, C) Plasma microfilaria in infected groups, D) Number of adult worms obtained from pleural cavity in infected groups at harvest (D70). Statistical analyses are 1-way or 2-way ANOVA, or t-tests as appropriate.

19.2.2 General EGFR inhibition has no significant impact on *L.sigmodontis* infection in BALB/c mice.

As described in 18.3, having established that BALB/c mice would tolerate Gefitinib in their water supply, we attempted to increase the dose to 100mg/kg. However, at this concentration the drug precipitated out of water, and collected at the bottom of the bottle. Therefore, we changed our mode of administration and mixed Gefitinib in with the animals' food, as detailed in 18.3. Again, there were no significant differences in weight between groups (Figure 19-9 A; only weight change in infected groups was documented). From day 55 until harvest at D74, Gefitinib-treated mice had significantly fewer plasma microfilaria compared to controls (analysis by 2-way ANOVA) (Figure 19-9 B). At end of experiment PLEC samples were analysed for both adult worms and microfilariae; there were no significant differences between infected groups (Figure 19-9 C+D).

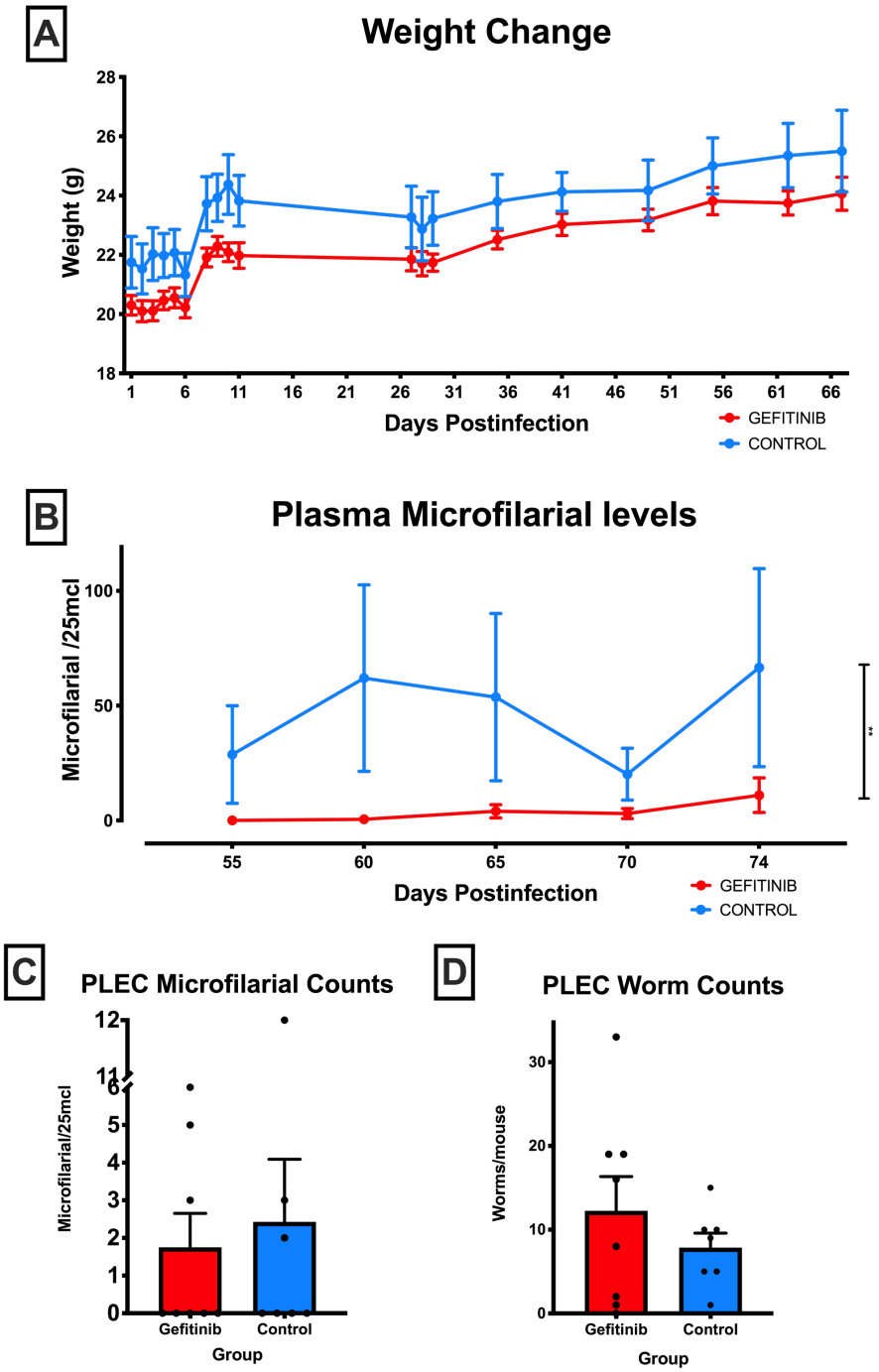

Figure 19-9 BALB/c mice infected with L.sigmodontis and treated with Gefitinib 100mg/kg in food 3x weekly. A) Weight change, B) Plasma microfilaria, C) PLEC microfilaria and D) Adult worms recovered from PLEC at end experiment. Please note uninfected groups were not weighed. Representative of 2 experiments. Statistical analyses are T-test with corrections for multiple comparisons where appropriate, except for B), where 2-way ANOVA was used.

Thoracic lymph node and PLEC samples were analysed for both cell numbers and cytokine staining. There was a trend to increased TH2 cells (by total number) in infected groups in thoracic lymph node, and a significant increase in the infected Gefitinib group compared to both gefitinib only and infected only (Figure 19-10 D). Aside from this, we saw no significant differences in cell proportions of CD4 T cells, CD8 T cells, TH1s, and Tregs (Figure 19-10 A – C & E).

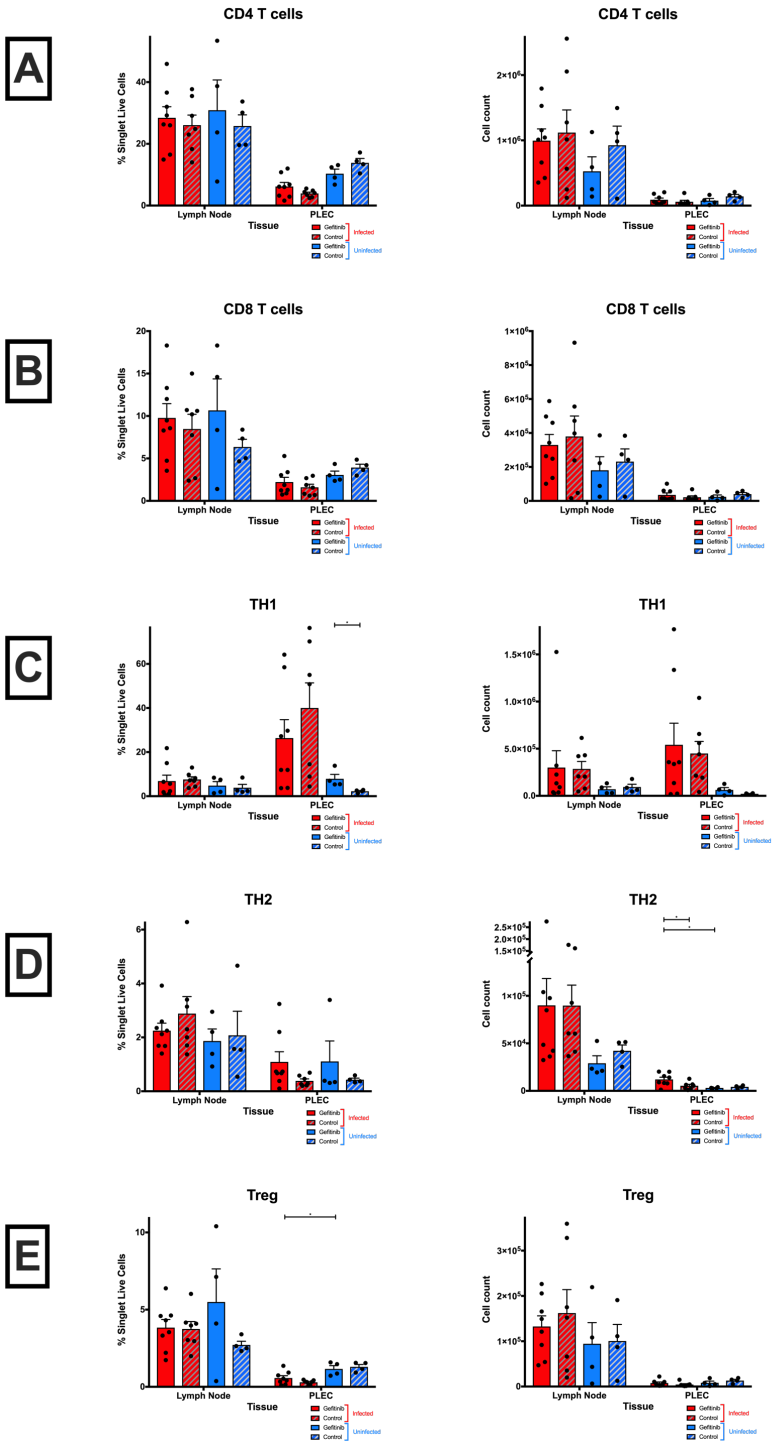

Figure 19-10 Cell proportions in thoracic lymph node and PLEC samples of BALB/c mice infected with L.sigmodontis and exposed to Gefitinib or control, with uninfected groups as comparators. A) CD4 T cells, B) CD8 T cell, C) TH1, D) TH2, & E) Treg cells. Representative of 2 experiments. Statistical analyses are ANOVA with secondary T-testing where appropriate.

We then analysed cytokine production in CD4 T cells (Figure 19-11) and TH2 cells in particular (Figure 19-12). There were no significant differences in cytokine expression in CD4 T cells of infected animals given Gefitinib compared to controls (Figure 19-11 A – E). Hypothesising that TH2 cells might be expressing Type 2 cytokines at an increased level, and that this signal might be masked by a lack of expression in other CD4 T cells, we analysed cytokine expression specifically on TH2 cells (defined as $CD4^+$ $GATA3^+$ lymphocytes). Again, we saw no significant differences in expression of IL-4, IL-5, IL-10 & IL-13 (Figure 19-12 A–D respectively).

From these data we concluded that, at the dose administered to these mice, a general, Gefitinib-mediated blockade of EGFR signalling does not significantly affect the outcome of *L.sigmodontis* infection in BALB/c mice, a known permissive host, and does not affect the function of CD4 T cells in general and TH2 cells in particular.

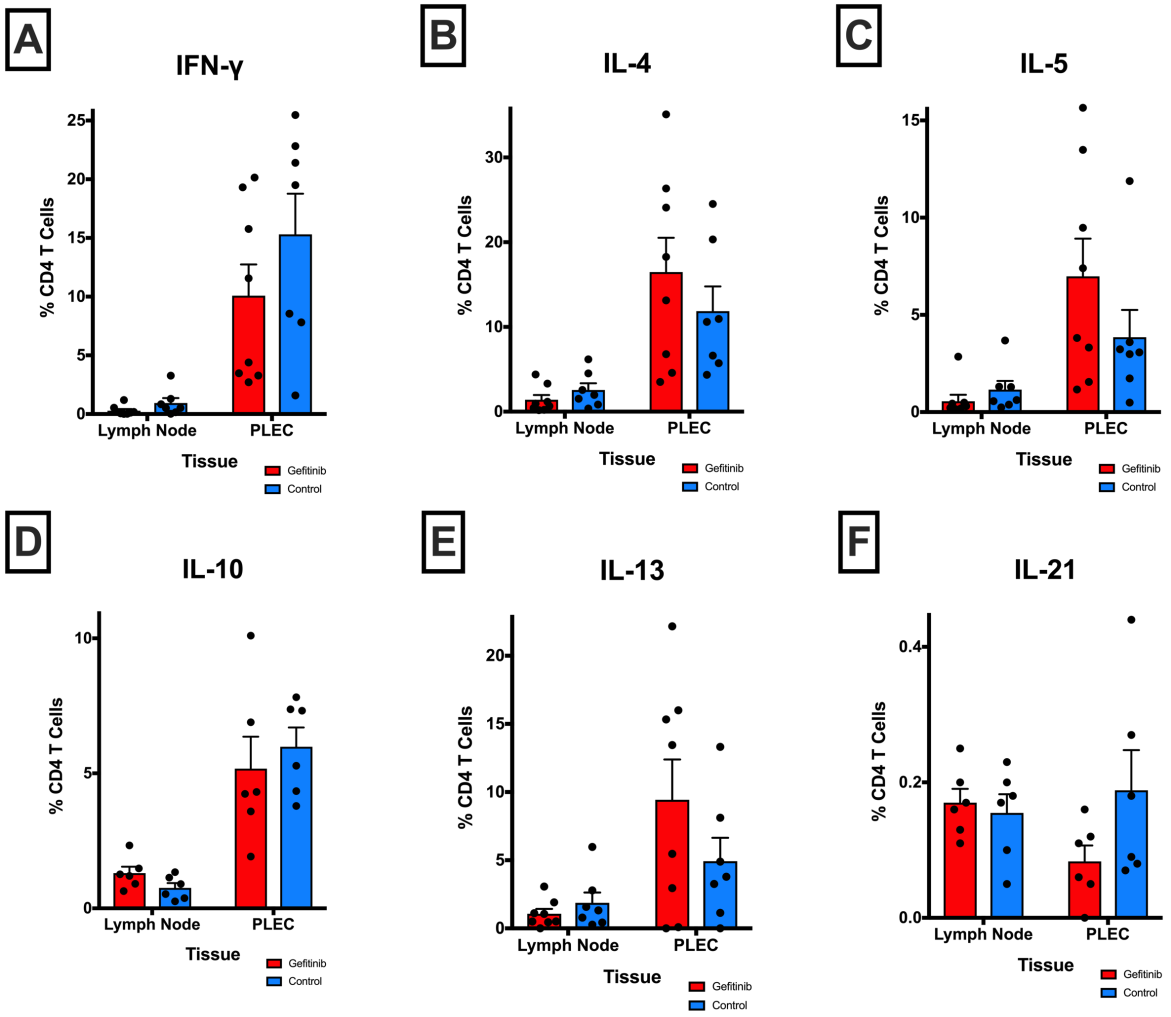

Figure 19-11 Intracellular cytokine staining of CD4 T cells in mice infected with L.sigmodontis in the presence or absence of Gefitinib. A) IFNγ, B) IL-4, C) IL-5, D) IL-10, E) IL-13, F) IL-21. Representative of 2 experiments. Statistical analyses are T-tests.

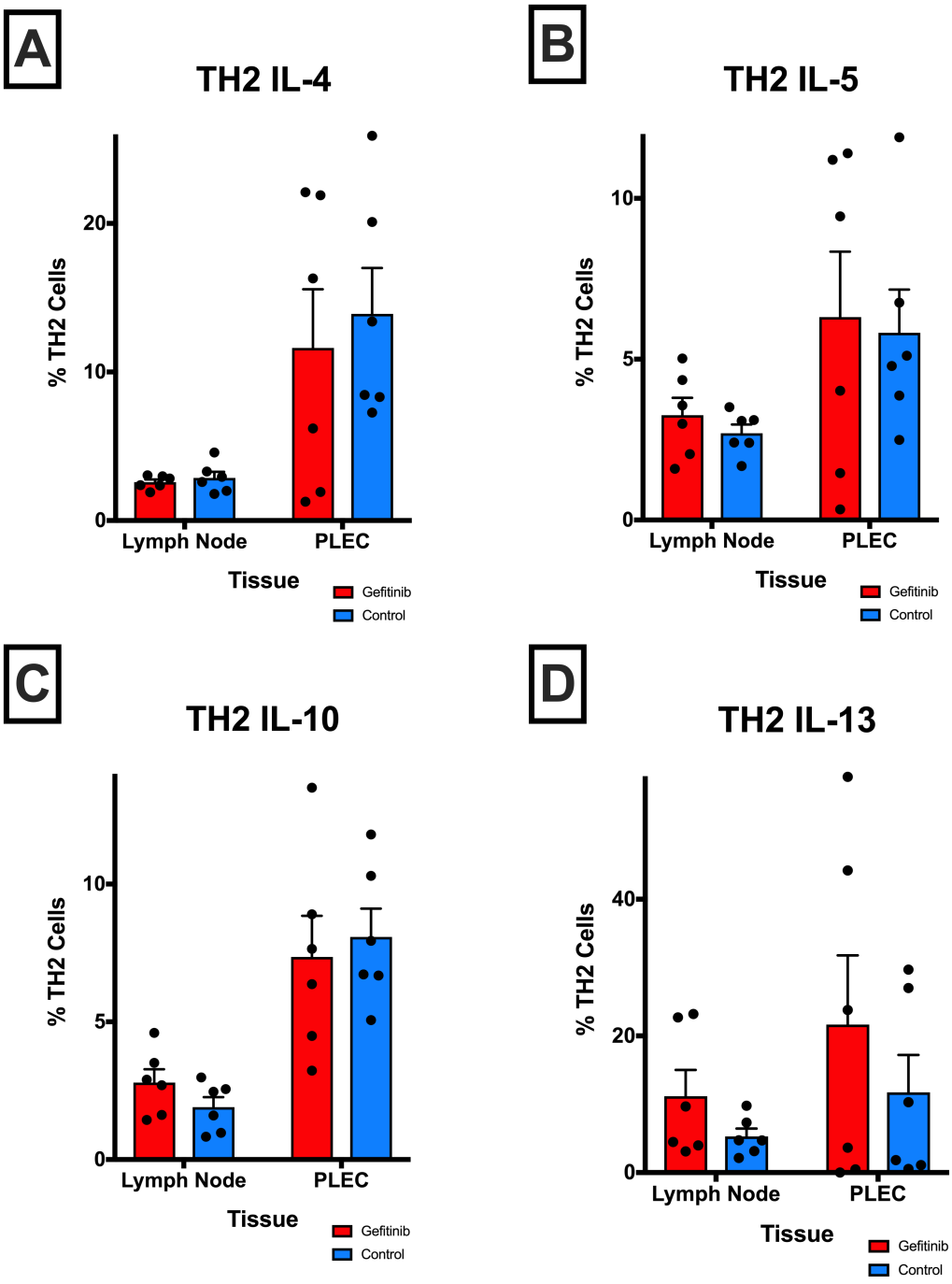

Figure 19-12 Intracellular cytokine staining of TH2 cells in mice infected with L.sigmodontis in the presence or absence of Gefitinib. A) IL-4, B) IL-5, C) IL-10, D) IL-13. Statistical analyses are T-tests.

20 Discussion

Our experiments showed that deletion of EGFR signalling on regulatory T cells biases C57BL/6 mice towards a TH2 response to *L.sigmodontis* infection, which is visible at D40 postinfection but not D14. However, there was no significant increase in expression of Type 2 cytokines in CD4 T cells at D14 or D40 (though there was a nonsignificant trend seen at D40). Mice deficient in Amphiregulin were no more susceptible to *L.sigmodontis* infection than wildtypes, and proportions of T cell subtypes and CD4 T cell Type 2 cytokine staining was similar.

These data would indicate that AREG-EGFR signalling on regulatory T cells is not a significant factor in the immune response to *L.sigmodontis* infection in C57BL/6 mice. Our hypothesis was that by blocking this signal (either by removal of EGFR on Treg or total deletion of *Areg* in the mouse) that Treg would be less activated, less suppressive, and therefore the mice would be more resistant to infection. Though it seems that there is a slight bias in $EGFR^{\Delta FOXP3}$ mice towards a TH2 response, and a trend at around the time of parasite expulsion for more Type 2 cytokine production, the difference between $EGFR^{\Delta FOXP3}$ and WT groups is not large. Also, when Amphiregulin is completely removed from the mouse, no differences are seen either in terms of T cell proportions or parasite length or number when compared to wildtype.

Previous work has demonstrated that Treg expansion predates TH2 response to chronic helminth infection, and that Treg depletion biases the immune response towards TH2 (Taylor, van der Werf, and Maizels 2012). If Treg were receiving an activation/expansion signal via EGFR, then this could explain the mild increase in TH2 cells we saw in $EGFR^{\Delta FOXP3}$ mice at D40. However, it would seem that Amphiregulin at least is not the signal of importance in this model. C57BL/6 is not a permissive host to *L.sigmodontis* infection, and as such we concluded that it was difficult to make them *more* resistant to infection than they already are. We decided to move to BALB/c experiments to study *L.sigmodontis* in a more permissive host.

Wildtype BALB/c mice treated with Gefitinib up to 100mg/kg 3x/week were not less susceptible to *L.sigmodontis* infection than controls, lymphocyte populations were not significantly different, and no significant differences in cytokine staining were observed either in CD4 T cells or TH2 cells.

To study the effects of a general blockade of EGFR signalling, we decided to use Gefitinib, a commercially available agent with a license for use in humans for a variety of cancers where EGFR overexpression is a feature (Carlson et al. 2012; Chen et al. 2013; Costanzo et al. 2011; Dutton et al. 2014; Köhler and Schuler 2013). Concerns surrounding long-term administration of Gefitinib meant that a thrice-weekly dosing schedule was devised; it was hoped that this would ensure enough Gefitinib present in the animals to generate an effect, if one was present. However,

we saw no differences in worm numbers or PLEC microfilaria at harvest; no difference in T cell numbers; and no difference in cytokine expression, either in CD4 T cells or specifically in TH2 cells. There were significantly fewer microfilaria in plasma at various timepoints up until experimental harvest, but this did not translate to fewer PLEC microfilaria or adult worms. Overall, these results would agree with our work in AREG$^{-/-}$ C57BL/6 mice, indicating that EGFR signalling is not an important influence on the behaviour either on Treg or T cells in general.

It is possible that our BALB/c mice were underdosed with Gefitinib: When the drug was added to water mice drunk at the same rate as controls; however, it was not possible to weigh food pots when we moved to administration in food (the mice would throw food around the cage, and the pots were contaminated with sawdust), and so we used weight gain throughout the experiment as a proxy for food consumption. This has the flaw that if the mice ate less on the days they were given Gefitinib-laced food, and over-ate on subsequent days, they could still have gained weight whilst not consuming the drug. Additionally, our calculations were based on average energy requirements, food consumption rates and desired drug dose per unit bodyweight; we had no guarantee that an individual mouse would be consuming this amount of food, and it is likely that there was variability in terms of actual drug delivered to any one individual. The use of 100mg/kg was intended to partially combat this (as well as being close to the equivalent dose used in humans), as effects have previously been seen using doses of 50mg/kg (Zheng et al. 2016; Song et al. 2016), albeit when administered in the short term.

Taken as a whole, we conclude that endogenous AREG-EGFR signalling on Treg (or Amphiregulin signalling in general) is not a significant factor in the context of *L.sigmodontis* infection either in a permissive or resistant host.

21 Supplemental Data

21.1 Time course of *L.sigmodontis* infection in C57BL/6 mice.

Animals were infected on the same date, and separate harvests at D7, D14 & D21 were performed. Cell proportions and CD4 cytokine staining results are given below.

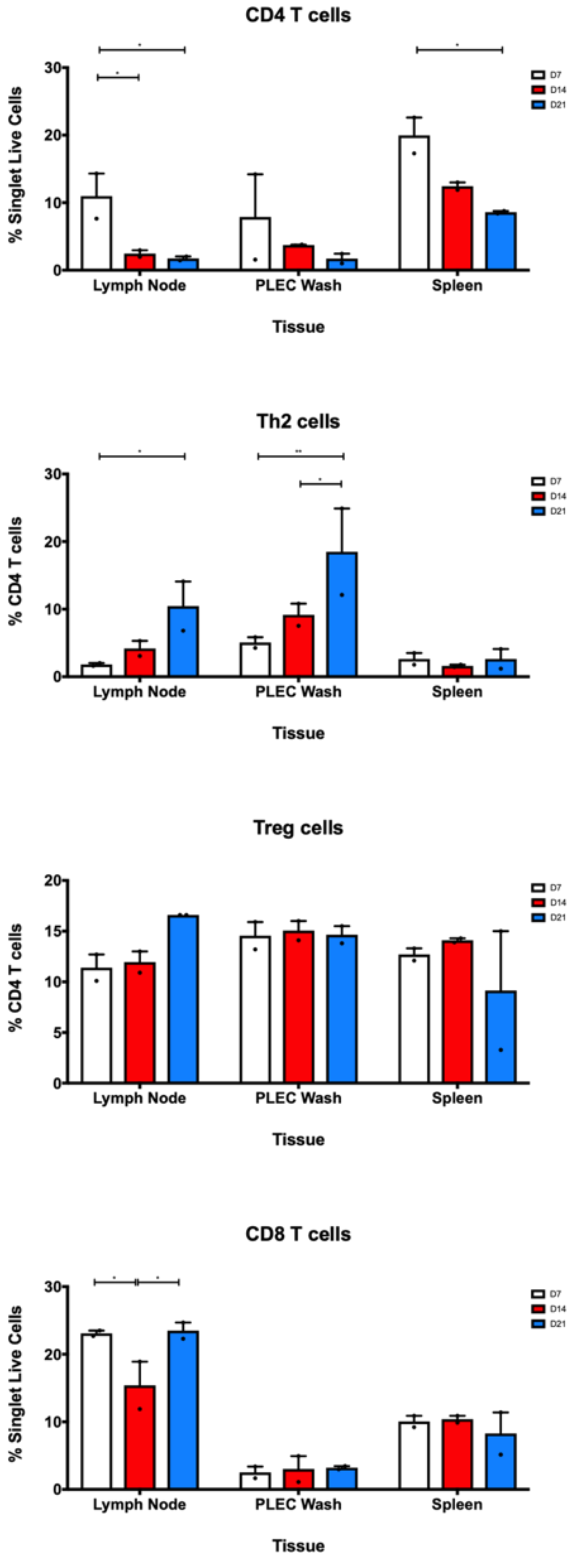

Figure 21-1 Cellular makeup of thoracic lymph node, PLEC wash and Spleen in C57BL/6 mice infected with L.sigmodontis. Analyses are t-tests with Bonferroni correction.

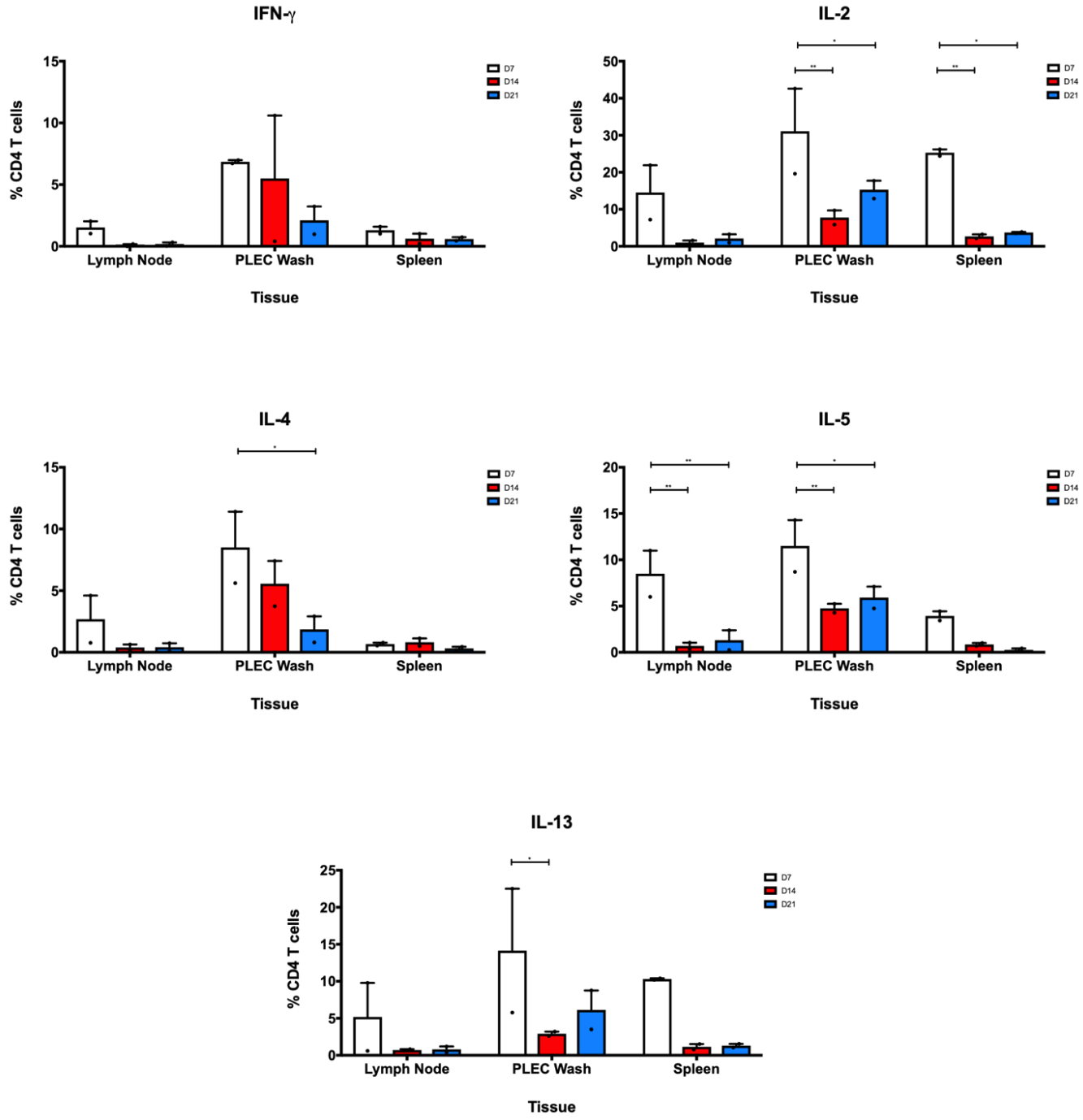

Figure 21-2 Cytokine Expression in thoracic lymph node, PLEC wash and Spleen of C57BL/6 mice infected with L.sigmodontis. Analyses are t-tests with Bonferroni correction.

Chapter 4: Determination of the cellular source of Amphiregulin in the lungs during a murine asthma model

22 Abstract

Previous work from the Maizels group with the murine helminth *Heligmosomoides polygyrus* has shown that *H.polygyrus* infection induces systemic Treg expansion, which can then suppress inflammation in an airway challenge model of lung inflammation. Exploratory work in my laboratory group noted that this effect was diminished in *Areg*$^{-/-}$ mice, implying that Amphiregulin-EGFR signalling was a cause of Treg activation in the lungs. Confirming this finding, and determining the cellular source of Amphiregulin, was the aim of this chapter.

We performed an airway sensitisation and challenge with Ovalbumin and compared wildtype and various transgenic strains of C57BL/6 mice that were either infected or uninfected with *H.polygyrus*. We did not see a decrease in BAL cellularity in animals infected with *H.polygyrus*, in contrast to previous experimentation.

Furthermore, deletion of EGFR on Tregs had no discernible effect on airway hyperresponsiveness. Additionally, deletion of Amphiregulin expression, either globally or in specific cell types, had no effect on cellularity or cell proportions. Infection with *H.polygyrus* promoted an increase in TH2 cytokine production but did not significantly alter cellularity in bronchoalveolar lavage fluid. We conclude that, as the initial finding of Treg-induced suppression of airway inflammation (obtained by

infecting mice with *H.polygyrus*) was not seen, that further interpretation of data is impossible.

23 Introduction

23.1 Asthma is a chronic TH2 inflammatory condition

Asthma is a chronic lung condition, thought to be multifactorial in origin, that affects an estimated 334m people worldwide (Global Asthma Network 2014; Stefan et al. 2019). It is an important cause of disability and death globally, and considerable efforts have gone towards understanding the immunological mechanisms that are involved in the pathogenesis of asthma (Song et al. 2016). The Hygiene Hypothesis is the idea that early exposure to pathogens 'trains' the immune system to recognise antigens correctly, and therefore reduces the risk of harmless antigens (e.g. house dust mite or pollen) being misidentified as serious (Brooks, Pearce, and Douwes 2013). Individuals not exposed to sufficient amounts of pathogen become atopic, and prone to develop the conditions eczema, allergic rhinitis and allergic asthma. These conditions are typified by a biased, TH2 response and in the case of asthma, infiltration of eosinophils, mast cells and lymphocytes into the lungs (Song et al. 2016). A role for early childhood infections, notably RSV, has been highlighted (Krishnamoorthy et al. 2012; Jackson et al. 2008).

Because of asthma's global importance, mouse models have been developed to mimic the disease; mice are exposed to an allergen (typically Ovalbumin or house dust mite antigen), and then challenged a short time later with this antigen, typically by nebulisation (though other methods are available, and are more invasive) (Reddy,

Lakshmi, and Reddy 2012; Stumm et al. 2011). Typical results show an infiltration of eosinophils, neutrophils and lymphocytes, but similar numbers of alveolar macrophages (Reddy, Lakshmi, and Reddy 2012).

23.2 *Heligmosomoides polygyrus* upregulates regulatory T cells *in vivo*

As previously discussed in Chapter 3, helminths have a range of mechanisms to evade and manipulate the immune system to their own advantage. These mechanisms typically involve specific cells such as regulatory T cells, regulatory B cells and TH2 cells, and commonly alter the expression of TH2 cytokines and the anti-inflammatory molecules IL-10 and TGFβ to promote an immunotolerant environment (McSorley, Hewitson, and Maizels 2013).

Heligmosomoides polygyrus is a gastrointestinal helminth parasite of mice, and an analogue of hookworm in humans (Reynolds, Filbey, and Maizels 2012). Due to the ease of maintaining the life cycle in the lab, as well as the relatively mild pathology in infected mice, *H.polygyrus* has been developed as a model for induction of TH2 and Treg responses, as well as the analysis of the effects of secreted helminth products on the host (Reynolds, Filbey, and Maizels 2012; Camberis, Le Gros, and Urban 2003; Johnston et al. 2015).

The life cycle of *H.polygyrus* has been described in Johnson et al. (Johnston et al. 2015): eggs from an infected host are passed in faeces, where they hatch in the environment after 24h into L1 larvae. After 2-3 days they moult to L2 larvae and begin feeding on environmental bacteria. Within another 3 days they moult once more into L3 larvae, where they are ready for ingestion by a murine host. Once ingested, L3 larvae migrate to the duodenum where they form a cyst by day 5 postinfection. Returning to the intestinal lumen by D8 as adults, they then mate and start producing eggs, which appear in the faeces by D14. Cambergris et al. have details of how to maintain the *H.polygyrus* life cycle in the laboratory (Camberis, Le Gros, and Urban 2003). It should be noted that C57BL/6 mice are more susceptible to *H.polygyrus* infection, as opposed to BALB/c mice, who are resistant, i.e. this is the opposite situation to that of *L.sigmodontis* infection.

Mice infected with *H.polygyrus* adopt an immunosuppressive phenotype, with downregulated allergic and autoimmune responses. Regulatory T cells are more populous and activated, B cells are hyperstimulated and antigen-presenting cells are skewed in phenotype so as to produce an tolerant form of TH2 immunity (Maizels et al. 2012). Despite this, TH2 cytokines such as IL-4 and IL-13 are essential for parasite clearance, which occurs at any time between 4 and 20 weeks depending on mouse strain susceptibility (Reynolds, Filbey, and Maizels 2012; Camberis, Le Gros, and Urban 2003). In particular, mast cells appear to be important for clearance of

H.polygyrus, as mast-cell deficient mice show impaired TH2 priming, and reduced levels of IL-25 and IL-33 (Hepworth et al. 2012). Finally, recent work in our lab has shown that IL-13 mediated clearance of *H.polygyrus* is dependent on signalling both from Amphiregulin-EGFR and IL-33-T1/ST2 signalling complexes, as both signals had to be present for the production of IL-13 from TH2 cells (Minutti et al. 2017).

23.2.1 HES

The main way *H.polygyrus* affects the immune system appears to be via the excretion of a variety of factors that affect the host, termed *H.polygyrus* Excretory-Secretory products, or HES (Maizels et al. 2012). In particular there is evidence that HES contains a mimic of TGFβ that, though structurally distinct from mammalian TGFβ, appears to be functionally identical, and induces the proliferation of Treg in the host (Johnston et al. 2017; Smyth et al. 2018; Grainger et al. 2010). HES has been used in a murine asthma model by McSorley et al., where addition of HES to OVA immunisation steps resulted in increased numbers of Treg in the bronchoalveolar lavage, fewer effector T cells and eosinophils, and fewer TH1, TH2 and TH17 cytokines, particularly IL-5 (McSorley et al. 2012). This is in addition to TGFβ produced by Tregs induced by *H.polygyrus* infection (Grainger et al. 2010), which has been seen in asthma modelling also (Wilson et al. 2005). Due to the fact that HES can be administered without the need to infect the target animal, and is more practical than the adoptive transfer of regulatory T cells (Wilson et al. 2005; Grainger

et al. 2010), researchers have been exploring its use as an immunomodulator (Maizels et al. 2012).

23.3 Treg-mediated immunosuppression of immune responses in a mouse asthma model is dependent on Amphiregulin-induced EGFR signalling

Previous work done by Dittrich et al. has highlighted the effects of Treg induction in this asthma model: Working with *L.sigmodontis*, they showed that Treg induction led to decreased airway hyperresponsiveness, BAL eosinophilia, TH2 cytokine production and increases of both Treg cells and TGFβ secretion overall (Dittrich et al. 2008). These effects were reversed partially or fully by TGFβ blockade or Treg depletion. Similarly, RSV infection has been correlated with impaired Treg function, which seems to lead to worsening asthma due to Treg cells class-switching to a TH2 phenotype (Krishnamoorthy et al. 2012).

Previous work performed by colleagues has shown that induction of Treg by coinfecting mice with *H.polygyrus* led to reduced lung infiltrates in a model of lung inflammation using both ovalbumin and house dust mite allergen, and that this was reversible with the use of an anti-CD25 antibody to deplete Treg (Wilson et al. 2005). Additionally, it was shown that IL-10 was dispensible for Treg-mediated

immunosuppression in this model, implying that TGFβ was the likely effector molecule of Treg-mediated inhibition of cellular infiltration. This role for TGFβ was also seen by Dittrich et al. HES-induced Tregs also suppress airway inflammation in asthma modelling (Grainger et al. 2010); as stated previously, HES also contains a TGFβ mimic, termed TGM, which induces Tregs *in-vivo* (Johnston et al. 2017).

We have previously shown that Treg express the EGFR under inflammatory conditions, and respond to Amphiregulin in a source-specific manner (Zaiss et al. 2013). Noting the above, we wondered if Amphiregulin-mediated EGFR signalling was important in the above asthma model. Preliminary work was performed in the Netherlands with wildtype and *Areg*$^{-/-}$ mice (by Dietmar Zaiss and Erinke Van Grisven), using ovalbumin as the sensitisation agent. They found that when WT mice were infected with *H.polygyrus* that there was a general reduction in BAL cellularity, in particular eosinophils; when *Areg*$^{-/-}$ mice were used, this effect was not seen, implying that Treg-mediated suppression of BAL infiltrate was dependent on Amphiregulin signalling. Determining the cellular source of Amphiregulin-mediated EGFR signalling in this model system was the aim of this chapter.

24 Hypothesis

We wished to determine which cellular population is the source of Amphiregulin-mediated EGFR signalling for regulatory T cells in a mouse airway inflammation model.

25 Methods

25.1 Animal strains used

C57BL/6J mice of various genotypes (see table 25-1) were bred and maintained at the University of Edinburgh in specific-pathogen free conditions. All mice were housed in individually ventilated cages at the Ashworth 3 Level 5 animal unit, King's Buildings, University of Edinburgh, until required for experiments, when they were transferred to the March Building, King's Buildings Campus, University of Edinburgh. Both sexes were used for experiments, but all mice in one experiment were of the same sex. Mice were 6-8-weeks old at the start of the experiment. Cages were randomly assigned to a treatment group; mice were not randomised within the cages themselves, but mice of different genotypes could be co-housed within the same cage. Experiments were performed in accordance with the United Kingdom Animals (Scientific Procedures) Act of 1986, and all researchers were accredited by the UK Home Office. Dispensation to carry out animal research at The University of Edinburgh was approved by the University of Edinburgh Animal Welfare and Ethical Review Body and granted by the UK government Home Office; all research was carried under the project licence 70/8470. All *in-vivo* experiments were conducted with groups of 5-7 animals unless otherwise stated.

Genotypes of mice used in this experiment were as follows:

Genotype	Phenotype
WT, *Egfr*$^{fl/fl}$ or *Areg*$^{fl/fl}$	Wildtype controls
Areg$^{-/-}$	Deletion of Amphiregulin signal from all cells
Areg$^{fl/fl}$ *x LysM*^{cre}	Deletion of Amphiregulin signal originating from Alveolar Macrophages
Areg$^{fl/fl}$ *x ROR*α^{cre}	Deletion of Amphiregulin signal originating from ILC2 cells
Egfr$^{fl/fl}$ *x FoxP3*^{cre}	Deletion of EGFR receptor on Treg

Table 25-1 List of transgenic strains of C57BL/6 mouse used to determine the cellular source of Amphiregulin in a murine lung inflammation model.

25.2 Heligmosomoides polygyrus

H. polygyrus and was maintained by serial passage through F1 mice (C57BL/6xCBA) as described previously (Johnston et al. 2015). L3 Larvae were stored in distilled water and refrigerated until ready for use. Life cycle was kindly maintained by Ms Elaine Robertson, of the Buck Laboratory, University of Edinburgh. On the day of infection, 200 L3 larvae (in 200μl distilled water) were administered to mice by oral gavage with a blunt-tipped needle.

25.3 Ovalbumin administration

This procedure has been described previously (Reddy, Lakshmi, and Reddy 2012). For sensitisation to ovalbumin (OVA), Grade V Ovalbumin was purchased (#A5503-5G, Sigma-Aldrich), and dissolved in PBS to a stock concentration of 1000μg/ml. A sensitisation dose of 10μg was used, dissolved 1 in 5 with PBS (i.e. 10μl OVA stock and 40μl PBS); this solution was mixed 1:2 with Alum (Imject Alum, #77161, Thermo Fisher) to give a final dose of 10μg OVA in 100μl. This was administered to mice via intraperitoneal injection on 2 occasions, at least 14 days apart, with the 2nd injection at least 7 days prior to nebulised exposure to OVA.

21 days after the first OVA injection, nebulisation occurred daily as follows: OVA nebulisation solution was composed of OVA stock diluted 1:10 in PBS, giving a concentration of 100μg/ml. 10ml of this was used on any one occasion. Mice were placed (maximum 15 at a time) into a nebulisation chamber and exposed to aerosolised ovalbumin for 20 minutes. Nebulising air driver was an Omron CompAIR; Nebulising chamber was PARI LC Star Reusable Nebulizer Set. Mice were observed throughout the nebulisation period for signs of distress, and also for a short period of time after returning to their cage.

25.4 Experimental Procedure

We gavaged mice of various genotypes with H.polygyrus in PBS or PBS alone, and then the following day started our sensitisation process to Ovalbumin as stated above. See figure 25-1 for details of timeline. 26 days after the first exposure to OVA i.p. the animals were harvested for analysis.

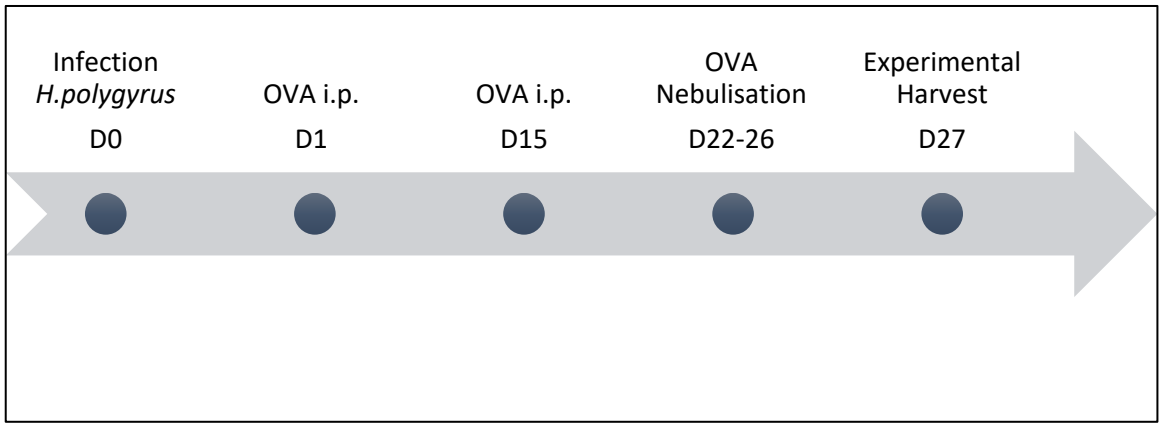

Figure 25-1 Timeline of Ovalbumin experiments. In some experiments H.polygyrus infection was carried out up to 14 days prior to the first dose of intraperitoneal ovalbumin.

25.5 Experimental Harvest

25.5.1 Culling

Animals were sacrificed by injection of 150μl of Pentobarbital (Euthatal 200mg/ml, Merial). After cessation of movement and heartbeat, animals were confirmed dead by dislocation of the neck.

25.5.2 Adult worm acquisition from bowel

The abdomen and thorax were opened by dissection with scissors, and the front ribs and sternum removed. An incision was made distal to the stomach, and the small and large intestine blunt-dissected up to the level of the caecum, where a second incision was made. Intestinal samples were collected into PBS. Adult worm burdens were later determined by exposing the intestinal lumen by dissection. Counting was performed by Ms A Fulton with a microscope.

25.5.3 Bronchoalveolar Lavage Acquisition

This method was based on a previously published protocol (Maus et al. 2001). After opening the thoracic cavity (to allow the lungs to expand fully during lavage), the neck was dissected open and the musculature surrounding the trachea removed. A White needle (19G, 1.1 x 40mm) was gently inserted into the tracheal lumen, and the

needle was clamped with artery forceps roughly 2mm proximal to the bevel. Using a 1ml syringe, serial lung lavages were performed using 500μl BAL buffer (see Section 3.8). Each 500μl wash was pushed in then aspirated 3 times before collection into a 1.5ml Eppendorf tube. This was repeated 3 more times, aiming to obtain a total of 1500μl fluid. Samples were placed on ice until analysis.

25.6 Flow Cytometric sample preparation and analysis

25.6.1 Sample preparation

Single cell suspensions were prepared as follows: samples were centrifuged (300g, 5min, 4°C) and resuspended in 210μl complete IMDM; 10μl was taken for cell counting, and 100μl into FACS tubes (for intracellular cytokine staining). the remainder aliquoted into a 96-well plate and used for surface staining.

25.6.2 Surface Staining

Samples contained in a 96-well place were centrifuged (300g, 5min, 4°C), the supernatant removed, and samples resuspended in 150μl PBS. Samples were then centrifuged again (300g, 5min, 4°C), supernatant removed, and the cell pellets loosened using a plate shaker.

Following this, samples were viability stained (IndoBlue, see section 25.8) for 10 minutes at room temperature, then stained with Fc block and antibodies for surface markers (see section 3.8), 50μl/well, for 30 minutes at 4°C. Following this, wells were 'washed' with 100μl FACS buffer, centrifuged (300g, 5min, 4°C) and the supernatant removed; this was repeated one more time. Samples were then placed in Paraformaldehyde 2% (100μl/well) and fixed for 20 minutes, before washing with 100μl FACS buffer, centrifugation (300g, 5min, 4°C) and resuspension in 150μl FACS buffer. Samples were stored at 4°C until analysis.

25.6.3 Intracellular Cytokine Staining

Samples were incubated (37°C, 5% CO2) for 6h in 200μl complete IMDM with a stimulatory anti-CD3 antibody (#553058, BD Pharmingen) at a concentration of 2μg/ml, and monensin 10μM (Invitrogen). This was performed in FACS tubes.

Following this, samples were washed in 3ml FACS buffer, centrifuged (5m, 300g, 4°C) and resuspended in 150μl PBS, then transferred to a 96-well plate. Samples were then viability stained (Zombie Aqua, see section 25.8) and left at room temperature for 10 minutes. Following this, samples were stained with antibodies for surface markers for CD4 and CD8 (see section 25.8) and incubated at 4°C for 30 minutes. For intracellular staining, samples were fixed with 2% paraformaldehyde (in PBS) 100μl/well at room temperature for 20 minutes, centrifuged (5m, 300g, 4°C)

and resuspended in 100μl FACS buffer; this was repeated once more. Samples were then centrifuged again and resuspended in 100μl 0.5% Saponin at room temperature for 20 minutes to permeabilise the cells. Following this samples were centrifuged (5m, 300g, 4°C) and resuspended in 50μl 0.5% Saponin containing antibodies to intracellular cytokines and incubated for 30 minutes at 4°C. Following this samples were washed in FACS buffer as detailed above and fixed in 100μl 2% paraformaldehyde (in PBS) for 20 minutes at room temperature, before resuspension in 150μl FACS buffer.

25.6.4 Flow Cytometry Analysis

Samples were analysed by flow cytometry using a BD FACSCanto flow cytometer and FlowJo software v10.3 (FlowJo LLC).

Cells were identified after gating for singlets and live cells, and CD45 positivity for surface staining. Cell types were then identified as follows:

Panel 1:

- CD4 T cells: Lymphocyte (FSc x SSc) / CD3+ / CD4+
- CD8 T cells: Lymphocyte (FSc x SSc) / CD3+ / CD4-
- B cells: Lymphocyte (FSc x SSc) / CD19+
- Alveolar Macrophages: CD11c + / SigF + / F4/80 +
- Neutrophils: Ly6G +
- Eosinophils: CD11c - / SigF +
- Monocytes: Ly6G - / Ly6C +

Panel 2:

- ILCs: Lin- (BV421) / CD11c- / CD11b- / CD90.2+
- Dendritic cells: Lin- (BV421) / CD11c- / MHCII+
- Mast cells: Lin- (BV421) / FCεRI+ / c-kit+
- Basophils: Lin- (BV421) / FCεRI+ / CD49b+

Intracellular cytokine staining samples were gated as follows: Singlets – Live – Lymphocyte gate on FSc x SSc – CD4 & CD8, followed by intracellular cytokine staining.

25.7 Statistical Analysis

Student's t-test was performed with GraphPad Prism 7 (GraphPad Software Inc.), with corrections for multiple comparisons where appropriate (See figure legends for details). Significant results were reported as follows: * = $p<0.05$, ** = $p<0.01$, *** = $p<0.001$.

25.8 Recipes

BAL wash:

- PBS 40 ml
- BSA 1% 10 ml (BSA 5% stock)
- EDTA 0.01mM 1 μl (EDTA 0.5M stock)

FACS Buffer (PBS with 2% FCS):

- PBS 500ml
- Fetal Calf Serum 10ml

Viability Stains:

- Intracellular cytokine stains:
    - Zombie Aqua Fixable Viability Kit, #423101, Biolegend
    - Dilute 1:500 in PBS, use 20μl per well.
- Surface stain for cellular characterisation in BALF samples:
    - Live/Dead Fixable Blue Dead Cell Stain Kit, L34961, Invitrogen
    - Dilute 1:300 in PBS, use 10μl per well.

Surface Staining Recipe (per sample):

- FACS buffer: 50μl
- Fc Block (1mg/ml) 0.25μl
- Surface Antibody 1:200 0.25μl

Intracellular Cytokine Staining Recipe (per sample):

- 0.5% a (in FACS buffer): 50μl
- Intracellular antibody 1:200 0.25μl

Antibodies used:

Antigen	Fluorophore	Product code	Manufacturer
CD3	BV421	100228	Biolegend
CD4	AF700	100536	Biolegend
CD4	FITC	11-0041-82	eBioscience
CD8	PCP/Cy5.5	100734	Biolegend
CD8	PE	553032	BD Pharmingen
CD11b	BV711	101241	Biolegend
CD11c	BV605	117334	Biolegend
CD19	APC	17-0193-82	eBioscience
CD45.2	PCP	108926	Biolegend
F4/80	Pe-Cy7	25-4801-82	eBioscience
IFNγ	FITC	505806	Biolegend
Ly6c	AF700	128024	Biolegend
Ly6g	APC-Cy7	127624	Biolegend
SiglecF	PE	552126	BD Pharmingen
IL-5	APC	504306	Biolegend
IL-13	PcPeFl710	46-7133-82	eBioscience
MHC-II	FITC	11-5321-82	eBioscience
CD49b	PE	558759	BD Biosciences
ckit	PeCy7	105813	Biolegend
FCεRI	APC/AF647	134309	Biolegend
CD90.2	APC-Cy7	105327	Biolegend
Lineage negative gate (Panel 2):	BV421	CD3: 100228 CD19: 115538 SigF: 562681 Ly6G: 127628 NK1.1: 108731	Biolegend Biolegend BD Horizon Biolegend Biolegend

26 Results

26.1 Deletion of EGFR on regulatory T cells does not affect total BAL cellularity

To determine the effects of deleting the EGFR signalling pathway on Tregs in a lung asthma model, we infected WT and EGFR$^{\Delta FOXP3}$ mice with *H.polygyrus*, and then sensitised them to ovalbumin (OVA) on D1 + D15 as described above. We then exposed the mice to nebulised OVA daily from D22-26 and culled for analysis on D27. Due to issues around colony health, we did not have enough female mice of genotype *Egfr$^{fl/fl}$ x FoxP3^{cre}* (hereafter termed EGFR$^{\Delta FOXP3}$) to conduct an experiment alongside our other genotypes: it was therefore decided to use males, comparing to 'wildtype' male controls (in fact these were littermate controls, *Egfr$^{fl/fl}$*, hereafter termed 'WT'). Please note that, due to constraints in mouse supply, it was not possible to include control mice that were exposed to nebulised PBS in place of OVA; consequently, this limits interpretation of this experiment.

26.1.1 Worm counts

Gut samples were taken at harvest (i.e. 27 days postinfection) to determine that there was no significant difference in infection rates between our 2 groups. This was true, with adult worm counts between 100 and 200 for each group (Figure 26-1; p=0.28).

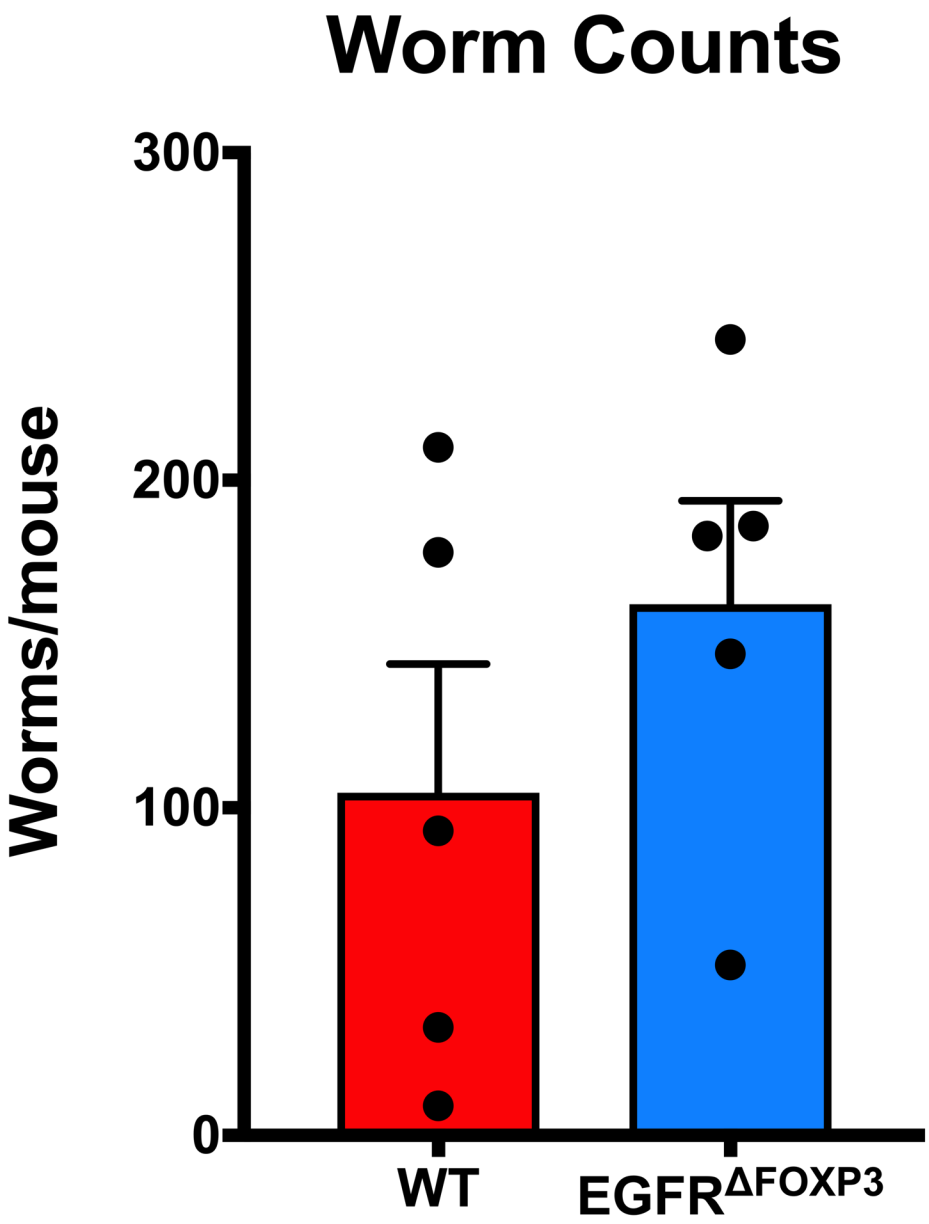

Figure 26-1 ***H.polygyrus adults worms found in intestinal lumen of WT and EGFR$^{\Delta FOXP3}$ mice, 27d postinfection. Note that D28 has been used previously as an analysis timepoint for H.polygyrus infection of C57BL/6 mice (Filbey et al. 2014).***

26.1.2 BAL cellularity

In contrast to previous investigations (as described in 23.3), we detected no discernible difference in amounts of BAL cellular infiltrate (defined as Trypan blue excluding cells, figure 26-2) in mice of either genotype, regardless of infection status.

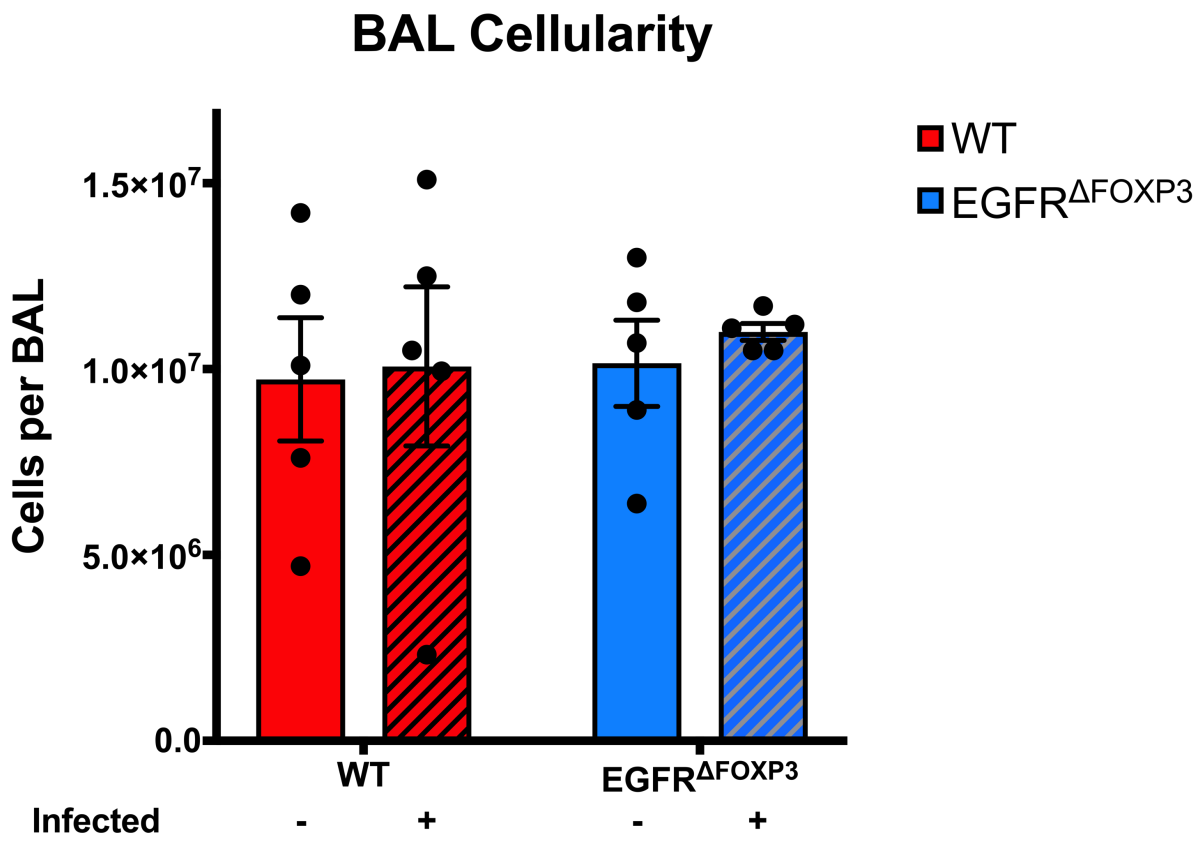

Figure 26-2 Total cellularity of BAL samples does not vary by genotype or infection status. Animals were sensitised (D1, D15) then exposed to OVA by nebulisation (D22-26) before culling & sample acquisition on D27. Samples were stained with Trypan blue and counted using a Cellometer Auto T4 (Nexelcom). Statistical analysis was with 2-way ANOVA.

26.1.3 Number of leukocyte populations are not significantly different in WT or EGFR$^{\Delta FOXP3}$ mice.

Following experimental harvest, we then analysed different leukocyte populations in BAL fluid, to see if these were present in different proportions. We saw no significant differences in proportions of granulocytes (Figure 26-3), mast cells, ILCs or dendritic cells (Figure 26-4 A – C). In the EGFR$^{\Delta FOXP3}$ group there was a small increase in basophils in infected animals (Figure 26-4D): the significance of this is unclear, and the result may be spurious.

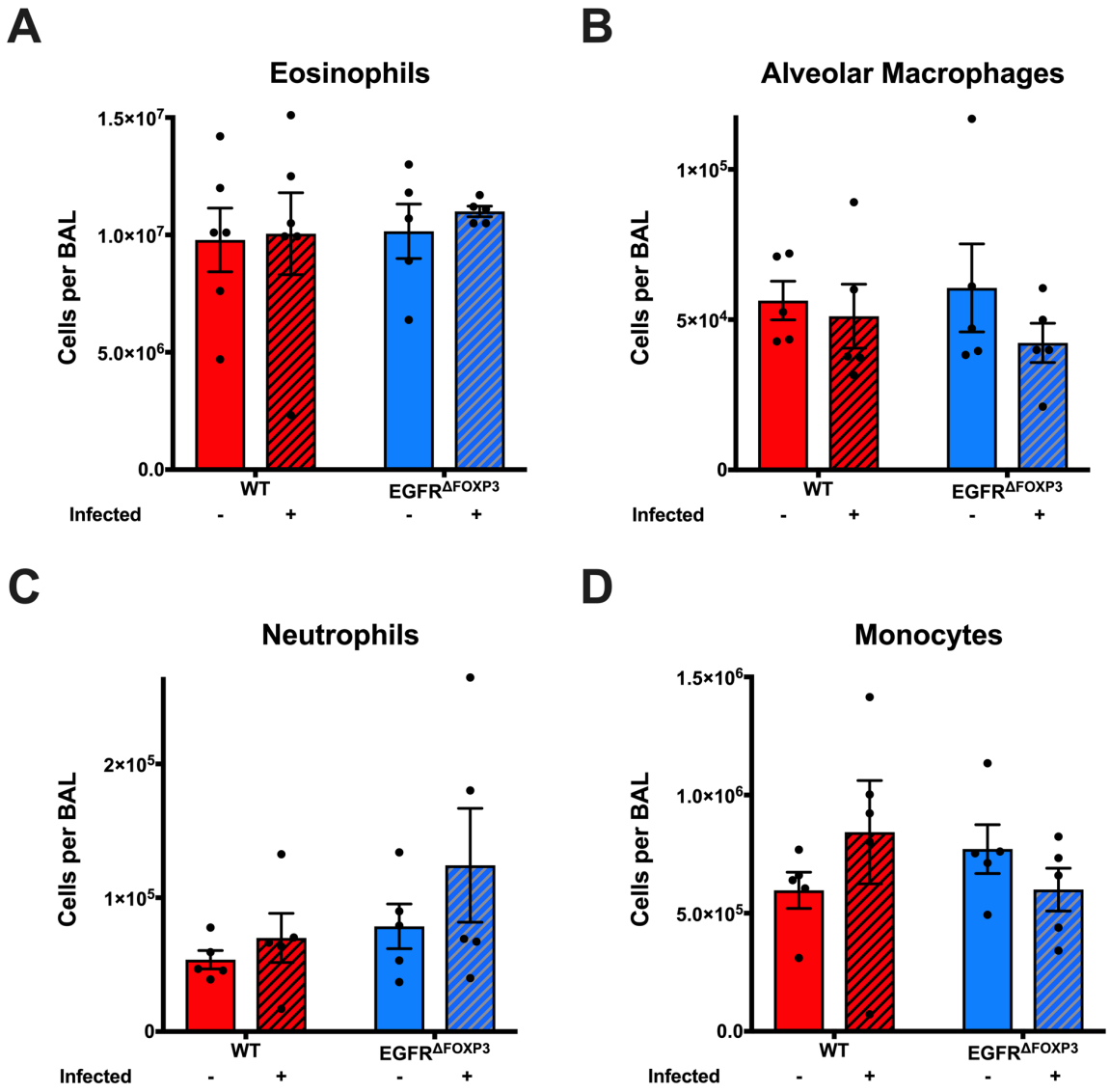

Figure 26-3 Granulocyte populations present in BAL samples of WT and EGFR$^{\Delta FOXP3}$ mice, infected or uninfected with H.polygyrus, exposed to OVA in an airway allergy model. A) Eosinophils, B) Alveolar macrophages, C) Neutrophils, D) Monocytes. Statistical analyses are 2-way ANOVA with subsequent t-testing where appropriate.

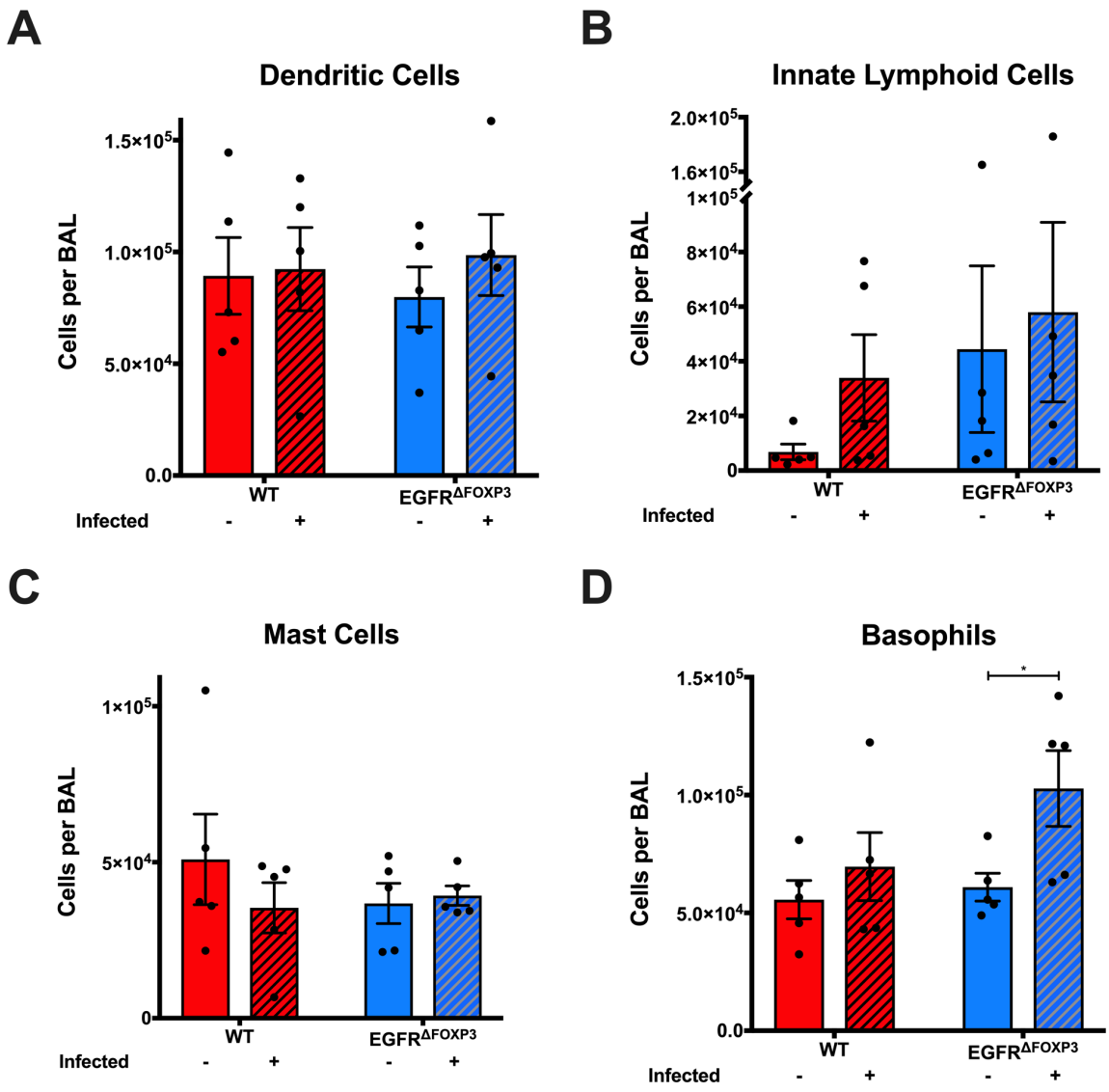

Figure 26-4 Other cell populations present in BAL samples of WT and EGFR$^{\Delta FOXP3}$ mice, infected or uninfected, exposed to OVA in an airway allergy model. A) Dendritic cells, B) Innate Lymphoid Cells, C) Mast cells, D) Basophils. Statistical analyses are 2-way ANOVA with subsequent t-testing where appropriate. The difference in basophil levels in infected vs uninfected EGFR$^{\Delta FOXP3}$ mice is significant, but may be spurious.

26.1.4 Lymphocyte populations and expression of intracellular cytokines is not significantly different in WT or EGFR$^{\Delta FOXP3}$ mice.

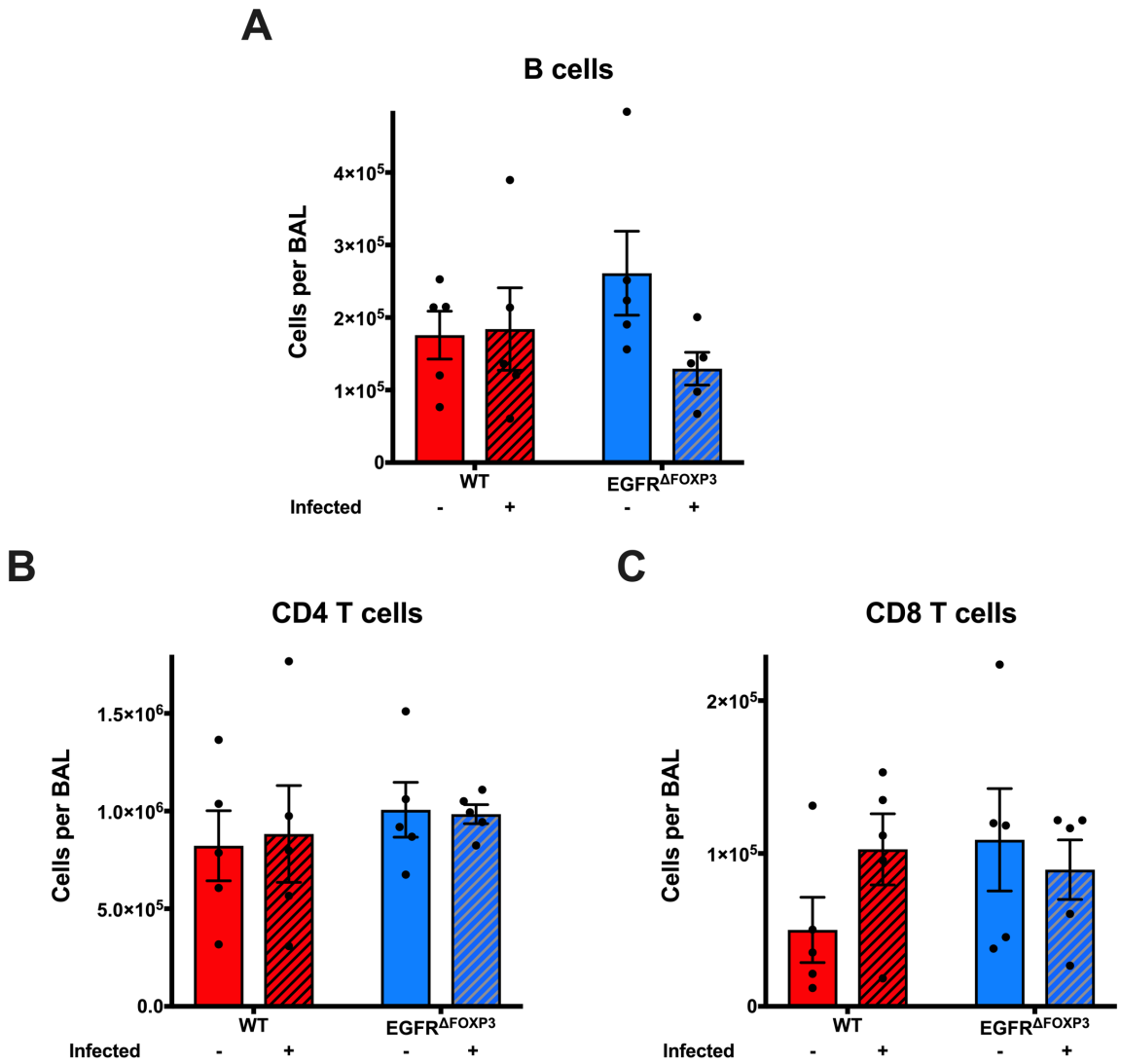

Figure 26-5 Lymphocyte populations present in BAL samples of WT and EGFR$^{\Delta FOXP3}$ mice, infected or uninfected with H.polygyrus, exposed to OVA in an airway allergy model. A) B cells, B) CD4 T cells, C) CD8 T cells. Statistical analyses are 2-way ANOVA with subsequent t-testing where appropriate.

Similarly, there were no significant differences in proportions of various lymphocyte populations between the groups (Figure 26-5). Analysis of intracellular cytokine expression in CD4 and CD8 T cells showed an increase in CD4 cell IFNγ in infected $EGFR^{\Delta FOXP3}$ that was not seen in noninfected $EGFR^{\Delta FOXP3}$; this was not seen in WT mice (Figure 26-6 A). This change was not seen in CD8 T cells (Figure 26-6 D). IL-5 and IL-13 expression was upregulated in the CD4 T cells of either group (Figure 26-6 B – C), but there were no differences between genotypes. In CD8 T cells there were no significant differences in IL-5 expression (Figure 26-6 E), and IL-13 expression was increased in infected WT but not $EGFR^{\Delta FOXP3}$ mice, but at a much lower level than CD4 T cells (Figure 26-6 F).

Based on these data, we concluded that EGFR deletion on regulatory T cells has no significant impact on the pathogenesis of airway hyperreactivity in an Ovalbumin sensitisation model, and that upregulation of TH2 immunity by *H.polygyrus* has no significant effect either.

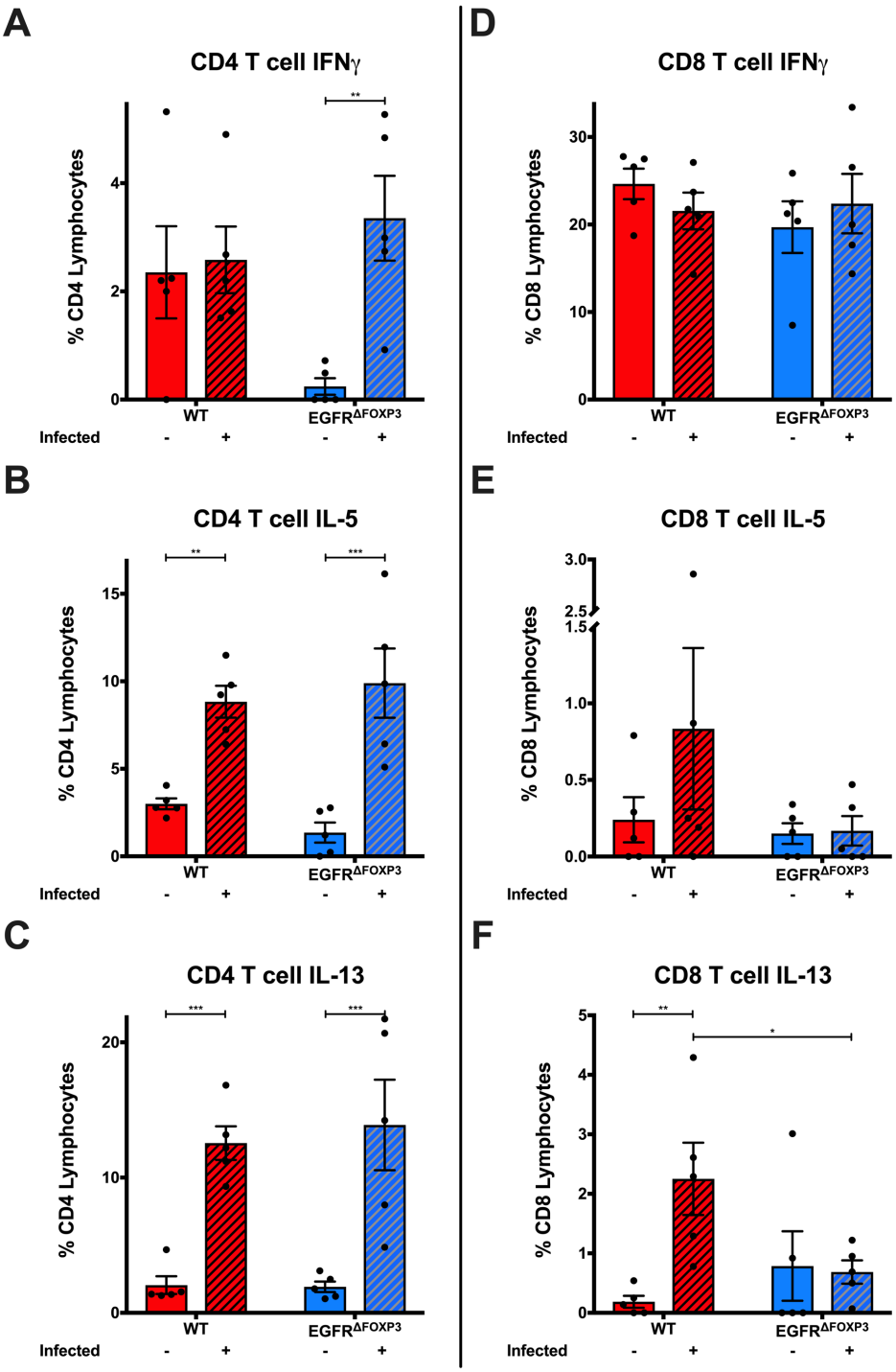

Figure 26-6 Cytokine expression in CD4 (left) and CD8 (right) T cell populations in BAL samples of WT and EGFR$^{\Delta FOXP3}$ mice, infected or uninfected with H.polygyrus, exposed to OVA in an airway allergy model. Cytokines analysed are IFNγ (A & D), IL-5 (B & E) and IL-13 (C & F). Statistical analyses are 2-way ANOVA with subsequent t-testing.

26.2 Identifying role of Amphiregulin in Treg activation in a murine asthma model.

To determine the role of amphiregulin in airway inflammation, and identify the cellular source of amphiregulin in the lung, we performed an Ovalbumin (OVA) airway sensitisation experiment with mouse of various genotypes, and infected half the groups with *H.polygyrus* (NB: due to constraints in mouse supply, there was no uninfected *Egfr*$^{fl/fl}$ *x LysM*^{cre} group). As described above, we infected the mice (or gavaged with PBS) on D1, Sensitised to OVA D2 & D15, then exposed them to nebulised OVA on D22-26 and harvested for sample acquisition on D27. Genotypes used were as detailed in table 25-1 and are hereafter referred to as (true genotype in brackets): WT (*Areg*$^{fl/fl}$); AREG$^{\Delta LysM}$ (*Areg*$^{fl/fl}$ *x LysM*^{cre}); AREG$^{\Delta ROR\alpha}$ (*Areg*$^{fl/fl}$ *x ROR*α^{cre}); and AREG$^{-/-}$ (*Areg*$^{-/-}$). LysM is a commonly used marker for alveolar macrophages, though it also induces deletions in neutrophils (Clausen et al. 1999; Abram et al. 2014). RORα was used as a lineage marker for ILC2 cells, as has been described previously (Spits et al. 2013).

26.2.1 Worm counts

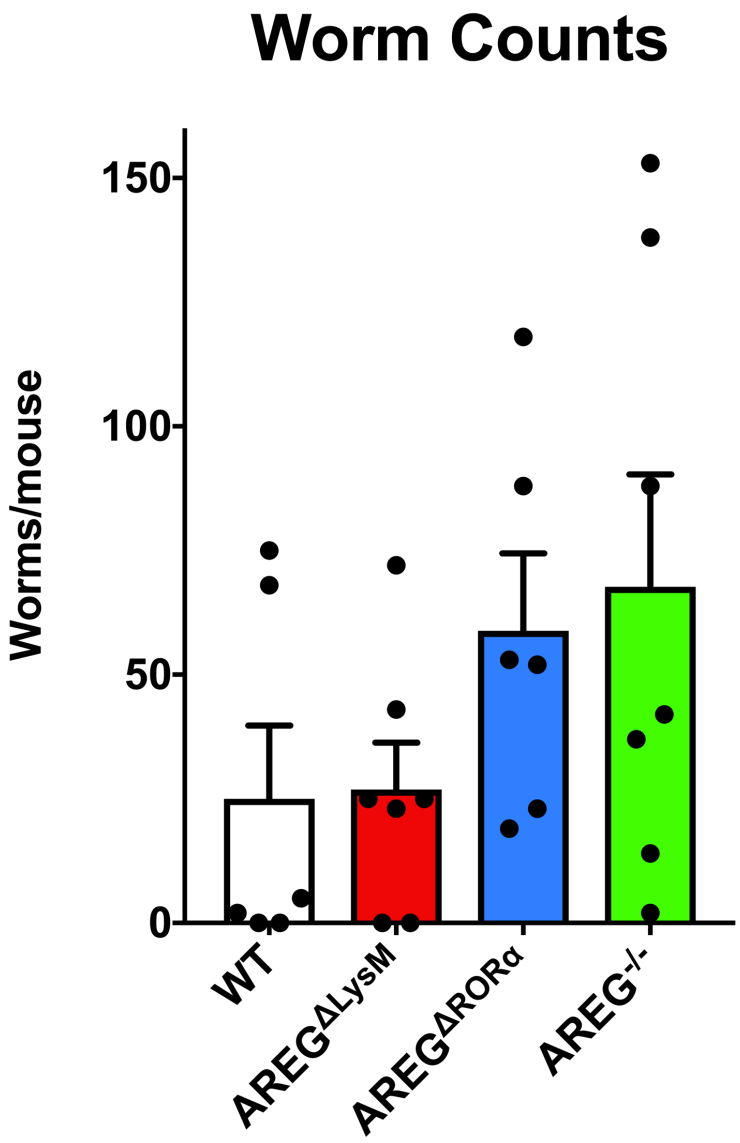

Figure 26-7 Gut worm counts from infected animals of various genotypes. Animals were infected with H.polygyrus and harvested 27 days later. Statistical analysis was 1-way ANOVA.

Though there was a trend towards greater numbers of worms in the AREG$^{-/-}$ and AREG$^{\Delta ROR\alpha}$ groups, there were no overall significant differences seen, implying that all groups were equally susceptible to infection (Figure 26-7).

26.2.2 BAL cellularity is not broadly similar across different genotypes, and the significance of this is unclear.

We then went on to analyse the cellularity of BAL samples. Looking first at wildtype groups, we saw a significant increase in cellularity when the animals were exposed to OVA as opposed to PBS by nebulisation (Figure 26-8 A). However, infection with *H.polygyrus* did not reduce the cellularity of BAL fluid, as has been previously observed.

Furthermore, there was heterogeneity of BAL cellularity both in uninfected and infected groups, with AREG$^{-/-}$ groups having significantly more cellularity than others (Figure 26-8 B – C).

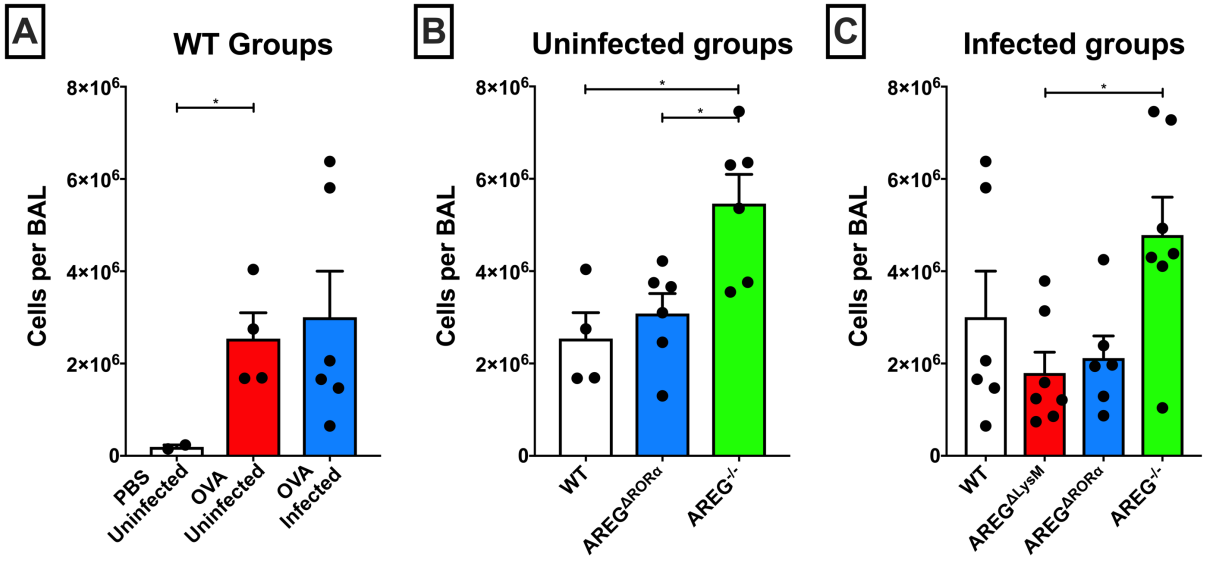

Figure 26-8 Comparison of BAL cellularity of A) all WT, B) all uninfected, and C) all infected groups. Animals were sensitised (D1, D15) then exposed to OVA by nebulisation (D22-26) before culling & sample acquisition on D27. Samples were then stained with Trypan blue and counted using a Cellometer Auto T4 (Nexelcom). Statistical analyses are 1-way ANOVA with secondary t-testing. Note AREG$^{-/-}$ is significantly more cellular than other groups, a feature not seen in previous experiments.

When comparing cellularity between uninfected and infected groups of each genotype, no significant differences were seen (Figure 26-9). Please note that, in the absence of an uninfected AREG$^{\Delta LysM}$ group, the infected AREG$^{\Delta LysM}$ group was compared to uninfected WT.

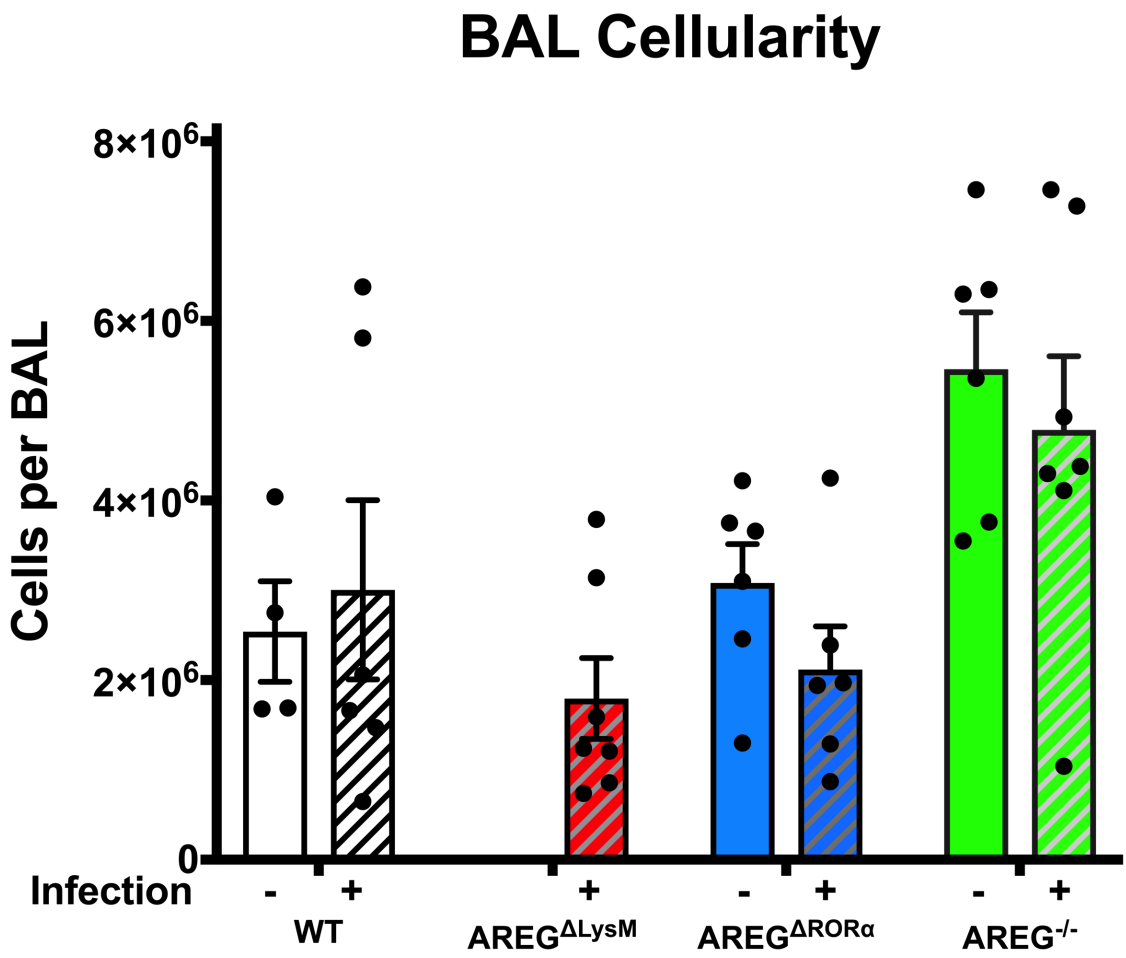

Figure 26-9 Comparison of BAL cellularity of different groups, by genotype and infection status (infected groups are patterned). The infected AREG$^{\Delta LysM}$ group was compared to uninfected WT, as no uninfected AREG$^{\Delta LysM}$ group was available. Statistical analyses are 2-way ANOVA with secondary t-testing between uninfected and infected groups.

26.2.3 Leukocyte populations are not significantly different in mice infected with *H.polygyrus*.

Noting the differences in BAL cellularity, we examined if there was any detectable difference in various leukocyte cell populations. Figure 26-10 shows the different numbers of granulocytes found in BAL; All groups exposed to OVA had significantly more eosinophils than PBS-treated WT controls, and also significantly fewer alveolar macrophages. There were no significant differences between infected and uninfected groups of each genotype for any of the cell populations studied, with the exception of monocytes in the AREG$^{\Delta ROR\alpha}$ group (significance unclear).

Figure 26-11 shows cell populations of dendritic cells, ILCs, mast cells and basophils. There was a slight decrease in dendritic cells seen in the AREG$^{-/-}$ infected group; again, given the lack of difference in other cell populations between the AREG$^{-/-}$ groups, the significance of this is doubtful.

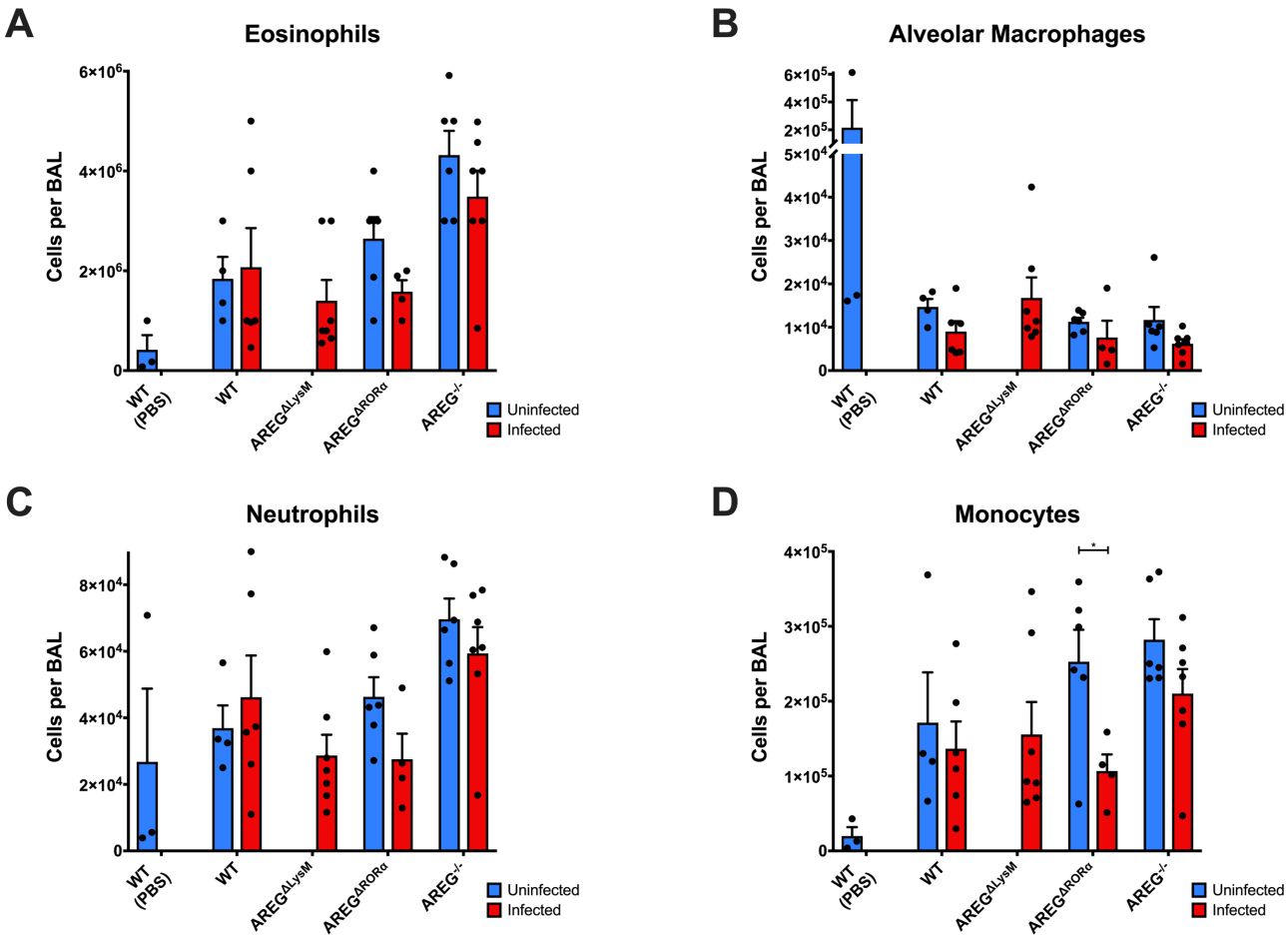

Figure 26-10 Granulocyte populations present in BAL samples of mice sensitised, then exposed to nebulised OVA. Groups uninfected with H.polygyrus are blue, infected are red. A) Eosinophils, B) Alveolar macrophages, C) Neutrophils, D) Monocytes. Statistical analyses are T-testing between infected and uninfected groups (infected AREG$^{\Delta LysM}$ compared to uninfected WT).

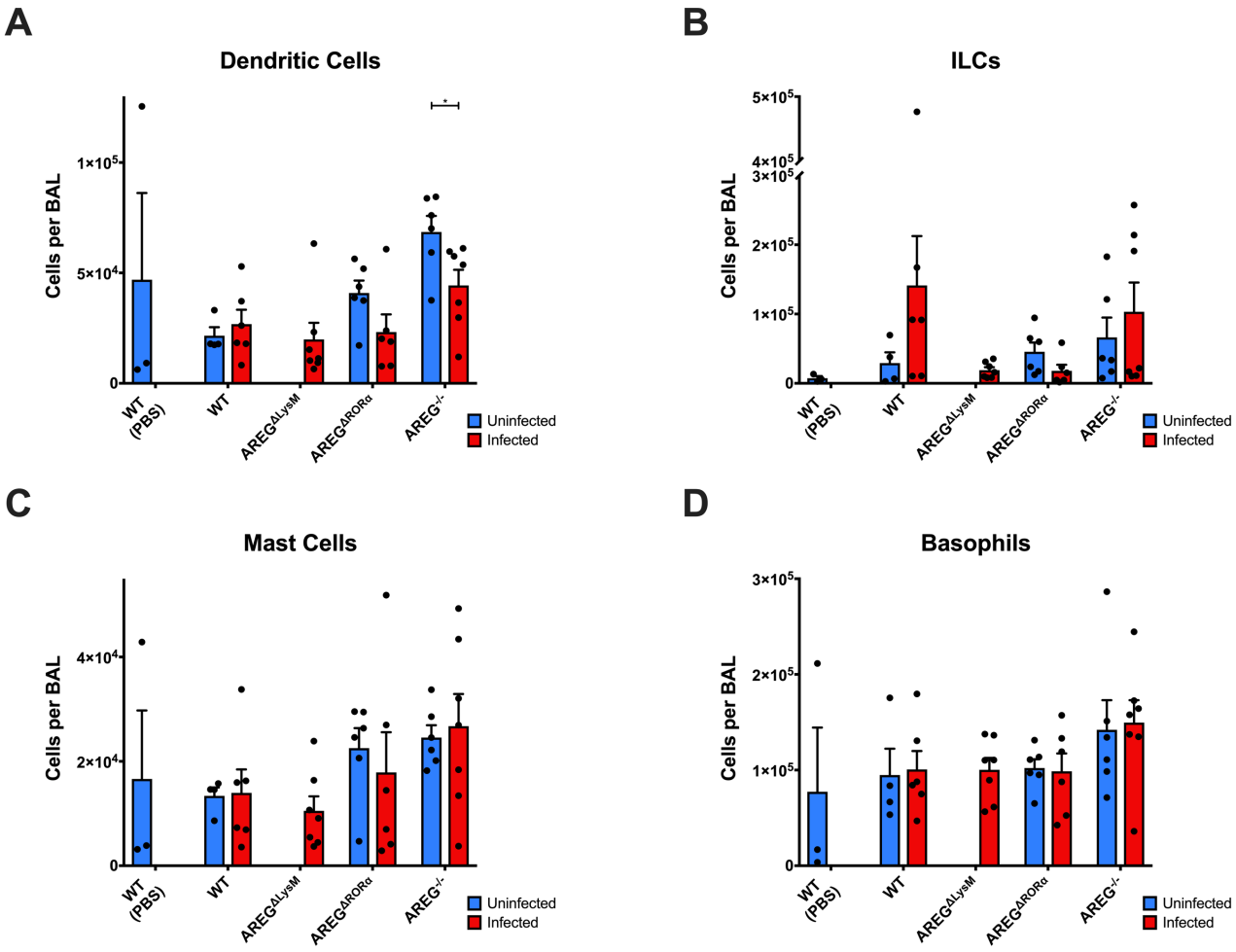

Figure 26-11 Other cell populations present in BAL samples of mice sensitised, then exposed to nebulised OVA. Groups uninfected with H.polygyrus are blue, infected are red. A) Dendritic cells, B) Innate Lymphoid Cells, C) Mast cells, D) Basophils. Statistical analyses are T-testing of infected and uninfected groups (infected AREG$^{\Delta LysM}$ compared to uninfected WT).

26.2.4 Lymphocyte populations and expression of intracellular cytokines is not significantly different.

Moving on to lymphocyte populations, we saw no between-group differences of infected and uninfected mice for B cells and CD4 T cells, and a small decrease in AREG$^{\Delta LysM}$ infected mice compared to WT uninfected (Figure 26-12).

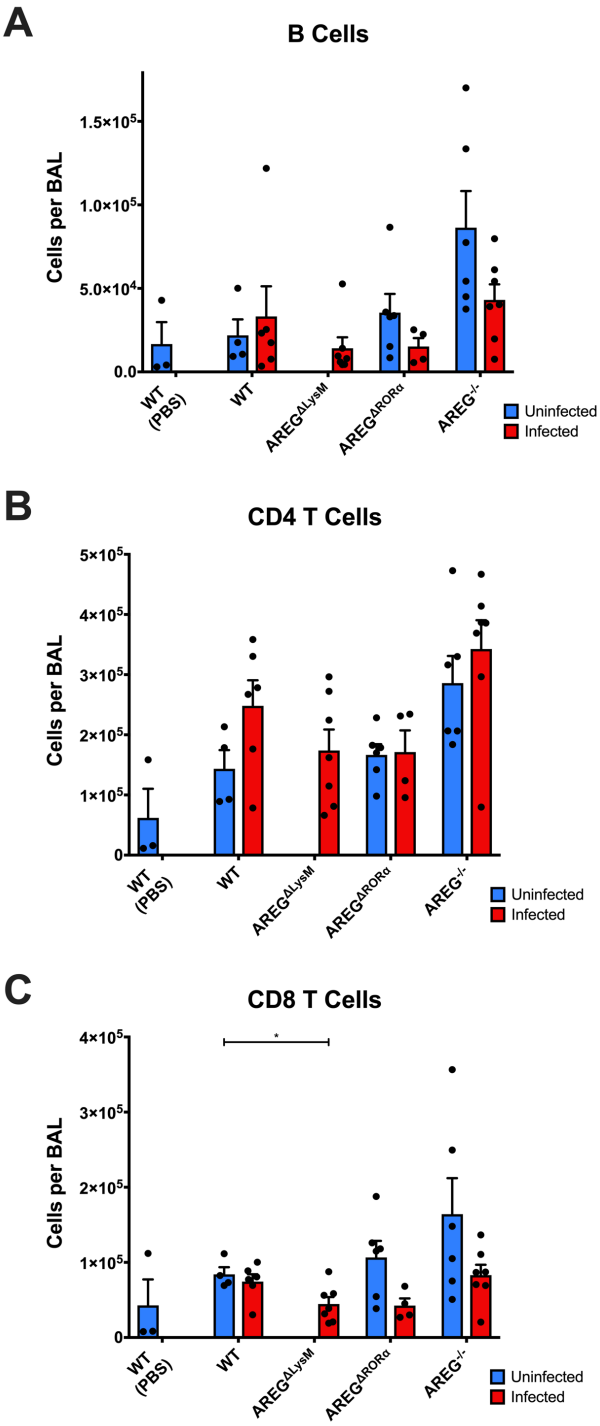

Figure 26-12 Lymphocyte populations present in BAL samples of mice sensitised, then exposed to nebulised OVA. Groups uninfected with H.polygyrus are blue, infected are red.. A) B cells, B) CD4 T cells, C) CD8 T cells. Statistical analyses are T-testing of infected and uninfected groups (infected AREG$^{\Delta LysM}$ compared to uninfected WT).

Levels of cytokine expression in CD4 and CD8 T cells were quantified (Figure 26-13); there were significant increases in CD4 T cell IL-5 and IL-13 expression in infected groups compared to uninfected. Total levels of these cytokines in CD8 T cells were much lower but tended to be higher in infected groups of any genotype. CD8 T cell IFNγ was higher in all infected groups than their uninfected controls, significantly so in $AREG^{\Delta ROR\alpha}$ and $AREG^{-/-}$ groups. We also compared the infected groups alone (Figure 26-14) and found increased IL-5 production on $AREG^{-/-}$ CD4 T cells relative to WT and $AREG^{\Delta LysM}$ groups, and IL-13 on $AREG^{\Delta ROR\alpha}$ CD8 T cells compared to WT only.

Based on these data, we concluded that whilst the presence of *H.polygyrus* promotes a significant increase in TH2 response, this had not been sufficient to alter cell populations significantly in the BAL when compared to uninfected controls in an Ovalbumin model of airway hyperreactivity. TH2 response seems to be more prominent in $AREG^{-/-}$ and $AREG^{\Delta ROR\alpha}$ groups when compared to WT and $AREG^{\Delta LysM}$.

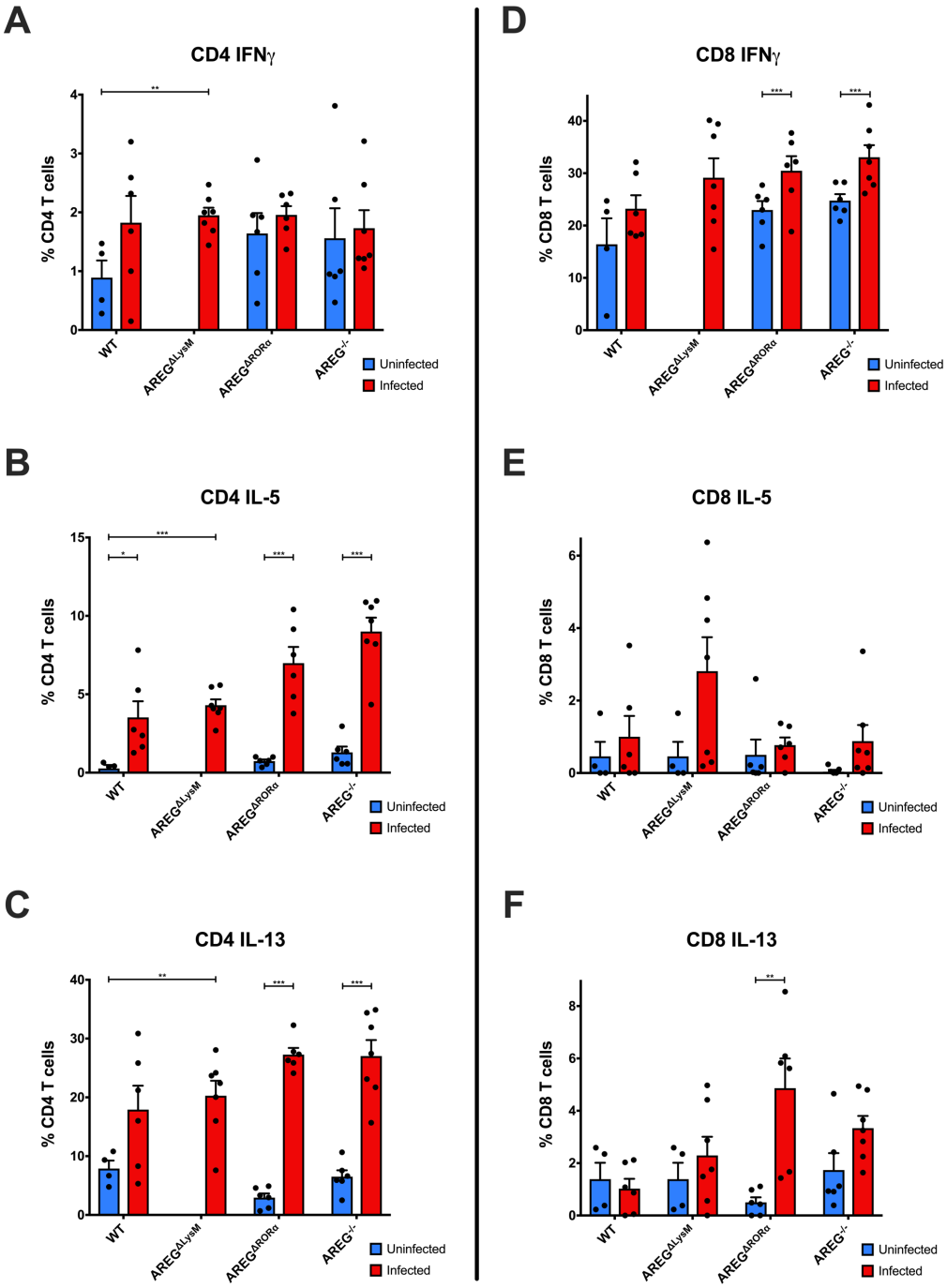

Figure 26-13 Cytokine expression in CD4 (left) and CD8 (right) T cells from BAL samples of mice sensitised, then exposed to nebulised OVA. Groups uninfected with H.polygyrus are blue, infected are red. Cytokines analysed are IFNγ (A & D), IL-5 (B & E) and IL-13 (C & F). Statistical analyses are T-testing of infected and uninfected groups (infected AREG$^{\Delta LysM}$ compared to uninfected WT)

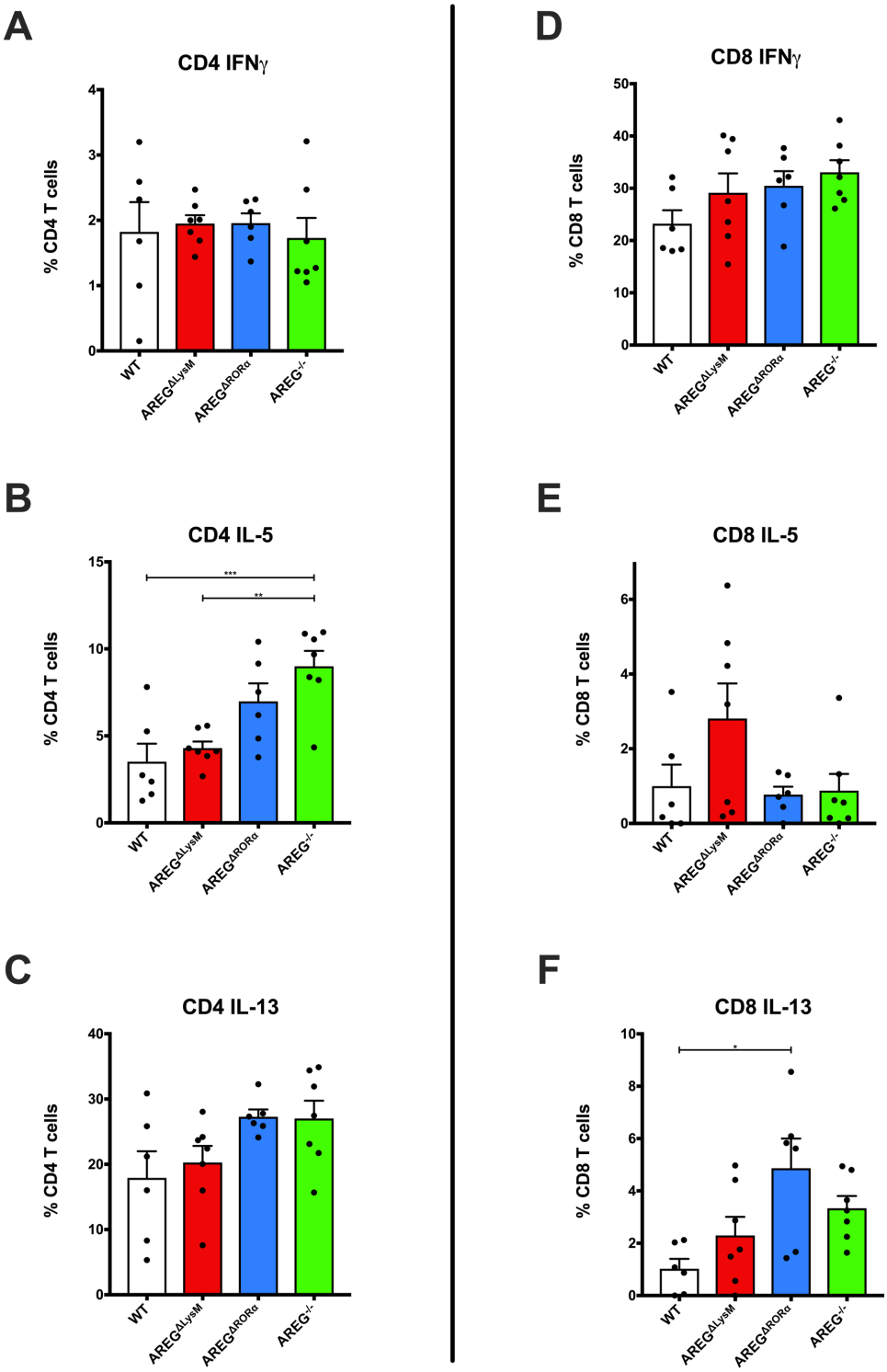

Figure 26-14 Cytokine expression in BAL-derived CD4 (left) and CD8 (right) T cells; infected groups only. Cytokines analysed are IFNγ (A & D), IL-5 (B & E) and IL-13 (C & F). Statistical analyses are 1-way ANOVA, with secondary T-testing.

27 Discussion

The findings of these experiments do not corroborate previous work done in our laboratory, or by others using helminth infection to induce Treg in asthma models (Dittrich et al. 2008; Wilson et al. 2005). These experiments showed that an increase in Treg numbers and activation led to a decrease in the severity of TH2 response to airway allergen challenge, i.e. the presence of a Treg-inducing helminth led to decreased lung inflammation. This basic finding was not seen in our experiments, where mouse populations infected with *H.polygyrus* did not have significantly less cellular BAL when compared to uninfected controls. There were some differences in BAL cellularity across genotype (notably AREG$^{-/-}$ groups had more cellular BAL than other groups, whether infected with *H.polygyrus* or not), which may point to a difference in immune responses to OVA challenge; however, this finding in the AREG$^{-/-}$ group conflicts with earlier work done in our laboratory, where there was no appreciable difference in BAL cellularity between WT and AREG$^{-/-}$ groups.

The reasons for these discrepancies are hard to explain: one possibility is that the mouse strains we used for these experiments are characteristically different to those used in our preliminary work: between experiments (several years apart) the microbiome of our mouse colonies was moved from a SOPF to an SPF background, due to an issue with anomalous results in the work of several groups using the Ashworth animal unit. In order to move our mice onto SPF background, newborn pups were fostered onto an C57BL/6 SPF mother, purchased from the Jackson

laboratory. This tends to produce mice with a 'hybrid' SPF/SOPF microbiome (Dr P Spence, Personal Communication), which, in combination with the phenotype of our transgenic strains, might have produced mice which are a) less susceptible to the effects of infection with *H.polygyrus* and b) broadly similar in their response to OVA airway challenge, regardless of genotype. It should be noted that there is a known interaction between *H.polygyrus* and the mouse microbiome during infection, and this has been shown to be important for *H.polygyrus*' immunosuppressive effect in a house dustmite airway sensitisation/challenge model (Zaiss et al. 2015). Therefore, it is possible that the alteration of our mouse microbiome had an influence on its susceptibility to alteration by *H.polygyrus* infection.

Another possibility is that changes in our experimental schedule led to our findings being discordant with our preliminary work. Our initial experiments involved a longer period between inoculation with *H.polygyrus* and the first injection of OVA; 28 days, as opposed to our shortened schedule, where mice were infected 1 day prior to first exposure to OVA. This shortened timeframe was chosen because the induction of regulatory T cells in *H.polygyrus* infection occurs early in infection, and ratios of Treg to conventional T cells have largely normalised by D28 (Finney et al. 2007; Rausch et al. 2008). By confining our experimental period to less than 28 days, we had hoped to capture our data during a period of optimal Treg expansion. However, please note that other experiments performed using $AREG^{\Delta LysM}$, $AREG^{-/-}$ and $AREG^{fl/fl}$ mice (data not shown above) used a gap of 14 days between infection with

H.polygyrus and first injection of OVA, and similar results on BAL cellularity and cell proportions was found.

Finally, it is possible that there were issues either with the ovalbumin we used or the quality of *H.polygyrus* larvae. We tried to mitigate for this by a) using new grade V Ovalbumin stock, and b) checking for established infection by examination of gut samples for adult worms (Figure 26-1). Judging by the obvious infiltration of inflammatory cells in OVA-treated samples relative to our PBS-treated control, and the presence of adult worms in our bowel samples (and no significant differences between our infected groups), we do not think these are likely causes of our experimental failure.

In conclusion, as we have failed to replicate the findings of previously published work, we do not believe any conclusions can be drawn concerning the cellular source of Amphiregulin for regulatory T cells in an airway inflammation model.

Concluding Remarks

This thesis aimed to study the relationship between EGFR activation on regulatory T cells and the outcome of infection. To achieve this, we used Vaccinia virus, a poxvirus known to produce a soluble EGFR ligand, and 2 separate helminth worm infections, which are known to induce regulatory T cells as part of the host response to infection.

Given the failure to replicate the findings of our initial experiments using *Heligmosomoides polygyrus*, it is difficult to infer anything from our data. Using *Litomosoides sigmodontis*, we found that EGFR signalling via AREG (or EGFR signalling on Treg in general) was dispensible for optimal Treg function *in-vivo*. *L.sigmodontis* infection produces a marked upregulation in Tregs, both systemically and in the pleural space (Taylor et al. 2005; 2007). This Treg induction is powerful enough to protect NOD mice from developing Type 1 Diabetes, even without biasing the immune response towards TH2, though TGFβ is still required (Hübner et al. 2012). As with most other helminth infections, *L.sigmodontis* produces a large number of excretory-secretory products, with over 300 molecules being identified in one study, most of these coming from adult gravid females (Armstrong et al. 2014). Many of these proteins have an immunomodulatory effect on the host, seemingly to benefit the survival of various stages of the parasite (Pfaff et al. 2002; Hartmann, Schramm, and Breloer 2015). Other researchers have found that, similar to *H.polygyrus*, *L.sigmodontis* produces an analogue to TGFβ, which induces Treg that subsequently express IL-10; this induction of TGFβ has been noted in other Helminthoses also (Grainger et al. 2010; Hartmann, Schramm, and Breloer 2015;

Maizels, Smits, and McSorley 2018). It is unlikely that this TGFβ analogue is the only excretory-secretory product that *L.sigmodontis* is releasing that affects Treg, given the diversity of molecules released from helminth worms (Maizels, Smits, and McSorley 2018); but even if so, it is likely that it is enough to overcome the effects of EGFR signalling inhibition in our Chapter 3 experiments. Hence, it seems that EGFR signalling is dispensible for activation of Treg in the context of *L.sigmodontis* infection.

Using Vaccinia virus infection of C57BL/6 mice, we have shown that:

1. Early protein products from UV-inactivated virus can induce Treg suppressive function *in-vitro*, and that with VACV that does not express VGF this effect is not seen;
2. *in-vivo* infection of $EGFR^{\Delta FOXP3}$ mice results in less weight loss and lower viral titres in the lung compared to WT;
3. BAL of VACV-infected $EGFR^{\Delta FOXP3}$ mice is more cellular; and
4. BAL supernatant of infected $EGFR^{\Delta FOXP3}$ mice contains less TGFβ than their WT counterparts. Based on these data, we conclude that VACV-derived VGF activates Treg at the site of infection, and these Treg subsequently suppress the immune response to VACV infection via TGFβ mediated immunosuppression. This is clearly beneficial to the virus, as reflected in higher lung viral titres and more weight loss in WT animals as compared to $EGFR^{\Delta FOXP3}$.

Concluding remarks

Almost 40% of the poxvirus genome is composed of immunomodulatory proteins, which are summarised elsewhere (Bidgood and Mercer 2015). Other researchers have demonstrated an interaction between VACV and T cells: VACV M2 protein, which is released from infected cells, can suppress T cell activation by binding CD80/CD86, preventing these from being ligated by CD28 or CTLA4 (Kleinpeter et al. 2019). However, to our knowledge this is the first time a direct interaction between Vaccinia virus and regulatory T cells has been shown. Given the wide number of immunomodulatory proteins poxviruses produce, and the discovery that activated Treg express EGFR and respond to EGFR ligands, it is perhaps not surprising that as well as suppressing the innate and adaptive immune responses through a variety of means, VACV also manipulates Treg to achieve the same objective of a locally immunosuppressive environment that benefits the pathogen.

As part of our work we decided to assess the influence of Gefitinib blockade on the outcome of VACV infection in WT mice; however, we were not able to complete these experiments as stated above in section 11.3.8, and time constraints meant that we had to discontinue this line of inquiry. If time had allowed, repeating this experiment using a monoclonal antibody inhibitor of EGFR might have been more tolerable for the experimental animals, and allowed us to establish the utility of EGFR inhibition in acute infection. Gefitinib was chosen as our inhibitor for practical reasons: it is commercially licensed for use in humans; the dosages used in humans and mice are comparable (after appropriate conversion); and treatment can be easily

ceased after resolution of infection (as opposed to monoclonal antibodies, which maintain their effect for several weeks after administration).

Future directions arising from this thesis should focus on the applicability of EGFR inhibition in various infective processes. As discussed previously, poxviruses currently cause little disease in the human population, due to the eradication of Smallpox (Variola virus) in the late 1970's. Concerns persist, however, about the use of Smallpox as a bioterrorism agent, and currently treatment in an attack using such an agent would be almost entirely supportive. Any medicine that improves the host response to infection without resulting in immune system-mediated damage to the host should be investigated further. EGFR-inhibiting medicines (TKIs and monoclonal antibodies) have mild side effect profiles when compared to older medicines, are already in mass-production and, in the case of TKIs, have a rapid onset and offset of effect. Given the importance of VGF and SPGF for providing optimal replication conditions for VACV and variola respectively, blocking the effects of these agents with EGFR inhibitors is a tempting avenue for future research.

Would EGFR inhibition be effective against other pathogens? This is less clear: Other viruses use EGFR as means of entry into cells, and some (such as CMV) use EGFR to change the behaviour of monocytes so as to benefit the virus (Chan, Nogalski, and Yurochko 2009); but there also appears to be considerable redundancy, with viruses using multiple methods to enter cells. Poxviruses uniquely

produce a soluble mediator with EGF-like properties, making them an ideal candidate for this study. Other pathogens, such as those listed in section 4.2, appear to use EGFR signalling to enter or manipulate their target cells, but the effects of EGFR blockade in these situations would have to be examined case-by-case. There are certainly some pathogens (e.g. *Helicobacter pylori*), where due to already effective treatments existing the benefits of this line of inquiry are doubtful. However, in some cases (such as influenza) where antimicrobial resistance is a rising concern, research is more readily justified.

In conclusion, Poxviruses use soluble growth factors with EGFR ligating properties to stimulate regulatory T cells, which in turn suppress the immune system using TGFβ, so as to create a locally immunosuppressive environment in which the virus can replicate. The use of EGFR inhibitors to mitigate this process should be examined further.

References

Abdullah, N. A., B. A. Torres, M. Basu, and H. M. Johnson. 1989. 'Differential Effects of Epidermal Growth Factor, Transforming Growth Factor-Alpha, and Vaccinia Virus Growth Factor in the Positive Regulation of IFN-Gamma Production'. *Journal of Immunology* 143 (1): 113–17.

Abe, M., J. G. Harpel, C. N. Metz, I. Nunes, D. J. Loskutoff, and D. B. Rifkin. 1994. 'An Assay for Transforming Growth Factor-Beta Using Cells Transfected with a Plasminogen Activator Inhibitor-1 Promoter-Luciferase Construct'. *Analytical Biochemistry* 216 (2): 276–84. https://doi.org/10.1006/abio.1994.1042.

Abi Abdallah, Delbert S., Charlotte E. Egan, Barbara A. Butcher, and Eric Y. Denkers. 2011. 'Mouse Neutrophils Are Professional Antigen-Presenting Cells Programmed to Instruct Th1 and Th17 T-Cell Differentiation'. *International Immunology* 23 (5): 317–26. https://doi.org/10.1093/intimm/dxr007.

Abram, Clare L., Gray L. Roberge, Yongmei Hu, and Clifford A. Lowell. 2014. 'Comparative Analysis of the Efficiency and Specificity of Myeloid-Cre Deleting Strains Using ROSA-EYFP Reporter Mice'. *Journal of Immunological Methods* 408: 89–100. https://doi.org/10.1016/j.jim.2014.05.009.

Adib-Conquy, Minou, Thierry Pedron, Anne-France Petit-Bertron, Olivier Tabary, Harriet Corvol, Jacky Jacquot, Annick Clément, and Jean-Marc Cavaillon. 2008. 'Neutrophils in Cystic Fibrosis Display a Distinct Gene Expression Pattern'. *Molecular Medicine* 14 (1–2): 36–44. https://doi.org/10.2119/2007-00081.Adib-Conquy.

Akira, Shizuo, Satoshi Uematsu, and Osamu Takeuchi. 2006. 'Pathogen Recognition and Innate Immunity'. *Cell* 124 (4): 783–801. https://doi.org/10.1016/j.cell.2006.02.015.

Allen, Judith E., and Tara E. Sutherland. 2014. 'Host Protective Roles of Type 2 Immunity: Parasite Killing and Tissue Repair, Flip Sides of the Same Coin'. *Seminars in Immunology* 26 (4): 329–40. https://doi.org/10.1016/j.smim.2014.06.003.

Amoah, Samuel, Beth C. Holbrook, Rama D. Yammani, and Martha A. Alexander-Miller. 2013. 'High Viral Burden Restricts Short-Lived Effector Cell Number at Late Times Postinfection through Increased Natural Regulatory T Cell Expansion'. *Journal of Immunology* 190 (10): 5020–29. https://doi.org/10.4049/jimmunol.1200971.

Andrade, Anderson A., Patrícia N. G. Silva, Anna C. T. C. Pereira, Lirlândia P. De Sousa, Paulo C. P. Ferreira, Ricardo T. Gazzinelli, Erna G. Kroon, Catherine Ropert, and Cláudio A. Bonjardim. 2004. 'The Vaccinia Virus-Stimulated Mitogen-Activated Protein Kinase (MAPK) Pathway Is Required for Virus Multiplication'. *The Biochemical Journal* 381 (2): 437–46. https://doi.org/10.1042/BJ20031375.

Armstrong, Stuart D., Simon A. Babayan, Nathaly Lhermitte-Vallarino, Nick Gray, Dong Xia, Coralie Martin, Sujai Kumar, et al. 2014. 'Comparative Analysis of the Secretome from a Model Filarial Nematode (Litomosoides Sigmodontis) Reveals Maximal Diversity in Gravid Female Parasites'. *Molecular & Cellular Proteomics* 13 (10): 2527–44. https://doi.org/10.1074/mcp.M114.038539.

Avraham, Roi, and Yosef Yarden. 2011. 'Feedback Regulation of EGFR Signalling: Decision Making by Early and Delayed Loops'. *Nature Reviews Molecular Cell Biology* 12 (2): 104–17. https://doi.org/10.1038/nrm3048.

Bachmanov, Alexander A., Danielle R. Reed, Gary K. Beauchamp, and Michael G. Tordoff. 2002. 'Food Intake, Water Intake, and Drinking Spout Side Preference of 28 Mouse Strains'. *Behavior Genetics* 32 (6): 435–43.

Barbier, Diane, Ignacio Garcia-Verdugo, Julien Pothlichet, Roxana Khazen, Delphyne Descamps, Karine Rousseau, David Thornton, et al. 2012. 'Influenza A Induces the Major Secreted Airway Mucin MUC5AC in a Protease–EGFR–Extracellular Regulated Kinase–Sp1–Dependent Pathway'. *American Journal of Respiratory Cell and Molecular Biology* 47 (2): 149–57. https://doi.org/10.1165/rcmb.2011-0405OC.

Becker, Yechiel. 2003. 'Vaccinia Virus Pathogenicity in Atopic Dermatitis Is Caused by Allergen-Induced Immune Response That Prevents the Antiviral Cellular and Humoral Immunity'. *Virus Genes* 27 (3): 269–282.

Beerli, Corina, Artur Yakimovich, Samuel Kilcher, Glennys V. Reynoso, Gotthold Fläschner, Daniel J. Müller, Heather D. Hickman, and Jason Mercer. 2019. 'Vaccinia Virus Hijacks EGFR Signalling to Enhance Virus Spread through Rapid and Directed Infected Cell Motility'. *Nature Microbiology* 4 (2): 216–25. https://doi.org/10.1038/s41564-018-0288-2.

Berasain, Carmen, and Matías A. Avila. 2014. 'Amphiregulin'. *Seminars in Cell & Developmental Biology* 28: 31–41. https://doi.org/10.1016/j.semcdb.2014.01.005.

Bethony, Jeffrey, Simon Brooker, Marco Albonico, Stefan M Geiger, Alex Loukas, David Diemert, and Peter J Hotez. 2006. 'Soil-Transmitted Helminth Infections: Ascariasis, Trichuriasis, and Hookworm'. *The Lancet* 367 (9521): 1521–32. https://doi.org/10.1016/S0140-6736(06)68653-4.

Beutler, Bruce. 2004. 'Innate Immunity: An Overview'. *Molecular Immunology* 40 (12): 845–59.

Bidgood, Susanna R., and Jason Mercer. 2015. 'Cloak and Dagger: Alternative Immune Evasion and Modulation Strategies of Poxviruses'. *Viruses* 7 (8): 4800–4825. https://doi.org/10.3390/v7082844.

Bles, Nathalie, Larissa Di Pietrantonio, Jean-Marie Boeynaems, and Didier Communi. 2010. 'ATP Confers Tumorigenic Properties to Dendritic Cells by Inducing Amphiregulin Secretion'. *Blood* 116 (17): 3219–26. https://doi.org/10.1182/blood-2010-01-265611.

Boran, Aislyn D. W., Joseph Seco, Vinodh Jayaraman, Gomathi Jayaraman, Shan Zhao, Sushmitha Reddy, Yibang Chen, and Ravi Iyengar. 2012. 'A Potential Peptide Therapeutic Derived from the Juxtamembrane Domain of the Epidermal Growth Factor Receptor'. *PloS One* 7 (11): e49702. https://doi.org/10.1371/journal.pone.0049702.

Bouchery, T., K. Ehrhardt, E. Lefoulon, W. Hoffmann, O. Bain, and C. Martin. 2012. 'Differential Tissular Distribution of Litomosoides Sigmodontis Microfilariae between Microfilaremic and Amicrofilaremic Mice Following Experimental Infection'. *Parasite* 19 (4): 351–58. https://doi.org/10.1051/parasite/2012194351.

Bouchery, Tiffany, Gaelle Dénécé, Tarik Attout, Katharina Ehrhardt, Nathaly Lhermitte-Vallarino, Muriel Hachet-Haas, Jean Luc Galzi, et al. 2012. 'The Chemokine CXCL12 Is Essential for the Clearance of the Filaria Litomosoides Sigmodontis in Resistant Mice'. *PloS One* 7 (4): e34971. https://doi.org/10.1371/journal.pone.0034971.

Boukamp, P., R. T. Petrussevska, D. Breitkreutz, J. Hornung, A. Markham, and N. E. Fusenig. 1988. 'Normal Keratinization in a Spontaneously Immortalized Aneuploid Human Keratinocyte Cell Line.' *The Journal of Cell Biology* 106 (3): 761–71. https://doi.org/10.1083/jcb.106.3.761.

Boyer, Olivier, David Saadoun, Julien Abriol, Mélanie Dodille, Jean-Charles Piette, Patrice Cacoub, and David Klatzmann. 2004. 'CD4+CD25+ Regulatory T-Cell Deficiency in Patients with Hepatitis C-Mixed Cryoglobulinemia Vasculitis'. *Blood* 103 (9): 3428–30. https://doi.org/10.1182/blood-2003-07-2598.

Brehm, Michael A., Keith A. Daniels, and Raymond M. Welsh. 2005. 'Rapid Production of TNF-α Following TCR Engagement of Naive CD8 T Cells'. *The Journal of Immunology* 175 (8): 5043–49. https://doi.org/10.4049/jimmunol.175.8.5043.

Brillard, Emilie, Jean-René Pallandre, David Chalmers, Bernhard Ryffel, Amandine Radlovic, Estelle Seilles, Pierre Simon Rohrlich, et al. 2007. 'Natural Killer Cells Prevent CD28-Mediated Foxp3 Transcription in CD4+CD25- T Lymphocytes'. *Experimental Hematology* 35 (3): 416–25. https://doi.org/10.1016/j.exphem.2006.12.004.

Brockmann, Leonie, Shiwa Soukou, Babett Steglich, Paulo Czarnewski, Lilan Zhao, Sandra Wende, Tanja Bedke, et al. 2018. 'Molecular and Functional

Heterogeneity of IL-10-Producing CD4+ T Cells'. *Nature Communications* 9 (1): 5457. https://doi.org/10.1038/s41467-018-07581-4.

Brooks, Collin, Neil Pearce, and Jeroen Douwes. 2013. 'The Hygiene Hypothesis in Allergy and Asthma: An Update'. *Current Opinion in Allergy and Clinical Immunology* 13 (1): 70–77. https://doi.org/10.1097/ACI.0b013e32835ad0d2.

Bublil, Erez M, and Yosef Yarden. 2007. 'The EGF Receptor Family: Spearheading a Merger of Signaling and Therapeutics'. *Current Opinion in Cell Biology*, Cell regulation, 19 (2): 124–34. https://doi.org/10.1016/j.ceb.2007.02.008.

Budhu, Sadna, David A. Schaer, Yongbiao Li, Ricardo Toledo-Crow, Katherine Panageas, Xia Yang, Hong Zhong, et al. 2017. 'Blockade of Surface-Bound TGF-β on Regulatory T Cells Abrogates Suppression of Effector T Cell Function in the Tumor Microenvironment'. *Science Signaling* 10: eaak9702. https://doi.org/10.1126/scisignal.aak9702.

Buller, R. M., S. Chakrabarti, J. A. Cooper, D. R. Twardzik, and B. Moss. 1988. 'Deletion of the Vaccinia Virus Growth Factor Gene Reduces Virus Virulence'. *Journal of Virology* 62 (3): 866–74.

Buller, R. Mark L., Sekhar Chakrabarti, Bernard Moss, and Torgny Fredricksont. 1988. 'Cell Proliferative Response to Vaccinia Virus Is Mediated by VGF'. *Virology* 164 (1): 182–192.

Burgel, P.-R., and J. A. Nadel. 2004. 'Roles of Epidermal Growth Factor Receptor Activation in Epithelial Cell Repair and Mucin Production in Airway Epithelium'. *Thorax* 59 (11): 992–96. https://doi.org/10.1136/thx.2003.018879.

Burzyn, Dalia, Wilson Kuswanto, Dmitriy Kolodin, Jennifer L. Shadrach, Massimiliano Cerletti, Young Jang, Esen Sefik, et al. 2013. 'A Special Population of Regulatory T Cells Potentiates Muscle Repair'. *Cell* 155 (6): 1282–95. https://doi.org/10.1016/j.cell.2013.10.054.

Camberis, Mali, Graham Le Gros, and Joseph Urban. 2003. 'Animal Model of Nippostrongylus Brasiliensis and Heligmosomoides Polygyrus'. *Current Protocols in Immunology* Chapter 19: Unit 19.12. https://doi.org/10.1002/0471142735.im1912s55.

Campbell, Sharon M, Johanna A Knipper, Dominik Ruckerl, Conor M Finlay, Nicola Logan, Carlos M Minutti, Matthias Mack, Stephen J Jenkins, Matthew D Taylor, and Judith E Allen. 2019. 'Myeloid Cell Recruitment versus Local Proliferation Differentiates Susceptibility from Resistance to Filarial Infection'. *ELife* 7: e30947. https://doi.org/10.7554/eLife.30947.

Carlson, Robert W., Anne O'eill, Tatiana Vidaurre, Henry L. Gomez, Sunil S. Badve, and George W. Sledge. 2012. 'A Randomized Trial of Combination

Anastrozole plus Gefitinib and of Combination Fulvestrant plus Gefitinib in the Treatment of Postmenopausal Women with Hormone Receptor Positive Metastatic Breast Cancer'. *Breast Cancer Research and Treatment* 133 (3): 1049–56. https://doi.org/10.1007/s10549-012-1997-5.

Carpenter, G, L King Jr, and S Cohen. 1978. 'Epidermal Growth Factor Stimulates Phosphorylation in Membrane Preparations in Vitro'. *Nature* 276 (5686): 409–10.

CDC. 2018. 'Parasites'. 30 August 2018. https://www.cdc.gov/parasites/index.html. Accessed July 2019.

Center for Drug Evaluation and Research. 2005. 'Guidance for Industry: Estimating the Maximum Safe Starting Dose in Initial Clinical Trials for Therapeutics in Adult Healthy Volunteers'. https://www.fda.gov/regulatory-information/search-fda-guidance-documents/estimating-maximum-safe-starting-dose-initial-clinical-trials-therapeutics-adult-healthy-volunteers. Accessed July 2019

Chakir, Habiba, Haiping Wang, David E. Lefebvre, John Webb, and Fraser W. Scott. 2003. 'T-Bet/GATA-3 Ratio as a Measure of the Th1/Th2 Cytokine Profile in Mixed Cell Populations: Predominant Role of GATA-3'. *Journal of Immunological Methods* 278 (1): 157–69. https://doi.org/10.1016/S0022-1759(03)00200-X.

Chan, Gary, Maciej T. Nogalski, and Andrew D. Yurochko. 2009. 'Activation of EGFR on Monocytes Is Required for Human Cytomegalovirus Entry and Mediates Cellular Motility'. *Proceedings of the National Academy of Sciences of the United States of America* 106 (52): 22369–74. https://doi.org/10.1073/pnas.0908787106.

Chang, W, J G Lim, I Hellström, and L E Gentry. 1988. 'Characterization of Vaccinia Virus Growth Factor Biosynthetic Pathway with an Antipeptide Antiserum.' *Journal of Virology* 62 (3): 1080–83.

Chen, Fei, Zhugong Liu, Wenhui Wu, Cristina Rozo, Scott Bowdridge, Ariel Millman, Nico Van Rooijen, Joseph F Urban Jr, Thomas A Wynn, and William C Gause. 2012. 'An Essential Role for TH2-Type Responses in Limiting Acute Tissue Damage during Experimental Helminth Infection'. *Nature Medicine* 18 (2): 260–66. https://doi.org/10.1038/nm.2628.

Chen, Jianchun, Fenghua Zeng, Steven J. Forrester, Satoru Eguchi, Ming-Zhi Zhang, and Raymond C. Harris. 2016. 'Expression and Function of the Epidermal Growth Factor Receptor in Physiology and Disease'. *Physiological Reviews* 96 (3): 1025–1069.

Chen, Xiaofeng, Yiqian Liu, Oluf Dimitri Røe, Yingying Qian, Renhua Guo, Lingjun Zhu, Yongmei Yin, and Yongqian Shu. 2013. 'Gefitinib or Erlotinib as

Maintenance Therapy in Patients with Advanced Stage Non-Small Cell Lung Cancer: A Systematic Review'. *PloS One* 8 (3): e59314. https://doi.org/10.1371/journal.pone.0059314.

Chung, Che-Sheng, Chein-Hung Chen, Ming-Yi Ho, Cheng-Yen Huang, Chung-Lin Liao, and Wen Chang. 2006. 'Vaccinia Virus Proteome: Identification of Proteins in Vaccinia Virus Intracellular Mature Virion Particles'. *Journal of Virology* 80 (5): 2127–40. https://doi.org/10.1128/JVI.80.5.2127-2140.2006.

Chung, Christine H., Kim Ely, Loris McGavran, Marileila Varella-Garcia, Joel Parker, Natalie Parker, Carolyn Jarrett, et al. 2006. 'Increased Epidermal Growth Factor Receptor Gene Copy Number Is Associated With Poor Prognosis in Head and Neck Squamous Cell Carcinomas'. *Journal of Clinical Oncology* 24 (25): 4170–76. https://doi.org/10.1200/JCO.2006.07.2587.

Clark, Jessica A., Andrew T. Clark, Richard S. Hotchkiss, Timothy G. Buchman, and Craig M. Coopersmith. 2008. 'Epidermal Growth Factor Treatment Decreases Mortality and Is Associated with Improved Gut Integrity in Sepsis'. *Shock* 30 (1): 36–42. https://doi.org/10.1097/shk.0b013e31815D0820.

Clark, R. H. 2006. 'Deletion of Gene A41L Enhances Vaccinia Virus Immunogenicity and Vaccine Efficacy'. *Journal of General Virology* 87 (1): 29–38. https://doi.org/10.1099/vir.0.81417-0.

Clausen, B. E., C. Burkhardt, W. Reith, R. Renkawitz, and I. Förster. 1999. 'Conditional Gene Targeting in Macrophages and Granulocytes Using LysMcre Mice'. *Transgenic Research* 8 (4): 265–77. https://doi.org/10.1023/a:1008942828960.

Collison, Lauren W., and Dario A. A. Vignali. 2011. 'In Vitro Treg Suppression Assays'. In *Regulatory T Cells: Methods and Protocols*, edited by George Kassiotis and Adrian Liston, 21–37. Methods in Molecular Biology. Humana Press. https://doi.org/10.1007/978-1-61737-979-6_2.

Cooper, Max D., and Matthew N. Alder. 2006. 'The Evolution of Adaptive Immune Systems'. *Cell* 124 (4): 815–22. https://doi.org/10.1016/j.cell.2006.02.001.

Cosson, Pierre, and Thierry Soldati. 2008. 'Eat, Kill or Die: When Amoeba Meets Bacteria'. *Current Opinion in Microbiology* 11 (3): 271–76. https://doi.org/10.1016/j.mib.2008.05.005.

Costanzo, Raffaele, Maria Carmela Piccirillo, Claudia Sandomenico, Guido Carillio, Agnese Montanino, Gennaro Daniele, Pasqualina Giordano, et al. 2011. 'Gefitinib in Non Small Cell Lung Cancer'. *BioMed Research International* 2011: e815269. https://doi.org/10.1155/2011/815269.

Cotter, Catherine A., Patricia L. Earl, Linda S. Wyatt, and Bernard Moss. 2015. 'Preparation of Cell Cultures and Vaccinia Virus Stocks'. *Current Protocols in Microbiology* 39: 14A.3.1-14A.318. https://doi.org/10.1002/9780471729259.mc14a03s39.

Cytographica.com. 2007. 'Lab Tools'. http://www.cytographica.com/lab/index.html. Accessed July 2019.

Dai, Kai, Ling Huang, Jing Chen, Lihua Yang, and Zuojiong Gong. 2015. 'Amphiregulin Promotes the Immunosuppressive Activity of Intrahepatic CD4+ Regulatory T Cells to Impair CD8+ T-Cell Immunity against Hepatitis B Virus Infection'. *Immunology* 144 (3): 506–17. https://doi.org/10.1111/imm.12400.

Dai, Peihong, Weiyi Wang, Hua Cao, Francesca Avogadri, Lianpan Dai, Ingo Drexler, Johanna A. Joyce, et al. 2014. 'Modified Vaccinia Virus Ankara Triggers Type I IFN Production in Murine Conventional Dendritic Cells via a CGAS/STING-Mediated Cytosolic DNA-Sensing Pathway'. *PLOS Pathogens* 10 (4): e1003989. https://doi.org/10.1371/journal.ppat.1003989.

Dassonville, O., J. L. Formento, M. Francoual, A. Ramaioli, J. Santini, M. Schneider, F. Demard, and G. Milano. 1993. 'Expression of Epidermal Growth Factor Receptor and Survival in Upper Aerodigestive Tract Cancer'. *Journal of Clinical Oncology* 11 (10): 1873–78. https://doi.org/10.1200/JCO.1993.11.10.1873.

Dietze, K. K., G. Zelinskyy, K. Gibbert, S. Schimmer, S. Francois, L. Myers, T. Sparwasser, K. J. Hasenkrug, and U. Dittmer. 2011. 'Transient Depletion of Regulatory T Cells in Transgenic Mice Reactivates Virus-Specific CD8+ T Cells and Reduces Chronic Retroviral Set Points'. *Proceedings of the National Academy of Sciences* 108 (6): 2420–25. https://doi.org/10.1073/pnas.1015148108.

Dittrich, Anna M., Annika Erbacher, Sabine Specht, Felix Diesner, Martin Krokowski, Angela Avagyan, Philippe Stock, et al. 2008. 'Helminth Infection with Litomosoides Sigmodontis Induces Regulatory T Cells and Inhibits Allergic Sensitization, Airway Inflammation, and Hyperreactivity in a Murine Asthma Model'. *The Journal of Immunology* 180 (3): 1792–99.

Dutton, Susan J, David R Ferry, Jane M Blazeby, Haider Abbas, Asa Dahle-Smith, Wasat Mansoor, Joyce Thompson, et al. 2014. 'Gefitinib for Oesophageal Cancer Progressing after Chemotherapy (COG): A Phase 3, Multicentre, Double-Blind, Placebo-Controlled Randomised Trial'. *The Lancet Oncology* 15 (8): 894–904. https://doi.org/10.1016/S1470-2045(14)70024-5.

Eierhoff, Thorsten, Eike R. Hrincius, Ursula Rescher, Stephan Ludwig, and Christina Ehrhardt. 2010. 'The Epidermal Growth Factor Receptor (EGFR) Promotes

Uptake of Influenza A Viruses (IAV) into Host Cells'. *PLoS Pathog* 6 (9): e1001099. https://doi.org/10.1371/journal.ppat.1001099.

Elson, C. O., Y. Cong, S. Brandwein, C. T. Weaver, R. P. McCabe, M. Mähler, J. P. Sundberg, and E. H. Leiter. 1998. 'Experimental Models to Study Molecular Mechanisms Underlying Intestinal Inflammation'. *Annals of the New York Academy of Sciences* 859: 85–95. https://doi.org/10.1111/j.1749-6632.1998.tb11113.x.

Ferguson, Brian J, Daniel S Mansur, Nicholas E Peters, Hongwei Ren, and Geoffrey L Smith. 2012. 'DNA-PK Is a DNA Sensor for IRF-3-Dependent Innate Immunity'. *ELife* 1: e00047. https://doi.org/10.7554/eLife.00047.

Ferris, Robert L, Elizabeth M Jaffee, and Soldano Ferrone. 2010. 'Tumor Antigen-Targeted, Monoclonal Antibody-Based Immunotherapy: Clinical Response, Cellular Immunity, and Immunoescape'. *Journal of Clinical Oncology* 28 (28): 4390–99. https://doi.org/10.1200/JCO.2009.27.6360.

Fields, Bernard N., David M. Knipe, Peter M. Howley, and Diane E. Griffin. 2013. *Fields Virology*. 6th Edition. Philadelphia, USA: Lippincott Williams & Wilkins.

Filbey, Kara J, John R Grainger, Katherine A Smith, Louis Boon, Nico van Rooijen, Yvonne Harcus, Stephen Jenkins, James P Hewitson, and Rick M Maizels. 2014. 'Innate and Adaptive Type 2 Immune Cell Responses in Genetically Controlled Resistance to Intestinal Helminth Infection'. *Immunology and Cell Biology* 92 (5): 436–48. https://doi.org/10.1038/icb.2013.109.

Filby, Andrew, Julfa Begum, Marwa Jalal, and William Day. 2015. 'Appraising the Suitability of Succinimidyl and Lipophilic Fluorescent Dyes to Track Proliferation in Non-Quiescent Cells by Dye Dilution'. *Methods* 82: 29–37. https://doi.org/10.1016/j.ymeth.2015.02.016.

Finney, Constance A M, Matthew D Taylor, Mark S Wilson, and Rick M Maizels. 2007. 'Expansion and Activation of CD4+CD25+ Regulatory T Cells in Heligmosomoides Polygyrus Infection'. *European Journal of Immunology* 37 (7): 1874–86. https://doi.org/10.1002/eji.200636751.

Flajnik, Martin F., and Masanori Kasahara. 2010. 'Origin and Evolution of the Adaptive Immune System: Genetic Events and Selective Pressures'. *Nature Reviews. Genetics* 11 (1): 47–59. https://doi.org/10.1038/nrg2703.

Foy, Susan P., Stefanie J. Mandl, Tracy dela Cruz, Joseph J. Cote, Evan J. Gordon, Erica Trent, Alain Delcayre, James Breitmeyer, Alex Franzusoff, and Ryan B. Rountree. 2016. 'Poxvirus-Based Active Immunotherapy Synergizes with CTLA-4 Blockade to Increase Survival in a Murine Tumor Model by Improving the Magnitude and Quality of Cytotoxic T Cells'. *Cancer Immunology, Immunotherapy* 65: 537–49. https://doi.org/10.1007/s00262-016-1816-7.

References

Freyschmidt, Eva-Jasmin, Clinton B. Mathias, Natalia Diaz, Daniel H. MacArthur, Amale Laouar, Narasimhaswamy Manjunath, Matthias D. Hofer, et al. 2010. 'Skin Inflammation Arising from Cutaneous Treg Deficiency Leads to Impaired Viral Immune Responses'. *Journal of Immunology* 185 (2): 1295–1302. https://doi.org/10.4049/jimmunol.0903144.

Fulton, A., S. A. Babayan, and M. D. Taylor. 2018. 'Use of the Litomosoides Sigmodontis Infection Model of Filariasis to Study Type 2 Immunity'. In *Type 2 Immunity*, edited by R. Lee Reinhardt, 1799:11–26. Humana, New York. https://doi.org/10.1007/978-1-4939-7896-0_2.

Galán, Jorge E., John Pace, and Michael J. Hayman. 1992. 'Involvement of the Epidermal Growth Factor Receptor in the Invasion of Cultured Mammalian Cells by Salmonella Typhimurium'. *Nature* 357 (6379): 588. https://doi.org/10.1038/357588a0.

Garrido, Greta, Pablo Lorenzano, Belinda Sánchez, Irene Beausoleil, Daniel F Alonso, Rolando Pérez, and Luis E Fernández. 2007. 'T Cells Are Crucial for the Anti-Metastatic Effect of Anti-Epidermal Growth Factor Receptor Antibodies'. *Cancer Immunology, Immunotherapy* 56 (11): 1701–10. https://doi.org/10.1007/s00262-007-0313-4.

Gause, William C., Thomas A. Wynn, and Judith E. Allen. 2013. 'Type 2 Immunity and Wound Healing: Evolutionary Refinement of Adaptive Immunity by Helminths'. *Nature Reviews. Immunology* 13 (8): 607–14. https://doi.org/10.1038/nri3476.

Georgana, Iliana, Rebecca P. Sumner, Greg J. Towers, and Carlos Maluquer de Motes. 2018. 'Virulent Poxviruses Inhibit DNA Sensing by Preventing STING Activation'. *Journal of Virology* 92 (10): e02145-17. https://doi.org/10.1128/JVI.02145-17.

Ghoreschi, Kamran, Arian Laurence, Xiang-Ping Yang, Cristina M. Tato, Mandy J. McGeachy, Joanne E. Konkel, Haydeé L. Ramos, et al. 2010. 'Generation of Pathogenic TH17 Cells in the Absence of TGF-β Signalling'. *Nature* 467 (7318): 967–71. https://doi.org/10.1038/nature09447.

Gilchuk, Pavlo, Tim M Hill, Clifford Guy, Sean R McMaster, Kelli L Boyd, Whitney A Rabacal, Pengcheng Lu, et al. 2016. 'A Distinct Lung Interstitium-Resident Memory CD8+ T Cell Subset Confers Enhanced Protection to Lower Respiratory Tract Infection'. *Cell Reports* 16 (7): 1800–1809. https://doi.org/10.1016/j.celrep.2016.07.037.

Glimcher, Laurie H., and Kenneth M. Murphy. 2000. 'Lineage Commitment in the Immune System: The T Helper Lymphocyte Grows Up'. *Genes & Development* 14 (14): 1693–1711. https://doi.org/10.1101/gad.14.14.1693.

Global Asthma Network. 2014. 'The Global Asthma Report 2014.' http://www.globalasthmareport.org/2014/index.php. Accessed July 2019.

Gomez-Escobar, Natalia, William F. Gregory, and Rick M. Maizels. 2000. 'Identification of Tgh-2, a Filarial Nematode Homolog of Caenorhabditis Elegans Daf-7 and Human Transforming Growth Factor Beta, Expressed in Microfilarial and Adult Stages of Brugia Malayi'. *Infection and Immunity* 68 (11): 6402–10.

Goulding, J., R. Bogue, V. Tahiliani, M. Croft, and S. Salek-Ardakani. 2012. 'CD8 T Cells Are Essential for Recovery from a Respiratory Vaccinia Virus Infection'. *The Journal of Immunology* 189 (5): 2432–40. https://doi.org/10.4049/jimmunol.1200799.

Goulding, John, Georges Abboud, Vikas Tahiliani, Pritesh Desai, Tarun E. Hutchinson, and Shahram Salek-Ardakani. 2014. 'CD8 T Cells Use IFN-γ To Protect against the Lethal Effects of a Respiratory Poxvirus Infection'. *The Journal of Immunology* 192 (11): 5415–25. https://doi.org/10.4049/jimmunol.1400256.

Grainger, John R., Katie A. Smith, James P. Hewitson, Henry J. McSorley, Yvonne Harcus, Kara J. Filbey, Constance A. M. Finney, et al. 2010. 'Helminth Secretions Induce de Novo T Cell Foxp3 Expression and Regulatory Function through the TGF-β Pathway'. *The Journal of Experimental Medicine* 207 (11): 2331–41. https://doi.org/10.1084/jem.20101074.

Graness, A, S Hanke, F D Boehmer, P Presek, and C Liebmann. 2000. 'Protein-Tyrosine-Phosphatase-Mediated Epidermal Growth Factor (EGF) Receptor Transinactivation and EGF Receptor-Independent Stimulation of Mitogen-Activated Protein Kinase by Bradykinin in A431 Cells.' *Biochemical Journal* 347 (2): 441–47.

Gschwind, Andreas, Oliver M. Fischer, and Axel Ullrich. 2004. 'The Discovery of Receptor Tyrosine Kinases: Targets for Cancer Therapy'. *Nature Reviews Cancer* 4 (5): 361–70. https://doi.org/10.1038/nrc1360.

Guglani, Lokesh, and Shabaana A. Khader. 2010. 'Th17 Cytokines in Mucosal Immunity and Inflammation'. *Current Opinion in HIV and AIDS* 5 (2): 120–27. https://doi.org/10.1097/COH.0b013e328335c2f6.

Haben, Irma, Wiebke Hartmann, Sabine Specht, Achim Hoerauf, Axel Roers, Werner Müller, and Minka Breloer. 2013. 'T-Cell-Derived, but Not B-Cell-Derived, IL-10 Suppresses Antigen-Specific T-Cell Responses in Litomosoides Sigmodontis-Infected Mice'. *European Journal of Immunology* 43 (7): 1799–1805. https://doi.org/10.1002/eji.201242929.

Haeryfar, S. M. M., R. J. DiPaolo, D. C. Tscharke, J. R. Bennink, and J. W. Yewdell. 2005. 'Regulatory T Cells Suppress CD8+ T Cell Responses Induced by Direct Priming and Cross-Priming and Moderate Immunodominance Disparities'. *The Journal of Immunology* 174 (6): 3344–51. https://doi.org/10.4049/jimmunol.174.6.3344.

Halim, Timotheus Y.F., Batika M.J. Rana, Jennifer A. Walker, Bernhard Kerscher, Martin D. Knolle, Helen E. Jolin, Eva M. Serrao, et al. 2018. 'Tissue-Restricted Adaptive Type 2 Immunity Is Orchestrated by Expression of the Costimulatory Molecule OX40L on Group 2 Innate Lymphoid Cells'. *Immunity* 48 (6): 1195–1207. https://doi.org/10.1016/j.immuni.2018.05.003.

Han, Qing, Neda Bagheri, Elizabeth M. Bradshaw, David A. Hafler, Douglas A. Lauffenburger, and J. Christopher Love. 2012. 'Polyfunctional Responses by Human T Cells Result from Sequential Release of Cytokines'. *Proceedings of the National Academy of Sciences of the United States of America* 109 (5): 1607–12. https://doi.org/10.1073/pnas.1117194109.

Hardbower, Dana M., Kshipra Singh, Mohammad Asim, Thomas G. Verriere, Danyvid Olivares-Villagómez, Daniel P. Barry, Margaret M. Allaman, et al. 2016. 'EGFR Regulates Macrophage Activation and Function in Bacterial Infection'. *The Journal of Clinical Investigation* 126 (9): 3296–3312. https://doi.org/10.1172/JCI83585.

Harrington, Laurie E., Robbert van der Most, J. Lindsay Whitton, and Rafi Ahmed. 2002. 'Recombinant Vaccinia Virus-Induced T-Cell Immunity: Quantitation of the Response to the Virus Vector and the Foreign Epitope'. *Journal of Virology* 76 (7): 3329–37. https://doi.org/10.1128/JVI.76.7.3329-3337.2002.

Harrison, Kate, Ismar R. Haga, Tali Pechenick Jowers, Seema Jasim, Jean-Christophe Cintrat, Daniel Gillet, Thomas Schmitt-John, Paul Digard, and Philippa M. Beard. 2016. 'Vaccinia Virus Uses Retromer-Independent Cellular Retrograde Transport Pathways To Facilitate the Wrapping of Intracellular Mature Virions during Virus Morphogenesis'. *Journal of Virology* 90 (22): 10120–32. https://doi.org/10.1128/JVI.01464-16.

Hartemann, Agnès, Gilbert Bensimon, Christine A. Payan, Sophie Jacqueminet, Olivier Bourron, Nathalie Nicolas, Michèle Fonfrede, Michelle Rosenzwajg, Claude Bernard, and David Klatzmann. 2013. 'Low-Dose Interleukin 2 in Patients with Type 1 Diabetes: A Phase 1/2 Randomised, Double-Blind, Placebo-Controlled Trial'. *The Lancet. Diabetes & Endocrinology* 1 (4): 295–305. https://doi.org/10.1016/S2213-8587(13)70113-X.

Hartmann, Wiebke, Christoph Schramm, and Minka Breloer. 2015. 'Litomosoides Sigmodontis Induces TGF-β Receptor Responsive, IL-10-Producing T Cells That Suppress Bystander T-Cell Proliferation in Mice'. *European Journal of Immunology* 45 (9): 2568–81. https://doi.org/10.1002/eji.201545503.

Heinrichs, Jessica, David Bastian, Anandharaman Veerapathran, Claudio Anasetti, Brain Betts, and Xue-Zhong Yu. 2016. 'Regulatory T-Cell Therapy for Graft-versus-Host Disease'. *Journal of Immunology Research and Therapy* 1 (1): 1–14.

Helden, Mary J. G. van, Peter J. S. van Kooten, Cornelis P. J. Bekker, Andrea Gröne, David J. Topham, Andrew J. Easton, Claire J. P. Boog, Dirk H. Busch, Dietmar M. W. Zaiss, and Alice J. A. M. Sijts. 2012. 'Pre-Existing Virus-Specific CD8(+) T-Cells Provide Protection against Pneumovirus-Induced Disease in Mice'. *Vaccine* 30 (45): 6382–88. https://doi.org/10.1016/j.vaccine.2012.08.027.

Hepworth, Matthew R., Emilia Daniłowicz-Luebert, Sebastian Rausch, Martin Metz, Christian Klotz, Marcus Maurer, and Susanne Hartmann. 2012. 'Mast Cells Orchestrate Type 2 Immunity to Helminths through Regulation of Tissue-Derived Cytokines'. *Proceedings of the National Academy of Sciences of the United States of America* 109 (17): 6644–49. https://doi.org/10.1073/pnas.1112268109.

Hoerauf, A., K. Pfarr, S. Mand, A. Y. Debrah, and S. Specht. 2011. 'Filariasis in Africa--Treatment Challenges and Prospects'. *Clinical Microbiology and Infection* 17 (7): 977–85. https://doi.org/10.1111/j.1469-0691.2011.03586.x.

Hoffmann, Isabelle, Emmanuel Eugène, Xavier Nassif, Pierre-Olivier Couraud, and Sandrine Bourdoulous. 2001. 'Activation of ErbB2 Receptor Tyrosine Kinase Supports Invasion of Endothelial Cells by Neisseria Meningitidis'. *The Journal of Cell Biology* 155 (1): 133–44. https://doi.org/10.1083/jcb.200106148.

Hübner, Marc P., Yinghui Shi, Marina N. Torrero, Ellen Mueller, David Larson, Kateryna Soloviova, Fabian Gondorf, et al. 2012. 'Helminth Protection against Autoimmune Diabetes in Nonobese Diabetic Mice Is Independent of a Type 2 Immune Shift and Requires TGF-β'. *The Journal of Immunology* 188 (2): 559–68. https://doi.org/10.4049/jimmunol.1100335.

Hübner, Marc P., Marina N. Torrero, John W. McCall, and Edward Mitre. 2009. 'Litomosoides Sigmodontis: A Simple Method to Infect Mice with L3 Larvae Obtained from the Pleural Space of Recently Infected Jirds (Meriones Unguiculatus)'. *Experimental Parasitology* 123 (1): 95–98. https://doi.org/10.1016/j.exppara.2009.05.009.

Hull, Caroline M., Mark Peakman, and Timothy I. M. Tree. 2017. 'Regulatory T Cell Dysfunction in Type 1 Diabetes: What's Broken and How Can We Fix It?' *Diabetologia* 60 (10): 1839–50. https://doi.org/10.1007/s00125-017-4377-1.

Huygelen, C. 1996. '[Jenner's cowpox vaccine in light of current vaccinology]'. *Verhandelingen - Koninklijke Academie Voor Geneeskunde Van Belgie* 58 (5): 479–536.

Iborra, Salvador, María Martínez-López, Sofía C. Khouili, Michel Enamorado, Francisco J. Cueto, Ruth Conde-Garrosa, Carlos del Fresno, and David Sancho. 2016. 'Optimal Generation of Tissue-Resident but Not Circulating Memory T Cells during Viral Infection Requires Crosspriming by DNGR-1+ Dendritic Cells'. *Immunity* 45 (4): 847–60. https://doi.org/10.1016/j.immuni.2016.08.019.

Jackson, Daniel J., Ronald E. Gangnon, Michael D. Evans, Kathy A. Roberg, Elizabeth L. Anderson, Tressa E. Pappas, Magnolia C. Printz, et al. 2008. 'Wheezing Rhinovirus Illnesses in Early Life Predict Asthma Development in High-Risk Children'. *American Journal of Respiratory and Critical Care Medicine* 178 (7): 667–72. https://doi.org/10.1164/rccm.200802-309OC.

Jacobs, Bertram L., Jeffrey O. Langland, Karen V. Kibler, Karen L. Denzler, Stacy D. White, Susan A. Holechek, Shukmei Wong, Trung Huynh, and Carole R. Baskin. 2009. 'Vaccinia Virus Vaccines: Past, Present and Future'. *Antiviral Research* 84 (1): 1–13. https://doi.org/10.1016/j.antiviral.2009.06.006.

Jiang, Xiaodong, Rachael A. Clark, Luzheng Liu, Amy J. Wagers, Robert C. Fuhlbrigge, and Thomas S. Kupper. 2012. 'Skin Infection Generates Non-Migratory Memory CD8+ TRM Cells Providing Global Skin Immunity'. *Nature* 483 (7388): 227–31. https://doi.org/10.1038/nature10851.

Jog, Neelakshi R., Eliza F. Chakravarty, Joel M. Guthridge, and Judith A. James. 2018. 'Epstein Barr Virus Interleukin 10 Suppresses Anti-Inflammatory Phenotype in Human Monocytes'. *Frontiers in Immunology* 9. https://doi.org/10.3389/fimmu.2018.02198.

Johnston, Chris J. C., Elaine Robertson, Yvonne Harcus, John R. Grainger, Gillian Coakley, Danielle J. Smyth, Henry J. McSorley, and Rick Maizels. 2015. 'Cultivation of Heligmosomoides Polygyrus: An Immunomodulatory Nematode Parasite and Its Secreted Products'. *Journal of Visualized Experiments* 98: e52412. https://doi.org/10.3791/52412.

Johnston, Chris J. C., Danielle J. Smyth, Ravindra B. Kodali, Madeleine P. J. White, Yvonne Harcus, Kara J. Filbey, James P. Hewitson, et al. 2017. 'A Structurally Distinct TGF-β Mimic from an Intestinal Helminth Parasite Potently Induces Regulatory T Cells'. *Nature Communications* 8: 1741. https://doi.org/10.1038/s41467-017-01886-6.

Kadoki, Motohiko, Ashwini Patil, Cornelius C. Thaiss, Donald J. Brooks, Surya Pandey, Deeksha Deep, David Alvarez, et al. 2017. 'Organism-Level Analysis of Vaccination Reveals Networks of Protection across Tissues'. *Cell* 171 (2): 398-413.e21. https://doi.org/10.1016/j.cell.2017.08.024.

Kanhere, Aditi, Arnulf Hertweck, Urvashi Bhatia, M. Refik Gökmen, Esperanza Perucha, Ian Jackson, Graham M. Lord, and Richard G. Jenner. 2012. 'T-Bet

and GATA3 Orchestrate Th1 and Th2 Differentiation through Lineage-Specific Targeting of Distal Regulatory Elements'. *Nature Communications* 3: 1268. https://doi.org/10.1038/ncomms2260.

Kastenmuller, W., G. Gasteiger, N. Subramanian, T. Sparwasser, D. H. Busch, Y. Belkaid, I. Drexler, and R. N. Germain. 2011. 'Regulatory T Cells Selectively Control CD8+ T Cell Effector Pool Size via IL-2 Restriction'. *The Journal of Immunology* 187 (6): 3186–97. https://doi.org/10.4049/jimmunol.1101649.

Keates, Sarah, Andrew C. Keates, Kianoosh Katchar, Richard M. Peek, and Ciaran P. Kelly. 2007. 'Helicobacter Pylori Induces Up-Regulation of the Epidermal Growth Factor Receptor in AGS Gastric Epithelial Cells'. *The Journal of Infectious Diseases* 196 (1): 95–103. https://doi.org/10.1086/518440.

Keates, Sarah, Stavros Sougioultzis, Andrew C. Keates, Dezhang Zhao, Richard M. Peek, Leslie M. Shaw, and Ciaran P. Kelly. 2001. 'Cag+ Helicobacter Pylori Induce Transactivation of the Epidermal Growth Factor Receptor in AGS Gastric Epithelial Cells'. *Journal of Biological Chemistry* 276 (51): 48127–34. https://doi.org/10.1074/jbc.M107630200.

Kim, H. S., Y. H. Lee, D. S. Min, J. S. Chang, S. H. Ryu, B. Y. Ahn, and P. G. Suh. 1995. 'Tyrosine Phosphorylation of Phospholipase C-Gamma 1 by Vaccinia Virus Growth Factor'. *Virology* 214 (1): 21–28. https://doi.org/10.1006/viro.1995.9958.

Kim, Mikyung, Hailin Yang, Sung-Kwon Kim, Pedro A. Reche, Rebecca S. Tirabassi, Rebecca E. Hussey, Yasmin Chishti, et al. 2004. 'Biochemical and Functional Analysis of Smallpox Growth Factor (SPGF) and Anti-SPGF Monoclonal Antibodies'. *Journal of Biological Chemistry* 279 (24): 25838–48. https://doi.org/10.1074/jbc.M400343200.

Kleinpeter, Patricia, Christelle Remy-Ziller, Eline Winter, Murielle Gantzer, Virginie Nourtier, Juliette Kempf, Julie Hortelano, et al. 2019. 'By Binding CD80 and CD86, the Vaccinia Virus M2 Protein Blocks Their Interactions with Both CD28 and CTLA4 and Potentiates CD80 Binding to PD-L1'. *Journal of Virology* 93 (11): e00207-19. https://doi.org/10.1128/JVI.00207-19.

Köhler, Jens, and Martin Schuler. 2013. 'Afatinib, Erlotinib and Gefitinib in the First-Line Therapy of EGFR Mutation-Positive Lung Adenocarcinoma: A Review'. *Onkologie* 36 (9): 510–18. https://doi.org/10.1159/000354627.

Kohri, K., I. F. Ueki, J.-J. Shim, P.-R. Burgel, Y.-M. Oh, D. C. Tam, T. Dao-Pick, and J. A. Nadel. 2002. 'Pseudomonas Aeruginosa Induces MUC5AC Production via Epidermal Growth Factor Receptor'. *European Respiratory Journal* 20 (5): 1263–70. https://doi.org/10.1183/09031936.02.00001402.

Koivisto, Leeni, Guoqiao Jiang, Lari Häkkinen, Bosco Chan, and Hannu Larjava. 2006. 'HaCaT Keratinocyte Migration Is Dependent on Epidermal Growth Factor Receptor Signaling and Glycogen Synthase Kinase-3α'. *Experimental Cell Research* 312 (15): 2791–2805. https://doi.org/10.1016/j.yexcr.2006.05.009.

Korn, Thomas, Estelle Bettelli, Mohamed Oukka, and Vijay K. Kuchroo. 2009. 'IL-17 and Th17 Cells'. *Annual Review of Immunology* 27 (1): 485–517. https://doi.org/10.1146/annurev.immunol.021908.132710.

Kretschmer, Karsten, Irina Apostolou, Elmar Jaeckel, Khashayarsha Khazaie, and Harald Von Boehmer. 2006. 'Making Regulatory T Cells with Defined Antigen Specificity: Role in Autoimmunity and Cancer'. *Immunological Reviews* 212 (1): 163–69. https://doi.org/10.1111/j.0105-2896.2006.00411.x.

Krishnamoorthy, Nandini, Anupriya Khare, Timothy B Oriss, Mahesh Raundhal, Christina Morse, Manohar Yarlagadda, Sally E Wenzel, et al. 2012. 'Early Infection with Respiratory Syncytial Virus Impairs Regulatory T Cell Function and Increases Susceptibility to Allergic Asthma'. *Nature Medicine* 18 (10): 1525–30. https://doi.org/10.1038/nm.2896.

Kumar, Bhavna, Kitrina G. Cordell, Julia S. Lee, Francis P. Worden, Mark E. Prince, Huong H. Tran, Gregory T. Wolf, et al. 2008. 'EGFR, P16, HPV Titer, Bcl-XL and P53, Sex, and Smoking As Indicators of Response to Therapy and Survival in Oropharyngeal Cancer'. *Journal of Clinical Oncology* 26 (19): 3128–37. https://doi.org/10.1200/JCO.2007.12.7662.

Kumar, Thomas J. Connors, and Donna L. Farber. 2018. 'Human T Cell Development, Localization, and Function throughout Life'. *Immunity* 48 (2): 202–13. https://doi.org/10.1016/j.immuni.2018.01.007.

Kung, Che-Pei, David G. Meckes, and Nancy Raab-Traub. 2011. 'Epstein-Barr Virus LMP1 Activates EGFR, STAT3, and ERK through Effects on PKCδ'. *Journal of Virology* 85 (9): 4399–4408. https://doi.org/10.1128/JVI.01703-10.

Lahl, Katharina, and Tim Sparwasser. 2011. 'In Vivo Depletion of FoxP3+ Tregs Using the DEREG Mouse Model'. In *Regulatory T Cells: Methods and Protocols*, edited by George Kassiotis and Adrian Liston, 157–72. Methods in Molecular Biology. https://doi.org/10.1007/978-1-61737-979-6_10.

Lai, Alexander C. -K., and Beatriz G. -T. Pogo. 1989. 'Attenuated Deletion Mutants of Vaccinia Virus Lacking the Vaccinia Growth Factor Are Defective in Replication in Vivo'. *Microbial Pathogenesis* 6 (3): 219–26. https://doi.org/10.1016/0882-4010(89)90071-5.

Langhammer, Stefan, Robert Koban, Constanze Yue, and Heinz Ellerbrok. 2011. 'Inhibition of Poxvirus Spreading by the Anti-Tumor Drug Gefitinib (Iressa™)'.

Antiviral Research 89 (1): 64–70. https://doi.org/10.1016/j.antiviral.2010.11.006.

Le Goff, Laetitia, Tracey J. Lamb, Andrea L. Graham, Yvonne Harcus, and Judith E. Allen. 2002. 'IL-4 Is Required to Prevent Filarial Nematode Development in Resistant but Not Susceptible Strains of Mice'. *International Journal for Parasitology* 32 (10): 1277–1284.

Lee, Yun Kyung, Henrietta Turner, Craig L. Maynard, James R. Oliver, Dongquan Chen, Charles O. Elson, and Casey T. Weaver. 2009. 'Late Developmental Plasticity in the T Helper 17 Lineage'. *Immunity* 30 (1): 92–107. https://doi.org/10.1016/j.immuni.2008.11.005.

Levi-Montalcini, R., and S. Cohen. 1960. 'Effects of the Extract of the Mouse Submaxillary Salivary Glands on the Sympathetic System of Mammals'. *Annals of the New York Academy of Sciences* 85: 324–41.

Li, Guiyun, Nanhai Chen, Zehua Feng, R. Mark L. Buller, John Osborne, Tiara Harms, Inger Damon, Chris Upton, and David J. Esteban. 2006. 'Genomic Sequence and Analysis of a Vaccinia Virus Isolate from a Patient with a Smallpox Vaccine-Related Complication'. *Virology Journal* 3 (1): 88. https://doi.org/10.1186/1743-422X-3-88.

Li, S., E. J. Gowans, C. Chougnet, M. Plebanski, and U. Dittmer. 2008. 'Natural Regulatory T Cells and Persistent Viral Infection'. *Journal of Virology* 82 (1): 21–30. https://doi.org/10.1128/JVI.01768-07.

Liao, Wei, Dustin E. Schones, Jangsuk Oh, Yongzhi Cui, Kairong Cui, Roh Tae-Young, Keji Zhao, and Warren J. Leonard. 2008. 'Priming for T Helper Type 2 Differentiation by Interleukin 2-Mediated Induction of IL-4 Receptor α Chain Expression'. *Nature Immunology* 9 (11): 1288–96. https://doi.org/10.1038/ni.1656.

Lim, Jun Feng, Heidi Berger, and I.-Hsin Su. 2016. 'Isolation and Activation of Murine Lymphocytes'. *Journal of Visualized Experiments* 116: e54596. https://doi.org/10.3791/54596.

Lindquist, H. D. Alan, and John H. Cross. 2017. '195 - Helminths'. In *Infectious Diseases (Fourth Edition)*, edited by Jonathan Cohen, William G. Powderly, and Steven M. Opal, 1763–79. Elsevier. https://doi.org/10.1016/B978-0-7020-6285-8.00195-7.

Linggi, Bryan, and Graham Carpenter. 2006. 'ErbB Receptors: New Insights on Mechanisms and Biology'. *Trends in Cell Biology* 16 (12): 649–56. https://doi.org/10.1016/j.tcb.2006.10.008.

Liu, Qiang, Goldie Djuricin, Catherine Nathan, Paolo Gattuso, Robert A. Weinstein, and Richard A. Prinz. 1997. 'The Effect of Epidermal Growth Factor on the Septic Complications of Acute Pancreatitis'. *Journal of Surgical Research* 69 (1): 171–77. https://doi.org/10.1006/jsre.1997.5069.

Liu, Siqi, Xin Cai, Jiaxi Wu, Qian Cong, Xiang Chen, Tuo Li, Fenghe Du, et al. 2015. 'Phosphorylation of Innate Immune Adaptor Proteins MAVS, STING, and TRIF Induces IRF3 Activation'. *Science* 347 (6227): aaa2630. https://doi.org/10.1126/science.aaa2630.

Ma, Chaoyu, Shruti Mishra, Erika L. Demel, Yong Liu, and Nu Zhang. 2017. 'TGF-β Controls the Formation of Kidney-Resident T Cells via Promoting Effector T Cell Extravasation'. *Journal of Immunology* 198 (2): 749–56. https://doi.org/10.4049/jimmunol.1601500.

MacDonald, Felicity, and Dietmar M. W. Zaiss. 2017. 'The Immune System's Contribution to the Clinical Efficacy of EGFR Antagonist Treatment'. *Frontiers in Pharmacology* 8: 575. https://doi.org/10.3389/fphar.2017.00575.

Mahtouk, Karene, Dirk Hose, Thierry Reme, John De Vos, Michel Jourdan, Jerome Moreaux, Genevieve Fiol, et al. 2005. 'Expression of EGF-Family Receptors and Amphiregulin in Multiple Myeloma. Amphiregulin Is a Growth Factor for Myeloma Cells'. *Oncogene* 24 (21): 3512–24. https://doi.org/10.1038/sj.onc.1208536.

Maizels, Rick M., James P. Hewitson, Janice Murray, Yvonne M. Harcus, Blaise Dayer, Kara J. Filbey, John R. Grainger, Henry J. McSorley, Lisa A. Reynolds, and Katherine A. Smith. 2012. 'Immune Modulation and Modulators in Heligmosomoides Polygyrus Infection'. *Experimental Parasitology* 132 (1): 76–89. https://doi.org/10.1016/j.exppara.2011.08.011.

Maizels, Rick M., Hermelijn H. Smits, and Henry J. McSorley. 2018. 'Modulation of Host Immunity by Helminths: The Expanding Repertoire of Parasite Effector Molecules'. *Immunity* 49 (5): 801–18. https://doi.org/10.1016/j.immuni.2018.10.016.

Marek-Trzonkowska, Natalia, Małgorzata Myśliwiec, Anita Dobyszuk, Marcelina Grabowska, Ilona Derkowska, Jolanta Juścińska, Radosław Owczuk, et al. 2014. 'Therapy of Type 1 Diabetes with CD4(+)CD25(High)CD127-Regulatory T Cells Prolongs Survival of Pancreatic Islets - Results of One Year Follow-Up'. *Clinical Immunology* 153 (1): 23–30. https://doi.org/10.1016/j.clim.2014.03.016.

Marsh, Y. V., and D. A. Eppstein. 1987. 'Vaccinia Virus and the EGF Receptor: A Portal for Infectivity?' *Journal of Cellular Biochemistry* 34 (4): 239–45. https://doi.org/10.1002/jcb.240340403.

Martin, Stefani, Daniel T. Harris, and Joanna Shisler. 2012. 'The C11R Gene, Which Encodes the Vaccinia Virus Growth Factor, Is Partially Responsible for MVA-Induced NF-KB and ERK2 Activation'. *Journal of Virology* 86 (18): 9629–39. https://doi.org/10.1128/JVI.06279-11.

Matsumoto, Kenji, Shuhei Fukuda, Yuri Nakamura, and Hirohisa Saito. 2009. 'Amphiregulin Production by Human Eosinophils'. *International Archives of Allergy and Immunology* 149 Suppl 1: 39–44. https://doi.org/10.1159/000210652.

Maus, U., S. Herold, H. Muth, R. Maus, L. Ermert, M. Ermert, N. Weissmann, et al. 2001. 'Monocytes Recruited into the Alveolar Air Space of Mice Show a Monocytic Phenotype but Upregulate CD14'. *American Journal of Physiology. Lung Cellular and Molecular Physiology* 280 (1): L58-68. https://doi.org/10.1152/ajplung.2001.280.1.L58.

McCart, J. Andrea, Jerrold M. Ward, John Lee, Yun Hu, H. Richard Alexander, Steven K. Libutti, Bernard Moss, and David L. Bartlett. 2001. 'Systemic Cancer Therapy with a Tumor-Selective Vaccinia Virus Mutant Lacking Thymidine Kinase and Vaccinia Growth Factor Genes'. *Cancer Research* 24: 8751–57.

McSorley, Henry J., Yvonne M. Harcus, Janice Murray, Matthew D. Taylor, and Rick M. Maizels. 2008. 'Expansion of Foxp3+ Regulatory T Cells in Mice Infected with the Filarial Parasite Brugia Malayi'. *The Journal of Immunology* 181 (9): 6456–66.

McSorley, Henry J., James P. Hewitson, and Rick M. Maizels. 2013. 'Immunomodulation by Helminth Parasites: Defining Mechanisms and Mediators'. *International Journal for Parasitology* 43 (3–4): 301–10. https://doi.org/10.1016/j.ijpara.2012.11.011.

McSorley, Henry J, Mary T O'Gorman, Natalie Blair, Tara E Sutherland, Kara J Filbey, and Rick M Maizels. 2012. 'Suppression of Type 2 Immunity and Allergic Airway Inflammation by Secreted Products of the Helminth Heligmosomoides Polygyrus'. *European Journal of Immunology* 42 (10): 2667–82. https://doi.org/10.1002/eji.201142161.

Melnick, Michael, George Abichaker, Khine Htet, Parish Sedghizadeh, and Tina Jaskoll. 2011. 'Small Molecule Inhibitors of the Host Cell COX/AREG/EGFR/ERK Pathway Attenuate Cytomegalovirus-Induced Pathogenesis'. *Experimental and Molecular Pathology* 91 (1): 400–410. https://doi.org/10.1016/j.yexmp.2011.04.014.

Melnick, Michael, Krysta A. Deluca, Parish P. Sedghizadeh, and Tina Jaskoll. 2013. 'Cytomegalovirus-Induced Salivary Gland Pathology: AREG, FGF8, TNF-α,

and IL-6 Signal Dysregulation and Neoplasia'. *Experimental and Molecular Pathology* 94 (2): 386–97. https://doi.org/10.1016/j.yexmp.2013.01.005.

Melnick, Michael, Parish P Sedghizadeh, Krysta A Deluca, and Tina Jaskoll. 2013. 'Cytomegalovirus-Induced Salivary Gland Pathology: Resistance to Kinase Inhibitors of the Upregulated Host Cell EGFR/ERK Pathway Is Associated with CMV-Dependent Stromal Overexpression of IL-6 and Fibronectin'. *Herpesviridae* 4: 1. https://doi.org/10.1186/2042-4280-4-1.

Mercer, Jason, Stephan Knébel, Florian I. Schmidt, Josh Crouse, Christine Burkard, and Ari Helenius. 2010. 'Vaccinia Virus Strains Use Distinct Forms of Macropinocytosis for Host-Cell Entry'. *Proceedings of the National Academy of Sciences of the United States of America* 107 (20): 9346–51. https://doi.org/10.1073/pnas.1004618107.

Miettinen, Päivi J., Joel E. Berger, Juanito Meneses, Yume Phung, Roger A. Pedersen, Zena Werb, and Rik Derynck. 1995. 'Epithelial Immaturity and Multiorgan Failure in Mice Lacking Epidermal Growth Factor Receptor'. *Nature* 6538: 337–41. https://doi.org/10.1038/376337a0.

Mikami, Fumi, He Gu, Hirofumi Jono, Ali Andalibi, Hirofumi Kai, and Jian-Dong Li. 2005. 'Epidermal Growth Factor Receptor Acts as a Negative Regulator for Bacterium Nontypeable Haemophilus Influenzae-Induced Toll-like Receptor 2 Expression via an Src-Dependent P38 Mitogen-Activated Protein Kinase Signaling Pathway'. *Journal of Biological Chemistry* 43: 36185–94. https://doi.org/10.1074/jbc.M503941200.

Miller, W. E., H. S. Earp, and N. Raab-Traub. 1995. 'The Epstein-Barr Virus Latent Membrane Protein 1 Induces Expression of the Epidermal Growth Factor Receptor'. *Journal of Virology* 69 (7): 4390–98.

Miltenyi Biotec. 2018. 'MACS Handbook'. 2018. https://www.miltenyibiotec.com/GB-en/resources/macs-handbook.html. Accessed July 2019.

Minutti, Carlos M., Sebastian Drube, Natalie Blair, Christian Schwartz, Jame C. McCrae, Andrew N. McKenzie, Thomas Kamradt, et al. 2017. 'Epidermal Growth Factor Receptor Expression Licenses Type-2 Helper T Cells to Function in a T Cell Receptor-Independent Fashion'. *Immunity* 47 (4): 710-722.e6. https://doi.org/10.1016/j.immuni.2017.09.013.

Minutti, Carlos M., Rucha V. Modak, Felicity Macdonald, Fengqi Li, Danielle J. Smyth, David A. Dorward, Natalie Blair, et al. 2019. 'A Macrophage-Pericyte Axis Directs Tissue Restoration via Amphiregulin-Induced Transforming Growth Factor Beta Activation'. *Immunity* 50 (3): 645-654.e6. https://doi.org/10.1016/j.immuni.2019.01.008.

Mölleken, Katja, Elisabeth Becker, and Johannes H. Hegemann. 2013. 'The Chlamydia Pneumoniae Invasin Protein Pmp21 Recruits the EGF Receptor for Host Cell Entry'. *PLoS Pathogens* 9 (4): e1003325. https://doi.org/10.1371/journal.ppat.1003325.

Mombaerts, P., J. Iacomini, R. S. Johnson, K. Herrup, S. Tonegawa, and V. E. Papaioannou. 1992. 'RAG-1-Deficient Mice Have No Mature B and T Lymphocytes'. *Cell* 68 (5): 869–77.

Monick, M. M. 2004. 'Activation of the Epidermal Growth Factor Receptor by Respiratory Syncytial Virus Results in Increased Inflammation and Delayed Apoptosis'. *Journal of Biological Chemistry* 280 (3): 2147–58. https://doi.org/10.1074/jbc.M408745200.

Monticelli, Laurel A., Gregory F. Sonnenberg, Michael C. Abt, Theresa Alenghat, Carly G. K. Ziegler, Travis A. Doering, Jill M. Angelosanto, et al. 2011. 'Innate Lymphoid Cells Promote Lung-Tissue Homeostasis after Infection with Influenza Virus'. *Nature Immunology* 12 (11): 1045–54. https://doi.org/10.1031/ni.2131.

Morris, C. Paul, Marina N. Torrero, David Larson, Holly Evans, Yinghui Shi, Rachel T. Cox, and Edward Mitre. 2013. 'Vaccination with Intestinal Tract Antigens Does Not Induce Protective Immunity in a Permissive Model of Filariasis'. *Experimental Parasitology* 135 (1): 87–95. https://doi.org/10.1016/j.exppara.2013.05.018.

Mosmann, T. R., H. Cherwinski, M. W. Bond, M. A. Giedlin, and R. L. Coffman. 1986. 'Two Types of Murine Helper T Cell Clone. I. Definition According to Profiles of Lymphokine Activities and Secreted Proteins.' *The Journal of Immunology* 136 (7): 2348–57.

Moss, Bernard. 2012. 'Poxvirus Cell Entry: How Many Proteins Does It Take?' *Viruses* 4 (5): 688–707. https://doi.org/10.3390/v4050688.

Moss, Bernard. 2013. 'Poxvirus DNA Replication'. *Cold Spring Harbor Perspectives in Biology* 5 (9): a010199. https://doi.org/10.1101/cshperspect.a010199.

Moss, Bernard. 2015. 'Poxvirus Membrane Biogenesis'. *Virology* 479–480: 619–26. https://doi.org/10.1016/j.virol.2015.02.003.

Moss, Bernard. 2016. 'Membrane Fusion during Poxvirus Entry'. *Seminars in Cell & Developmental Biology* 60: 89–96. https://doi.org/10.1016/j.semcdb.2016.07.015.

Mottet, Christian, Holm H. Uhlig, and Fiona Powrie. 2003. 'Cutting Edge: Cure of Colitis by CD4+CD25+ Regulatory T Cells'. *The Journal of Immunology* 170 (8): 3939–43. https://doi.org/10.4049/jimmunol.170.8.3939.

Muniz-Feliciano, Luis, Jennifer Van Grol, Jose-Andres C. Portillo, Lloyd Liew, Bing Liu, Cathleen R. Carlin, Vern B. Carruthers, Stephen Matthews, and Carlos S. Subauste. 2013. 'Toxoplasma Gondii-Induced Activation of EGFR Prevents Autophagy Protein-Mediated Killing of the Parasite'. *PLoS Pathog* 9 (12): e1003809. https://doi.org/10.1371/journal.ppat.1003809.

Murphy, Kenneth M., and Steven L. Reiner. 2002. 'Decision Making in the Immune System: The Lineage Decisions of Helper T Cells'. *Nature Reviews Immunology* 2 (12): 933–44. https://doi.org/10.1038/nri954.

Muruganandah, Visai, Harindra D. Sathkumara, Severine Navarro, and Andreas Kupz. 2018. 'A Systematic Review: The Role of Resident Memory T Cells in Infectious Diseases and Their Relevance for Vaccine Development'. *Frontiers in Immunology* 9: 1574. https://doi.org/10.3389/fimmu.2018.01574.

Nath, Artika P., Asolina Braun, Scott C. Ritchie, Francis R. Carbone, Laura K. Mackay, Thomas Gebhardt, and Michael Inouye. 2019. 'Comparative Analysis Reveals a Role for TGF-β in Shaping the Residency-Related Transcriptional Signature in Tissue-Resident Memory CD8+ T Cells'. *PLOS ONE* 14 (2): e0210495. https://doi.org/10.1371/journal.pone.0210495.

NC3Rs. 2019. 'Mouse: Tail Vein Sampling'. 2019. https://www.nc3rs.org.uk/mouse-tail-vein-non-surgical. Accessed July 2019.

Norton, A, G R Peplinski, and K Tsung. 1996. 'Expression of Secreted Platelet-Derived Growth Factor-B by Recombinant Nonreplicating and Noncytopathic Vaccina Virus.' *Annals of Surgery* 224 (4): 555–62.

Nosbaum, Audrey, Nicolas Prevel, Hong-An Truong, Pooja Mehta, Monika Ettinger, Tiffany C. Scharschmidt, Niwa H. Ali, Mariela L. Pauli, Abul K. Abbas, and Michael D. Rosenblum. 2016. 'Regulatory T Cells Facilitate Cutaneous Wound Healing'. *Journal of Immunology* 196 (5): 2010–14. https://doi.org/10.4049/jimmunol.1502139.

National Research Council (US) Subcommittee on Laboratory Animal Nutrition. 1995. 3, *Nutrient Requirements of the Mouse*. Nutrient Requirements of Laboratory Animals: Fourth Revised Edition. National Academies Press (US). https://www.ncbi.nlm.nih.gov/books/NBK231918/.

O'Garra, Anne, and Kenneth Murphy. 1994. 'Role of Cytokines in Determining T-Lymphocyte Function'. *Current Opinion in Immunology* 6 (3): 458–66. https://doi.org/10.1016/0952-7915(94)90128-7.

Okoye, Isobel S., Stephanie M. Coomes, Victoria S. Pelly, Stephanie Czieso, Venizelos Papayannopoulos, Tanya Tolmachova, Miguel C. Seabra, and Mark S. Wilson. 2014. 'MicroRNA-Containing T-Regulatory-Cell-Derived

Exosomes Suppress Pathogenic T Helper 1 Cells'. *Immunity* 41 (1): 89–103. https://doi.org/10.1016/j.immuni.2014.05.019.

Ouyang, Ping, Krzysztof Rakus, Steven J. van Beurden, Adrie H. Westphal, Andrew J. Davison, Derek Gatherer, and Alain F. Vanderplasschen. 2014. 'IL-10 Encoded by Viruses: A Remarkable Example of Independent Acquisition of a Cellular Gene by Viruses and Its Subsequent Evolution in the Viral Genome'. *The Journal of General Virology* 95 (2): 245–62. https://doi.org/10.1099/vir.0.058966-0.

Pan, Fan, Huimin Fan, Ling Lu, Zhongmin Liu, and Shuiping Jiang. 2011. 'The Yin and Yang of Signaling in Tregs and TH17 Cells'. *Science Signaling* 4 (165): mr4. https://doi.org/10.1126/scisignal.2001709.

Pasare, Chandrashekhar, and Ruslan Medzhitov. 2003. 'Toll Pathway-Dependent Blockade of CD4+CD25+ T Cell-Mediated Suppression by Dendritic Cells'. *Science* 299 (5609): 1033–36. https://doi.org/10.1126/science.1078231.

Patel, Achchhe L., Xiaofei Chen, Scott T. Wood, Elizabeth S. Stuart, Kathleen F. Arcaro, Doris P. Molina, Snezana Petrovic, Cristina M. Furdui, and Allen W. Tsang. 2014. 'Activation of Epidermal Growth Factor Receptor Is Required for Chlamydia Trachomatis Development'. *BMC Microbiology* 14 (1): 277. https://doi.org/10.1186/s12866-014-0277-4.

Patton, John B., David George, and Kyeong-Ok Chang. 2011. 'Bile Acids Promote HCV Replication through the EGFR/ERK Pathway in Replicon-Harboring Cells'. *Intervirology* 54 (6): 339–48. https://doi.org/10.1159/000321452.

Pechenick Jowers, Tali, Rebecca J. Featherstone, Danielle K. Reynolds, Helen K. Brown, John James, Alan Prescott, Ismar R. Haga, and Philippa M. Beard. 2015. 'RAB1A Promotes Vaccinia Virus Replication by Facilitating the Production of Intracellular Enveloped Virions'. *Virology* 475: 66–73. https://doi.org/10.1016/j.virol.2014.11.007.

Peters, Nicholas E., Brian J. Ferguson, Michela Mazzon, Aodhnait S. Fahy, Ewelina Krysztofinska, Raquel Arribas-Bosacoma, Laurence H. Pearl, Hongwei Ren, and Geoffrey L. Smith. 2013. 'A Mechanism for the Inhibition of DNA-PK-Mediated DNA Sensing by a Virus'. *PLoS Pathogens* 9 (10). https://doi.org/10.1371/journal.ppat.1003649.

Petit, G., M. Diagne, P. Maréchal, D. Owen, D. Taylor, and O. Bain. 1992. 'Maturation of the Filaria Litomosoides Sigmodontis in BALB/c Mice; Comparative Susceptibility of Nine Other Inbred Strains'. *Annales de Parasitologie Humaine et Comparée* 67 (5): 144–50. https://doi.org/10.1051/parasite/1992675144.

Pfaff, Alexander W, Hartwig Schulz-Key, Peter T Soboslay, David W Taylor, Karen MacLennan, and Wolfgang H Hoffmann. 2002. 'Litomosoides Sigmodontis Cystatin Acts as an Immunomodulator during Experimental Filariasis'. *International Journal for Parasitology* 32 (2): 171–78. https://doi.org/10.1016/S0020-7519(01)00350-2.

Postigo, Antonio, Morag C Martin, Mark P Dodding, and Michael Way. 2009. 'Vaccinia-Induced Epidermal Growth Factor Receptor-MEK Signalling and the Anti-Apoptotic Protein F1L Synergize to Suppress Cell Death during Infection'. *Cellular Microbiology* 11 (8): 1208–18. https://doi.org/10.1111/j.1462-5822.2009.01327.x.

Pratt, Zachary L., Jingzhu Zhang, and Bill Sugden. 2012. 'The Latent Membrane Protein 1 (LMP1) Oncogene of Epstein-Barr Virus Can Simultaneously Induce and Inhibit Apoptosis in B Cells'. *Journal of Virology* 86 (8): 4380–93. https://doi.org/10.1128/JVI.06966-11.

Prenzel, N. 2001. 'The Epidermal Growth Factor Receptor Family as a Central Element for Cellular Signal Transduction and Diversification'. *Endocrine Related Cancer* 8 (1): 11–31. https://doi.org/10.1677/erc.0.0080011.

Puksuriwong, Suttida, Muhammad S. Ahmed, Ravi Sharma, Madhan Krishnan, Sam Leong, Teresa Lambe, Paul S. McNamara, Sarah C. Gilbert, and Qibo Zhang. 2019. 'MVA-NP+M1 Vaccine Activates Mucosal M1-Specific T Cell Immunity and Tissue-Resident Memory T Cells in Human Nasopharynx-Associated Lymphoid Tissue'. *The Journal of Infectious Diseases*, :jiz593. https://doi.org/10.1093/infdis/jiz593.

Qi, Yilin, Darwin J. Operario, Steve N. Georas, and Tim R. Mosmann. 2012. 'The Acute Environment, Rather than T Cell Subset Pre-Commitment, Regulates Expression of the Human T Cell Cytokine Amphiregulin'. *PloS One* 7 (6): e39072. https://doi.org/10.1371/journal.pone.0039072.

Rausch, Sebastian, Jochen Huehn, Dennis Kirchhoff, Justyna Rzepecka, Corinna Schnoeller, Smitha Pillai, Christoph Loddenkemper, et al. 2008. 'Functional Analysis of Effector and Regulatory T Cells in a Parasitic Nematode Infection'. *Infection and Immunity* 76 (5): 1908–19. https://doi.org/10.1128/IAI.01233-07.

Read, Simon, Rebecca Greenwald, Ana Izcue, Nicholas Robinson, Didier Mandelbrot, Loise Francisco, Arlene H. Sharpe, and Fiona Powrie. 2006. 'Blockade of CTLA-4 on CD4+CD25+ Regulatory T Cells Abrogates Their Function in Vivo'. *Journal of Immunology* 177 (7): 4376–83. https://doi.org/10.4049/jimmunol.177.7.4376.

Reddy, Aravind T., Sowmya P. Lakshmi, and Raju C. Reddy. 2012. 'Murine Model of Allergen Induced Asthma'. *Journal of Visualized Experiments*, 63: 3771. https://doi.org/10.3791/3771.

Reddy, Pradeep B. J., Taylor H. Schreiber, Naveen K. Rajasagi, Amol Suryawanshi, Sachin Mulik, Tamara Veiga-Parga, Toshiro Niki, Mitsuomi Hirashima, Eckhard R. Podack, and Barry T. Rouse. 2012. 'TNFRSF25 Agonistic Antibody and Galectin-9 Combination Therapy Controls Herpes Simplex Virus-Induced Immunoinflammatory Lesions'. *Journal of Virology* 86 (19): 10606–20. https://doi.org/10.1128/JVI.01391-12.

Redpath, Stephen A., Nienke van der Werf, Ana M. Cervera, Andrew S. MacDonald, David Gray, Rick M. Maizels, and Matthew D. Taylor. 2013. 'ICOS Controls Foxp3 $^{+}$ Regulatory T-Cell Expansion, Maintenance and IL-10 Production during Helminth Infection: Immunity to Infection'. *European Journal of Immunology* 43 (3): 705–15. https://doi.org/10.1002/eji.201242794.

Resch, Wolfgang, Kim K. Hixson, Ronald J. Moore, Mary S. Lipton, and Bernard Moss. 2007. 'Protein Composition of the Vaccinia Virus Mature Virion'. *Virology* 358 (1): 233–47. https://doi.org/10.1016/j.virol.2006.08.025.

Reuter, Dajana, Tim Sparwasser, Thomas Hünig, and Jürgen Schneider-Schaulies. 2012. 'Foxp3+ Regulatory T Cells Control Persistence of Viral CNS Infection'. *PLoS ONE* 7 (3): e33989. https://doi.org/10.1371/journal.pone.0033989.

Reynolds, Lisa A., Kara J. Filbey, and Rick M. Maizels. 2012. 'Immunity to the Model Intestinal Helminth Parasite Heligmosomoides Polygyrus'. *Seminars in Immunopathology* 34 (6): 829–46. https://doi.org/10.1007/s00281-012-0347-3.

Roberts, Kim L., and Geoffrey L. Smith. 2008. 'Vaccinia Virus Morphogenesis and Dissemination'. *Trends in Microbiology* 16 (10): 472–79. https://doi.org/10.1016/j.tim.2008.07.009.

Rodo, Miguel J., Virginie Rozot, Elisa Nemes, One Dintwe, Mark Hatherill, Francesca Little, and Thomas J. Scriba. 2019. 'A Comparison of Antigen-Specific T Cell Responses Induced by Six Novel Tuberculosis Vaccine Candidates'. *PLOS Pathogens* 15 (3): e1007643. https://doi.org/10.1371/journal.ppat.1007643.

Rojas, José M., Miguel Avia, Verónica Martín, and Noemí Sevilla. 2017. 'IL-10: A Multifunctional Cytokine in Viral Infections'. *Journal of Immunology Research* 2017: 6104054. https://doi.org/10.1155/2017/6104054.

Romagnani, Sergio. 2000. 'The Role of Lymphocytes in Allergic Disease'. *Journal of Allergy and Clinical Immunology* 105 (3): 399–408. https://doi.org/10.1067/mai.2000.104575.

Romano, M., V. Ricci, A. Di Popolo, P. Sommi, C. Del Vecchio Blanco, C. B. Bruni, U. Ventura, et al. 1998. 'Helicobacter Pylori Upregulates Expression of Epidermal Growth Factor-Related Peptides, but Inhibits Their Proliferative Effect in MKN 28 Gastric Mucosal Cells'. *The Journal of Clinical Investigation* 101 (8): 1604–13. https://doi.org/10.1172/JCI1174.

Romano, Marco, Giorgia Fanelli, Caraugh Jane Albany, Giulio Giganti, and Giovanna Lombardi. 2019. 'Past, Present, and Future of Regulatory T Cell Therapy in Transplantation and Autoimmunity'. *Frontiers in Immunology* 10: 43. https://doi.org/10.3389/fimmu.2019.00043.

Salek-Ardakani, Shahram, Magdalini Moutaftsi, Shane Crotty, Alessandro Sette, and Michael Croft. 2008. 'OX40 Drives Protective Vaccinia Virus-Specific CD8 T Cells'. *Journal of Immunology* 181 (11): 7969–76.

Sánchez-Puig, Juana M, Laura Sánchez, Garbiñe Roy, and Rafael Blasco. 2004. 'Susceptibility of Different Leukocyte Cell Types to Vaccinia Virus Infection'. *Virology Journal* 1: 10. https://doi.org/10.1186/1743-422X-1-10.

Schenkel, Jason M., and David Masopust. 2014. 'Tissue-Resident Memory T Cells'. *Immunity* 41 (6): 886–97. https://doi.org/10.1016/j.immuni.2014.12.007.

Schlessinger, Joseph. 2000. 'Cell Signaling by Receptor Tyrosine Kinases'. *Cell* 103 (2): 211–25. https://doi.org/10.1016/S0092-8674(00)00114-8.

Schneider, Marlon R., and Yosef Yarden. 2014. 'Structure and Function of Epigen, the Last EGFR Ligand'. *Seminars in Cell & Developmental Biology* 28: 57–61. https://doi.org/10.1016/j.semcdb.2013.12.011.

Schrick, Livia, Simon H. Tausch, P. Wojciech Dabrowski, Clarissa R. Damaso, José Esparza, and Andreas Nitsche. 2017. 'An Early American Smallpox Vaccine Based on Horsepox'. *The New England Journal of Medicine* 377 (15): 1491–92. https://doi.org/10.1056/NEJMc1707600.

Sehrawat, Sharvan, Susmit Suvas, Pranita P. Sarangi, Amol Suryawanshi, and Barry T. Rouse. 2008. 'In Vitro-Generated Antigen-Specific CD4+ CD25+ Foxp3+ Regulatory T Cells Control the Severity of Herpes Simplex Virus-Induced Ocular Immunoinflammatory Lesions'. *Journal of Virology* 82 (14): 6838–51. https://doi.org/10.1128/JVI.00697-08.

Seo, Benjamin, Eric W. Choy, Stuart Maudsley, William E. Miller, Brenda A. Wilson, and Louis M. Luttrell. 2000. 'Pasteurella Multocida Toxin Stimulates Mitogen-Activated Protein Kinase via Gq/11-Dependent Transactivation of the Epidermal Growth Factor Receptor'. *Journal of Biological Chemistry* 275 (3): 2239–45. https://doi.org/10.1074/jbc.275.3.2239.

Setiady, Yulius Y., Jennifer A. Coccia, and Peter U. Park. 2010. 'In Vivo Depletion of CD4+FOXP3+ Treg Cells by the PC61 Anti-CD25 Monoclonal Antibody Is Mediated by FcgammaRIII+ Phagocytes'. *European Journal of Immunology* 40 (3): 780–86. https://doi.org/10.1002/eji.200939613.

Shankaran, Harish, Danielle L Ippolito, William B Chrisler, Haluk Resat, Nikki Bollinger, Lee K Opresko, and H Steven Wiley. 2009. 'Rapid and Sustained

Nuclear–Cytoplasmic ERK Oscillations Induced by Epidermal Growth Factor'. *Molecular Systems Biology* 5: 332. https://doi.org/10.1038/msb.2009.90.

Sibilia, Maria, and Erwin F. Wagner. 1995. 'Strain-Dependent Epithelial Defects in Mice Lacking the EGF Receptor'. *Science* 269 (5221): 234.

Singh, Bhuminder, Graham Carpenter, and Robert J. Coffey. 2016. 'EGF Receptor Ligands: Recent Advances'. *F1000Research* 5: 2270. https://doi.org/10.12688/f1000research.9025.1.

Singh, Bhuminder, and Robert J Coffey. 2014. 'From Wavy Hair to Naked Proteins: The Role of Transforming Growth Factor Alpha in Health and Disease'. *Seminars in Cell & Developmental Biology* 28: 12–21. https://doi.org/10.1016/j.semcdb.2014.03.003.

Slanina, Heiko, Sabrina Mündlein, Sabrina Hebling, and Alexandra Schubert-Unkmeir. 2014. 'Role of Epidermal Growth Factor Receptor Signaling in the Interaction of Neisseria Meningitidis with Endothelial Cells'. *Infection and Immunity* 82 (3): 1243–55. https://doi.org/10.1128/IAI.01346-13.

Smith, Geoffrey L., Camilla T. O. Benfield, Carlos Maluquer de Motes, Michela Mazzon, Stuart W. J. Ember, Brian J. Ferguson, and Rebecca P. Sumner. 2013. 'Vaccinia Virus Immune Evasion: Mechanisms, Virulence and Immunogenicity'. *The Journal of General Virology* 94 (11): 2367–92. https://doi.org/10.1099/vir.0.055921-0.

Smith, Geoffrey L., Alain Vanderplasschen, and Mansun Law. 2002. 'The Formation and Function of Extracellular Enveloped Vaccinia Virus'. *The Journal of General Virology* 83 (12): 2915–31. https://doi.org/10.1099/0022-1317-83-12-2915.

Smith, Kendall A. 2011. 'Edward Jenner and the Small Pox Vaccine'. *Frontiers in Immunology* 2: 21. https://doi.org/10.3389/fimmu.2011.00021.

Smyth, Danielle J., Yvonne Harcus, Madeleine P.J. White, William F. Gregory, Janina Nahler, Ian Stephens, Edward Toke-Bjolgerud, et al. 2018. 'TGF-β Mimic Proteins Form an Extended Gene Family in the Murine Parasite Heligmosomoides Polygyrus'. *International Journal for Parasitology* 48 (5): 379–85. https://doi.org/10.1016/j.ijpara.2017.12.004.

Solic, N., and D. E. Davies. 1997. 'Differential Effects of EGF and Amphiregulin on Adhesion Molecule Expression and Migration of Colon Carcinoma Cells'. *Experimental Cell Research* 234 (2): 465–76. https://doi.org/10.1006/excr.1997.3635.

Song, Liqiang, Huanzhang Tang, Dapeng Liu, Jiao Song, Yunfu Wu, Shuoyao Qu, and Yan Li. 2016. 'The Chronic and Short-Term Effects of Gefinitib on Airway

Remodeling and Inflammation in a Mouse Model of Asthma'. *Cellular Physiology and Biochemistry* 38 (1): 194–206. https://doi.org/10.1159/000438621.

Soroceanu, Liliana, Armin Akhavan, and Charles S. Cobbs. 2008. 'Platelet-Derived Growth Factor-α Receptor Activation Is Required for Human Cytomegalovirus Infection'. *Nature* 455 (7211): 391–95. https://doi.org/10.1038/nature07209.

Specht, Sabine, Matthew D. Taylor, Marieke A. Hoeve, Judith E. Allen, Roland Lang, and Achim Hoerauf. 2012. 'Over Expression of IL-10 by Macrophages Overcomes Resistance to Murine Filariasis'. *Experimental Parasitology* 132 (1): 90–96. https://doi.org/10.1016/j.exppara.2011.09.003.

Spesock, April H., Brice E. Barefoot, Caroline A. Ray, Daniel J. Kenan, Michael D. Gunn, Elizabeth A. Ramsburg, and David J. Pickup. 2011. 'Cowpox Virus Induces Interleukin-10 Both in Vitro and in Vivo'. *Virology* 417 (1): 87–97. https://doi.org/10.1016/j.virol.2011.05.010.

Spits, Hergen, David Artis, Marco Colonna, Andreas Diefenbach, James P. Di Santo, Gerard Eberl, Shigeo Koyasu, et al. 2013. 'Innate Lymphoid Cells — a Proposal for Uniform Nomenclature'. *Nature Reviews Immunology* 13 (2): 145–49. https://doi.org/10.1038/nri3365.

Stack, Julianne, Ismar R. Haga, Martina Schröder, Nathan W. Bartlett, Geraldine Maloney, Patrick C. Reading, Katherine A. Fitzgerald, Geoffrey L. Smith, and Andrew G. Bowie. 2005. 'Vaccinia Virus Protein A46R Targets Multiple Toll-like–Interleukin-1 Receptor Adaptors and Contributes to Virulence'. *The Journal of Experimental Medicine* 201 (6): 1007–18. https://doi.org/10.1084/jem.20041442.

Stefan, Mihaela S., Meng-Shiou Shieh, Kerry A. Spitzer, Penelope S. Pekow, Jerry A. Krishnan, David H. Au, and Peter K. Lindenauer. 2019. 'Association of Antibiotic Treatment With Outcomes in Patients Hospitalized for an Asthma Exacerbation Treated With Systemic Corticosteroids'. *JAMA Internal Medicine*. 179 (3): 333-339. https://doi.org/10.1001/jamainternmed.2018.5394.

Stern, Kathryn A., Trenton L. Place, and Nancy L. Lill. 2008. 'EGF and Amphiregulin Differentially Regulate Cbl Recruitment to Endosomes and EGF Receptor Fate'. *Biochemical Journal* 410 (3): 585–94. https://doi.org/10.1042/BJ20071505.

Stittelaar, Koert J., Thijs Kuiken, Rik L. de Swart, Geert van Amerongen, Helma W. Vos, Hubert G. M. Niesters, Pim van Schalkwijk, et al. 2001. 'Safety of Modified Vaccinia Virus Ankara (MVA) in Immune-Suppressed Macaques'. *Vaccine* 19 (27): 3700–3709. https://doi.org/10.1016/S0264-410X(01)00075-5.

Stroobant, Paul, Andrew R. Rice, William J. Gullick, Dorothy J. Cheng, Ian M. Kerr, and Michael D. Waterfield. 1985. 'Purification and Characterization of Vaccinia Virus Growth Factor'. *Cell* 42 (1): 383–93. https://doi.org/10.1016/S0092-8674(85)80133-1.

Stumm, Camila Leindecker, Scott H. Wettlaufer, Sonia Jancar, and Marc Peters-Golden. 2011. 'Airway Remodeling in Murine Asthma Correlates with a Defect in PGE2 Synthesis by Lung Fibroblasts'. *American Journal of Physiology. Lung Cellular and Molecular Physiology* 301 (5): L636-644. https://doi.org/10.1152/ajplung.00158.2011.

Swanson, Karen V., J. McLeod Griffiss, Vonetta L. Edwards, Daniel C. Stein, and Wenxia Song. 2011. 'Neisseria Gonorrhoeae-Induced Transactivation of EGFR Enhances Gonococcal Invasion'. *Cellular Microbiology* 13 (7): 1078–90. https://doi.org/10.1111/j.1462-5822.2011.01603.x.

Tario, Joseph D., Alexis N. Conway, Katharine A. Muirhead, and Paul K. Wallace. 2018. 'Monitoring Cell Proliferation by Dye Dilution: Considerations for Probe Selection'. *Methods in Molecular Biology* 1678: 249–99. https://doi.org/10.1007/978-1-4939-7346-0_12.

Taylor, Mark J, Achim Hoerauf, and Moses Bockarie. 2010. 'Lymphatic Filariasis and Onchocerciasis'. *The Lancet* 376 (9747): 1175–85. https://doi.org/10.1016/S0140-6736(10)60586-7.

Taylor, Matthew D., Anjanette Harris, Simon A. Babayan, Odile Bain, Abigail Culshaw, Judith E. Allen, and Rick M. Maizels. 2007. 'CTLA-4 and CD4+ CD25+ Regulatory T Cells Inhibit Protective Immunity to Filarial Parasites in Vivo'. *The Journal of Immunology* 179 (7): 4626–4634.

Taylor, Matthew D., Laetitia LeGoff, Anjanette Harris, Eva Malone, Judith E. Allen, and Rick M. Maizels. 2005. 'Removal of Regulatory T Cell Activity Reverses Hyporesponsiveness and Leads to Filarial Parasite Clearance in Vivo'. *The Journal of Immunology* 174 (8): 4924–4933.

Taylor, Matthew D., Nienke van der Werf, and Rick M. Maizels. 2012. 'T Cells in Helminth Infection: The Regulators and the Regulated'. *Trends in Immunology* 33 (4): 181–89. https://doi.org/10.1016/j.it.2012.01.001.

Taylor, Matthew, Nienke van der Werf, Anjanette Harris, Andrea L Graham, Odile Bain, Judith E Allen, and Rick M Maizels. 2009. 'Early Recruitment of Natural CD4+ Foxp3+ Treg Cells by Infective Larvae Determines the Outcome of Filarial Infection'. *European Journal of Immunology* 39 (1): 192–206. https://doi.org/10.1002/eji.200838727.

Threadgill, D. W., A. A. Dlugosz, L. A. Hansen, T. Tennenbaum, U. Lichti, D. Yee, C. LaMantia, et al. 1995. 'Targeted Disruption of Mouse EGF Receptor: Effect of

Genetic Background on Mutant Phenotype'. *Science* 269 (5221): 230–34. https://doi.org/10.1126/science.7618084.

Townsley, Alan C., Andrea S. Weisberg, Timothy R. Wagenaar, and Bernard Moss. 2006. 'Vaccinia Virus Entry into Cells via a Low-PH-Dependent Endosomal Pathway'. *Journal of Virology* 80 (18): 8899–8908. https://doi.org/10.1128/JVI.01053-06.

Tscharke, David C., Gunasegaran Karupiah, Jie Zhou, Tara Palmore, Kari R. Irvine, S.M. Mansour Haeryfar, Shanicka Williams, et al. 2005. 'Identification of Poxvirus CD8+T Cell Determinants to Enable Rational Design and Characterization of Smallpox Vaccines'. *The Journal of Experimental Medicine* 201 (1): 95–104. https://doi.org/10.1084/jem.20041912.

Tsung, K., J. H. Yim, W. Marti, R. M. Buller, and J. A. Norton. 1996. 'Gene Expression and Cytopathic Effect of Vaccinia Virus Inactivated by Psoralen and Long-Wave UV Light'. *Journal of Virology* 70 (1): 165–71.

Tuettenberg, Andrea, Susanne A. Hahn, Johanna Mazur, Aslihan Gerhold-Ay, Jetse Scholma, Iris Marg, Alexander Ulges, et al. 2016. 'Kinome Profiling of Regulatory T Cells: A Closer Look into a Complex Intracellular Network'. *PLoS ONE* 11 (2): e0149193. https://doi.org/10.1371/journal.pone.0149193.

Tzahar, E, J D Moyer, H Waterman, E G Barbacci, J Bao, G Levkowitz, M Shelly, et al. 1998. 'Pathogenic Poxviruses Reveal Viral Strategies to Exploit the ErbB Signaling Network.' *The EMBO Journal* 17 (20): 5948–63. https://doi.org/10.1093/emboj/17.20.5948.

Tzahar, E, H Waterman, X Chen, G Levkowitz, D Karunagaran, S Lavi, B J Ratzkin, and Y Yarden. 1996. 'A Hierarchical Network of Interreceptor Interactions Determines Signal Transduction by Neu Differentiation Factor/Neuregulin and Epidermal Growth Factor.' *Molecular and Cellular Biology* 16 (10): 5276–87.

UpToDate. 2019. 'Cidofovir: An Overview'. https://www.uptodate.com/contents/cidofovir-an-overview. Accessed July 2019.

Vanderplasschen, Alain, Elizabeth Mathew, Michael Hollinshead, Robert B. Sim, and Geoffrey L. Smith. 1998. 'Extracellular Enveloped Vaccinia Virus Is Resistant to Complement Because of Incorporation of Host Complement Control Proteins into Its Envelope'. *Proceedings of the National Academy of Sciences of the United States of America* 95 (13): 7544–49.

Veiga-Parga, Tamara, Sharvan Sehrawat, and Barry T. Rouse. 2013. 'Role of Regulatory T Cells during Virus Infection'. *Immunological Reviews* 255 (1): 182–196. https://doi.org/10.1111/imr.12085.

Vermeer, Paola D., Julia McHugh, Tatiana Rokhlina, Daniel W. Vermeer, Joseph Zabner, and Michael J. Welsh. 2007. 'Vaccinia Virus Entry, Exit, and Interaction with Differentiated Human Airway Epithelia'. *Journal of Virology* 81 (18): 9891–99. https://doi.org/10.1128/JVI.00601-07.

Volkmann, L., O. Bain, M. Saeftel, S. Specht, K. Fischer, F. Brombacher, K. I. Matthaei, and A. Hoerauf. 2003. 'Murine Filariasis: Interleukin 4 and Interleukin 5 Lead to Containment of Different Worm Developmental Stages.' *Medical Microbiology and Immunology* 192 (1): 23–31. https://doi.org/10.1007/s00430-002-0155-9.

Volkmann, L., M. Saeftel, O. Bain, K. Fischer, B. Fleischer, and A. Hoerauf. 2001. 'Interleukin-4 Is Essential for the Control of Microfilariae in Murine Infection with the Filaria Litomosoides Sigmodontis.' *Infection and Immunity* 69 (5): 2950–56. https://doi.org/10.1128/IAI.69.5.2950-2956.2001.

Volkmann, Lars, Kerstin Fischer, Mark Taylor, and Achim Hoerauf. 2003. 'Antibiotic Therapy in Murine Filariasis (Litomosoides Sigmodontis): Comparative Effects of Doxycycline and Rifampicin on Wolbachia and Filarial Viability'. *Tropical Medicine & International Health* 8 (5): 392–401. https://doi.org/10.1046/j.1365-3156.2003.01040.x.

Vos, Theo, Christine Allen, Megha Arora, Ryan M Barber, Zulfiqar A Bhutta, Alexandria Brown, Austin Carter, et al. 2016. 'Global, Regional, and National Incidence, Prevalence, and Years Lived with Disability for 310 Diseases and Injuries, 1990–2015: A Systematic Analysis for the Global Burden of Disease Study 2015'. *The Lancet* 388 (10053): 1545–1602. https://doi.org/10.1016/S0140-6736(16)31678-6.

Wang, Shen-Wu, Chad K. Oh, Seong H. Cho, Guanghui Hu, Rachel Martin, Sossiena Demissie-Sanders, Kang Li, Matthew Moyle, and Zhengbin Yao. 2005. 'Amphiregulin Expression in Human Mast Cells and Its Effect on the Primary Human Lung Fibroblasts'. *The Journal of Allergy and Clinical Immunology* 115 (2): 287–94. https://doi.org/10.1016/j.jaci.2004.11.037.

Wang, Sihua, Yuan Zhang, Yan Wang, Ping Ye, Jun Li, Huabin Li, Qingqing Ding, and Jiahong Xia. 2016. 'Amphiregulin Confers Regulatory T Cell Suppressive Function and Tumor Invasion via the EGFR/GSK-3β/Foxp3 Axis'. *Journal of Biological Chemistry* 291 (40): 21085–95. https://doi.org/10.1074/jbc.M116.717892.

Wang, Xin, Shu-Mei Huong, Marie L Chiu, Nancy Raab-Traub, and Eng-Shang Huang. 2003. 'Epidermal Growth Factor Receptor Is a Cellular Receptor for Human Cytomegalovirus'. *Nature* 424 (6947): 456–61. https://doi.org/10.1038/nature01818.

Whibley, Natasha, Andrea Tucci, and Fiona Powrie. 2019. 'Regulatory T Cell Adaptation in the Intestine and Skin'. *Nature Immunology* 20 (4): 386–96. https://doi.org/10.1038/s41590-019-0351-z.

WHO. 2019. 'Neglected Tropical Diseases'. WHO. 2019. http://www.who.int/neglected_diseases/en/. Accessed July 2019.

Wiedemann, Agnès, Lily Mijouin, Mohammed Akli Ayoub, Emilie Barilleau, Sylvie Canepa, Ana Paula Teixeira-Gomes, Yves Le Vern, Manon Rosselin, Eric Reiter, and Philippe Velge. 2016. 'Identification of the Epidermal Growth Factor Receptor as the Receptor for Salmonella Rck–Dependent Invasion'. *The FASEB Journal* 30 (12): 4180–91. https://doi.org/10.1096/fj.201600701R.

Wilson, Mark S., Matthew D. Taylor, Adam Balic, Constance A.M. Finney, Jonathan R. Lamb, and Rick M. Maizels. 2005. 'Suppression of Allergic Airway Inflammation by Helminth-Induced Regulatory T Cells'. *The Journal of Experimental Medicine* 202 (9): 1199–1212. https://doi.org/10.1084/jem.20042572.

Wipff, Pierre-Jean, Daniel B. Rifkin, Jean-Jacques Meister, and Boris Hinz. 2007. 'Myofibroblast Contraction Activates Latent TGF-B1 from the Extracellular Matrix'. *The Journal of Cell Biology* 179 (6): 1311–23. https://doi.org/10.1083/jcb.200704042.

Worthington, John J., Aoife Kelly, Catherine Smedley, David Bauché, Simon Campbell, Julien C. Marie, and Mark A. Travis. 2015. 'Integrin Avβ8-Mediated TGF-β Activation by Effector Regulatory T Cells Is Essential for Suppression of T-Cell-Mediated Inflammation'. *Immunity* 42 (5): 903–15. https://doi.org/10.1016/j.immuni.2015.04.012.

Wu, Shiying, Qian Zhang, Fei Zhang, Fansen Meng, Shengduo Liu, Ruyuan Zhou, Qingzhe Wu, et al. 2019. 'HER2 Recruits AKT1 to Disrupt STING Signalling and Suppress Antiviral Defence and Antitumour Immunity'. *Nature Cell Biology* 21 (8): 1027–40. https://doi.org/10.1038/s41556-019-0352-z.

Wu, Xuejie, Pin Wu, Yifei Shen, Xiaodong Jiang, and Feng Xu. 2018. 'CD8+ Resident Memory T Cells and Viral Infection'. *Frontiers in Immunology* 9: 2093. https://doi.org/10.3389/fimmu.2018.02093.

Wynn, Thomas A., Ajay Chawla, and Jeffrey W. Pollard. 2013. 'Origins and Hallmarks of Macrophages: Development, Homeostasis, and Disease'. *Nature* 496 (7446): 445–55. https://doi.org/10.1038/nature12034.

Xiao, Zhengguo, Julie M. Curtsinger, Martin Prlic, Stephen C. Jameson, and Matthew F. Mescher. 2007. 'The CD8 T Cell Response to Vaccinia Virus Exhibits Site-Dependent Heterogeneity of Functional Responses'. *International Immunology* 19 (6): 733–43. https://doi.org/10.1093/intimm/dxm039.

Yan, Fang, Hanwei Cao, Rupesh Chaturvedi, Uma Krishna, Stuart S. Hobbs, Peter J. Dempsey, Richard M. Peek, et al. 2009. 'Epidermal Growth Factor Receptor Activation Protects Gastric Epithelial Cells from Helicobacter Pylori-Induced Apoptosis'. *Gastroenterology* 136 (4): 1297-e3. https://doi.org/10.1053/j.gastro.2008.12.059.

Yan, Y., Y. Lu, M. Wang, H. Vikis, R. Yao, Y. Wang, R. A. Lubet, and M. You. 2006. 'Effect of an Epidermal Growth Factor Receptor Inhibitor in Mouse Models of Lung Cancer'. *Molecular Cancer Research* 4 (12): 971–81. https://doi.org/10.1158/1541-7786.MCR-06-0086.

Yang, Guilin, Ailian Liu, Qing Xie, Taylor B. Guo, Bing Wan, Boping Zhou, and Jingwu Z. Zhang. 2007. 'Association of CD4+CD25+Foxp3+ Regulatory T Cells with Chronic Activity and Viral Clearance in Patients with Hepatitis B'. *International Immunology* 19 (2): 133–40. https://doi.org/10.1093/intimm/dxl130.

Yang, Hailin, Sung-Kwon Kim, Mikyung Kim, Pedro A. Reche, Tiara J. Morehead, Inger K. Damon, Raymond M. Welsh, and Ellis L. Reinherz. 2005. 'Antiviral Chemotherapy Facilitates Control of Poxvirus Infections through Inhibition of Cellular Signal Transduction'. *Journal of Clinical Investigation* 115 (2): 379–87. https://doi.org/10.1172/JCI200523220.

Yoder, Jennifer D., Tsefang S. Chen, Cliff R. Gagnier, Srilakshmi Vemulapalli, Claudia S. Maier, and Dennis E. Hruby. 2006. 'Pox Proteomics: Mass Spectrometry Analysis and Identification of Vaccinia Virion Proteins'. *Virology Journal* 3 (1): 10. https://doi.org/10.1186/1743-422X-3-10.

Yu, Fang, Suveena Sharma, Julie Edwards, Lionel Feigenbaum, and Jinfang Zhu. 2015. 'Dynamic Expression of T-Bet and GATA3 by Regulatory T Cells Maintains Immune Tolerance'. *Nature Immunology* 16 (2): 197–206. https://doi.org/10.1038/ni.3053.

Zaccone, Paola, Oliver Burton, Nigel Miller, Frances M. Jones, David W. Dunne, and Anne Cooke. 2009. 'Schistosoma Mansoni Egg Antigens Induce Treg That Participate in Diabetes Prevention in NOD Mice'. *European Journal of Immunology* 39 (4): 1098–1107. https://doi.org/10.1002/eji.200838871.

Zaiss, Dietmar M., Li Yang, Pranav R Shah, James J Kobie, Joseph F Urban, and Tim R Mosmann. 2006. 'Amphiregulin, a TH2 Cytokine Enhancing Resistance to Nematodes'. *Science* 314 (5806): 1746. https://doi.org/10.1126/science.1133715.

Zaiss, Dietmar M.W., William C. Gause, Lisa C. Osborne, and David Artis. 2015. 'Emerging Functions of Amphiregulin in Orchestrating Immunity, Inflammation and Tissue Repair'. *Immunity* 42 (2): 216–26. https://doi.org/10.1016/j.immuni.2015.01.020.

Zaiss, Dietmar M.W., Jorg van Loosdregt, Andrea Gorlani, Cornelis P.J. Bekker, Andrea Grone, Maria Sibilia, Paul M. P. van Bergen en Henegouwen, Rob C. Roovers, Paul J. Coffer, and Alice J. A. M. Sijts. 2013. 'Amphiregulin Enhances Regulatory T Cell Suppressive Function via the Epidermal Growth Factor Receptor'. *Immunity* 38 (2): 275–84. https://doi.org/10.1016/j.immuni.2012.09.023.

Zaiss, Mario, Alexis Rapin, Luc Lebon, Lalit Kumar Dubey, Ilaria Mosconi, Kerstin Sarter, Alessandra Piersigilli, et al. 2015. 'The Intestinal Microbiota Contributes to the Ability of Helminths to Modulate Allergic Inflammation'. *Immunity* 43 (5): 998–1010. https://doi.org/10.1016/j.immuni.2015.09.012.

Zelinskyy, Gennadiy, Kirsten K. Dietze, Yvonne P. Hüsecken, Simone Schimmer, Savita Nair, Tanja Werner, Kathrin Gibbert, et al. 2009. 'The Regulatory T-Cell Response during Acute Retroviral Infection Is Locally Defined and Controls the Magnitude and Duration of the Virus-Specific Cytotoxic T-Cell Response'. *Blood* 114 (15): 3199–3207. https://doi.org/10.1182/blood-2009-03-208736.

Zeng, Hanyu, Rong Zhang, Boquan Jin, and Lihua Chen. 2015. 'Type 1 Regulatory T Cells: A New Mechanism of Peripheral Immune Tolerance'. *Cellular and Molecular Immunology* 12 (5): 566–71. https://doi.org/10.1038/cmi.2015.44.

Zhang, Hongtao, Alan Berezov, Qiang Wang, Geng Zhang, Jeffrey Drebin, Ramachandran Murali, and Mark I. Greene. 2007. 'ErbB Receptors: From Oncogenes to Targeted Cancer Therapies'. *Journal of Clinical Investigation* 117 (8): 2051–58. https://doi.org/10.1172/JCI32278.

Zhang, Jing, Hui Li, Jinzhao Wang, Zheng Dong, Shahzad Mian, and Fu-Shin X. Yu. 2004. 'Role of EGFR Transactivation in Preventing Apoptosis in Pseudomonas Aeruginosa–Infected Human Corneal Epithelial Cells'. *Investigative Ophthalmology & Visual Science* 45 (8): 2569–76. https://doi.org/10.1167/iovs.03-1323.

Zhang, Nan, Bernd Schröppel, Girdhari Lal, Claudia Jakubzick, Xia Mao, Dan Chen, Na Yin, et al. 2009. 'Regulatory T Cells Sequentially Migrate from Inflamed Tissues to Draining Lymph Nodes to Suppress the Alloimmune Response'. *Immunity* 30 (3): 458–69. https://doi.org/10.1016/j.immuni.2008.12.022.

Zheng, Kai, Kaio Kitazato, and Yifei Wang. 2014. 'Viruses Exploit the Function of Epidermal Growth Factor Receptor'. *Reviews in Medical Virology* 24 (4): 274–86. https://doi.org/10.1002/rmv.1796.

Zheng, Kai, Yangfei Xiang, Xiao Wang, Qiaoli Wang, Meigong Zhong, Shaoxiang Wang, Xiaoyan Wang, Jianglin Fan, Kaio Kitazato, and Yifei Wang. 2014. 'Epidermal Growth Factor Receptor-PI3K Signaling Controls Cofilin Activity To Facilitate Herpes Simplex Virus 1 Entry into Neuronal Cells'. *MBio* 5 (1): e00958-13. https://doi.org/10.1128/mBio.00958-13.

References

Zheng, Nan, Can Zhao, Xi-Ran He, Shan-Tong Jiang, Shu-Yan Han, Guo-Bing Xu, and Ping-Ping Li. 2016. 'Simultaneous Determination of Gefitinib and Its Major Metabolites in Mouse Plasma by HPLC–MS/MS and Its Application to a Pharmacokinetics Study'. *Journal of Chromatography B* 1011: 215–22. https://doi.org/10.1016/j.jchromb.2016.01.006.

Zhou, Yang, Jae-Young Lee, Chang-Min Lee, Won-Kyung Cho, Min-Jong Kang, Jonathan L. Koff, Pyeong-Oh Yoon, et al. 2012. 'Amphiregulin, an Epidermal Growth Factor Receptor Ligand, Plays an Essential Role in the Pathogenesis of Transforming Growth Factor-β-Induced Pulmonary Fibrosis'. *The Journal of Biological Chemistry* 287 (50): 41991–0. https://doi.org/10.1074/jbc.M112.356824.

Zhu, Jinfang, Hidehiro Yamane, and William E. Paul. 2010. 'Differentiation of Effector CD4 T Cell Populations'. *Annual Review of Immunology* 28: 445–89. https://doi.org/10.1146/annurev-immunol-030409-101212.

Zhu, Lingxiang, Pak-kei Lee, Wai-ming Lee, Yuhua Zhao, Dongfang Yu, and Yin Chen. 2009. 'Rhinovirus-Induced Major Airway Mucin Production Involves a Novel TLR3-EGFR–Dependent Pathway'. *American Journal of Respiratory Cell and Molecular Biology* 40 (5): 610–19. https://doi.org/10.1165/rcmb.2008-0223OC.

Zitvogel, Laurence, Lionel Apetoh, François Ghiringhelli, and Guido Kroemer. 2008. 'Immunological Aspects of Cancer Chemotherapy'. *Nature Reviews Immunology* 8 (1): 59–73. https://doi.org/10.1038/nri2216.